3/17

SANDIA REPORT

SAND94–2162 • UC–122
Unlimited Release
Printed February 1995

Development of the Multi-Level Seismic Receiver (MLSR)

G. E. Sleefe, B. P. Engler, P. M. Drozda, R. J. Franco, Jeff Morgan

Prepared by
Sandia National Laboratories
Albuquerque, New Mexico 87185 and Livermore, California 94550
for the United States Department of Energy
under Contract DE-AC04-94AL85000

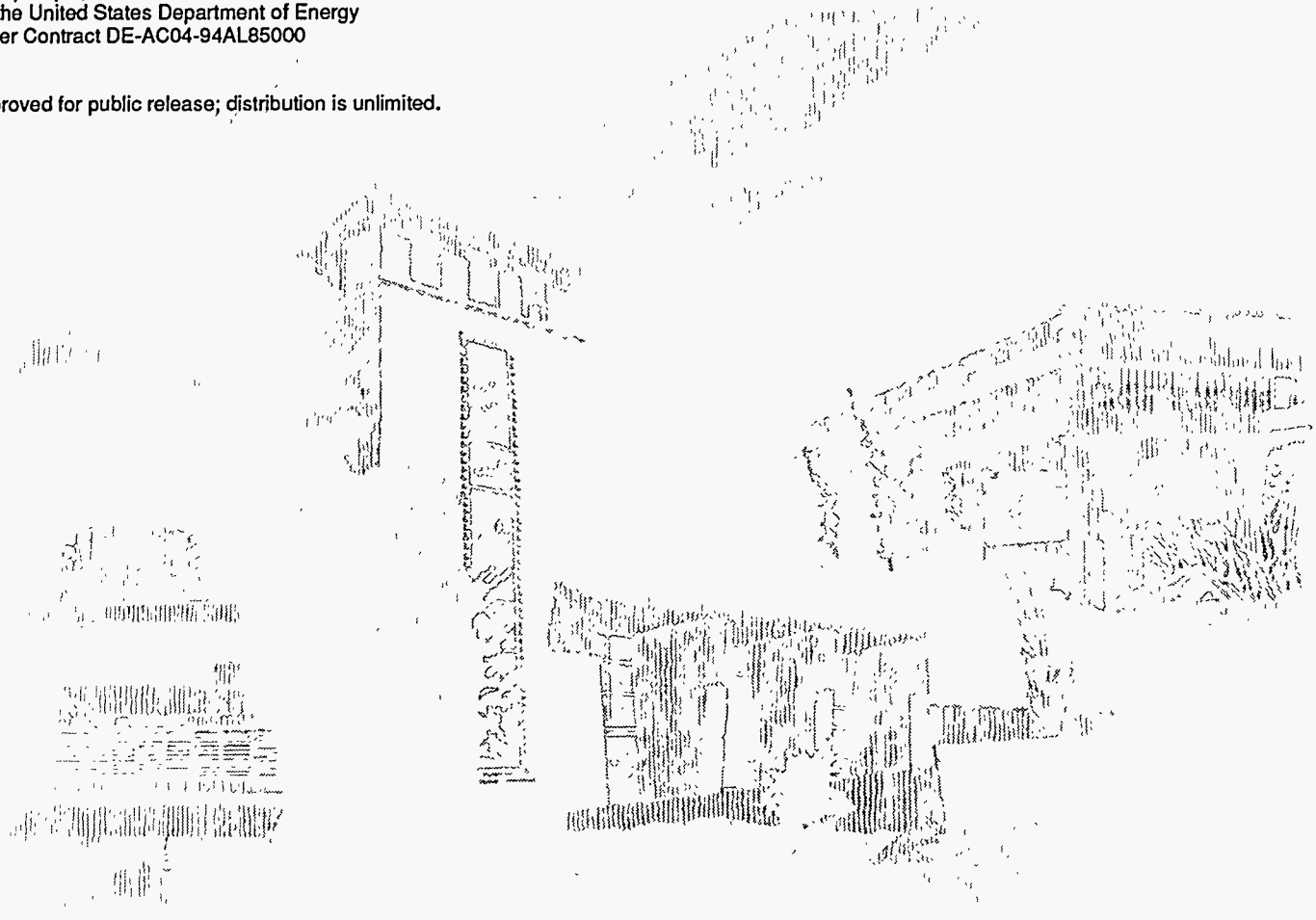

SF2900Q(8-81)

Issued by Sandia National Laboratories, operated for the United States Department of Energy by Sandia Corporation.

Available to DOE and DOE contractors from
Office of Scientific and Technical Information
PO Box 62
Oak Ridge, TN 37831

Prices available from (615) 576-8401, FTS 626-8401

Available to the public from
National Technical Information Service
US Department of Commerce
5285 Port Royal Rd
Springfield, VA 22161

NTIS price codes
Printed copy: A11
Microfiche copy: A01

Distribution
Category UC-122

SAND94-2162
Unlimited Release
Printed February 1995

Development of the Multi-Level Seismic Receiver (MLSR)

G. E. Sleefe, B. P. Engler, and P. M. Drozda
Advanced Geophysical Technology Department, 6114

R. J. Franco and Jeff Morgan
Telemetry Technology Development Department, 2664

Sandia National Laboratories
Albuquerque, NM 87185

January 24, 1995

Abstract

The Advanced Geophysical Technology Department (6114) and the Telemetry Technology Development Department (2664) have, in conjunction with the Oil Recovery Technology Partnership, developed a Multi-Level Seismic Receiver (MLSR) for use in crosswell seismic surveys. The MLSR was designed and evaluated with the significant support of many industry partners in the oil exploration industry. The unit was designed to record and process superior quality seismic data operating in severe borehole environments, including high temperature (up to 200°C) and static pressure (10,000 psi). This development has utilized state-of-the-art technology in transducers, data acquisition, and real-time data communication and data processing. The mechanical design of the receiver has been carefully modeled and evaluated to insure excellent signal coupling into the receiver.

BS

TABLE OF CONTENTS

TABLE OF FIGURES

Table of Tables

I. Introduction and Background

I.1. INTRODUCTION

Looking for petroleum in underground reservoirs is an expensive, time-consuming operation. Even after an oil-producing area appears to have been depleted, petroleum-bearing formations can go undetected in-between existing wells. In the United States alone, an estimated 300 billion barrels remain undetected.

In order to help identify underground oil-bearing formations, the oil industry has routinely used seismic waves to generate sub-surface images. The conventional seismic technique uses seismic-wave generators and sensors that are situated on the earth's surface. Unfortunately, the surface seismic technique has very limited resolution when imaging deep formations, due to wave attenuation, dispersion, and inaccurate seismic coupling. Thus, the surface seismic technique has limited utility for determining formation properties between existing oil and gas wells.

During the past several years, it has been recognized that a new seismic technique, referred to as cross-well seismic imaging, can provide a quantitative image of the reservoir. With this method, as illustrated in Figure I.1, a seismic source is placed in one well and is used to propagate seismic energy into the formation. In an adjacent well, a seismic receiver is used to measure the variations of the seismic energy through the formation, and infer the properties of the region between the two wells. The cross-well seismic imaging method holds great promise in providing high resolution (less than 5 m) images and could prove useful in finding bypassed oil and assessing the effectiveness of enhanced oil recovery processes.

The primary reason that cross-well seismic imaging is not routinely used is the lack of cost-effective instrumentation to generate and receive the seismic waves. Conventional borehole seismic receivers can record data at only one depth at a time. As such, the conventional receivers require extensive, time-consuming movement up and down the well in order to sample the full seismic wave-field. Because the cross-well method is targeted at active producing wells, the down-time required during imaging makes the cross-well technique prohibitively expensive when conventional receivers are utilized. Therefore, the primary objective of this project was to develop a seismic receiver system which is suitable for use in production wells, and simultaneously measures the seismic wave-field at multiple depths. Such a system is referred to as a multi-level borehole seismic receiver.

I.2. PROJECT STRUCTURE AND HISTORICAL PERSPECTIVE

This section briefly describes the structure of this development effort in terms of funding sources, industry participants, and key personnel. This section also serves to give a historical perspective of the project.

In 1988, the U.S. Department of Energy established the Oil Recovery Technology Partnership. The mission of the Partnership was to establish and fund projects that would bring National Laboratories' technologies and expertise to solving oil and gas recovery related projects. Also in 1988, a subset of the Partnership was formed and was referred to as the Crosswell Seismic Forum. The mission of the

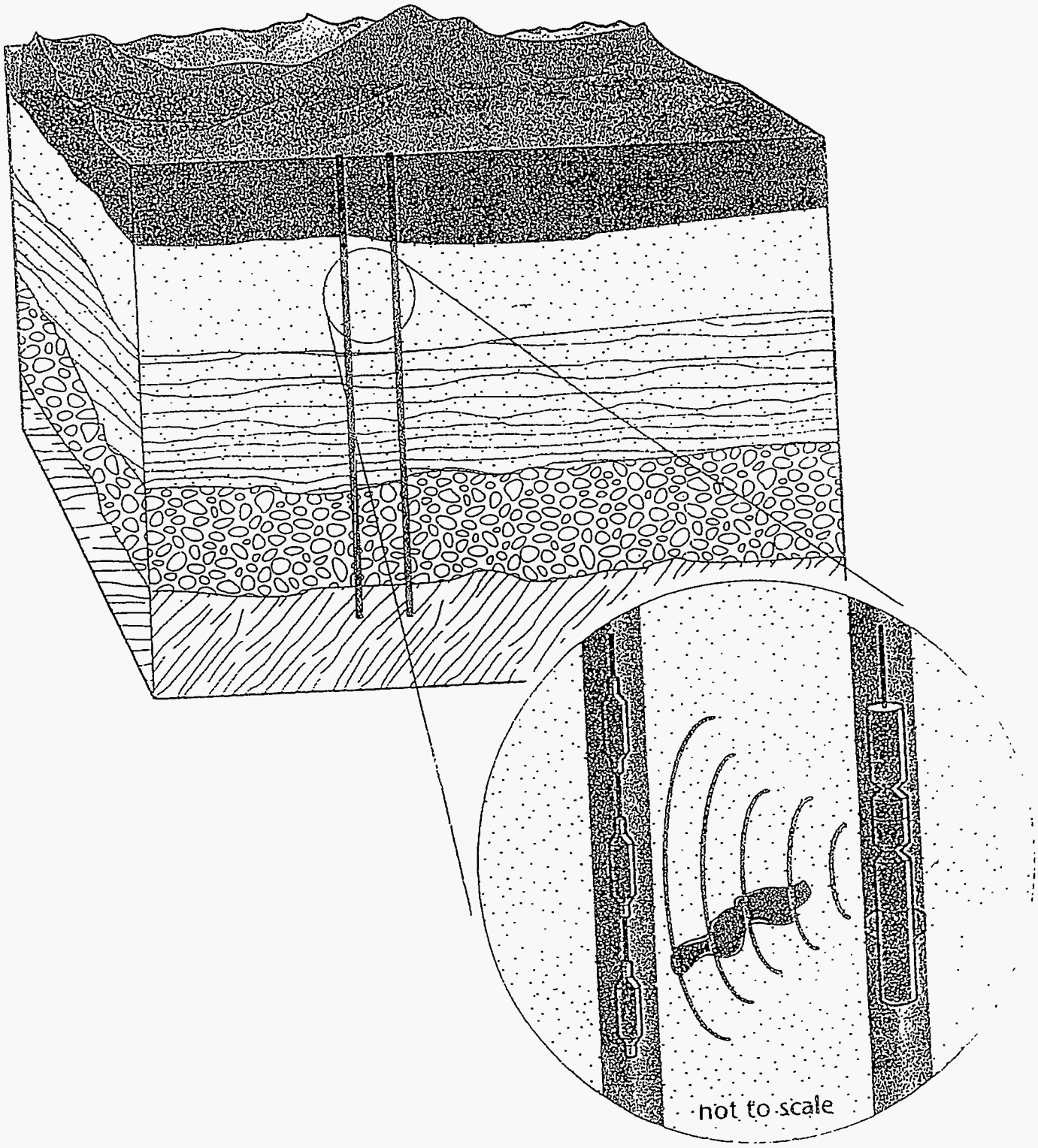

Figure I.1: Crosswell seismic imaging configuration. A seismic source (inset, right), generates seismic waves in the formation. Seismic receivers (inset. left), detect the waves that have traversed the formation.

Forum was to bring National Laboratories' technologies and expertise to solve technical issues associated with the new cross-well seismic imaging technique. A major thrust of the Forum was to establish teams between the Laboratories and the Oil and Gas Industry to develop new cross-well technologies. The Forum consisted of over twenty participating companies, each of which contributed a nominal, one-time fee. These formal participants provided reviews and evaluations of proposals presented by Laboratory/Industry teams. This feedback was used by the Partnership and DOE to select new projects.

The first meeting of the Forum was held in December of 1988. At this meeting, Gerry Sleefe presented a conceptual proposal to the Forum on the need for a multi-level seismic receiver. The presentation focused on the technical challenges posed by multi-level receivers and possible ways in which Sandia could bring weapons technology to help solve the problem. The second meeting of the Forum was held in April of 1989. At this meeting, five formal proposals were presented to the Forum for evaluation. Gerry Sleefe and Paul Hommert presented a formal proposal for the development of the MLSR. Gerry presented the development program as involving the investigation and implementation of three key technologies; seismic sensors, mechanical clamping, and data telemetry. Paul presented the key business plan for the proposal; the establishment of an industry partner to assist in the development and eventually become the commercial supplier for the new technologies. Of the five proposals presented at this Forum meeting, the MLSR proposal received the highest ranking from the Forum participants. As a result, DOE provided initial funding of the MLSR program to Sandia in June of 1989.

One of the early primary tasks of the program was to establish an industry partner. The partner selection was made by soliciting oil and gas service and instrumentation companies to participate. The solicitation was achieved through a formal Request For Quotation (RFQ) issued by Sandia National Laboratories. The RFQ asked the companies to submit a proposal to Sandia to indicate their interest in teaming with Sandia on this project. The proposals were to contain two key aspects; a summary of the company's technical capabilities appropriate for this development effort, and a proposal for participating in a cost-shared arrangement with Sandia. Of the more than a dozen companies asked to quote, three submitted formal proposals. These proposals were evaluated and scored by weighing the technical expertise with the cost-shared effort. The RFQ process resulted in a contract award to OYO Geospace Corporation in March of 1990.

OYO Geospace Corporation, based in Houston, TX, is a major manufacturer and supplier of sensors and instrumentation for the seismic industry. Their main product line consists of geophone sensors, digital seismic data recorders, digital plotters, and a variety of borehole sensor packages. OYO Geospace Corp. participated in this development effort through a 50% cost-shared contract. The time and materials contract resulted in OYO Geospace paying for 50% of their development costs. OYO Geospace contributed $250,000 in direct development costs plus approximately $200,000 of in-kind efforts to this project. This cost-shared effort greatly leveraged the approximate $1,400,000 provided by DOE.

In addition to the OYO Geospace participation, numerous U.S. oil companies teamed with Sandia. The participating oil companies provided field-test facilities and equipment, field-test personnel, use of seismic sources, data acquisition services, and data processing services. Participating oil companies

were; Amoco, Chevron, Conoco, Exxon, and Texaco. The total in-kind support provided by these companies exceeded $1,000,000. In essence, between the cost shared efforts of OYO Geospace and the oil companies, DOE received approximately an even match for their funds.

This project involved a large number of key personnel that provided valuable contributions towards the development of the MLSR. A list of the personnel and their role in the development of the MLSR is provided in Appendix A.

I.3. PROJECT OBJECTIVES

The objectives of this project was to design, develop, and field-test a multi-level, three-component borehole seismic receiver system. To meet the needs for accurate reservoir imaging, the following major design goals were established for the MLSR:

(1) an accurate 3-component vibration response for stimuli ranging from 10 Hz to above 1000 Hz;

(2) true multi-level clamping for at least four, but preferably up to 32 levels;

(3) simultaneous broad-band data acquisition for all down-hole sensors in the MLSR, and a means for carrying the sensor data to the surface;

(4) the incorporation of fail-safe mechanisms to minimize the possibility of system failure while in the borehole; and

(5) the ability to operate the system at temperatures up to 200°C.

The system developed under this program generally meets all of the above goals. A detailed set of specifications that describes the conformance of the system to these goals is provided in Chapter II.

There were three significant technical development areas required to achieve the design goals:

(1) the selection of the appropriate seismic sensors for the cross-well application;

(2) the detailed mechanical design of the clamped packages and interconnects so that clamp resonances were minimal in the 10 Hz to 1000 Hz range; and

(3) the development of a telemetry scheme for carrying the high-fidelity seismic signals to the surface.

Each of these three technical areas are incorporated into the final MLSR system and will be discussed in detail in subsequent chapters.

I.4. LIMITATIONS OF PRIOR ART

Prior to the start of this project, almost all seismic receivers were single level; i.e. only one receiver could be operated in the well. There were a few crude multi-level receivers in existence, but they lacked many of the required features for high-resolution cross-well imaging. This section summarizes the limitations of the prior art. In summary, the fundamental limitations of the prior art were limited multi-level capability and limited bandwidth.

I.4.a Lack of Multi-Level Capabilities

The conventional approach for acquiring full wave-field borehole seismic data is to utilize a wall-locking three-component geophone instrument in the survey well. The instrument is typically locked at a particular depth to sample the wave-field generated by a seismic source located either at the surface (VSP mode) or in an adjacent well (CHSP mode). The receiver instrument must then be moved and locked at other depths in order to sample the full seismic wave-field. Once the full seismic wave-field is sampled, an image formation process such as tomography can be utilized. The obvious limitation to this conventional approach is the excessive time consumed by the frequent movement of the receiver instrument. When the survey is performed in a production well, the time-consuming nature of the receiver movements results in long shut-in times, and hence lost production. Therefore, it would be extremely desirable to utilize a receiver instrument capable of locking into the borehole at multiple depths and simultaneously sample the seismic wave-field at multiple depths. Such a system is often referred to as a multi-level receiver. The ability to simultaneously clamp multiple sondes in a borehole is therefore essential to the commercial success of three-component cross-well surveys.

Previous efforts towards the development of multi-station seismic receivers have been summarized in [I.1]. Prior multi-station receivers can be classified into one of two categories; fluid-coupled hydrophone receivers [I.2], and wall-locking three-component receivers [I:3]. Although multi-station hydrophone receivers offer the advantage of simple deployment, they lack the vector wave-field capabilities of wall-locked sensors. Additionally, hydrophone receivers are adversely affected by receiver well tube-wave phenomena including direct and reflected wave-field saturation and increased noise [I.4].

I.4.b Limited Seismic Bandwidth Capabilities

The bandwidth associated with conventional surface-seismic and VSP techniques for imaging deep petroleum reservoirs [I.5] is typically less than 150 Hz. With the advent of cross-well seismic techniques, the bandwidth is potentially increased well beyond 150 Hz due to the shorter propagation paths and the improved seismic coupling at depth. As a result, there is now a need for both borehole seismic sources and receivers that have bandwidths on the order of 1000 Hz to take advantage of the high resolution capabilities of cross-well imaging [I.6].

Several factors have contributed to the limited bandwidth in the prior art. These factors include tool resonance, sensor limitations, and data acquisition limitations. These limiting factors are described in the following subsections.

I.4.c Receiver Resonances

It has long been recognized [I.7] that conventional VSP wall-locked sondes exhibit vibrational resonances in the 150 Hz to 400 Hz range. The presence of such tool resonances results in significant distortion of the seismic signals recorded during high-resolution cross-well surveys.

It is essential that the clamped seismic receiver instrument faithfully record the particle motion of the seismic wave-field that is incident on the borehole. The conventional VSP wall-locking geophone instrument generally does not enable the accurate measurement of particle motion over a wide frequency range. Two limitations of the conventional receiver can cause this limited frequency response. The first limitation, known as structural resonances, results from structural elements within the receiver that act like "tuning forks". When the receiver is excited with seismic energy, these structural modes cause spurious vibrations within the receiver. These modes are sensed by the geophones, and cause narrow-band signals to occur at the natural frequencies of the modes.

The second limitation is known as locking resonance, and results from inadequate coupling of the geophones to the borehole over a wide frequency band. When the locking arm of the instrument extends to clamp the unit to the borehole, the geophones are coupled to the borehole only at relatively low frequencies. At some higher frequency, the motions of the clamping unit do not follow the motions of the borehole wall. In conventional VSP geophone receivers, as illustrated in Figure I.2, the locking resonant frequency is typically in the 200 Hz to 400 Hz range. Therefore, conventional VSP instruments can only be used for accurate polarization measurements for seismic excitations below about 200 Hz.

I.4.d Limited Bandwidth Due to Seismic Sensor Selection

While conventional geophones are clearly the appropriate sensor for low-frequency surface and VSP applications [I.8], their performance degrades at the cross-well seismic frequencies. Conventional geophones, as illustrated in Figure I.3, exhibit spurious modes which are due to off-axis excitation of the geophone springs [I.8]. The spurious mode manifests itself as a resonance effect which occurs at a frequency which is approximately 25 times higher than the natural frequency of the geophone. For example, a 10 Hz geophone can exhibit spurious modes at and above 250 Hz, thus limiting its usefulness above 250 Hz. Additionally, the low frequency end of the geophone does not accurately measure particle motion due to phase shifts within the first few octaves above the natural frequency. Even if these inaccuracies in the sensor could be eliminated or corrected for, the geophone suffers from high-frequency self-noise [I.9] which reduces the potential signal-to-noise ratio above approximately 200 Hz. Therefore, a seismic sensor other than the conventional geophone is desirable for increasing the bandwidth of cross-well seismic data acquisition.

LRS-1300 Downhole Receiver Tool

The LRS-1300 three-component downhole receiver tool* from LRS offers greater sensing precision and more flexibility in field operations than does any comparable tool available today. The high-performance characteristics make the LRS-1300 suitable for standard well-site seismic applications, such as checkshot, VSP, and salt-dome proximity surveys, as well as a growing number of borehole-to-borehole surveys.

Design Features

- Excellent frequency response: flat to 350 Hz for vertical components and 150 Hz for horizontal components
- Excellent shear-wave particle motion reproducibility free of resonance up to 150 Hz
- High clamp-force-to-weight ratio (up to 7.3:1), permitting cable slacking to reduce cable induced noise and improve acoustic coupling
- Suitable for borehole diameters up to 20 inches
- Fail-safe mechanism that releases arm upon loss of power
- Optional gimbal-mounting that keeps elements normal to each other at up to 60° tilt*
- Isolation box that reduces pickup of 60 Hz and its harmonics 90 dB down from peak signal level
- Optional wireline simulator for testing and calibration
- Quick disassembly into two units, one for electronics and the other for all mechanical components

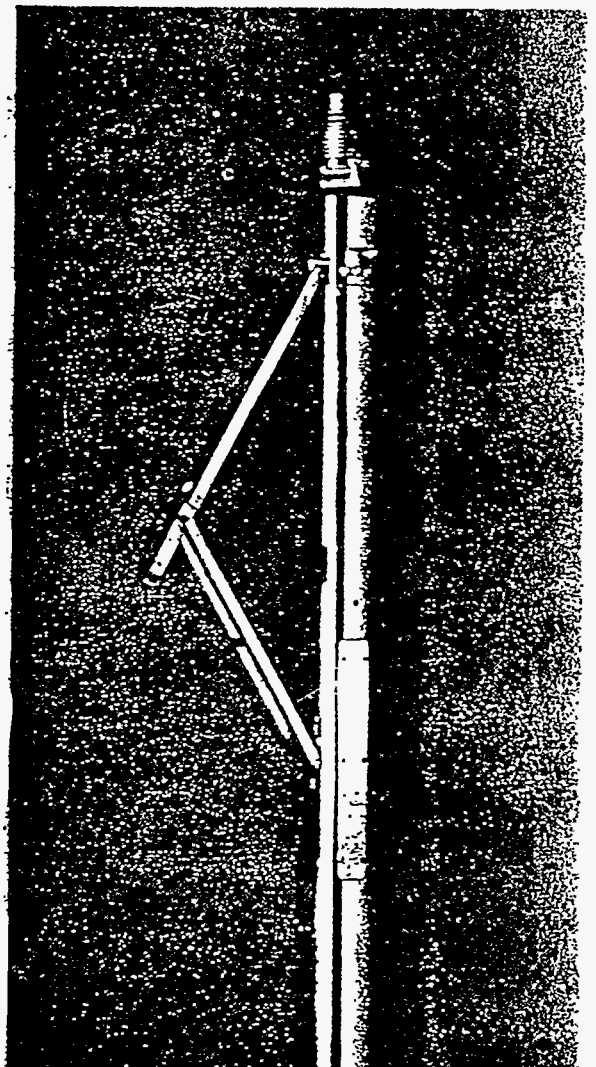

Excellent frequency response (flat below 150 Hz) and advanced operating features make the LRS-1300 tool the ideal choice for downhole seismic applications.

Western Atlas International
A Litton/Unocal Company

LRS

Figure I.2: Typical prior-art single-level seismic receiver

I.4.e Limited Data Acquisition and Telemetry Capabilities

An essential feature for a multi-level receiver is the transmission of multi-channel data from the borehole to the surface. There are two basic techniques which have been used for data acquisition and telemetry. The first approach, known as the multi-conductor cable method, transmits each sensor signal on a separate pair of wires to the surface. These analog signals are then recorded on the surface by a conventional multi-channel digital seismograph. Note that for a 5-level 3-component system, a total of 15 pairs of wires would need to be incorporated into the wireline cable. This approach has been implemented by several vendors, but has some serious limitations. In particular, the multi-conductor wireline cables and associated connectors are expensive and fragile. Additionally, the multi-conductor approach makes it impractical to expand beyond about 5 levels of receivers. Furthermore, the transmission of the analog signals over several miles of cable can cause noise corruption.

The second technique utilized for data acquisition and telemetry is referred to as the downhole digitizing method. With this approach, a digital data acquisition system is included downhole in the local vicinity of the sensor signals. The data acquisition system converts the analog sensor signals to a digital representation, and transmits the digital signals from all channels over a single wire to the surface.

Prior art attempts at the downhole digitizing method resulted in significant limitations. An example of a typical prior art multi-level receiver is illustrated in Figure I.4. A particular limitation of these receivers is that the sample rates utilized were generally too slow for high-bandwidth acquisition. Downhole sample rates of 2 msec were common, which provided a useable bandwidth of only 200 Hz. Clearly, more than an order of magnitude increase in bandwidth is required for crosswell applications. Probably the most limiting factor of prior downhole digitizing systems is that they transmitted the data over standard 7-conductor wireline. Due to the limited bandwidth of standard 7-conductor wireline, the digitizing systems needed to store the digital data in a memory buffer prior to transmitting it to the surface at a slower rate. The need for downhole memory buffers and micro-controllers resulted in extremely complex electronics which generally could not withstand the 200oC borehole environment. Worst of all, the downhole digitizing with buffering approach could slow down the cross-well survey because of the finite time required to transmit the data over the wireline.

To illustrate the effect of downhole buffering, a mathematical model was developed to determine the acquisition time for different acquisition methodologies. The total time required to perform a cross-well seismic survey can be estimated from the following formula:

$$T_t = T_d + T_u + m*k_d + m*k_u + N^2*(T_s + T_r)/m + N*(T_m + T_l)/m \qquad (I.1)$$

where T_t is the total time to perform the cross-well survey, T_d is the time required to get the receiver string down to depth prior to starting the survey, T_u is the time required to get the receiver string back to the surface after completing the survey, m is the number of receivers in the string, k_d is the timerequired to load each receiver into the hole, k_m is the time required to get each receiver out of the hole after the survey, N is the # of source depths in the survey (assumed to be the same as the number of

GS-14

GEOPHONE

REPRESENTATIVE FREQUENCY RESPONSE CURVES*

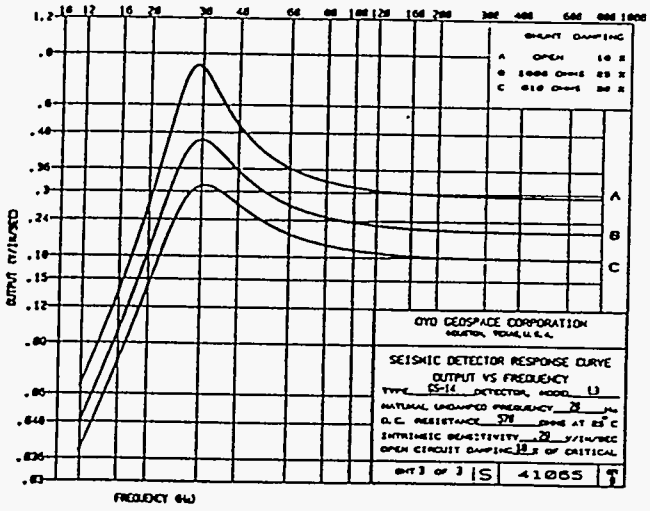

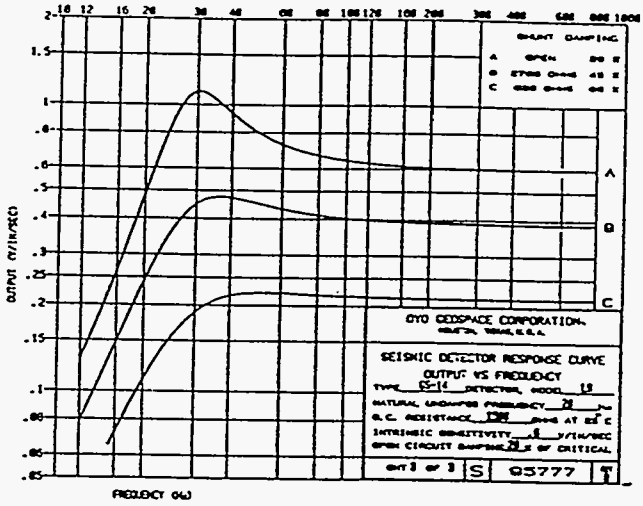

SPECIFICATIONS

	GS-14-L3	GS-14-L9
Functional		
Sensitivity ± 15%	290 mV/ips	600 mV/ips
Natural Frequency ± 20%	28 Hz	28 Hz
Coil Resistance ± 5%	570 ohms	1500 ohms
Coil Inductance	45 mh	90 mh
Damping Factor ± 30%	0.18	0.28
Damping Constant	172	738
Displacement Limit	0.09 in	0.09 in
Inertial Mass	0.076 oz	0.076 oz
Orientation Angle	± 180°	± 180°
Mechanical		
Height	0.68 in	0.74 in
Diameter	0.66 in	0.75 in
Weight	0.67 oz	0.95 oz
Environmental		
Operating Temperature	– 40° to 160° F	– 40° to 160° F
Storage Temperature	– 65° to 185° F	– 65° to 185° F
Shock	5000 G	1000 G

GS-14-L3

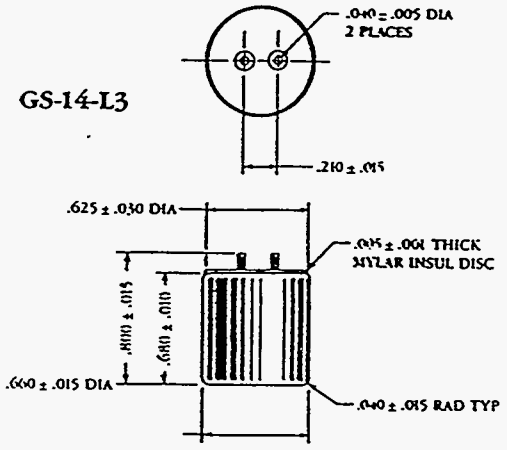

Note: All dimensions shown in inches.

NOTES:

1. Reference temperature for functional parameters is 75° F.
2. Orientation angle is referenced to vertical.
3. Damping factor is ratio of critical damping.
4. Sensitivity, natural frequency, coil resistance and damping factor are 100% tested. Consult the factory for special tests required to guarantee other functional parameters and shock limits.

*These frequency response curves illustrate amplitude vs frequency of excitation (velocity of motion).

Specifications are subject to change without notice.

OYO GEOSPACE

7334 N. Gessner • Houston, TX 77040 U.S.A.
TEL (713) 939-9700 • TLX 790433 • FAX (713) 937-8262
Bay R, 1350 42nd Ave. S.E. • Calgary, Alberta T2G-4V6, Canada
TEL (403) 287-3050 • TLX 03-821172 • FAX (403) 243-6220

Figure I.3: Typical prior-art seismic sensor

AMG

MULTILOCK(1)

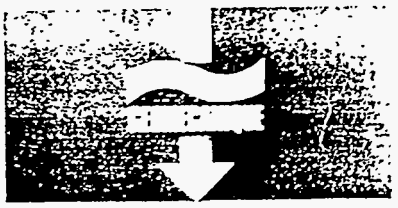

ACQUISITION EQUIPMENT

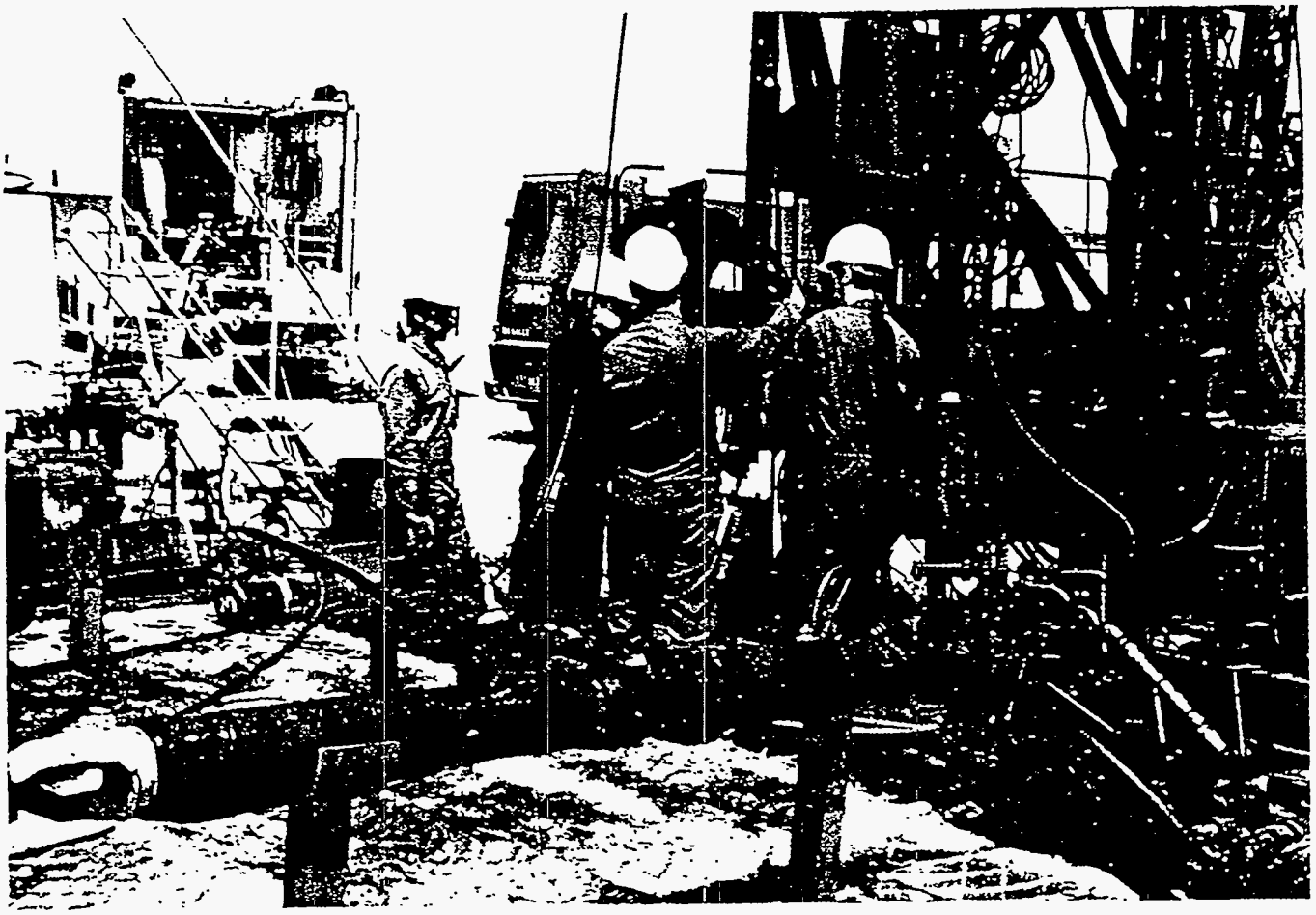

MULTILEVEL DIGITAL BOREHOLE SEISMIC SYSTEM FOR SHORTER RIG DOWNTIME AND BETTER DATA

- Efficient and safe in both cased and open, vertical or deviated holes, with very fast depth changes
- Complete acquisition and QC (correlation) system available
- Multilevel capacity reducing rig time at wellsite
- Identical response for all three components up to 160 Hz
- Noise filtering inherent to geophone string
- Compatible with standard 7-conductor logging cable
- Temperature up to 180°C (350°F), pressure up to 1200 bars (17,400 psi)
- Continuous monitoring to prevent wedging during downtrip
- DTU (downhole telemetry unit) in uppermost module
- Many years' experience worldwide in commercial and scientific applications.

Figure I.4: Typical prior-art multi-level seismic receiver

receiver depths points; i.e. the survey is NxN points or N^2 ray paths), T_s is the time required to move and re-shoot the source, T_r is the time in excess of T_s that it takes to telemeter the receiver data, T_m is the time required to move all receivers in the string from one station to the next, and T_l is the time required to lock all receivers in the string once they are on station.

Equation I.1 has been applied to determine the effect of different telemetry configurations. Table I.1 summarizes the parameters selected in the calculations. Figure I.5 is a plot of Equation I.1 for the situation where a clamped, swept seismic source is utilized. The time required to perform the survey is plotted as a function of the number of receivers in the string. Two different telemetry configurations are indicated. A 7-conductor telemetry system, which transmits at an effective data rate of 100 KBaud is shown. For comparison, a real-time telemetry system, such as one which utilizes the multi-conductor cable approach, or a high bandwidth fiber-optic cable is also illustrated. It is clear from this figure that for a small number of sondes in the string (less than 5), the time to perform the survey is independent of the telemetry method. This is because the receiver data is telemetered while the source is moving to its next shot location, and the data transmission is completed by the time the source is ready to shoot again. For a larger number of sondes, however, more data is acquired, and the 7-conductor approach takes longer to transmit this larger quantity of data. As a result, when more than 4 sondes are used, the survey slows down in-between shots, because of the wait for data transmissions. Therefore, with the swept source, there is no advantage to using more than 4 sondes in the string. It is also important to note that with 4 sondes, the swept source approach requires 40 hours to complete the survey. Clearly, in order to make such a source commercially attractive, real-time telemetry must be utilized to bring the survey below 40 hours.

Figure I.6 is a plot of Equation I.1 for the situation where an impulsive, non-clamped seismic source is utilized. For this case, the source is often weak and requires signal stacking. Three scenarios are indicated. In the first, real-time telemetry is performed and stacking is performed on the surface. In the second, a 7-conductor telemetry system is used and all data is sent to the surface and stacked at the surface. The third case is where the data is stacked downhole, although this requires a sophisticated down-hole micro-processor. From the figure, it is obvious that down-hole stacking must be implemented in order to make the 7-conductor telemetry system commercially viable. The figure also indicates that with a large number of sondes in the string (greater than 5), the survey is slowed down when 7-conductor telemetry is utilized.

In summary, 7-conductor data telemetry has serious limitations when one wants to implement more than 4 or 5 receivers in the string. In practice, 7-conductor telemetry is limited to 4 or 5 receivers, and down-hole stacking must be implemented. Therefore, in order to expand beyond 5 receivers, and avoid complicated down-hole electronics, real-time telemetry is preferred.

I.5. ADVANCEMENTS OVER PRIOR ART

The MLSR developed under this program provides significant advancements over the prior art described in the previous section. The improvements will be summarized in the following sub-sections.

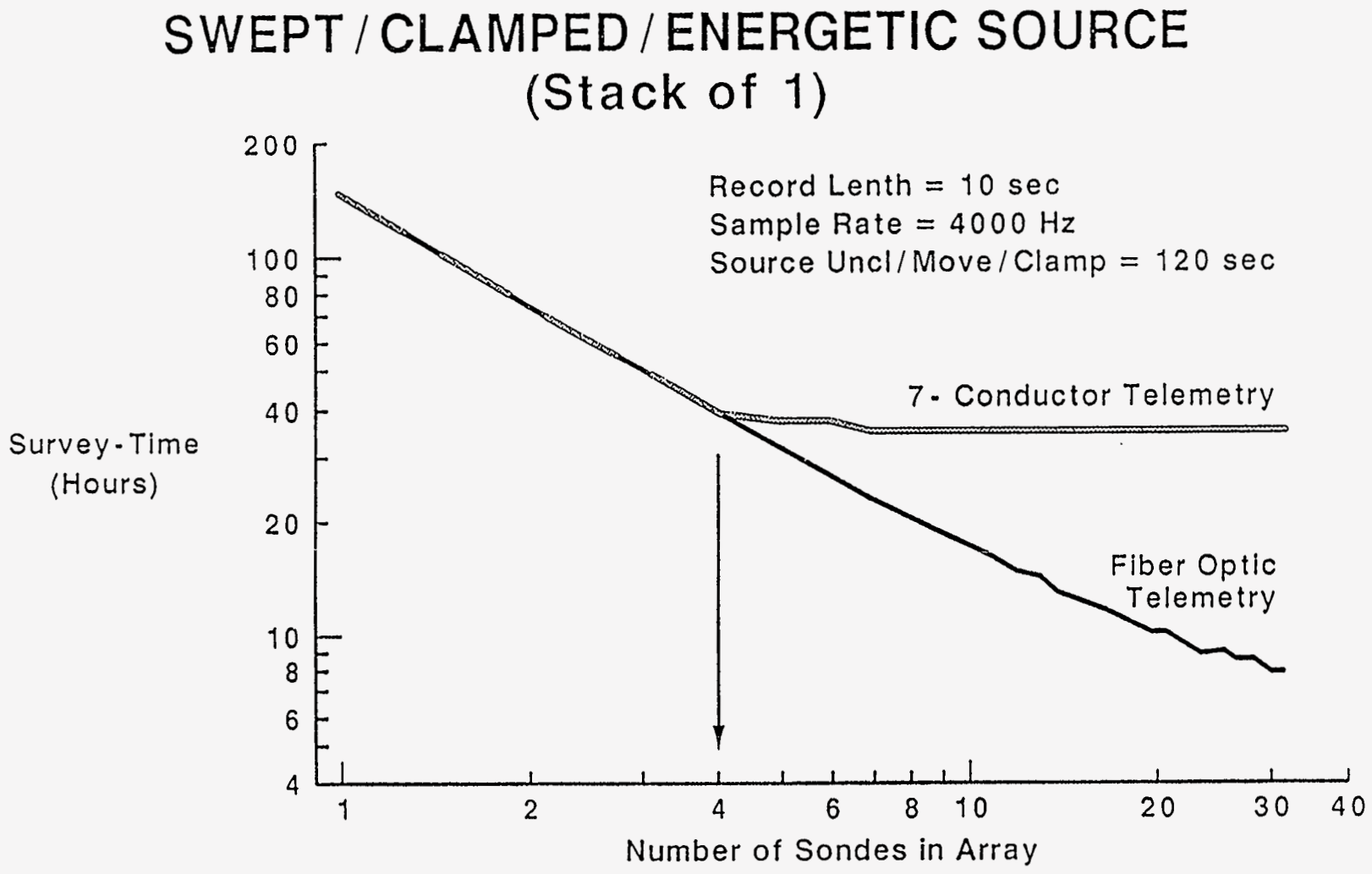

Figure I.5: Estimated time to perform a crosswell seismic survey using a swept-seismic source and a multi-level receiver

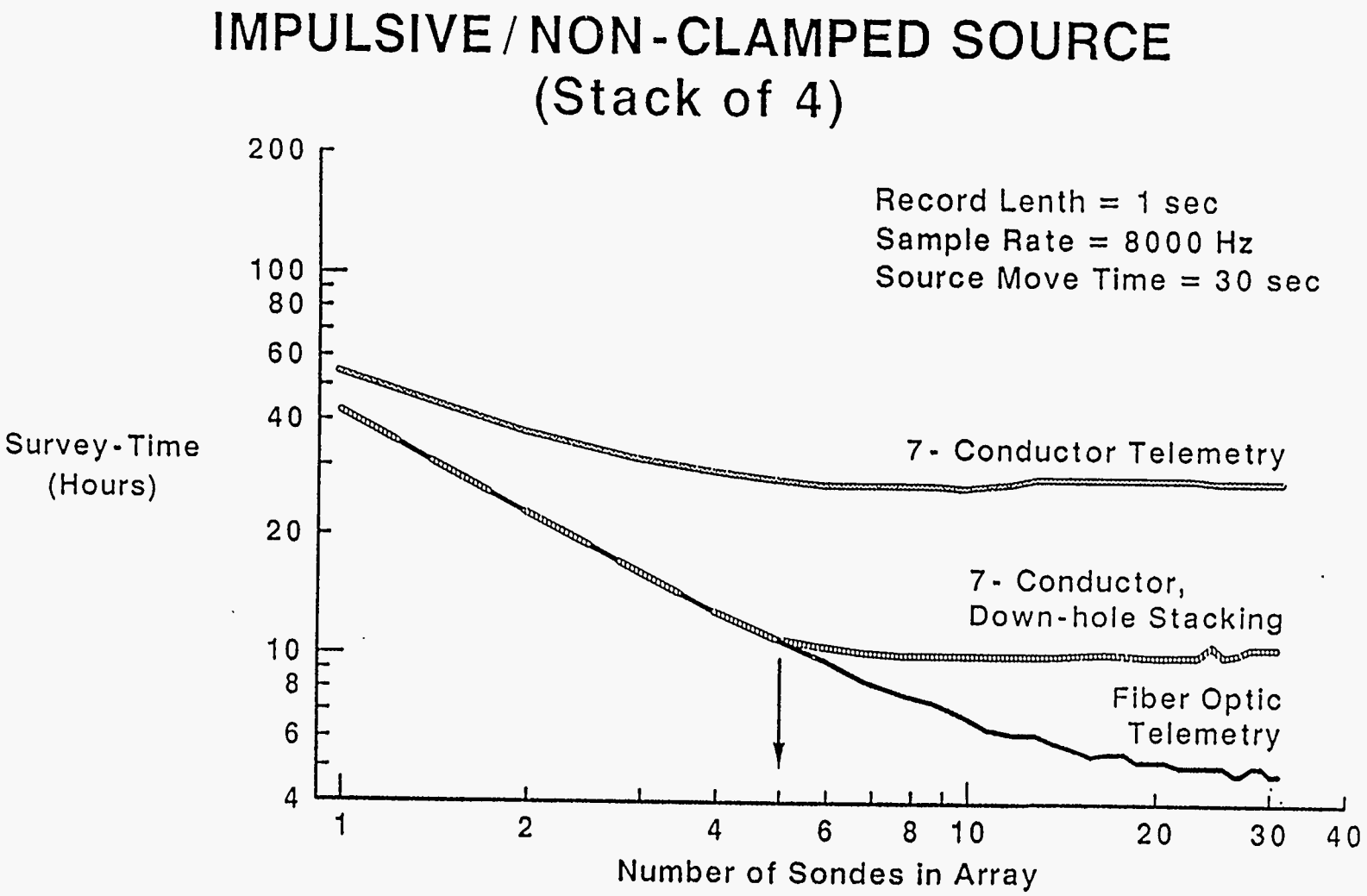

Figure I.6: Estimated time to perform a crosswell seismic survey using an impulsive seismic source

RECEIVER "ECONOMICS" CALCULATIONS

IMPLEMENTATION

- algorithm developed, runs under MS-DOS

SAMPLE CALCULATIONS

- many sample cases run, conclusions similar

Following examples:

- 64 x 64 survey
- survey depth = 6000 ft
- sondes deployed in groups of 4
- 10-minute penalty for every 4 sondes
- receiver clamp / unclamp / move time = 50 secs / sonde

Table I.1

I.5.a Multi-Level Expansion Capabilities

The developed MLSR offers true multi-level capabilities. The system is flexible and expandable; from 1 to 10 receivers can be placed in the string, with future expansion capability to 32 receivers. Each of the receivers are 3-component wall-locking sondes, which permits full-wavefield measurements. Due to the small size and easy-interconnect features, the system is easily and rapidly deployed in production wells. Full data acquisition and telemetry capabilities are included.

I.5.b Increased Seismic Bandwidth Capabilities

The developed MLSR has a much higher seismic bandwidth capability than the prior art. The mechanical design minimizes resonances below 1000 Hz, thereby increasing mechanical coupling to the formation. Additionally, state-of-the-art accelerometers are utilized in place of geophones, which results in a dramatic increase in frequency response above approximately 200 Hz. Furthermore, real-time telemetry with 1/8 ms sample rates and wide dynamic range provides high-fidelity signal recording. These improvements, which are discussed in the following subsections, provide for an effective seismic bandwidth of 10 Hz to more than 1000 Hz.

I.5.c Higher Resonant Frequencies

A mechanical clamp design was developed to provide accurate vibrational coupling to the borehole. Structural resonances are well above 2000 Hz, and locking resonances are typically above 1000 Hz. The method for achieving this improved vibrational response was the use of extensive finite element modeling of various receiver designs. The modeling helped identify potential resonant frequencies, and enabled engineering design iterations that pushed the resonant frequencies above the frequency band of interest. To help verify the modeling approach, extensive free-body and clamped-tool vibration experiments were performed. The final result was that all free body structural modes were above 2000 Hz and that locking resonances were generally above 1000 Hz. This is nearly an order of magnitude increase in seismic bandwidth relative to the prior art.

I.5.d Increased Bandwidth With Accelerometers

The low-noise piezo-electric accelerometers utilized in the receiver offer significant advantages over conventional geophones. In particular, these accelerometers do not exhibit the spurious resonance problem common to geophones. Additionally, accelerometers are insensitive to their mounting orientation and therefore do not require the gimbal mounts often utilized in geophone-based sondes. Another difference, and perhaps most important, is that these custom-designed low-noise piezo-electric accelerometers are more sensitive than geophones at the higher seismic frequencies. The high-frequency sensitivity improvement is due to the fact that the electronic noise of the custom accelerometer is lower than the electronic noise of the best geophones at frequencies above approximately 150 Hz. A 10:1 improvement in signal detection (and hence signal-to-noise ratio) at 1000 Hz has been achieved. This signal-to-noise improvement has been demonstrated with this

accelerometer-based receiver in numerous wells throughout the U.S. The specifications for these unique borehole accelerometers were developed by Sandia and resulted in a custom sensor which is now available from Wilcoxon Research as model 731-20.

I.5.e Improved Data Acquisition and Telemetry Capabilities

To overcome the limitations of traditional borehole telemetry systems, a system was developed that transmits the data through a fiber optic wireline. With the fiber optic approach, the data are digitized downhole with minimal circuitry. The data is then transmitted directly into an optical fiber for real-time data transmission to the surface. The advantage of the fiber optic approach is that there is no slow-down of the survey due to data transmissions. Additionally, the memory buffers for the data are uphole, allowing for very long record lengths, and real-time uphole stacking.

All of the electronic components used in the downhole portion have been proven to operate at 200°C. This is a primary advantage of fiber optic telemetry; no memory or micro-processors are required in the high temperature environment.

The downhole digitizer used in the MLSR provides wide-bandwidth, high dynamic range recording. The system samples data at a rate of 8000 samples/sec for each channel. The useable recorded bandwidth is 3000 Hz. An instantaneous floating point (IFP) gain-ranging approach is utilized. This results in a demonstrated dynamic range of 116 dB at temperatures below 150°C and a dynamic range of at least 100 dB at 200°C. This high fidelity recording capability is a significant improvement over the prior art.

I.6 SUMMARY

An advanced three-component multi-level borehole seismic receiver system has been designed, developed, and field tested. The system acquires data from multiple three-component wall-locking accelerometer packages and telemeters digital data to the surface in real-time. Due to the multiplicity of measurement stations and the real-time data link, acquisition time for the borehole seismic survey is significantly reduced. The seismic receiver system developed herein is protected by U.S. Patent 5,189,262 and U.S. Copyrights for both the BHDAS and BHDSP software (described in later chapters).

Subsequent chapters will describe the technical details of the system and its performance in numerous field trials. The field data will demonstrate that the MLSR provides significant enhancements relative to the prior art receivers; drastically improved signal-to-noise ratio, increased signal bandwidth, the detection of multiple reflectors, the observation of elastic wave conversions, and a true multi-level reduction in survey time.

II. SYSTEM DESCRIPTION AND OVERVIEW

This chapter provides a brief description and overview of the Multi-Level Seismic Receiver (MLSR). A general system and subsystem overview is provided. Additionally, a set of specifications are provided for the system.

II.1. SYSTEM OVERVIEW

The Multi-Level Seismic Receiver system (OYO Geospace trade-name of Advanced Borehole Recording System) is depicted in Figure II.1. The system consists of multiple wall-locking receivers that are interconnected with standard electrical cables. Each receiver contains three seismic sensors which are digitized by instantaneous floating point (IFP) circuitry. The sample rate of the digitizers is typically 8000 samples per second per channel. Up to 10 receivers (30 sensor channels) can be deployed in this fashion.

The digital data which streams out of the receiver packages are Manchester encoded and formatted by the Wireline Interface Unit (WIU) and driven onto a fiber optic wireline for transmission to the surface. With a 5-level receiver system, the data streaming to the surface is at a real-time rate of 5 Mbits/sec. The fiber optic wireline also contains electrical conductors which are utilized for power and command signals. At the surface, the digital optical data stream is converted back to an electrical signal, decoded, and checked for transmission errors. The data are streamed in real-time into a Borehole Data Acquisition System (BHDAS), which is a modified version of the OYO Geospace DFM-480. The acquisition unit performs the features of both a conventional seismograph and field processing system. The BHDAS also serves as the control system for the down-hole receivers, providing for clamp-motor control, setting of acquisition parameters, and acquiring temperature and diagnostic information from the downhole instruments. The BHDAS has a user-friendly interface and is fully menu-driven with windowing software.

The MLSR uses a unique data sampling scheme. Each receiver digitizes at a fixed rate of 8000 samples/sec/channel. This wideband data is transmitted over the fiber optic link in real-time to the surface. The BHDAS, however, provides for digital data filtering and decimation, which allows the recording of sample rates of 1/8, 1/4, 1, or 2 ms. The record length is set by the user and is limited only by the size of the uphole memory (16 second recording length is the current memory limitation). A further unique sampling feature, is that the data is sampled downhole as two simultaneous 16-bit words. One of these 16-bit words has unity gain and the second has a gain of 32. Both of these words are transmitted over the fiber optic link. The BHDAS restructures the two words in real-time to form a single 21-bit data sample. This sampling procedure eliminates the need for downhole gain ranging and downhole data processing.

The MLSR data acquisition and telemetry design is based on a digital interconnect bus architecture which is flexible and expandable. The digital interconnect scheme permits variable interconnect cable lengths, variable number of sondes in the array, and maintains superior dynamic range when compared to analog data transmission means. While the existing design is tailored to operation with a maximum

Multi-Station Seismic System

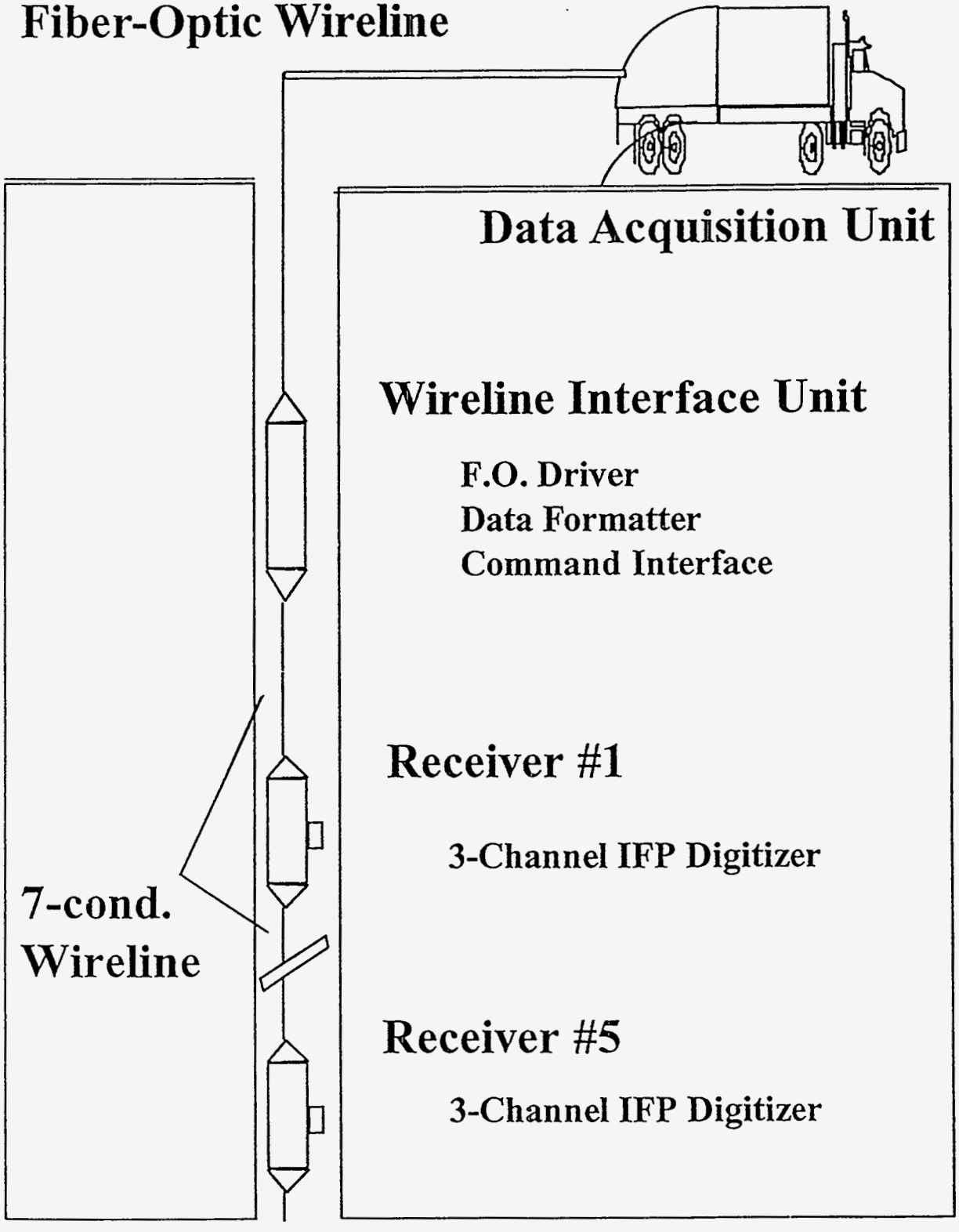

FIGURE II.1 Multi-level Seismic Receiver System

of five Data Receivers, this can be extended to ten if custom interconnects are available. The data acquisition and telemetry functions of the MLSR can be divided into four functional units: **Data Receivers, Data Formatter, Data Transmission Link, and Command Link.** The separation of these functional units can be described from the "Field Layout" diagram of Figure II.2. The Data Formatter, and Command Link Circuitry are physically housed together in the Wireline Interface Unit. These subsystems will be described in detail in subsequent sections.

II.2. SUB-SYSTEMS OVERVIEW

II.2.a Receiver Module (Clamping Package)

The receiver module is a rugged stainless steel package which consists of two pressure-sealed compartments. A schematic of the receiver module is shown in Figure II.3 and a photograph of a receiver module is shown in Figure II.4. A 3-component seismic sensor is housed in one section, and receiver electronics and the locking d.c. motor are in the second section. The drive mechanism for the locking arm is mechanically protected inside the central portion of the receiver but is exposed to the wellbore pressure. The locking arm drive mechanism consists of a right-angle gear drive and a lead-screw-piston arrangement. The locking arm is radially driven perpendicular to the longitudinal axis of the receiver, and has a total travel of 1.5". The clamp-force-to-tool-weight-ratio developed by this design is a function of the gearset selected and can vary from 5:1 to 20:1.

At the end of the locking arm, a user-defined contact shoe may be attached. The shoe serves two purposes; to allow clamping in large diameter boreholes, and to provide a fail-safe release mechanism. The contact shoe can be sheared off with a longitudinal pull of 600 lbs. The shearable portion of the locking shoe is attached to the receiver with a short cable. Thus, when the shoe is sheared, the broken piece swings below the receiver module and is retrieved when the array is brought uphole.

II.2.b Seismic Sensors

Either OYO Geospace SMC-1850 high temperature geophones or Wilcoxon 731-20HT accelerometers can be used as the sensors. The sensors are configured in a triaxial arrangement. The H1 sensor is oriented in the direction of the locking arm travel. The H2 sensor is oriented perpendicular to the direction of the locking arm travel. The third sensor is oriented longitudinally with respect to the receiver, and is referred to as the vertical component, V. OYO Geospace provides identical triaxial sensor packages for both accelerometers and geophones, so one sensor type can quickly be replaced by the other if desired. Referring to Section I.5.d, it is important to note that the accelerometers are preferred over the geophones when recording seismic data above 200 Hz. Thus, geophones would generally be used for ordinary VSP surveys, and the accelerometers would generally be used for high resolution VSP and CHSP surveys. However, the current accelerometers are limited to temperatures below 170°C, so geophones should be utilized for all extreme temperature applications.

FIGURE II.2 Field Applications of MLSR

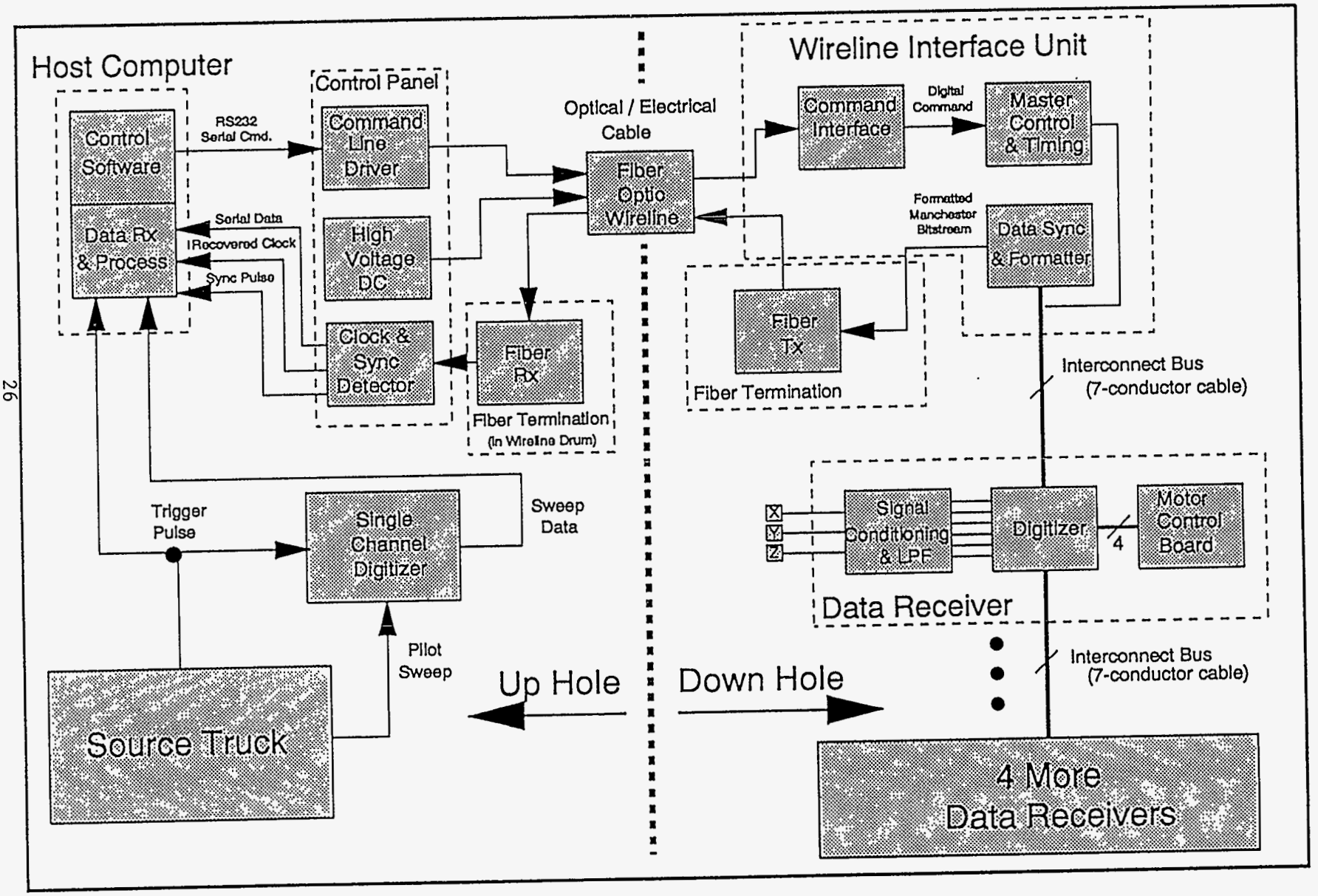

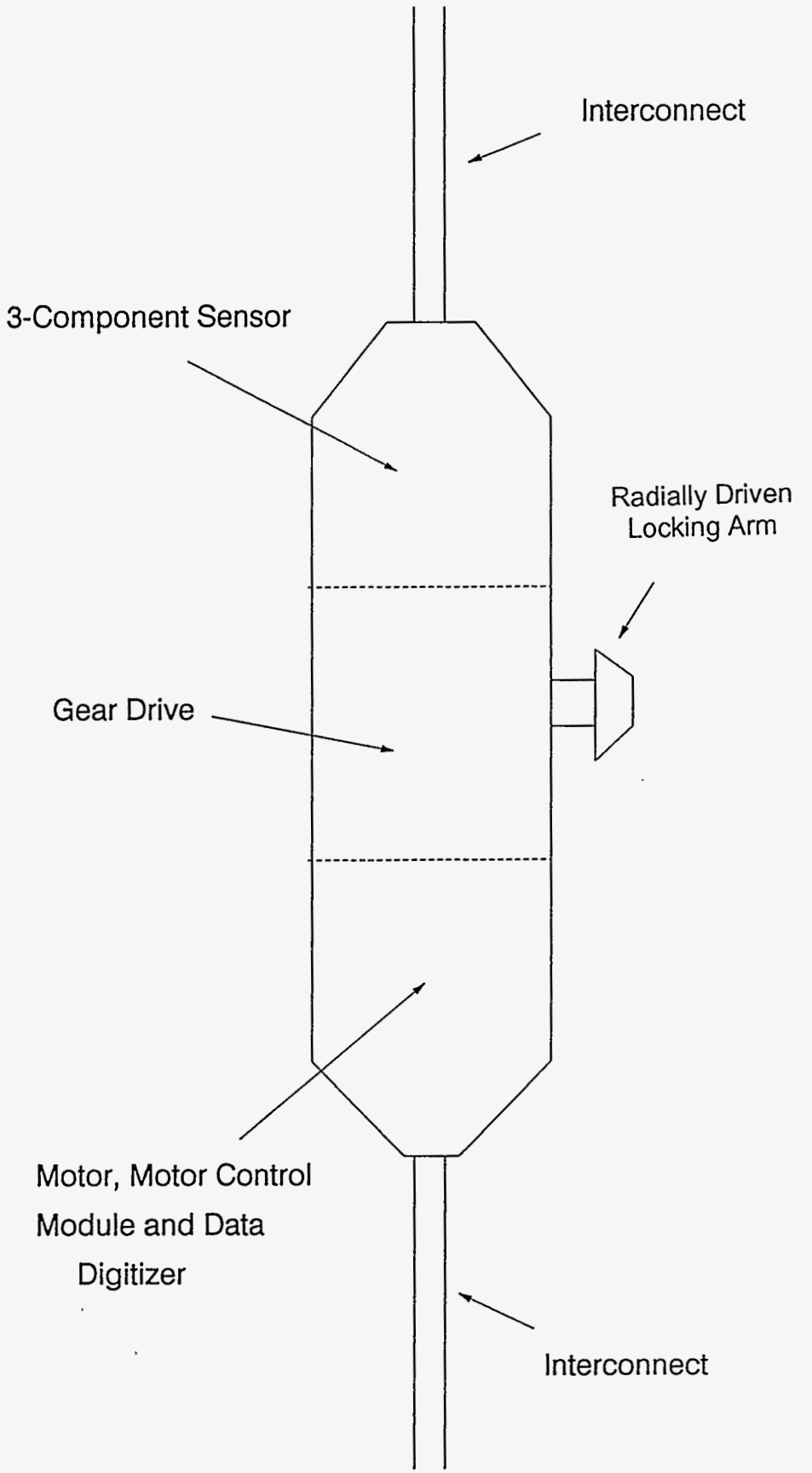

Figure II.3 - The basic features of the Borehole Receiver Module

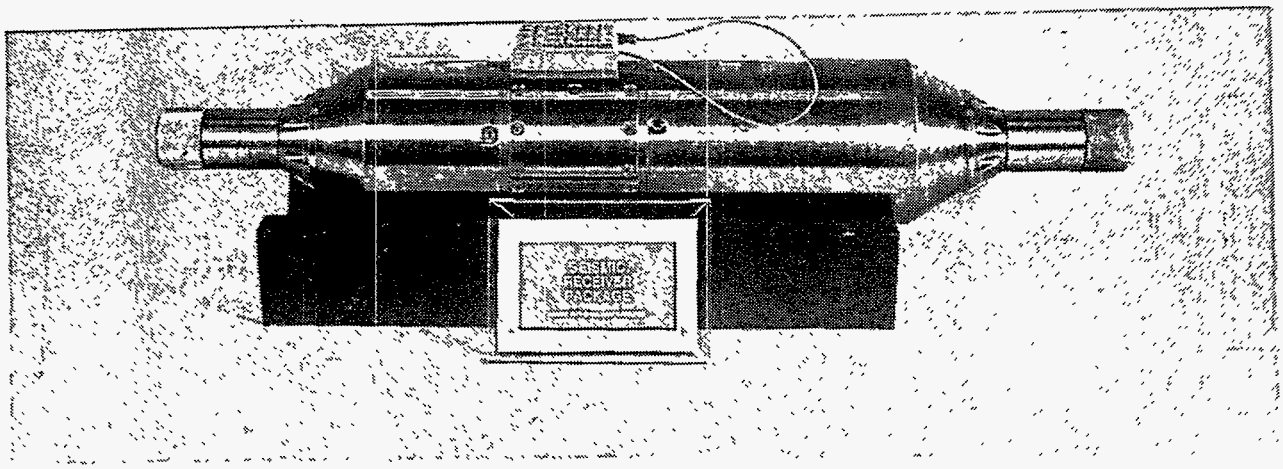

Figure II.4 Photo of the Seismic Receiver Module

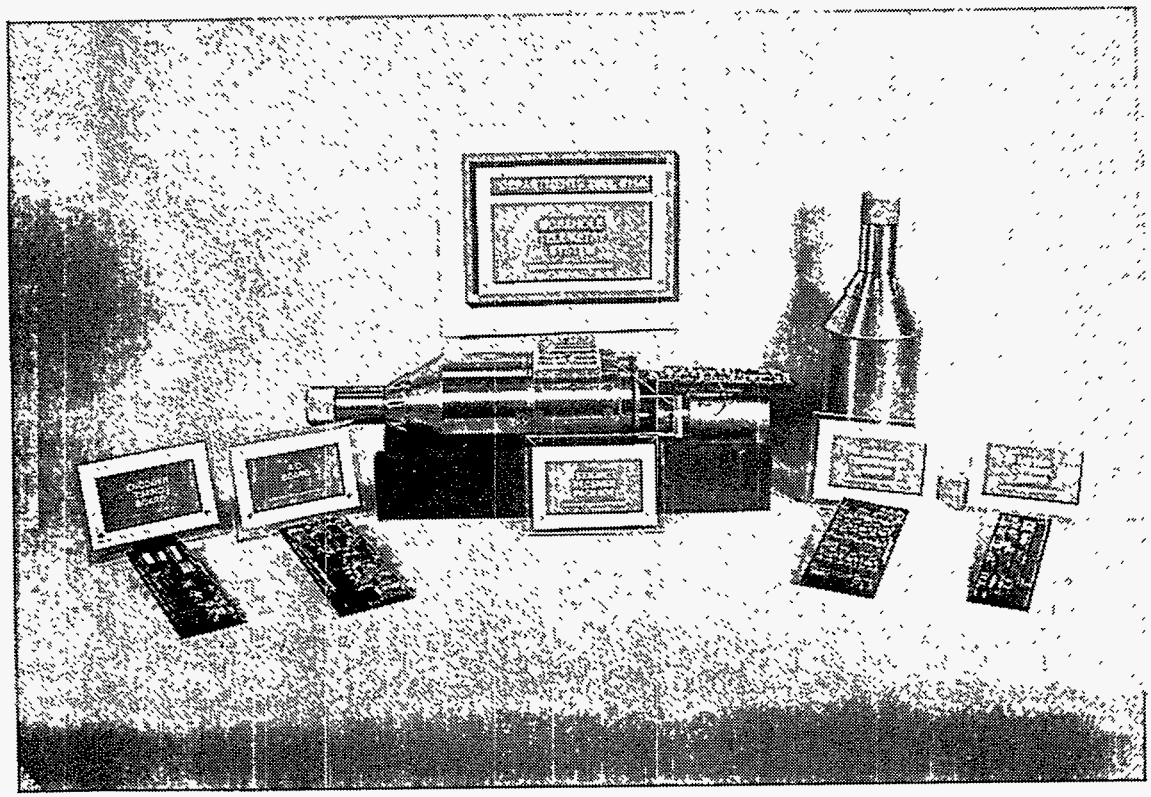

Figure II.5 Data Receiver Electronics

II.2.c Receiver Electronics

The electronics contained within each seismic receiver can be identified in the lower right of Figure II.2. A seismic receiver with the electronics installed is referred to as a Data Receiver. A photograph of the Data Receiver electronics is shown in Figure II.5. Each of the Data Receivers includes three channels of signal conditioning and a three channel digitizer to allow processing of a three axis acceleration measurement. Also included in each of the Data Receiver packages is a motor control circuit which decodes a digital control signal, allowing each clamp motor to be individually addressed. The five Data Receivers are interconnected with standard multi-conductor electrical cables which serve as a parallel interconnect bus. The data and clock from all receivers share two common wires in the bus. The receivers share these lines in a time multiplexed fashion, with the inactive receivers tristated. Note, that this parallel bus architecture allows operation of the system with any number of receivers connected. Also, any combination of receivers may be connected (For instance one could operate Receivers #1, #3, #5 as a set.) The power, control and sampling strobe signals are shared by all five receivers.

II.2.d Interconnect Cables

If five or fewer Data Receivers are used in the array, the receiver interconnects can be constructed with standard 7-conductor wireline using Gearhart Owens connectors, as illustrated in Figure II.6. The use of 7-conductor interconnects limits the separation between receivers to 10 ft. If more than five receivers, or longer interconnects are desired, the interconnects must be fabricated using twisted wire pairs to accommodate the large data bandwidth.

Interconnects are constructed so that the lower end connection is weaker than the top connection. If the array must be forcibly removed from the well, this feature ensures that the minimum amount of equipment is left in the well.

II.2.e Data Formatter

The Data Formatter is housed in the Wireline Interface Unit, as illustrated in Figure II.7, and connects immediately above the top Data Receiver. This function is identified as the "Data Sync and Formatter" block in Figure II.2. The primary function of the Data Formatter is to convert the time multiplexed, "bursted" data from the interconnect bus into a continuously clocked, formatted data stream for transmission on the optical fiber to the surface. This requires buffering the bursted data from the interconnect bus and injecting error codes and sync words to formulate a continuous serial bitstream. The Data Formatter also provides a Manchester encoder and line driver to interface to the fiber optic transmitter. The Manchester code is used to allow recovery of the clock from the data signal, so that a separate fiber is not required to transmit the clock.

II.2.f Data Transmission Link

The Data Transmission Link includes the "Fiber Tx, Fiber Optic Wireline, and Fiber Rx" blocks from Figure II.2. In the current configuration this Transmission Link resides in a wireline truck system provided by Chevron, as illustrated in Figure II.8. The top end of the Wireline Interface package (including the Data Formatter) is connected electrically to the fiber optic drivers which are housed in a cylindrical package which terminates the down hole end of the Fiber Optic Wireline. The fiber optic receivers at the up hole end of the Fiber Optic Wireline convert the optical signal back into the electrical Manchester coded signal. Circuitry in the Control Panel recovers the clock and data from the Manchester code and drives the Host Computer serial inputs (Figure II.2).

The Control Panel also provides data synchronization functions. Frame synchronization is provided by a fixed, 16-bit sync code, which marks the MSB of the first word of each frame. This detected sync pattern provides a top of frame strobe to the Host Computer. This frame strobe can also be used to synchronize down hole data to pilot sweeps or data from other sources.

II.2.g Command Link

The Command Link includes the "Command Interface" block in the Wireline Interface Unit (on the down hole end of the wireline) and terminates to the "Command Line Driver" on the up hole side. This link is a simple RS232 serial control feature which operates at low frequency (150 baud) over copper conductors in the fiber optic wireline. Commands implemented in the link include motor control, digital initialization, and calibration functions. The host computer transmits the desired command and detects the echo from the down hole command receiver. If the echo matches the transmitted command, a verify code is transmitted down hole to permit the command to be executed. If no verify code is sent, the command is not executed. This simple handshake scheme allows high reliability in the Command Link. This is critical in our application since it controls motor clamping.

II.2.h Surface Recorder

The surface recording system is built around a ruggedized OYO Geospace DFM-480 digital field monitor, and is shown in Figure II.9. The DFM-480 is a PC-compatible 80486 computer. It has a special interface board which contains a high speed digital signal processor (DSP) and a large memory buffer. The DSP receives the seismic data through its high speed synchronous serial port. The DSP performs several real-time operations on the seismic data stream. The real-time data stream can undergo the following real-time operations; gain and offset calibrations, IFP computation (converts two 16 bit words to a 21 bit seismic word), stacking, filtering, and storage to mass memory. Once the seismic data is in mass memory, the 486 processor takes control of the data and various functions can be performed; wiggle trace display on the CRT and thermal plotter, permanent storage on hard disk or 9-track tape, cross-correlation, and a variety of Q/A routines such as FFT, noise monitors, and AGC.

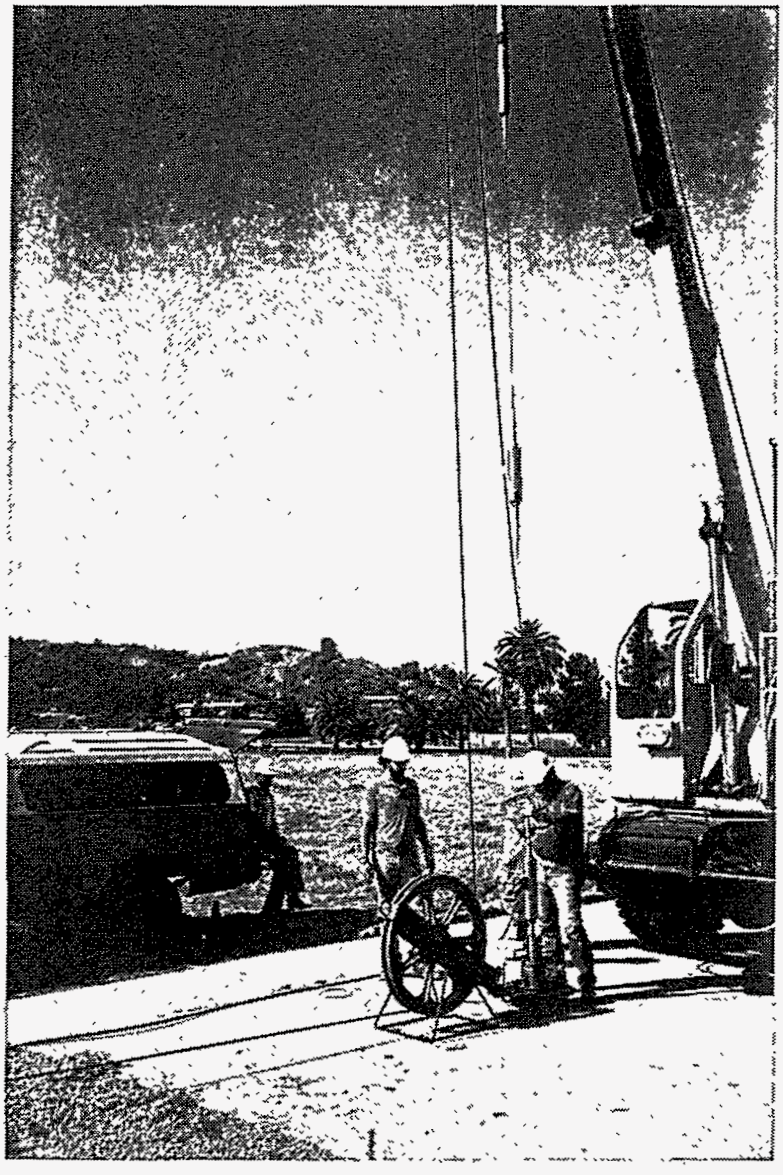

Figure II.6 Photo of MLSR showing inter-connected Data Receivers.

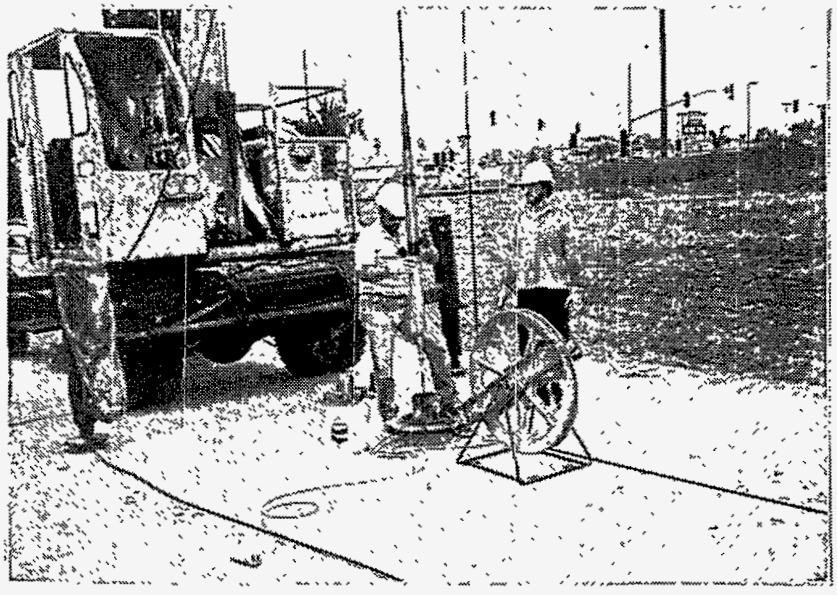

Figure II.7 Wireline Interface Unit

Figure II.8 Truck which houses the fiber optic wireline and Borehole Data Acquisition System.

a)

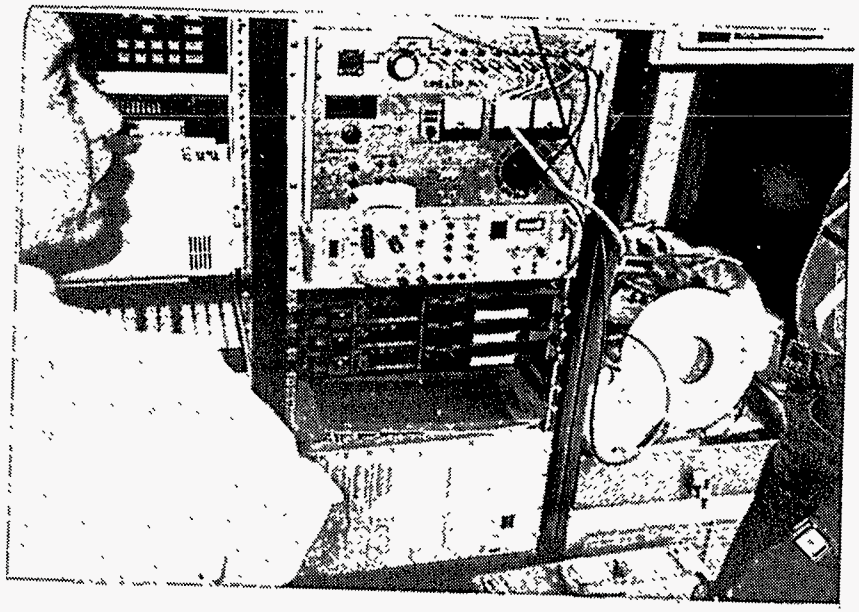

b)

Figure II.9 a) **DFM-480 computer serves as Borehole Data Data Acquisition System (BHDAS).**

b) **Control panel which interfaces BHDAS to the fiber optic wireline.**

II.2.i Field Processing

The BHDAS can store the seismic data on a variety of different media in a variety of formats. Data formats include SEG-D, SEG-Y, SEG-2, MICROMAX, and Binary formats. Media include 9-track tape, 4-mm tape, hard disk, floppy disk, and file transmission over Ethernet. The recorded data can be processed off line by any standard seismic processing system. Additionally, the data can be processed immediately on the DFM-480. Any seismic processing software that runs on a 486 computer can run on the DFM-480. The DFM-480 is typically packaged with the MICROMAX field processing software, enabling rapid on-line processing of field data.

II.2.j Single Receiver Analog Option

The above paragraphs have been couched in terms of the multi-level configuration of the seismic receiver system. It is possible, however, to operate a single seismic receiver as a stand-alone unit. In this configuration, as illustrated in Figure II.10, only one seismic receiver is placed downhole. No electronics are placed in the receiver module. The receiver is connected to a standard 7-conductor wireline using a standard Gearhart Owens connector. Six of the seven wires are connected directly to the accelerometers. The analog accelerometer signals are carried directly over the long wireline. Each accelerometer requires two wires for proper operation. The seventh wire in the wireline is connected to the d.c. clamp motor, with motor ground connected to the armor of the cable. The uphole configuration is quite simple; amplifiers/power supplies are used to condition the accelerometer signals, and the signals are fed into a standard surface seismograph. A control panel is used to deliver the d.c. power to the motor.

II.3. SYSTEM SPECIFICATIONS

This section presents the specifications of the MLSR which are of most importance to future users of this technology. Due to the complexity of the subsystems, only the most important specifications are compiled here. More detailed specifications can be found in later chapters.

Figure II.10 Operation of a single receiver in analog mode.

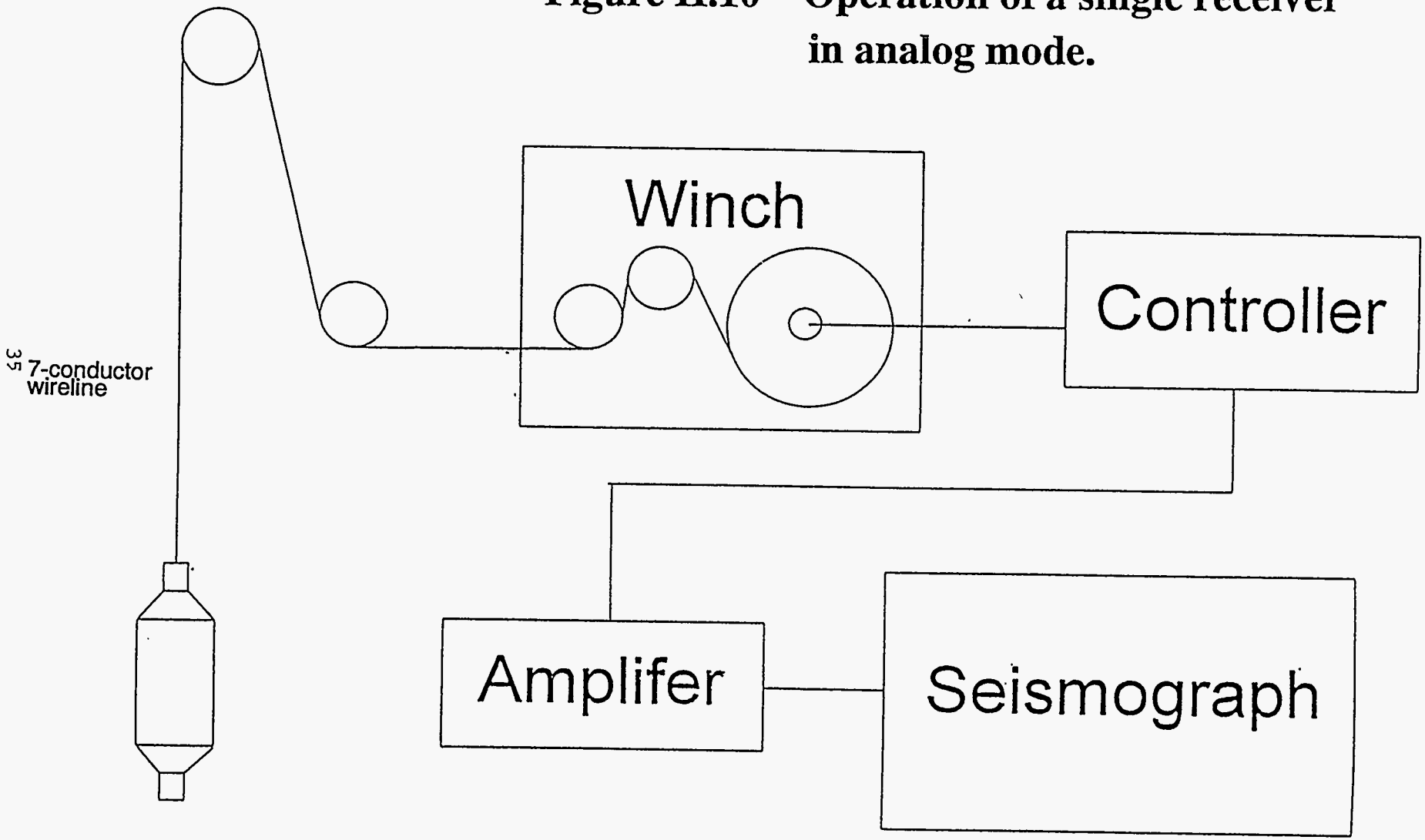

TABLE II.1. Mechanical/Environmental Specifications

Receiver Module		
Length	-	17 in
Diameter	-	4 in
Weight	-	35 lbs
Clamp force-to-weight ratio	-	5:1 to 20:1 (selectable)
Well Diameter	-	4.25 - 9 in
Working pressure limit	-	10,000 psi
Working Temperature limit	-	130°C (demonstrated)
	-	200°C (targeted)
First Resonance - Free Body	-	2400 Hz
First Resonance - Clamped	-	Above 1000 Hz
Wireline Interface Unit		
Length	-	30 in
Diameter	-	3.5 in
Weight	-	40 lbs
Working Pressure limit	-	10,000 psi
Working Temperature limit	-	130°C (demonstrated)
		200°C (targeted)
Fiber Optic Wireline Head (Chevron Version)		
Length	-	36 in
Diameter	-	3.5 in
Weight	-	30 lbs
Working Pressure Limit	-	10,000 psi
Working Temperature Limit	-	125°C
Fiber Optic Wireline (Chevron Version)		
Length	-	7000 ft
Diameter	-	15/32 in
Working Pressure Limit	-	10,000 psi
Working Temperature Limit	-	150°C

Table II.2. Data Acquisition Specifications

Downhole Sample Rate	-	1/8 ms
Downhole Low pass filter	-	3000 Hz (9 pole)
Downhole Hi pass filter	-	8 Hz (1 pole)
Downhole Pre-amp	-	0 to 40 dB,jumper select
Recorded Sample Rate	-	1/8 - 2 ms, soft select
Digital Anti-alias filter	-	yes
Record Length	-	1/8 - 16 s, soft select
Gain Ranging	-	2-stage IFP
Seismic Word Resolution	-	21 bits
Dynamic Range	-	114 dB (demonstrated)
System Seismic Bandwidth	-	10 - 1500 Hz (demonstrated)

III. SEISMIC SENSOR SUB-SYSTEM

This chapter provides the technical details on the sensor sub-system implemented in the Multi-Level Seismic Receiver (MLSR). Due to the high-resolution requirements of cross-well seismic imaging, new seismic sensor methods were investigated and implemented. This chapter details the design criteria and performance for the high resolution seismic sensor.

III.1. INTRODUCTION TO SENSOR SUBSYSTEM

An extensive study was undertaken to determine the optimal 3-component seismic sensor for cross-well surveys. This study involved the theoretical and experimental comparison between conventional geophones and low-noise piezo-electric accelerometers. Performance criteria included; frequency response, dynamic range, noise-floor, spurious response, and high-temperature behavior. It was found that properly designed accelerometers offer several significant advantages over geophones when used in the cross-well configuration. This chapter illustrates how accelerometers can be used to improve signal-to-noise ratios at frequencies above 100 Hz. Furthermore, accelerometers have the advantage that they do not require gimbal mounts, and they do not exhibit spurious resonances. At present, however, the charge amplifiers required for the piezo-electric accelerometers limit their operation to about 170°C.

III.2. SENSOR REQUIREMENTS

The objective of this study was to determine if it was possible to develop a sensor that exceeded the performance specifications of conventional geophones when used in the cross-well configuration. The incentive for this development program was that geophone sensors were developed for low-frequency surface seismic applications and were probably not optimally suited for the higher-frequency cross-well applications. Therefore, the following general requirements were set forth in the development of a new seismic sensor:

- flat frequency response from 10 Hz to at least 1000 Hz.

- absence of any spurious resonances or phase distortions from 10 Hz - 1000 Hz

- self noise that is comparable to or below the typical ambient seismic noise from 50Hz to 1000Hz
- the ability to mount without a gimbal assembly (i.e. sensor mounts/operates in any orientation)

- a size that is compatible or smaller than conventional geophones

- the ability to operate at temperatures up to at least 150°C, but preferably up to 200°C.

- be lightweight, yet rugged enough to suit the borehole environment.

In order to achieve these objectives, an engineering evaluation and design process was undertaken. Initially, a large number of commercially-available geophones and accelerometers were evaluated in terms of their performance. The evaluation established those technologies which could potentially

meet the cross-well requirements. It was determined that low-noise accelerometers offered significant improvements over conventional geophones when used in cross-well applications. At that point, a detailed set of design specifications were generated for the optimum seismic accelerometer. These specifications were developed into a Request For Quotation (RFQ) and commercial vendors were solicited to partner with Sandia and manufacture a custom accelerometer to the desired specifications. The result was a novel accelerometer that is now commercially available from Wilcoxon Research Inc.

III.3. SENSOR EVALUATION STUDY

A study was undertaken to evaluate the performance differences between conventional geophones and advanced piezo-electric accelerometers. For this study, both experimental and theoretical comparisons were made. Experimental studies were based on the following criteria; frequency response, sensitivity, noise floor, cross-axis sensitivity and linearity. Theoretical studies concentrated on noise floor, sensitivity, and frequency response performance. A summary of these studies is presented in the following sub-sections.

III.3.a Frequency Response

A fundamental relationship worth stating is that an accelerometer provides a voltage which is proportional to the vibrational acceleration of its base, while a geophone provides a voltage which is proportional to the vibrational velocity of its base. Therefore, although both accelerometers and geophones measure vibrational energy, the resulting signals are not the same. The relationship between the two sensors is easily computed from simple calculus. If one assumes sensors that have flat frequency response in their measurement domain, then accelerometers and geophones can be related from the following equation:

$$A(t) = dV(t)/dt \qquad \text{(III.1)}$$

where A(t) is the accelerometer output signal and V(t) is the geophone output signal. Hence, the accelerometer signal is simply the time-derivative of the geophone signal. Equation III.1 can be expressed in the frequency domain by applying well known Fourier-transform identities:

$$A(f) = 2*pi*f*V(f) \qquad \text{(III.2)}$$

In other words, the frequency spectrum of the accelerometer is equivalent to the frequency spectrum of the geophone, but increases in proportion to frequency. This means that the accelerometer tends to amplify high-frequency components of vibrational energy when compared to a geophone. To illustrate this point, Figure III.1 plots the theoretical sensitivity of accelerometers compared with geophones. This figure illustrates how accelerometers accentuate higher frequencies. Figure III.1, however, can be misleading to the novice. It may appear at first that a high sensitivity accelerometer (e.g. 10 volts/g) can be used which would be more sensitive than geophones. This was a common misunderstanding applied by early scientists when attempting to substitute accelerometers for geophones.

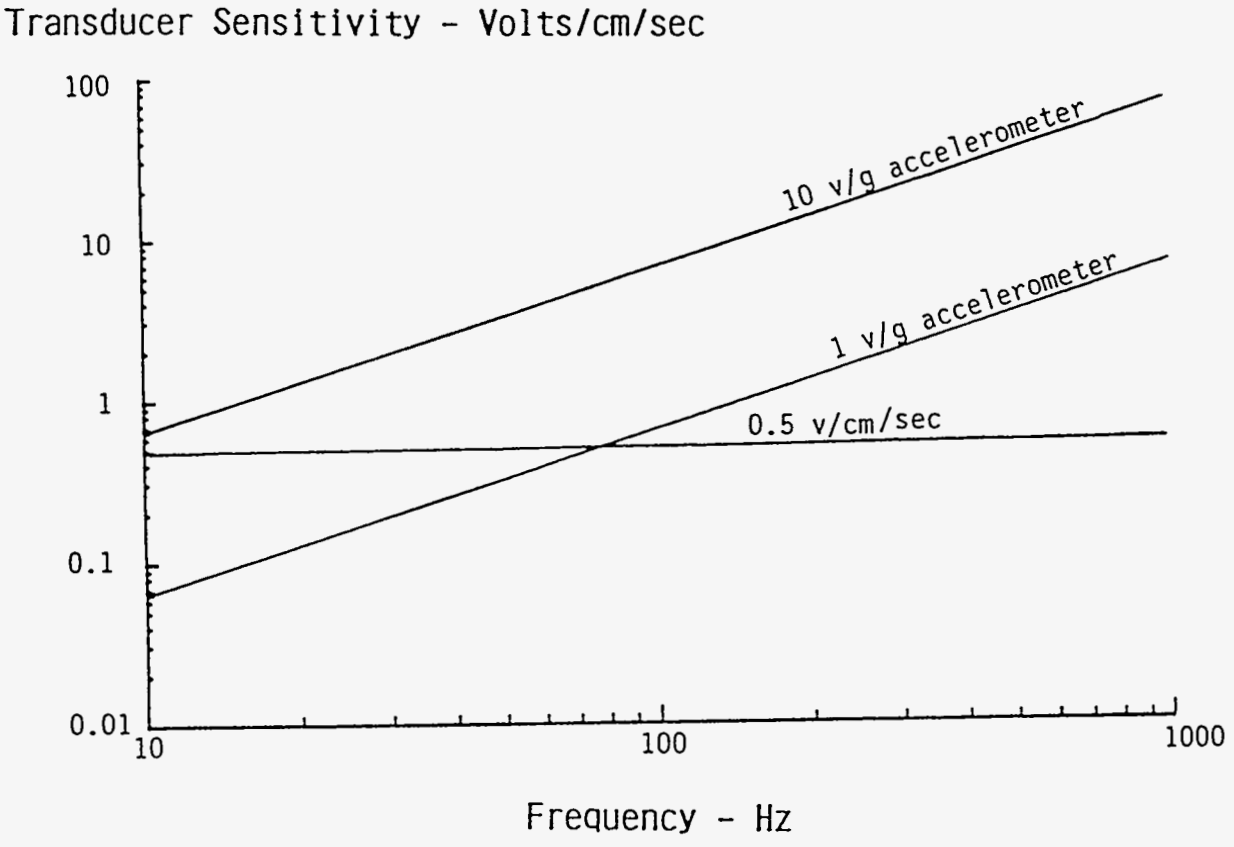

Figure III.1 Theoretical sensitivity of various vibration transducers.

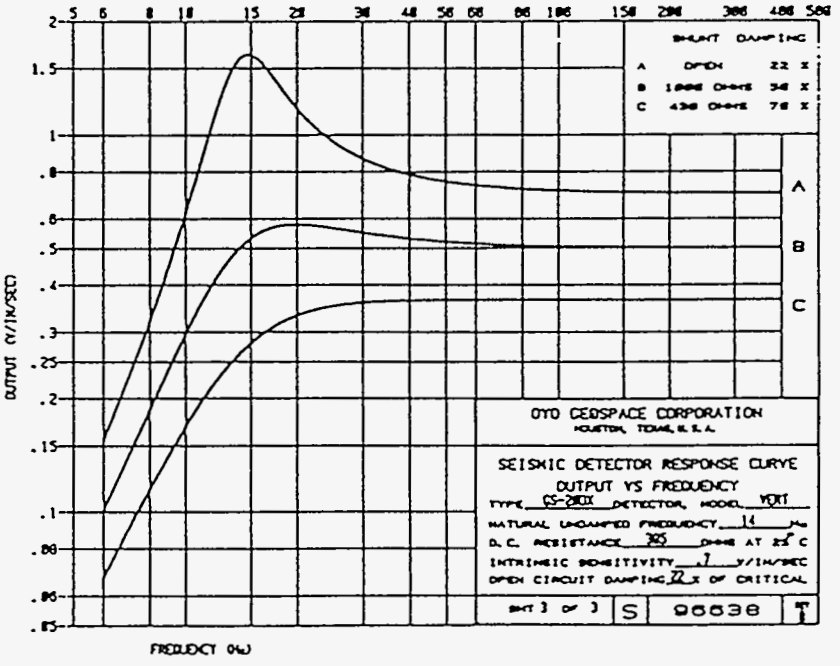

Figure III.2 Typical Geophone Frequency Response

IT MUST BE REMEMBERED THAT THE RATED SENSITIVITY OF A SENSOR IS ONLY A MEASURE OF ITS AMPLIFICATION FACTOR AND NOT ITS ABSOLUTE DETECTABILITY.

Absolute detectability is determined solely by noise floor and not rated sensitivity, as will be illustrated in a later subsection.

Figure III.2 plots the frequency response of a typical geophone, as used for conventional seismic measurements. Note that the velocity output is essentially constant as a function of frequency. The geophone does show a pronounced departure from ideal at its resonant frequency (e.g. 14 Hz). Both amplitude and phase distortions occur around the resonant frequency, so that reliable measurements are made only at frequencies well above the resonant frequency.

Figure III.3 plots the frequency response of the accelerometer developed under this program for cross-well seismic measurements. Note that the acceleration output is essentially constant as a function of frequency. The accelerometer, however, has a resonance that is around 2200 Hz. This means that the accelerometer provides accurate measurements at frequencies below its resonance. In practice, the accelerometer provides a nominally flat response from 1 Hz up to about 1250 Hz. This bandwidth exceeds that of the geophone. Furthermore, since the accelerometer accentuates high frequencies, it is particularly useful for amplifying weaker high-frequency energy. These issues will be illustrated in field data provided in subsequent chapters.

III.3.b Cross-Axis Sensitivity

An important attribute of a seismic sensor is cross-axis sensitivity. Cross-axis sensitivity is defined as the output voltage that occurs when the sensor is mechanically excited in a direction orthogonal to its sensitive axis. Cross axis sensitivity is usually expressed as a percentage of on-axis output under the same excitation. All sensors exhibit some degree of off-axis sensitivity due to both mechanical misalignment of the sensor elements, and off-axis resonant modes. For the geophone, off-axis spring modes usually occur at a frequency that is between 15-25 times the on-axis resonance. For example, a 14 Hz geophone would typically have an off-axis resonant mode in the 200-400 Hz range. Accelerometers, because of their high on-axis resonant frequency, generally do not exhibit off-axis modes in the measurement band. Therefore, the off-axis sensitivity of accelerometers is due almost exclusively to mechanical misalignments within the sensor housing.

Figure III.4 plots the measured off axis sensitivity for three commercially available seismic sensors. The "14 Hz Geophone" utilized in this test was an extremely low-cost unit which lacked published specifications for off-axis sensitivity. It is obvious from Figure 4 that this 14 Hz geophone has unacceptable off-axis response (up to 45% at 150 Hz). This sensor would be totally unacceptable for cross-well measurements, and illustrates the importance of cross-axis sensitivity specifications. Also shown in Figure 4 is the results from a high quality 28 Hz geophone. This sensor has less severe off-axis sensitivity (less than 15% at 400 Hz), but would still cause significant errors in 3-component measurements.

Figure III.3 Resonant frequency for typical unamplified 731-20 accelerometers at various temperatures.

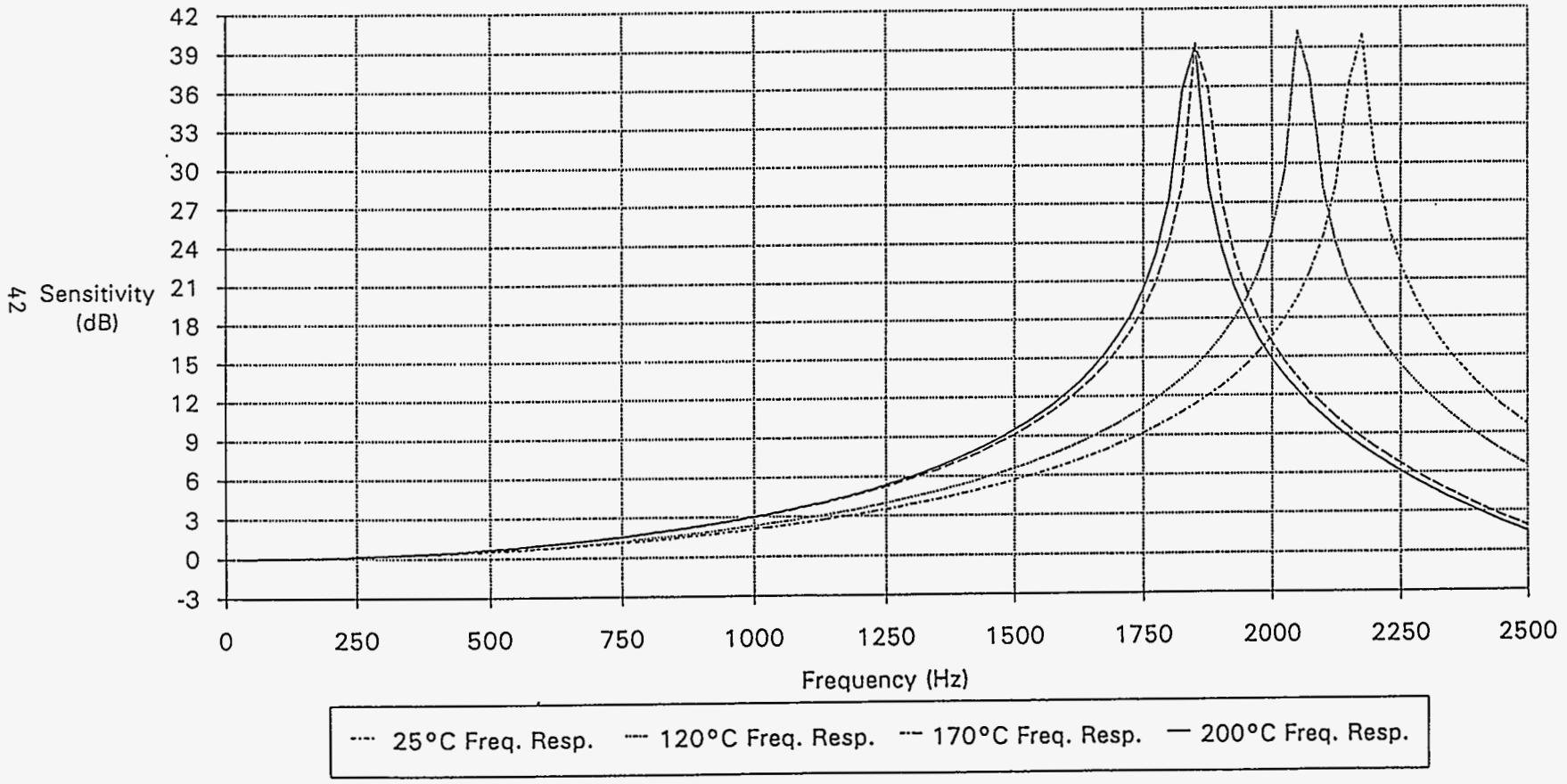

Figure III.4

Cross-Axis Sensitivity Data

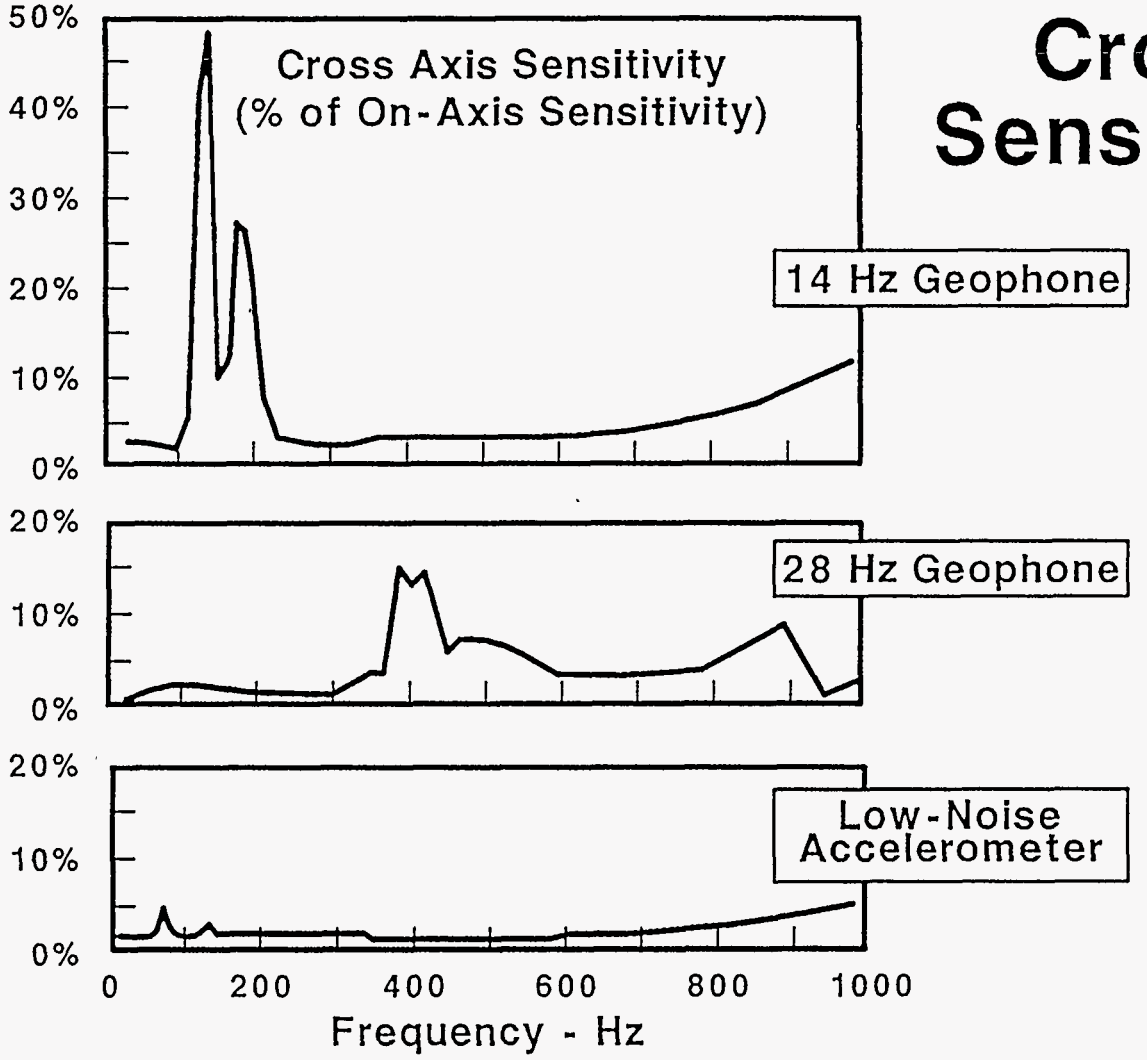

Figure 4 also shows the measured off-axis sensitivity for a low noise accelerometer (the Wilcoxon Model 731-200 was used for the measurements). This sensor is rated to have an off-axis sensitivity of less than 5%, and is confirmed by the data. Furthermore, the off-axis sensitivity curve does not exhibit spurious resonance modes, which enables a clean frequency response throughout the cross-well seismic frequency range.

III.3.c Seismic Noise Floor

An extremely important criteria for selecting a seismic sensor is a measure of its electronic noise floor. The electronic noise floor limits the minimum seismic vibration that can be detected. It is important that the electronic noise floor of the sensor be below the expected ambient seismic noise. When this is the case, the weakest seismic events can still be detected. Electronic noise floors are determined by both the electrical characteristics of the sensor element and the electrical characteristics of the pre-amplifier connected to the sensor element. An electrical model for a geophone is shown in Figure III.5. Also shown in Figure III.5 is the theoretical relationship for the electronic noise floor. At low frequencies, the geophone is purely a resistive device. As such, it is possible in practice to select very low-noise bipolar-polar op-amps such that the electronic noise is limited only by the thermal noise of the coil resistance (sqrt(4kTR)/G). Unfortunately, the physics of the geophone are such that for a given size coil, decreasing the coil resistance results in decreased sensitivity. Hence, the geophones on the market have pushed the theoretical limits of the design and have a finite thermal electronic noise. The geophone noise model also indicates that at relatively low frequencies, the noise floor is independent of frequency. For practical geophones, this flat noise relationship ("white noise") is valid for frequencies below about 2000 Hz.

An electrical model for piezo-electric accelerometers is shown in Figure III.6. Also shown in Figure 6 is the theoretical relationship for the electronic noise floor for these sensors. Note that the piezo-electric device is a high-impedance, reactive component. As such, its noise floor is very much affected by the amplifier to which it is connected. Bi-polar amplifiers are inappropriate for use with accelerometers since they have high current noise. JFET amplifiers are preferred, but must be carefully designed to avoid low-frequency "1/f" noise. Therefore, the technique for developing an extremely low-noise accelerometer is as follows:

1.) maximize the transduction efficiency of the transducer. This is performed by lowering the resonant frequency as much as possible and using mechanical amplification (e.g. cantilevered-mass designs).

2.) optimize the amplifier/crystal design such that the piezo-electric crystal and the amplifier are "noise matched". This requires a thorough understanding of JFET amplifier design techniques.

In order to verify the sensor noise models, it was essential to evaluate the noise floor of existing commercial sensors. There are two methods for measuring the noise floor of seismic sensors. The first method, known as element-simulation, requires that the active sensing element be disconnected from the amplifier and replaced by its equivalent impedance circuit. Typically, the coil of the

geophone would be replaced by a fixed resistor and the piezo-electric crystal would be replaced by a fixed capacitor. The element-substitution method has been found to give experimental results consistent with the theoretical models.

The second sensor noise measurement approach is called absolute-measurement. This technique, although experimentally difficult, can provide true measurements of absolute detectability of the seismic sensors. The absolute-measurement approach also helps confirm the validity of the element-simulation method for routine sensor noise-floor checks.

Figure III.7 shows an experimental facility developed for absolute measurement of seismic noise floors. The apparatus isolates the sensor from mechanical and acoustic stimulus. In other words, the sensor is placed in a seismically quiet chamber, and its noise floor is monitored.

In making absolute seismic noise floor measurements, it is important to understand the nature of ambient seismic noise that would be expected in boreholes. Prior to this study, there was no information in the literature on ambient seismic noise above 100 Hz. In Figure III.8, the ambient noise for boreholes is plotted for frequencies below 100 Hz (as obtained from references [III.1 and III.2]. The noise level labeled "typical" borehole noise is based on well data obtained from wells in industrial nations. The ultra-quiet borehole represents the lowest noise wells found in the world, and are far from industrial centers. Figure III.8 shows an extrapolation to frequencies above 100 Hz, and this was used as a nominal design goal for the new seismic sensor.

Figure III.9 plots absolute-measured noise floors for the lowest noise sensors that were commercially available at the time of this study. These measurements were obtained using the facility depicted in Figure III.7. Note that the measured geophone noise was lower than "typical" borehole noise below 150 Hz but was above this level at higher frequencies. On the other hand, the accelerometer noise floors tended to track the slope of the borehole noise curves. In particular, the 2500 Hz accelerometer (Wilcoxon Model 731-200) exhibited a noise floor that was fairly comparable to typical borehole noise. The 1000 Hz accelerometer (Wilcoxon Model 731) had a noise floor that was significantly below typical well noise. Unfortunately, the 1000 Hz accelerometer was unsuitable for borehole application since it was too large (2.5" diameter), had a low bandwidth (highest useable frequency was 700 Hz), and was too fragile (damage could occur at only 10 g's of shock).

Based on the study presented here, it was found that a piezo-electric accelerometer could have a lower self-noise than the conventional geophone. This attribute would enable accelerometers to provide improved signal-to-noise ratios when measuring seismic phenomena above approximately 100 Hz.

III.4. SUMMARY OF COMPARISON BETWEEN GEOPHONES AND ACCELEROMETERS

Based on the theoretical and experimental sensor study undertaken in this project, a formal comparison can be made between geophones and accelerometers. Table III.1 compares the features of geophones and accelerometers. This table shows that low-noise accelerometers are generally preferred over geophones for broadband (>1000 Hz) cross-well seismic work. Accelerometers offer lower noise floors, flatter frequency response, and improved 3-component response when compared to conventional geophones. For low frequency applications (<100 Hz), accelerometers offer no significant advantages over geophones, and the sensor choice would be a matter of preference. Furthermore, for very high-

Figure III.5

Noise Limits of Geophones

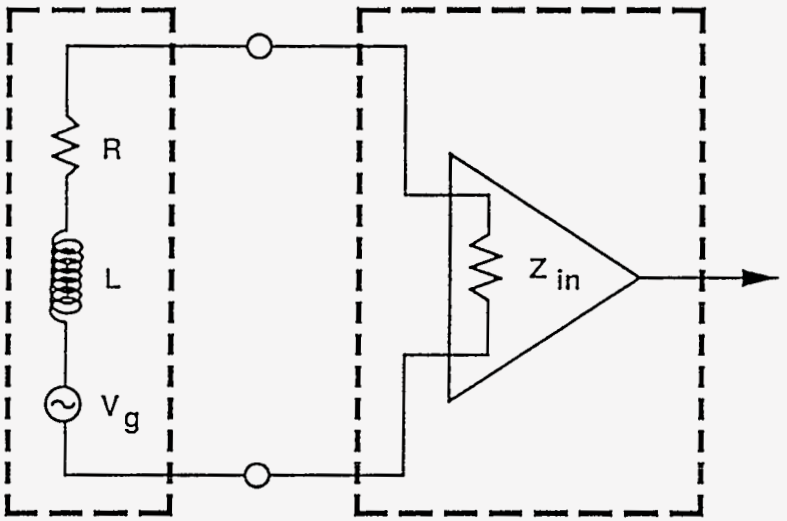

Velocity Noise

$$v_n = \frac{1}{G}\sqrt{e_n^2 + i_n^2(R^2+\omega^2 L^2) + 4\,kTR}$$

$(m/sec/\sqrt{Hz})$

e_n	=	Amplifier input voltage noise $(volts/\sqrt{Hz})$
i_n	=	Amplifier input current noise $(amps/\sqrt{Hz})$
G	=	Geophone transduction constant (volts/m/sec)
R, L	=	Geophone coil resistance and inductance
k	=	Boltzman's constant
T	=	Temperature (Kelvin)
ω	=	Radian frequency

NOTE: Most parameters depend on frequency and temperature

Figure III.6

Noise Limits of Piezo-Electric Accelerometers

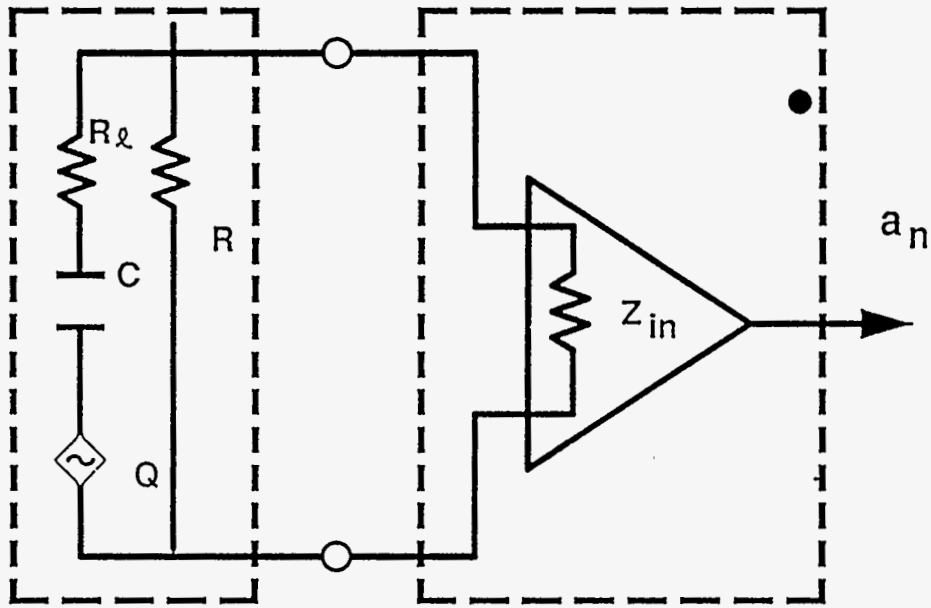

Accelerometer Noise Model

Low-Noise Amplifier

Accelerometer Noise

$$a_n = \frac{1}{Q}\sqrt{\frac{i_n^2}{\omega^2} + e_n^2 C^2 + \frac{4kTC\eta}{\omega}}$$

$(g/\sqrt{Hz})$

e_n, i_n = Amplifier input voltage noise and current noise
Q = Accelerometer crystal charge sensitivity (pC/g)
C = Accelerometer crystal capacitance
ω = Radian frequency
η = Loss Factor = $\omega R_\ell L$

NOTE: Most parameters function of frequency and temperature

Figure III.7

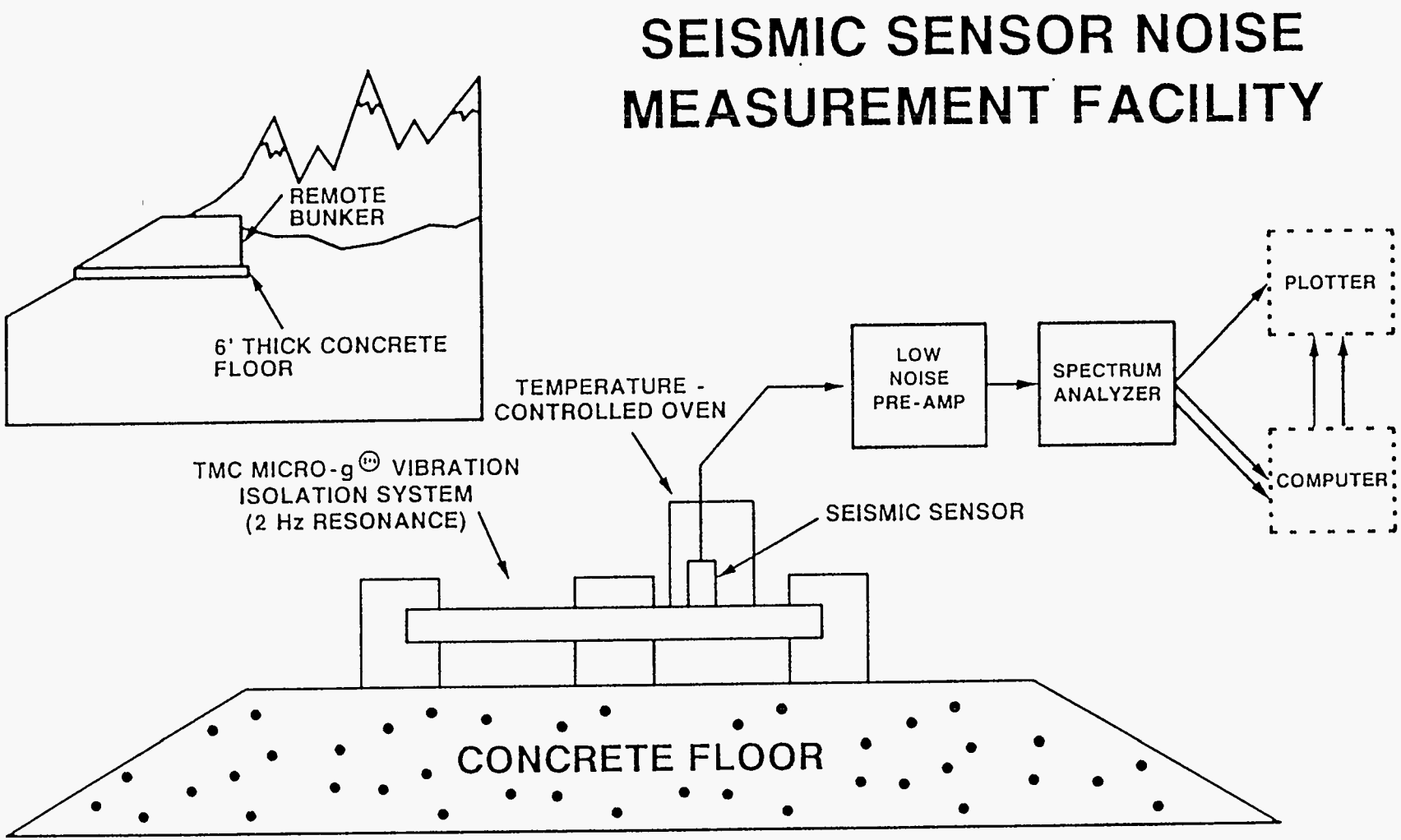
SEISMIC SENSOR NOISE
MEASUREMENT FACILITY
REMOTE
BUNKER
6' THICK CONCRETE
FLOOR
TEMPERATURE -
CONTROLLED OVEN
LOW
NOISE
PRE-AMP
SPECTRUM
ANALYZER
PLOTTER
COMPUTER
TMC MICRO-g VIBRATION
ISOLATION SYSTEM
(2 Hz RESONANCE)
SEISMIC SENSOR
CONCRETE FLOOR

temperature borehole applications, geophones would generally be preferred since the present technology accelerometer pre-amplifiers have not been demonstrated to operate at temperatures above 170° C.

III.5. ADVANCED ACCELEROMETER SPECIFICATIONS

Under this program, an advanced accelerometer was developed to meet the needs of high-resolution cross-well seismic imaging. The developed accelerometer is now commercially available from Wilcoxon Research as Model 731-20. This accelerometer is a significant advancement over its predecessor, the model 731-200. The improvements were made as a result of Sandia's recommendations and technical guidance. The major improvements are:

- reduction of seismic noise floor by at least 6 dB at all frequencies
- increase of operating temperature from 80° C to 125° C
- housing constrained to be case-isolated in a 1" diameter package
- quality control over performance such as cross-axis sensitivity and linearity.

A detailed specification sheet for the advanced accelerometer is shown in Figure III.10. The Model 731-20 has been fully implemented and tested in the Multi-Level Receiver System, and is considered the standard sensor for the commercially available system from OYO Geospace Corporation.

The original Model 731-20 accelerometer was limited in operation to temperatures below 125° C. Further development efforts resulted in a higher temperature version, and is referred to as Model 731-20HT. The Model 731-20HT operates at temperatures up to 170° C, but has approximately 3dB higher noise level than the 731-20. Detailed information on the Model 731-20HT can be obtained from the manufacturer.

Figure III.8

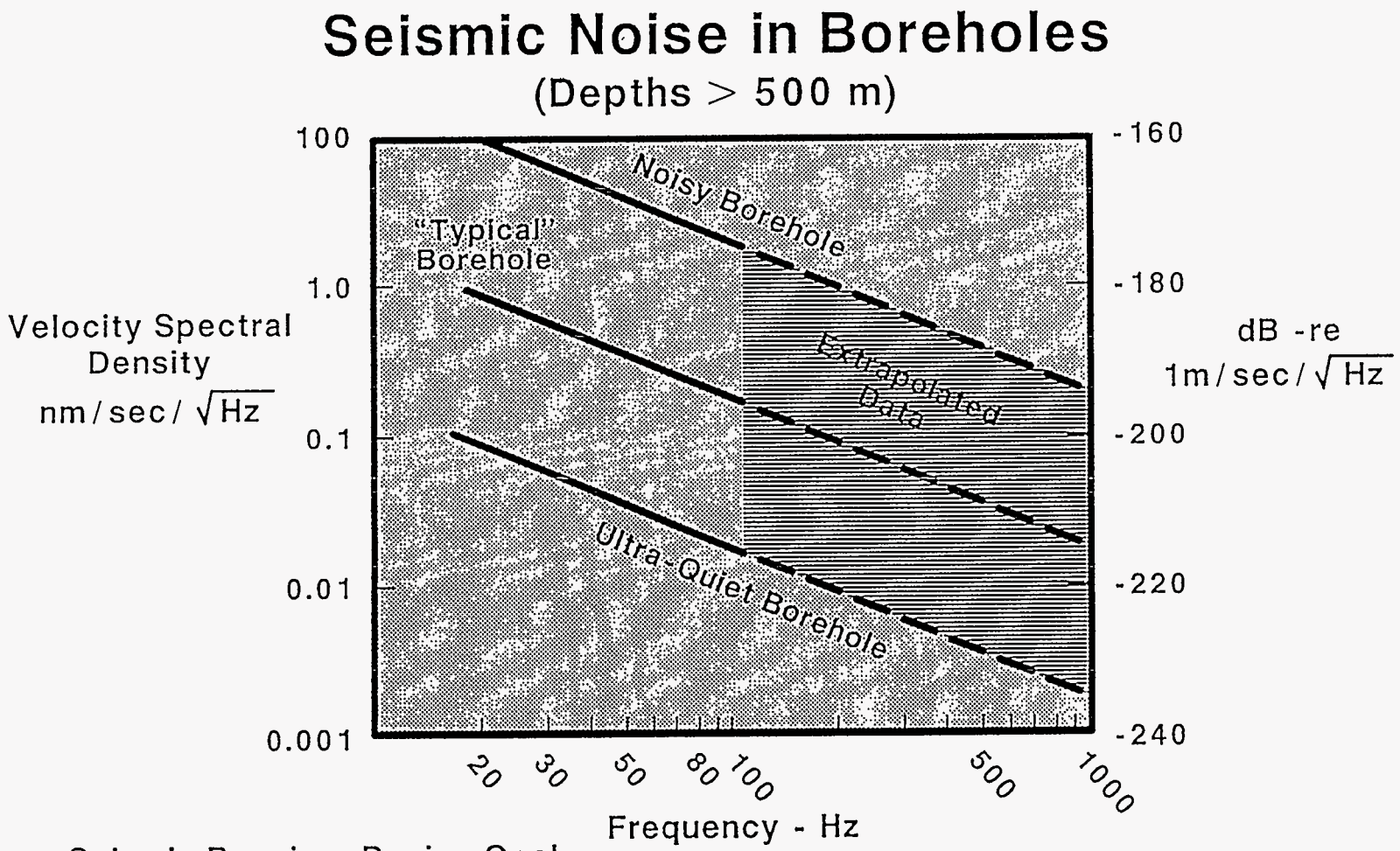

- Seismic Receiver Design Goal

  Receiver noise < "typical" borehole noise at all frequencies

Table III.1

SENSOR COMPARISON	GEOPHONE	ACCELEROMETER
NOMINALLY FLAT RESPONSE 20 Hz - 1500 Hz	YES	YES
FLAT PHASE	NO	YES
OFF - AXIS SENSITIVITY	CAN BE SIGNIFICANT	LOW (<4%)
REDUCED NOISE AT HIGH-FREQUENCIES (>200 Hz)	NO	YES
LINEARITY PROBLEMS	NO	NO
MOUNT IN ANY ORIENTATION	NO	YES
OPERATE AT 200°C	YES	PROBABLY
INSENSITIVE TO EMI	NO	GENERALLY, YES
SMALL, LIGHT WEIGHT	YES	YES

Figure III.9

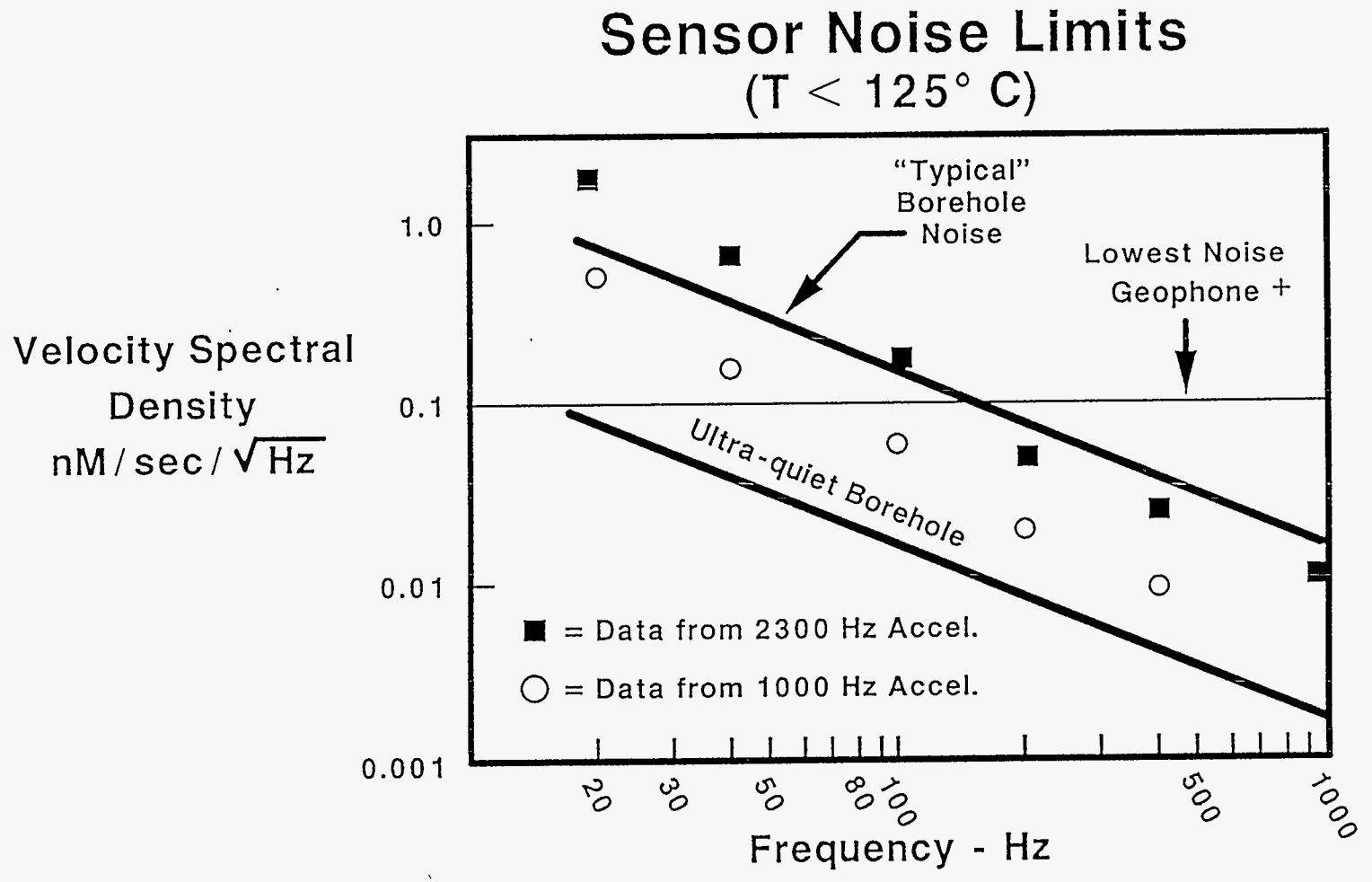

+ 0.5 V/cm/sec., 1 KΩ Geophone with OPA37HT High-temperature amplifier

WR New Product Data

Figure III.10

Seismic Accelerometer

Specifications @ 25 °C

DYNAMIC	
Sensitivity, ±10 %	20 V/g
Acceleration Range[1]	0.2 g peak
Amplitude Nonlinearity	1 %
Frequency Response:	
±5 %	1.5 - 400 Hz
±10 %	1.0 - 600 Hz
±3 dB	0.5 - 1000 Hz
Resonance Frequency, mounted	>2000 Hz
Transverse Sensitivity, max.	<2 % of axial
Temperature Response	TBD[2]
ELECTRICAL	
Power Requirement, voltage source	18 - 30 VDC
current regulating diode[3]	4 - 10 mA
Electrical Noise, equiv. g, nom	
Broadband, 2.0 Hz to 20 kHz	<1 µg
Spectral 20 Hz	-150 dB re g/√Hz
100 Hz	-158 dB re g/√Hz
1000 Hz	-163 dB re g/√Hz
Output Impedance, max.[3]	<1000 Ω
Bias Output Voltage	10 ±1 VDC
Grounding	case isolated
ENVIRONMENTAL	
Temperature Range	-40 to 120 °C
Vibration Limit	TBD[2]
Shock Limit	TBD[2]
Electromagnetic Sensitivity, equiv. g	TBD[2]
Base Strain Sensitivity	TBD[2]
PHYSICAL	
Weight	68.0 grams
Case Material	nickel plated aluminum
Mounting	adhesive
Connector	Microdot 10-32

NOTES: [1]Acceleration range decreases approximately 50 % at 120 °C.
[2]To Be Determined
[3]Current regulating diode may be reduced to 2 mA with a slight reduction in sensitivity and an increase in output impedance.

ACCESSORIES AVAILABLE: Cementing studs, power supplies, amplifiers, signal conditioners, cable assemblies.

Due to continued research and product development, Wilcoxon Research reserves the right to amend these specifications without notice.

Rev. 1 Wilcoxon Research, 2096 Gaither Road, Rockville MD 20850 • (301) 330-8811 • Fax: (301) 330-8873 5/90
Customer Service: 1-800-VIB-SENS

IV. CLAMPING PACKAGE SUB-SYSTEM

IV.1. INTRODUCTION

The present configuration of the Advanced Borehole Receiver consists of two pressure housings terminated with standard Gearhart-Owens seven conductor cable connectors, one on either end of a clamping assembly section. One housing contains the triaxially arranged accelerometers and the other the electric gearmotor. This gearmotor drives a rectangular piston perpendicular to the tool using a right angle translation unit to clamp the tool into the borehole. Since the right angle translation unit resides outside of the pressure housings, a high temperature and pressure rotary seal is used to insure integrity where the drive shaft breaches the gearmotor bulkhead.

Existing borehole receiver tools vary in the way in which they clamp into position from electro-mechanical scissor type to hydraulic piston arrangements. The clamp mechanism to be used in the Sandia/OYO MLSR was an area of primary concern due to size restriction, the wide frequency range requirement, and the desire to string several receivers together for use at one time. These requirements dictated that the clamp/motor subsystem be compact in size, powerful in nature, simple in operation and free of any resonant frequencies in the range of interest. Several concepts were considered, each of which had strengths and weaknesses. First, hydraulics can be powerful, compact clamp devices but require either a surface supply or a downhole reservoir. Also, the surface supply involves using hoses which are not easily deployed and the downhole reservoir will effect the frequency range of interest. The second possibility, a cantilevered arm clamp allows for the tool to be used in a wide range of casing sizes, but again there seems to be an effect on the frequency range. As a result an electro-mechanical clamp that involves an electric motor driving a piston normal from the axis of the receiver was decided upon. This clamp mechanism has the capability to supply sufficient clamp force while being compact in size. Analyses and design iterations of the prototype demonstrate that the MLSR system can operate through the frequency range of interest free of resonances.

IV.2. FINITE ELEMENT ANALYSIS OF EXISTING TECHNOLOGY

The borehole receiver tools presently being used within industry have a limited usable frequency range on the order of 0 - 350 Hz. Thus, before beginning the design of the MLSR, a survey of several tools routinely utilized in the field was performed. Information was collected which included the following; 1) overall tool weight, length and diameter, 2) general mechanical construction, 3) component layout, 4) the type of clamping mechanism used. The tools included in the survey turned out to have several things in common. All of the electro-mechanical tools were heavy, with a large length to width aspect ratio, and used either a scissor type or a cantilever arm clamp mechanism.

A finite element model was then constructed based upon this database in order to identify the factors which contribute to their limited frequency range. The model was constructed with beam elements which represent the various components of the tool and imitate their mechanical properties such as stiffness, mass and type of motion. Beams modeling the tool body are pinned appropriately to separate them from beam elements modeling the clamp mechanism. A 6 in. borehole was selected as the standard size to be used in all analyses. The only constraints applied to the model were vertical

movement within the borehole and either an increase or a decrease in the overall diameter of the model once it was clamped into position. This would allow for the worst case scenario such as rotation about a point on the clamp and yield the majority of the modes. Practical application could then be applied to prioritize the results.

The analysis determined the frequencies and the mode shapes of the model with the clamp pinned to the borehole wall, and also in the case of the main body of the tool pinned at either end to the wall. Kenneth Gwinn, 1524 [IV.1] conducted the analyses utilizing the finite element code Nastran [IV.2] with the mesh generation and plotting being performed by Patran [IV.3].

IV.2.a Modal Analysis Results

The results of the modal analysis are shown in Table IV.1 in which the modal frequencies below 1000 Hz are listed. The modes result from deformation of the model, however, the modes of practical importance are the modes that constitute motion at or near the sensor mount. Some of these modes will result in large motion at this location while others will produce little or no motion at all.

The first mode is caused by the bending of the main body of the tool and results in the frequency of 215 Hz. The second mode is orthogonal to the first and is found at 221 Hz. This mode is shifted slightly because the tool is nonsymmetric in stiffness due to the clamp mechanism.

The third mode which occurs at 269 Hz is due to the bending of the clamp assembly and should result in little motion at the sensor location.

The fourth and fifth mode which occur at 313 and 314 Hz. respectively are due to the second bending modes of the main tool body. The modes result in considerable motion at the sensor location.

The other modes are all due to deformation of the clamp assembly. Again little motion at the sensor is expected as a result of these modes.

An iteration of the analysis was then performed to determine if any change in the modes could be acquired by reasonably altering the sizes of the clamping components. Importantly, no change was observed in the first five modes since the main tool body properties dominate in this region, while above 350 Hz, deformation of the clamp assembly is all that is taking place.

Again, due to applied constraints no modes in the axial direction are produced. The modes in this direction would be controlled by the friction between the clamp and the borehole and the configuration of the clamp in contact with the borehole. Since the age of casing, the type of material that may be found on the casing and the geometry of clamping (i.e.. point versus line contact) may vary, the analysis was simplified.

Table IV.1. Modal Frequencies for General Receiver	
Mode #	Frequency (Hz)
1	215
2	221
3	269
4	313
5	314
6	397
7	460
8	592
9	620
10	842
11	990

IV.2.b Conclusions for General Receiver Analysis

The first modes encountered are the modes due to the bending of the main body of the receiver tool. These modes would also cause most of the motion at the sensor location utilized within this model. These modes must be changed in order to make measurements at higher frequencies. This can be accomplished by moving the sensor location away from high deformation areas, increasing the stiffness of the overall tool, and decreasing the mass of the receiver.

IV.3. FINITE ELEMENT ANALYSIS OF PROTOTYPE RECEIVER

Once the finite element analysis for the general receiver was completed the initial design for the MLSR borehole receiver was started. This design incorporated the conclusions of the previous analysis in order to eliminate modal frequencies from 0-2 KHz. This would be confirmed by repeating the finite element analysis after a preliminary design concept was laid out.

Keeping the receiver as short, as light and as stiff as possible should help eliminate many of the modal frequencies below 400 Hz. However, problems with modes associated with the lever arm clamp assembly still remained in the range of interest. Also, by utilizing a hydraulic clamp mechanism either a downhole hydraulic pump/motor built into the receiver or hoses run from the surface would need to be used. The pump/motor would add greatly to the complexity of the system and increase to the overall tool weight and length. The requirement of running hoses from a surface pump to the tool would increase the manpower and equipment necessary for operation and in the case of a multiple receiver array increase the cost of the interconnects and possibility of crosstalk within the system. It is important to note that the generation of a multiple array system was considered an intended outcome of the program, and the elimination of modes due to the interconnects themselves or from one receiver to another is necessary but not trivial. As a result the initial concept incorporated an electro-mechanical

clamp system in which an electric motor would drive out a rectangular piston perpendicularly from the longitudinal axis of the tool via a right-angle gearbox.

An electric motor with interchangeable gearing that would allow variation in the clamp force to tool weight ratio was chosen. The initial layout packaged the motor within one housing and placed the sensor mount within another housing to minimize the tool size and weight. These two housings would be placed on either side of the clamp mechanism in such a way as to keep the sensor mount as close as possible to the clamp and reduce motion at the sensor due modes elsewhere. A finite element analysis was done on this initial design to be sure that all modes would be removed from the frequency range of interest.

A drawing of the initial concept is shown in Figure IV.1. The cylindrical tool is composed of three sections separated by two bulkheads. The three sections are 1) the motor section, 2) the clamp section and 3) the sensor section. A piston driven by a threaded rod is used to make contact with the borehole casing. A motor extends and retracts the piston by turning the threaded rod through a ninety degree gearbox.

A finite element model of this concept was constructed in a similar manner as that utilized previously. A three dimensional model was used to allow as much design detail as possible. The model used 2130 4-node elements and contained 1990 nodes. Shell elements were used to model the bulkheads and the piston. The piston was constrained to allow for translation normal to the axis of the tool while rotations about the surface of contact were allowed. This should effectively model the piston as a sliding operation where some movement is allowed to account for the part tolerances.

The sensor package was modeled using a rigid beam element which placed the center-of-gravity of the mount at the correct point. The shells in contact with the mount were modeled as very thick elements thus causing bending of the shell elements at the edge of the mount in order to simulate the actual response.

A worst case scenario was assumed for the analysis where minimal contact between the tool and the casing was achieved. This was modeled by using a simple support to the casing with contact only at the ends of the tool and the piston. Contact was further constrained to the centerline of each part. This approach was conservative in nature since any additional contact between the tool and the casing would result in increasing a mode to a higher frequency. While any contact off of the centerline would constrain motion out of the tool centerline plane. This assumption was necessary for design purposes realizing that field testing would determine the quality of contact with the borehole.

IV.3.a Analysis Results

The results of the analysis are listed in Table IV.2. The first mode found at 460 Hz results in deformation of the motor case used to operate the piston clamp. The existence of this mode required a design change in the way in which the motor was mounted to the bulkhead and could possibly include some form of support for the case. This could be accomplished by use of a high density foam which would distribute the support over the entire case or by implementing a local support at the end opposite the mount that is integrated to the motor housing. The first attempt to remove this mode will use only

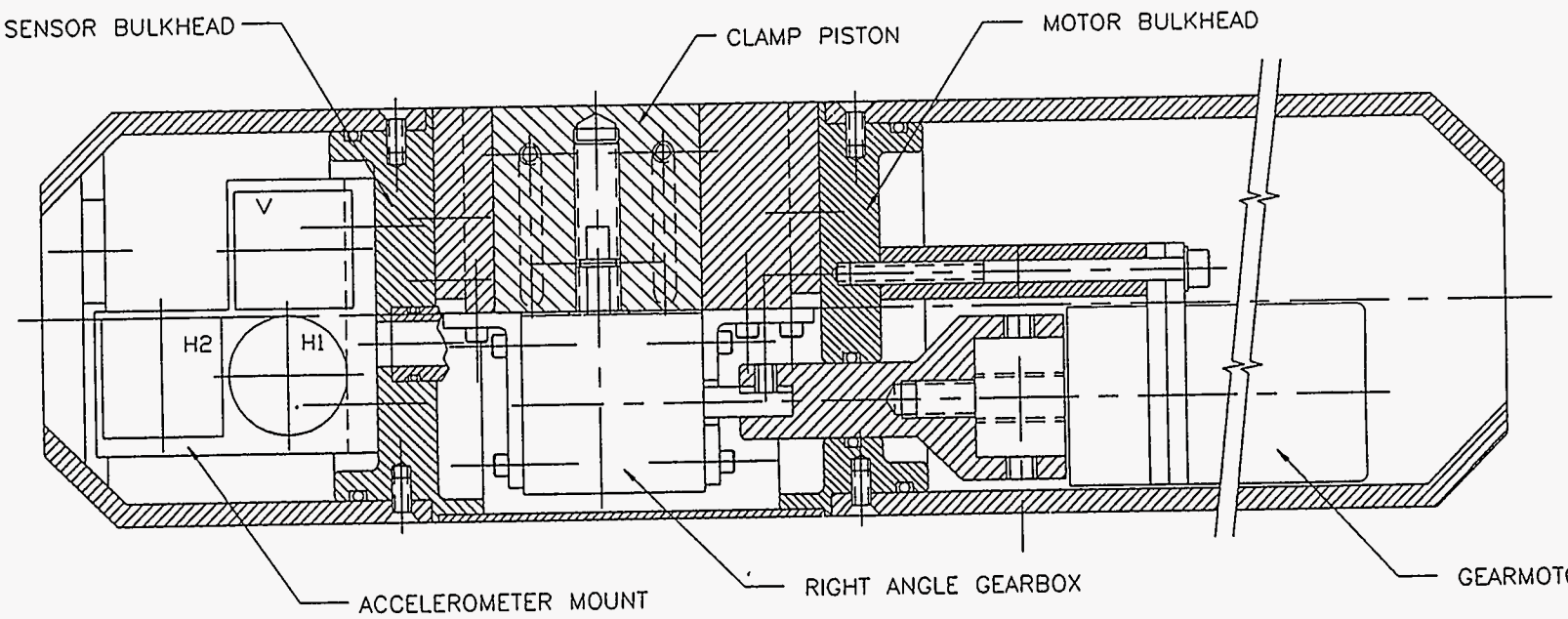

Figure IV.1

REVISIONS			
REV	DESCRIPTION	DATE	APPROVED

SANDIA NATIONAL LAB.

BOREHOLE RECEIVER CONCEPT DRAWING

ENGR. BY: B. ENGLER	SIZE C	FSCM NO	DWG NO / REV
DRAWN BY: B. ENGLER	SCALE 1X		SHEET 1 OF 1

the change in the manner in which the motor is mounted to the bulkhead thus maximizing available space within the housing for future options. The second mode found at 484 Hz is similar to the first mode in deformation, but the bending is normal to the first mode in direction. The design changes will also apply to removal of this mode. Little motion is observed in the sensor mount for either of these modes. As a result these modes should pose no problem.

The first mode which involves significant deformation of the tool was the third mode at 1404 Hz. This bending mode is a combination of the cylindrical body and the piston surface. It is important to note here that only the piston surface was modeled for the sake of simplicity. Thus, the piston surface bending observed was greatly exaggerated and not likely to occur. By increasing the thickness of the piston this mode was significantly raised and was no longer considered a problem. Due to the bending of the tool however some motion of the sensor mount was noted, primarily along the longitudinal axis.

Bending of the piston drive rod in combination with twisting of the piston surface produce the fourth mode at 1580 Hz. The portion of the mode due to twisting of the piston was decreased by simply increasing the rotational constraints on the piston. Also, the bending of the piston drive rod was reduced by increasing the rod diameter which raises the frequency of the mode. Originally this mode was found in the range of 500 Hz. By modifying the model to include simple rotational constraints, increasing piston thickness, and choosing a minimum drive rod diameter of 0.25 in., the mode was raised to the listed value. Additional increases along these lines should result in even further improvement. Again, some slight motion in the sensor mount was observed from this mode.

The fifth mode was due to bending and twisting of the piston surface as modeled along with some localized bending of the tool housing at the sensor location. This mode occurs at 1750 Hz and can be adjusted by applying not only the above modifications but by also providing support for the sensor mount and by improving the way in which it is mounted to the bulkhead. One method by which support for the sensor mount could be achieved is through the use of a high density foam for example.

The sixth mode was caused by the bending of the bulkhead on which the motor was mounted, resulting in axial movement of the motor. Some bending of other parts of the drive rod assembly take place. However, since this mode occurs at the upper end of the design specification and at a frequency near the beginning of the resonant frequency of the accelerometers this mode should not present a problem. Also, the motor motion produces little motion in the sensor mount and can be reduced through support of the motor as previously mentioned.

The next two modes involve higher order bending of the tool and motion of the sensor package. The seventh mode at 2270 Hz. was caused by bending of the tool and deformation of the piston surface. There is significant lateral motion of the sensor mount with this mode. The eighth mode at 2480 hz. results in major motion of the sensor mount due to localized bending of the tool housing.

Table IV.2. Modal Frequencies for Initial MLSR Design		
Mode #	Mode Description	Frequency (Hz)
1	Drive Motor Bending	460
2	Drive Motor Bending	484
3	1st Case Bending	1404
4	Shoe Twist, Rod Bending	1580
5	Shoe Bending	1750
6	Bulkhead Bending	1970
7	2nd Case Bending	2270
8	Sensor Mount Bending	2480

IV.3.b Design Modifications

1. Improve method of mounting the motor to the bulkhead. Secondarily, provide distributed support to the motor through the use of high density foam.

2. Increase thickness of the piston. This modification was fulfilled before the analysis was completed. The model incorporated a slim plate more than a piston for two reasons. The first being simplicity and the second being that the initial design used this type to achieve maximum flexibility in the size of casing the receiver could clamp into. However, it became evident that the design was too fragile to withstand the force which is produced in the clamping process, and that retraction in the borehole environment could easily be defeated.

3. Prevent rotational motion of the piston.

4. Increase the diameter of the piston drive rod to 0.25 in. minimum.

5. Move the sensor mount to the bulkhead and if necessary provide support similar to that used in the first modification.

IV.3.c Conclusions

With an improved motor mounting design, the first mode that results in major bending of the tool occurs at 1404 Hz. Thus the tool should respond in a linear fashion at least through the range of 0 - 1200 Hz. By maintaining better contact with the borehole other than the three point contact modeled, the first bending mode will increase significantly. The overall system design will be aimed at producing a tool clamp that should yield this result. The technique that will be utilized to do this will be based on radial conformation of the outside diameter of the tool or contact surfaces with the inside diameter of the borehole. If the clamp consists of large surface area contacts and not point contacts as modeled, the result should be an increased mode that can be experimentally confirmed.

IV.4. MECHANICAL DESIGN DEVELOPMENT

IV.4.a Clamp Force

With the finite element analysis of the prototype design in hand, the details of the design could be considered. The first area to be defined involves the clamp sub-assembly in which a piston moves along a threaded rod.

Although the size of the piston was ultimately restricted by the outside diameter of the tool and by the centerline offset distance of the motor mount, the stiffness of the piston/bulkhead assembly and the drive rod strength must be taken into account. A rectangular piston was chosen that would maximize the available surface area, maintain the appropriate stiffness and allow for simple constraints. The rectangular shape would, itself, constrain the piston rotationally and through the use of close tolerances, the piston would be constrained laterally. Guide pins were incorporated into the mount which would prohibit the piston from overrunning the threaded drive rod and also allow for minor adjustments to the lateral constraints.(Appendix B).

The size of the threaded rod and the number of threads per inch necessary to drive the piston with appropriate clamping force depend upon several factors. The output of the electric motor to be used, the torque multiplication factor of the gearset that will be used and the clamp force to tool weight ratio are some examples. A Globe Motor was chosen because it was of a size that could be mounted into the tool, various interchangeable torque multiplying gearsets are available and it can be ordered as a high temperature device.

To get an idea of which model of electric motor to use, the output torque was first calculated based on an assumed required axial force. This assumption was based on an estimated tool weight of 20 lbs. and a clamp force to tool weight ratio of 5:1.

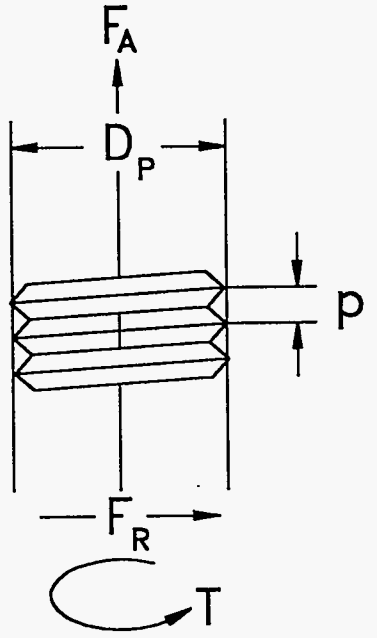

F_A = AXIAL FORCE
F_R = ROTATIONAL FORCE
T = TOTAL TORQUE
T_f = FRICTIONAL TORQUE
T_I = IDEAL TORQUE
D_P = PITCH DIAMETER
p = THREAD PITCH
N = NO. THREADS PER INCH

If friction is neglected then:

$$1) T_I = F_R \frac{D_p}{2}$$

or

$$2) F_R = 2\frac{T_I}{D_p}$$

So if we set up a proportion:

$$3) \frac{F_R}{F_A} = \frac{p}{D_p} = \frac{1}{ND_p}$$

$$4) F_A = F_R N D_p$$

By substituting equation no. 2 into equation no. 4, the result is:

$$5) F_A = 2T_IN$$

or

$$6) T_I = \frac{F_A}{2N}$$

By using equation no.6, an estimated output torque can be calculated. The weight of the tool and the tool weight to clamp force ratio will determine the value of the axial force used. And the number of threads per inch are controlled by the threaded drive rod being evaluated.

Example: Not considering friction, the required output torque is:

$$If: \quad F_A = 100 \ (lbs.)$$

$$N = 16 \ (\frac{threads}{inch})$$

$$Then: \ T_I = \frac{100}{32} = 3.125 \ (inch\text{-}lb.) = 50.0 \ (oz.\text{-}inch)$$

In order to maintain a 5:1 tool weight to clamp force ratio, a gearmotor with an output of at least 50 ounce-inches is needed.

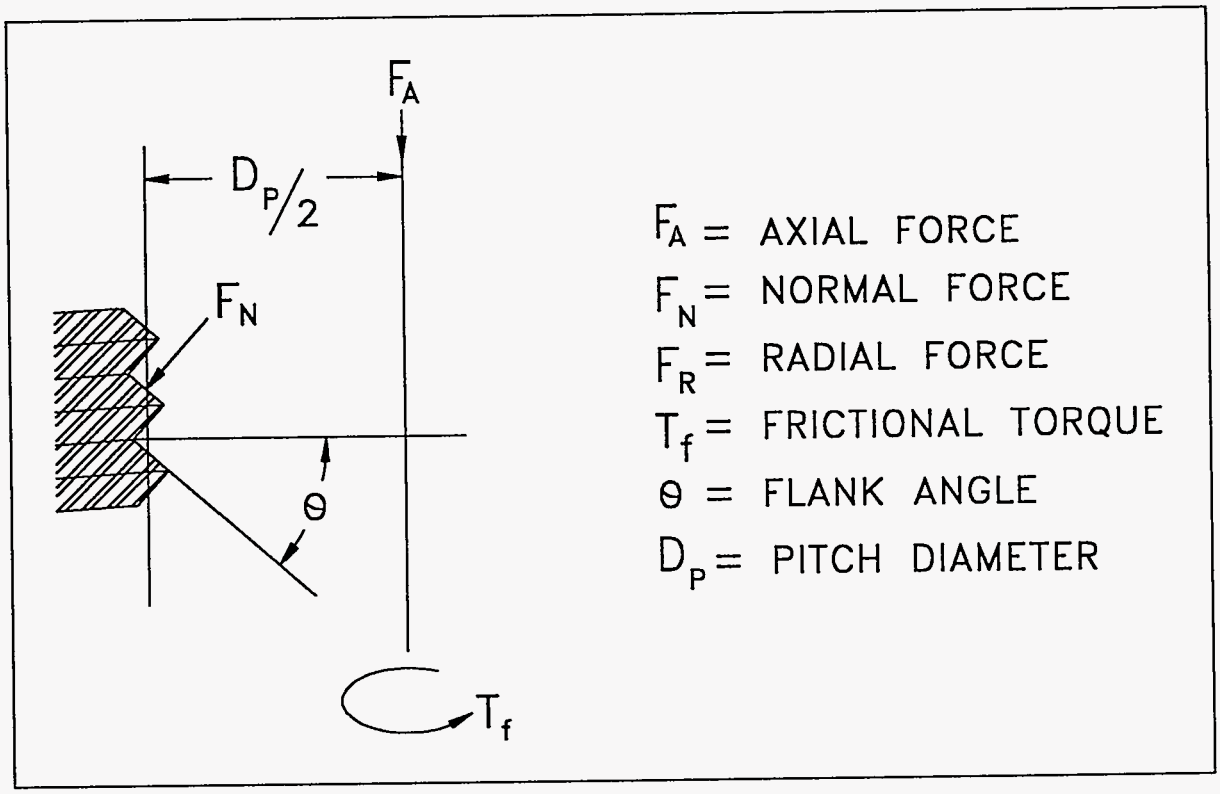

$$F_A = F_N \cos\theta$$

$$F_R = \mu F_N = \frac{\mu F_A}{\cos\theta}$$

If friction is not neglected then:

Therefore: $$T_f = \frac{F_R D_p}{2} = \frac{\mu F_A D_p}{2\cos\theta}$$

And the total torque is $$T = T_l + T_f$$

So:

$$T = \frac{F_A}{2N} + \frac{\mu F_A D_p}{2\cos\theta}$$

$$T = F_A[\frac{1}{2N} + \frac{\mu D_p}{2\cos\theta}$$

$$F_A = \frac{T}{\frac{1}{2N} + \frac{\mu D_p}{2\cos\theta}}$$

Example: If

$T = 3.125$ *inch-lb.* (Max *Continuous Rating*)

$N = 16$ *threads per inch*

$\mu = 0.2$

$D_p = 0.3344$ *inch*

$\theta = 30°$

Then:

$$F_A = \frac{3.125}{\frac{1}{2(16)} + \frac{(0.2)(0.3344)}{2\cos\theta}}$$

So:

$$F_A = 44.7\ lb.$$

And if:

$$T = 8.9\ \textit{inch-lb.}\ \textit{(Theoretical Stall Torque)}$$

Then:

$$F_A = 127.4\ lb.$$

When friction is no longer neglected and a friction coefficient of 0.2 is used, the axial force produced by the 50 ounce-inch motor reduces significantly. This friction coefficient represents a newly machined, well lubricated drive system and as the system ages the coefficient will increase resulting in further decrease in axial force produced. However, with an appropriate maintenance schedule, drive material selection and proper lubrication this trend can be minimized.

As the results show, the amount of the axial force produced can also be increased if the theoretical stall torque of the motor is used to provide the clamping force. This stall torque value varies with the model of the motor. Also, because of brush drop and field distortion the theoretical value will not always be attainable. However with the selection of a motor paired with an interchangeable gearset, the resulting axial force can be varied easily to accommodate cases as they are encountered.

Another method used to calculate the amount of axial force produced treats the clamping system as a translation or power screw [IV.4]. Although Acme, modified square and buttress threads are the most commonly used in this type of application, Unified threads will be considered here. This type of thread can be economically produced and may operate satisfactorily at the loads anticipated. If larger forces are encountered, the decrease in efficiency or the increase in wear become a problem then the other types of threads will be evaluated.

The results of this method gives the following equation:

$$\textit{(Output Force)}\quad Q = \frac{2T}{d}\left[\frac{\cos\alpha - \mu[\tan\lambda]}{\cos\alpha[\tan\lambda] + \mu}\right]$$

So for example: If

$$Thread\ size = \frac{3}{8} - 16$$

$$\mu = 0.2$$

$$Lead\ (\lambda) = 3°'$$

$$Flank\ (\alpha) = 30°$$

$$Pitch\ Diameter\ (d) = 0.3344$$

$$Torque\ (T) = 3.125\ \ inch\text{-}lb.$$

Then:

$$Q = 63.5\ \ lbs.$$

And if:

$$Torque\ (T) = 8.9\ \ inch\text{-}lb.$$

Then:

$$Q = 180.8 \ lbs.$$

This calculation is a little more comprehensive, however, the results again show a decrease in the output force of the motor when friction is taken into account. According to the power screw calculation in order to achieve an output force of 100 pounds under the same conditions:

$$T = \frac{Q\,d}{2}\cos\alpha\tan\lambda + \mu\frac{}{\cos\alpha - \mu\tan\lambda}$$

$$T = 4.9 \ inch\text{-}lbs.$$

Also the efficiency of the Unified thread screw can be calculated from this method.

$$\eta = \tan\lambda\alpha - \mu[\tan\lambda]\overline{[\cos\alpha\tan\lambda] + \mu}$$

For the case of a 3/8 - 16 thread:

$$\eta = 20.2\ \%$$

Figure IV-2 shows the variation of efficiency as a function of lead angle for an Acme, a Buttress and a Unified thread with a coefficient of friction of 0.2. In all cases the efficiency is low when the led angle is very small or very large. The efficiency can be adjusted by not only varying the lead angle within a series but also by incorporating multiple-start threads. It is important to note that the torque requirement was considered to be of primary importance and the efficiency was secondary at this time.

IV.4.b Motor Selection

Taking this number as an approximation of the required output, the Globe Motor model #BL102A175-18 with a 19X torque multiplier was chosen as the first gearmotor to evaluate. The criteria used to make this choice are as follows; 1) The maximum continuous torque rating for the gearbox is 6.0 inch-pounds, 2) The maximum continuous torque rating for the assembly is 5.9 inch-lbs., 3) The calculated stall torque is 16.34 inch-lbs., 4) The motor operates at 115 VDC and 5) The motor will fit into the

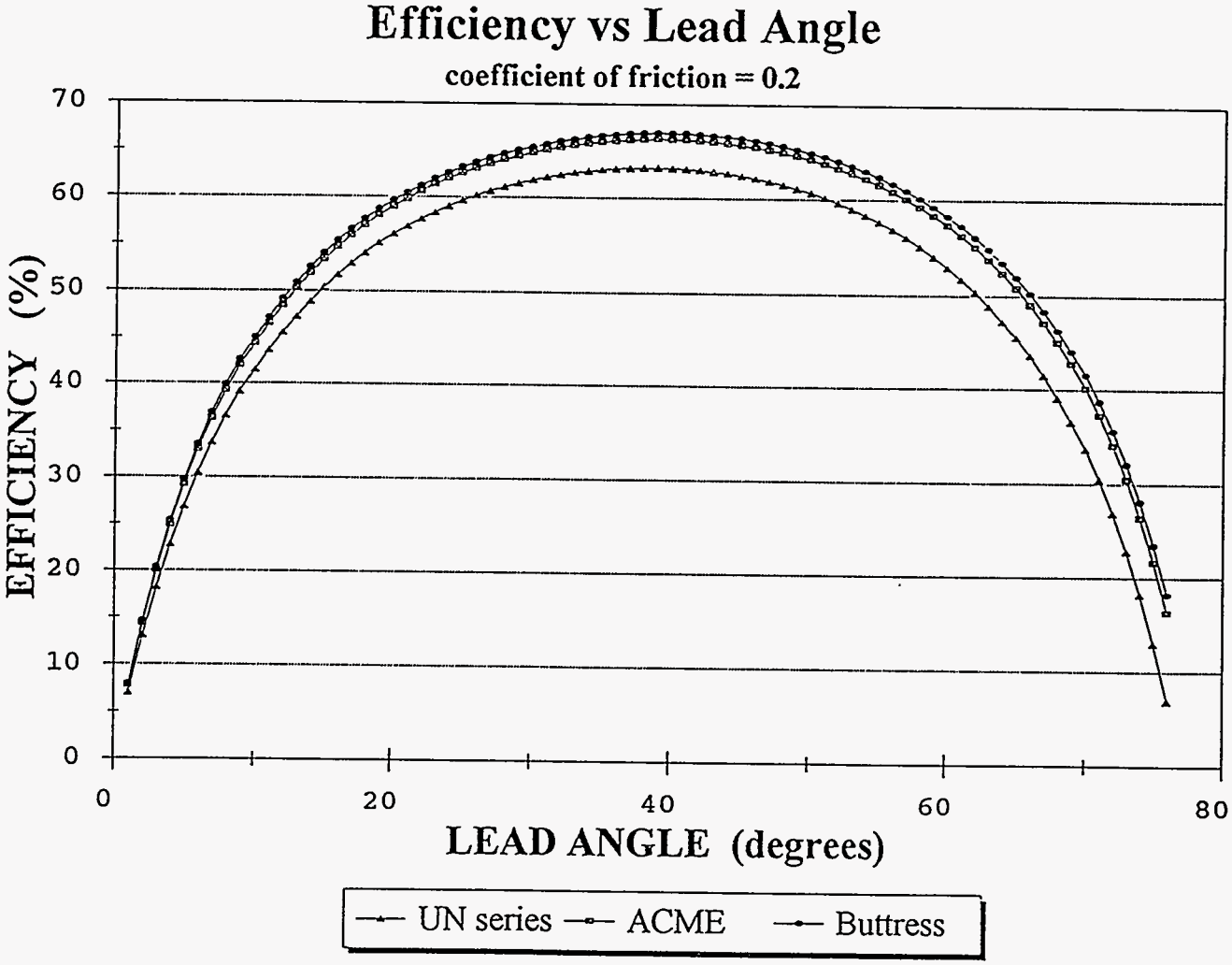
Efficiency vs Lead Angle
coefficient of friction = 0.2
EFFICIENCY (%)
70
60
50
40
30
20
10
0
0
20
40
60
80
LEAD ANGLE (degrees)
UN series
ACME
Buttress

Figure IV.2

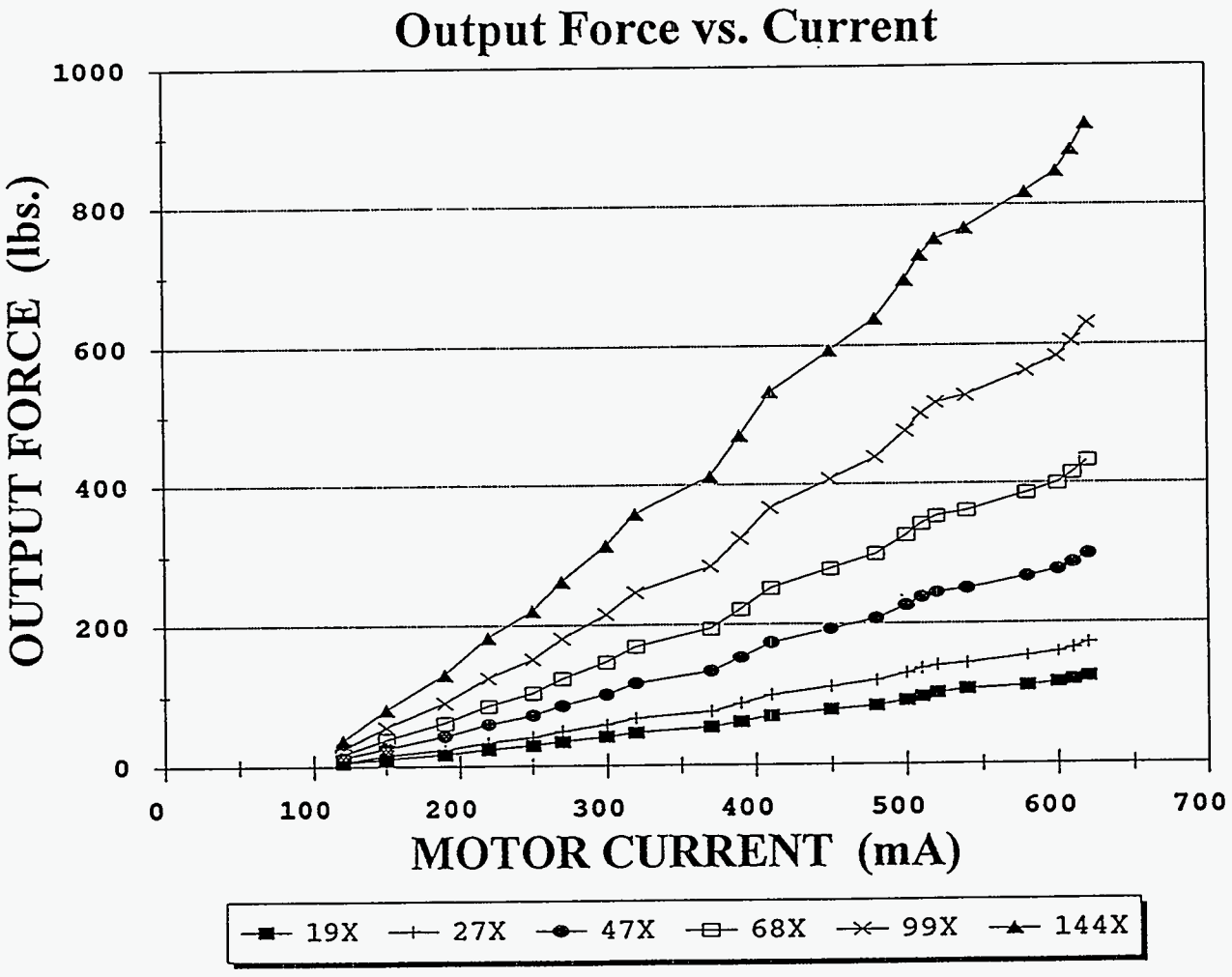
Output Force vs. Current
OUTPUT FORCE (lbs.)
1000
800
600
400
200
0
0
100
200
300
400
500
600
700
MOTOR CURRENT (mA)
19X
27X
47X
68X
99X
144X

Figure IV.3

MODEL 102A175-18

Fa = (T / ((1 / (2* N)) + ((Coeff. of Friction * Dp) / (2 * COS(ALPHA)))))

THREAD SIZE	SERIES	FRICTION COEFFICIENT μ	NUMBER of THREADS N	FLANK ANGLE α	COS ALPHA	PITCH DIAMETER Dp
1/4-20	UNC	0.2	20	30°	0.8660	0.2175
3/8-16	UNC	0.2	16	30°	0.8660	0.3344
1/2-13	UNC	0.2	13	30°	0.8660	0.45
1/4-28	UNF	0.2	28	30°	0.8660	0.2268
3/8-24	UNF	0.2	24	30°	0.8660	0.3479
1/2-20	UNF	0.2	20	30°	0.8660	0.4675
1/4-32	UNEF	0.2	32	30°	0.8660	0.2297
3/8-32	UNEF	0.2	32	30°	0.8660	0.3547
1/2-28	UNEF	0.2	28	30°	0.8660	0.4768

THREAD SIZE	MOTOR TORQUE 13 X	OUTPUT FORCE	MOTOR TORQUE 19 X	OUTPUT FORCE	MOTOR TORQUE 27 X	OUTPUT FORCE	MOTOR TORQUE 47 X	OUTPUT FORCE	MOTOR TORQUE 68 X	OUTPUT FORCE	MOTOR TORQUE 99 X	OUTPUT FORCE	MOTOR TORQUE 144 X	OUTPUT FORCE	THEORETICAL STALL TORQUE 19 X	THEORETICAL STALL OUTPUT FORCE
	T	Q	T	Q	T	Q	T	Q	T	Q	T	Q	T	Q	T	Q'
1/4-20	4.06	81.06	5.94	118.48	8.44	168.36	14.69	293.08	21.25	424.03	30.94	617.33	45.00	897.94	16.34	326.05
3/8-16	4.06	58.15	5.94	84.99	8.44	120.77	14.69	210.23	21.25	210.23	30.94	304.17	45.00	644.12	16.34	233.89
1/2-13	4.06	44.93	5.94	65.66	8.44	93.31	14.69	162.43	21.25	162.43	30.94	235.01	45.00	497.66	16.34	180.71
1/4-28	4.06	92.23	5.94	134.80	8.44	191.56	14.69	333.46	21.25	333.46	30.94	482.45	45.00	1021.66	16.34	370.98
3/8-24	4.06	66.59	5.94	97.33	8.44	138.31	14.69	240.76	21.25	240.76	30.94	348.33	45.00	737.64	16.34	267.85
1/2-20	4.06	51.44	5.94	75.18	8.44	106.83	14.69	185.96	21.25	185.96	30.94	269.05	45.00	569.75	16.34	206.88
1/4-32	4.06	96.39	5.94	140.87	8.44	200.19	14.69	348.47	21.25	348.47	30.94	504.17	45.00	1067.65	16.34	387.68
3/8-32	4.06	71.80	5.94	104.94	8.44	149.12	14.69	259.58	21.25	259.58	30.94	375.56	45.00	795.30	16.34	288.78
1/2-28	4.06	55.72	5.94	81.43	8.44	115.72	14.69	201.44	21.25	201.44	30.94	291.44	45.00	617.17	16.34	224.10

Table IV.3

MODEL 102A175-18

$$Q = (T * 2 / d) * ((COS (ALPHA) - (\mu *(TAN(LAMBDA)))) / ((COS(ALPHA) * TAN(LAMBDA))+ \mu))$$

THREAD SIZE	SERIES	FRICTION COEFFICIENT μ	LEAD ANGLE λ	TAN λ	FLANK ANGLE α	COS ALPHA	PITCH DIAMETER d	EFFICIENCY
1/4-20	UNC	0.2	4°11′	0.0731	30°	0.8660	0.2175	0.236
3/8-16	UNC	0.2	3°24′	0.0594	30°	0.8660	0.3344	0.202
1/2-13	UNC	0.2	3°07′	0.0544	30°	0.8660	0.46	0.188
1/4-28	UNF	0.2	2°52′	0.0501	30°	0.8660	0.2268	0.176
3/8-24	UNF	0.2	2°11′	0.0381	30°	0.8660	0.3479	0.140
1/2-20	UNF	0.2	1°57′	0.0340	30°	0.8660	0.4675	0.127
1/4-32	UNEF	0.2	2°29′	0.0434	30°	0.8660	0.2297	0.157
3/8-32	UNEF	0.2	1°36′	0.0279	30°	0.8660	0.3547	0.107
1/2-28	UNEF	0.2	1°22′	0.0239	30°	0.8660	0.4768	0.093

THREAD SIZE	MOTOR TORQUE 13 X		OUTPUT FORCE	MOTOR TORQUF 19 X		OUTPUT FORCE	MOTOR TORQUE 27 X		OUTPUT FORCE	MOTOR TORQUE 47 X		OUTPUT FORCE	MOTOR TORQUE 68 X		OUTPUT FORCE	MOTOR TORQUE 99 X		OUTPUT FORCE	MOTOR TORQUE 144 X		OUTPUT FORCE	THEORETICAL STALL TORQUE 19 X	THEORETICAL STALL OUTPUT FORCE
	T		Q	T		Q	T		Q	T		Q	T		Q	T		Q	T		Q	T	Q'
1/4-20	4.06		120.77	5.94		176.52	8.44		250.84	14.69		436.64	21.25		631.74	30.94		919.74	45.00		1337.80	16.34	485.77
3/8-16	4.06		82.53	5.94		120.63	8.44		171.42	14.69		298.39	21.25		431.72	30.94		628.53	45.00		914.22	16.34	331.97
1/2-13	4.06		62.47	5.94		91.30	8.44		129.75	14.69		225.86	21.25		326.77	30.94		475.74	45.00		691.98	16.34	251.27
1/4-28	4.06		126.01	5.94		184.17	8.44		261.71	14.69		455.57	21.25		659.12	30.94		959.60	45.00		1395.79	16.34	506.83
3/8-24	4.06		86.03	5.94		125.74	8.44		178.69	14.69		311.05	21.25		450.03	30.94		655.18	45.00		952.99	16.34	346.04
1/2-20	4.06		65.07	5.94		95.10	8.44		135.15	14.69		235.26	21.25		340.37	30.94		495.54	45.00		720.79	16.34	261.73
1/4-32	4.06		127.66	5.94		186.58	8.44		265.14	14.69		461.53	21.25		667.75	30.94		972.17	45.00		1414.06	16.34	513.46
3/8-32	4.06		87.92	5.94		128.49	8.44		182.59	14.69		317.85	21.25		459.87	30.94		669.51	45.00		973.83	16.34	353.61
1/2-28	4.06		66.51	5.94		97.21	8.44		138.14	14.69		240.46	21.25		347.90	30.94		506.51	45.00		736.74	16.34	267.52

Table IV.4

prototype housing. This motor should not only be capable of producing the required force in a continuous duty cycle but also if the clamping procedure involves running the motor to stall. Presently the duty cycle for the clamping of the receiver should be light enough so as to allow running the motor to stall. If the drive train is designed to handle the force and torque produced at stall, this would eliminate the necessity for a control feedback system and/or manual monitoring since these steps are usually taken to insure that the gearmotor assembly is not over torqued.

With the gearmotor model chosen the output force for a subset of the available interchangeable torque multipliers was calculated for three different sizes and three separate Unified series (Table IV-3 and Table IV-4). Experimentally the output force of the 19X torque multiplied gearmotor was determined. A load cell measured the force produced at various current levels by limiting the supply voltage. Assuming a linear relationship between the torque multipliers and their output, the curves for the rest of the multipliers were based on the response of the 19X. Figure IV-3 shows the output of the gearmotors as a function of current where 620 mA is the stall current. Not only does this graph show the flexibility of the output force produced but also shows the importance of determining the voltage line loss in the system. If this fact is ignored, the motor will be operating at a voltage and current that is less than ideal. This will result in a clamp force smaller than that produced at stall at 115 Vdc and 620 mA.

IV.4.c Clamp Time

This particular model of motor has a no load speed of 5,500 to 7,000 revolutions per minute. The gear assembly has a speed reduction ratio of 21.1:1 which results in a final output speed of 261 to 332 RPM. To calculate the travel time that it would take the piston to move from the initial position to the clamped position the following equation was used.

$$t = \frac{D\,N\,60}{R_s}$$

Where:

t = *Time* (*seconds*)

D = *Distance traveled for clamp* (1.0 *inch*)

$$N = 16 \textit{ threads per inch}$$

$$R = 300 \textit{ RPM}$$

$$t = \frac{(1.0)\ (16)\ 60}{300}$$

$$t = 3.2 \textit{ seconds}$$

So if an average speed of 300 RPM is used then it will take the piston 3.2 seconds to travel 1.0 inch. As different gear sets are interchanged with the basic motor not only does the torque multiplication factor change but so does the speed reduction ratio. Thus, the trade off for more output force is a reduction in speed which will add to the clamp time of the receiver. For example in the case of the 99X torque multiplier gear set with a speed reduction ratio of 117:1

$$R = 53.5 RPM$$

$$t = 17.9 \textit{ seconds}$$

In this case with an average speed of 53.5 RPM it will take the piston 17.9 seconds to travel the 1.0 inch to clamp. Again as larger torque multipliers are used, a higher speed reduction ratio is applied resulting in longer clamp times.

IV.4.d Torsional Strength of Shaft Assembly

There are several methods for calculating the design criteria for a circular shaft linkage. In practice the allowable stress that is generally used for a small, short shaft is 8500 pounds per square inch [1]. Using this stress, the allowable twisting moment for a circular shaft is:

$$T = S_s * Z_p$$

Where:

T = Torsional or twisting moment in inch-pounds

S_s = Allowable torsional shearing stress in pounds per $inch^2$

Z_p = Polar section modulus in $inches^3$

So for a 0.25 inch diameter shaft:

$$T = 8500 \frac{lbs}{inch^2} * \frac{\pi D^3}{16}$$

$$T = 26.08 \; inch\text{-}lbs.$$

If the motor is to be run to stall in the clamping procedure and the gearsets are to be interchangeable then the shaft must be capable of handling the associated torque produced.

The following are the calculated stall torque produced for the respective torque multipliers:

Torque Multiplier	Stall Torque (in.-lb.)
19X	16.34
27X	23.22
47X	40.42
68X	58.48
99X	85.14
144X	123.84

Table IV.5

As indicated only the first two torque multipliers can be used with this procedure if the allowable shearing stress of 8500 pounds per square inch is to be maintained.

However another approach to the problem is to utilize the torsion formula to determine the ultimate strength in torsion.

$$\tau = \frac{Tr}{J}$$

Bars of ductile material usually break in shear when twisted to failure, the surface of the fracture being normal to the axis of the bar. The torsion formula applies only when the maximum stress does not exceed the elastic limit of the material. If it is used with the T (torque) equal to the twisting moment at failure then a fictitious value called the modulus of rupture in torsion is obtained. For solid steel bars this value drops to about 80% of the ultimate tensile strength when the length becomes 25 times the diameter [IV.5]. In this case the length will be less than 25 times the diameter but this percentage will be used here to produce a conservative value. For common structural steel the yield point is 33,000 pounds per square inch, which results in a modulus of rupture of 26,400 pounds per square inch. By rearranging the torsion formula to solve for the corresponding torque value the following formula is obtained;

$$T = \frac{J\,\tau}{r}$$

And so for a 0.25 inch diameter shaft:

$$T = 80.99 \textit{ inch-lbs.}$$

With this method which is based on the yield point of the material, the torque multipliers through the 68X gearset can be used while maintaining at least a 1.4 safety factor. Finally, brittle materials such as hardened tool steel are generally stronger than in shear than in tension and therefor the maximum normal stress theory of failure should be applied. The diameter of a shaft made of brittle material and with a pure torsional load may be determined from the following formula:

$$T = \frac{D^3\,S_t}{5.1\,(K_t)}$$

Where:

S_t = *maximum allowable tensile stress* (*inch-lbs.*)

D = *diameter of the shaft*

K_t = *combined shock /fatigue factor* (1.0 - 1.5)

And if:

$$D = 0.25\ inch$$

$$K_t = 1.5\ (for\ suddenly\ applied\ /minor\ shock\ load)$$

$$S_t = 100{,}000\ (\frac{lbs}{inch^2})$$

Then:

$$T = 204.2\ \ inch\text{-}lbs.$$

From the preceding analysis, through the use of a hardened steel shaft all of the gearsets can be used in conjunction with the motor. This is highly recommended since the effects of such features as keyways and coupling devices are not covered here. One or more of these features could be utilized in the final design and the result of their use will be to lower the allowable stall torque. However with the proper selection of material and the acceptance of a lower safety factor, the gearsets through the 68X can probably be used with a high degree of confidence. Once the design of the drive-train is completed, the shaft can be experimentally tested in order to determine a more accurate modulus of rupture.

IV.4.e Linear Deflection

When designing steel shafting, it is considered good practice to limit the maximum linear deflection to 0.010 inches per foot of shaft length. In order to avoid linear deflection in excess of this amount, the maximum distance in feet between bearings is determined by the formula [IV.6]:

$$L = 8.95\ \sqrt[3]{D^2}$$

this formula is used in the case where the shaft is subjected to no bending action except its own weight.

So for a 0.25 inch diameter shaft:

$$L = 8.95 \sqrt[3]{00.25^2}$$

$$L = 3.55 \ ft.$$

No bearings are required in this case to maintain the accepted value of 0.010 inches of linear deflection per foot of length. However by creating a ratio between this value at 3.55 feet and the actual length of the shaft, the actual linear deflection can be calculated. If the shaft length is 2.13 inches then:

$$\frac{0.010 \ inch}{3.55 \ feet} = \frac{X \ inch}{0.1775 \ feet}$$

$$X = 0.0005 \ feet = 0.006 \ inches$$

Depending on the rotary shaft seal chosen, this 6 thousands of linear deflection could produce excessive wear and/or seal failure. Therefor care must be taken in the design of the seal subsystem to account for the possibility of this linear deflection or a bearing such as a oil impregnated bushing can be used. At this time no bearing will be incorporated and the system will be monitored in order to determine if a bearing/bushing is necessary.

IV.5. LABORATORY TESTING AND RESULTS

A number of laboratory tests were performed on the prototype receiver sonde in order to verify that the initial design meet the appropriate requirements. These tests also served as the baseline data to which all future modifications would be compared.

1.) Pressure Testing: In order to assure that the receiver and all internal components would survive borehole pressures, the sonde was tested to 3000 psi.

2.) Clamp Arm Testing: Clamp system reliability was tested by repeatedly clamping/unclamping the sonde in a dry steel casing. Clamp force was measured and estimated for several gearsets, and the tool weight to clamp force ratio was found to be in excess of 5:1.

3) Free-body Frequency Response Test: The receiver was placed on a shake table in its unclamped mode. Reference accelerometers were placed on different parts of the receiver and compared with

the internal mounted accelerometers. No tool resonances were found within the range of the experimental setup (10 Hz to 1000 Hz).

4) Clamped Receiver Frequency Response: All the shake table setups/fixtures exhibited resonances below 1000 Hz. As a result confirmation of no resonant frequencies in the clamped mode below 1000 Hz proved to be extremely difficult. The best fixture found was a solid block of granite (36 inches on a side) with a water filled 5 inch hole. Due to the finite size of the block however, block modes were excited at frequencies above 800 Hz. A reaction type shaker was used as the excitation source and the clamped accelerometer responses were compared with reference accelerometers cemented to the walls of the water filled hole. The results of these tests showed that the clamped receiver exhibited a flat response to at least 800 Hz.

5) Shoe Safety Release Test: To prove the viability of the shoe release mechanism, the receiver was clamped into a piece of casing with a 1/4 inch thick ring of steel welded to the inside. In the clamped position the receiver was then extruded free of the casing while monitoring the force required (Figure IV.4). This reasonable simulation of attempting to free the sonde as if it were stuck in the borehole was equivalent to overcoming a 1/2 inch borehole offset. The test showed that the shoe did indeed break free of the piston at the appropriate place and at the approximate shear value. Also the fasteners at the housings and the connector end showed no damage due to the 4400 lbs. of force required to free the sonde.

6) Rail Adapter Test: To improve the quality of the clamp and the centering of the receiver in the borehole upon clamping, rails were adapted to the receiver. Several tests were performed in order to determine the appropriate configuration of the rails. These tests involved rails ranging from small pads up to rails with an aspect ratio equal to the receiver. From these tests the rails that were the length of the sonde and sized diametrically so that the length of the piston travel was 1 1/4 inches maximum showed to be acceptable. The receiver housings were modified to incorporate the capability of running the sondes with rails if necessary.

IV.6. FUTURE DEVELOPMENT

With the design and the laboratory tests completed, field testing should indicate any weak areas that will require further consideration. A few areas to watch for at this time are the shaft /bulkhead interface and the right angle gearbox. Both should be inspected and maintained on a regular basis, looking for any signs of early wear or possible failure. The rotary seal is presently serving not only as the seal but also as the bearing surface for the shaft. Even though the calculations do not indicate the necessity of a bearing, one may become necessary if wear or leakage at the seal is indicated. Also depending on the torque multiplier used, the shaft should be inspected for signs of over torquing such as twisting of the coupling interface. If such signs become evident then another material or harding of the shaft is recommended. The gears in the right angle gearbox should also be inspected and greased on a regular basis to ensure proper performance. This will also allow for a determination of the lifetime of the unit before normal replacement can be expected. At this time hardening of the gears is recommended as soon as gears of the appropriate material are found. These steps will help to improve the design in the future and provide a more reliable tool.

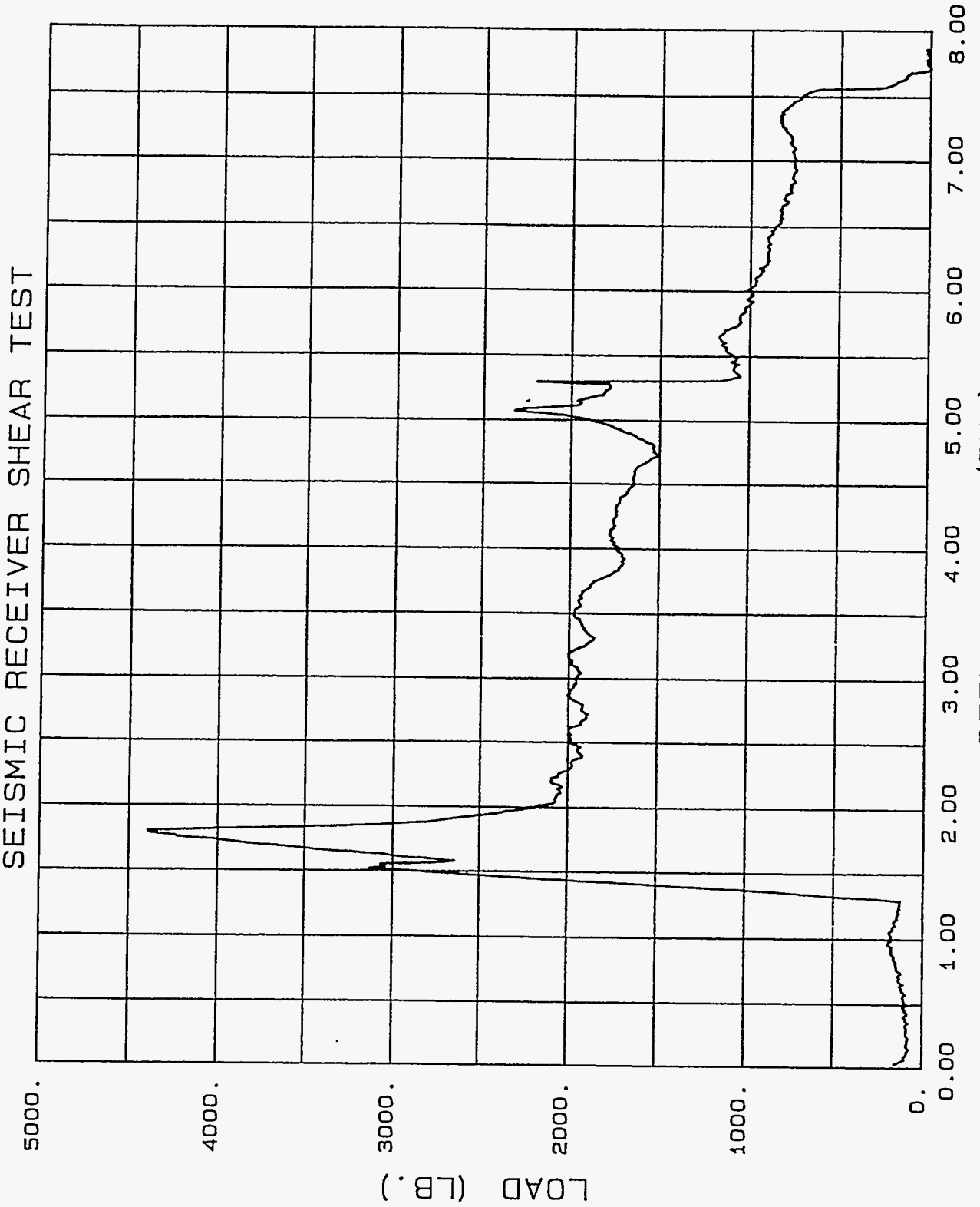
SEISMIC RECEIVER SHEAR TEST
LOAD (LB.)
5000.
4000.
3000.
2000.
1000.
0.
0.00
1.00
2.00
3.00
4.00
5.00
6.00
7.00
8.00
DEFLECTION (IN.)

Figure IV.4

A need in the future will be the capability to orient the sondes in the borehole or the ability to determine the sondes orientation as they hang. At present no appreciable headway has been made in the ability of manually orienting the sondes before loading into the borehole. Of course even a torque balanced wireline interconnect has some twist depending on the load it is subjected to. In the case where several sondes are strung together, the load at each interconnect is different and the result is a slightly different orientation of each sonde. Attempts at correcting this twist have resulted in the ability to orient the sondes to within +/- 15 degrees of each other. A mechanism which allows for a smaller amount of adjustment may improve this number. However to accomplish the proper alignment over the entire string, enough headroom must be available to observe the string in the final configuration. This may not be practical or available at all sites.

Even if the sondes were oriented at the surface in an acceptable fashion, the absolute orientation of the sondes would be unknown after entering the borehole. This is due to the fact that the wireline will twist as it unwinds off of the spool and proceeds down the borehole. So the present effort is to locate, adapt and test a device that will allow the absolute orientation of each sonde to be determined downhole as it hangs in the string.

V. SEISMIC TELEMETRY AND DATA ACQUISITION SUB-SYSTEM

V.1. DESIGN OBJECTIVES AND PHILOSOPHY

The fundamental desire to produce an expandable architecture for operation with one to five Data Receivers using standard seven conductor interconnects resulted in a parallel interconnect bus design. While the existing design is tailored to operation with a maximum of five Data Receivers, this can be extended to ten if custom interconnects are available. From the outset of the design of the data acquisition electronics for the MLSR two key challenges have dominated the effort. First, the unit must function for hours at a time at temperatures up to 200° C. This requirement drove an interest to minimize downhole circuitry and to keep the circuit functions simple and robust. For this reason there is no automatic gain ranging, filter selection, or data compression circuitry down hole. The design is based on low level digital components such as standard CMOS logic and Erasable Programmable Logic Devices (EPLD). These devices were chosen to avoid the need for complex, highly integrated devices such as microprocessors or high density semiconductor memory devices. Minimizing the complexity of timing functions and analog processing was pursued in the interest of a robust design which would operate well in the high temperature environment. Another key restraining factor in the design of the Data Receiver electronics was that of a limited volume in the package. This consideration also drives the interest to minimize circuitry.

V.2. DATA ACQUISITION AND TELEMETRY SPECIFICATIONS

In order to meet a broad array of seismic survey applications a detailed and demanding set of specifications were generated. These specifications comprised a working document which evolved as the challenges of high temperature operation and the functional needs of the oil industry were identified in the early planning of the development. Department 6114 carries the primary responsibility for setting specifications in response to the needs of the oil industry which is the ultimate user. The overall system specifications and requirements are defined in Table V.1.

Data Acquisition specifications have been developed to insure high quality performance in seismic survey applications. The data acquisition is based on a sixteen bit digitizer with low noise signal conditioning front end amplifiers. A detailed set of specification for the data acquisition system is provided in Table V.2.

The Data Transmission requirements for the MLSR reflect the desire to maintain a high quality data link for real time operation. The data is transferred to the surface over a fiber optic link of 7,000 feet length. The data integrity issue is addressed by utilizing an eight bit checksum for each sample of data, allowing errors to be detected and tagged. Data Transmission and Control Specifications are provided in Table V.3. Detailed discussion concerning the design implementation of the MLSR is included in later sections.

Table V.1: MLSR System Specifications	
Receiver Description	Three Axis Acceleration Pre Amps Integral to Accelerometers 3-channel, Dual Gain Digitizer Addressable Motor Control
# of Data Receivers	5 Currently (Expansion to 10)
Sampling Skew	0.5 μsec (Chan X, Station to Station)
Receiver Data Bus	Time Multiplexed, Tri-State Serial Data with Coherent Clock
Receiver Interconnects	7 Conductor (20 awg) with armor
Receiver String Length	50 feet total (5 receivers, 10 foot spacing)
Data Transmission to Surface	4.992 Mbits/sec (Manchester Code) Real Time Fiber Optic Link
Control Features	RS232 Serial Command (150 baud) Digitizer Reset Down Hole Calibration Diagnostics Test Mode Addressable Motor Control
Operating Temperature	130° C (demonstrated) 200° C (targeted)
Accelerometer	Wilcoxen Research Model #731-20
Wireline	7,000 feet 1 Optical Fiber required 7 Conductors (20 awg) 1 conductive armor (> 20 awg)

Table V.2: Receiver Specifications	
# of Channels	3 axis acceleration 5 diagnostic monitors
Sample Rate	1/8 msec (per channel, fixed)
Dynamic Range	120 dB (ambient to 130° C) 100 dB (to 200°C, anticipated)
ADC Resolution	15 bit + sign bit
Receiver Input Range	± 3.0 V maximum
Pre-amplifier (jumper selected)	Constant Current, 0/40 dB gain Single-Ended, 0/40 dB gain
Input Impedance	20 kΩ, Constant Current Input 40 kΩ,, Differential Input
Noise	5nv/√Hz (maximum, 10 to 3000 Hz) (with 40 dB gain pre-amp)
Total Harmonic Distortion	0.4 % (maximum)
Gain Ranging	Instantaneous Floating Point, 2 steps
Sample Resolution	60 dB (minimum)
Chan/Chan Sampling Skew	42 μsec (maximum, X to Y) 84 μsec (maximum, X to Z) 0.5 μsec (maximum, X to Xhold)
Bandwidth	10 to 3125 Hz
Anti-Alias Filter	9-pole LPF @ 3125 Hz
Diagnostics	3 Receiver Supply Voltages Calibration Source Reference Temperature
Output Data Format	Bursted Serial Data Bus 32 bits/sample, 3 samples/receiver
Supply Current (per Receiver)	+15V @ 270 ma. (4 watts) -15V @ 140 ma. (2.1 watts)

Table V.3: Data Transmission Link & Command Link Specifications	
Data Transmission Link:	
Input Format (from Receivers)	Serial Data Bus, Bursted 4.992 Mbits/sec
Output Format (to Fiber Tx)	Continuous, Formatted Manchester Code @ 4.992 Mbits/sec
Sync Pattern	"EBEB" marks top of Frame
Error code	8 bit checksum (per Receiver per frame)
Transmission Delay	0.375 μsec (fixed sample delay) 56 μsec (Data Hold to Up Hole Sync)
Control Link:	
Command Format	RS232, PC Compatible (8 data bit, one start, one stop)
Baud Rate	150 bits/sec
Handshake	Transmit Code with Echo & Verify
Command Override	DC Voltage Control for "Panic"
Current Required*	*15V @ 250 ma (4 watts) -15V @ 50 ma (0.8 Watts)

* Includes current to drive one optical fiber at 100 ma.

V.3. DATA ACQUISITION AND TELEMETRY DESIGN

V.3.a Data Receiver Design Overview

The Data Receiver serves the basic functions of converting three accelerometer inputs into high resolution digital data and transmitting the data onto the interconnect bus. A block diagram of the Data Receivers is provided as Figure V.1. The circuitry which implements these functions resides on three of the four boards which are housed in each receiver package; the Encoder Timing, Digitizer A/D, and Signal Conditioning Boards. The fourth board in the receiver is the Motor Control Board and will be discussed separately. The wiring diagram for the Data Receiver is provided in Figure V.2.

Each accelerometer input is filtered and digitized at unity gain and at 30 dB gain. The two samples are taken simultaneously so that the signals can be point-by-point merged into a single unsaturated measurement at the surface. That is, two 16-bits words are sent to the surface for each accelerometer sample and the Host computer does a real-time merge operation to discard the 30 dB signal whenever its over driven. Thus, a total of six conversion operations are required for each 3-axis data frame which occurs at 1/8 msec. rate. The common 1/8 msec. strobe forces of all the receivers in operation to sample their inputs simultaneously. Considerable care was exercised to maintain nearly ideal performance from the 16-bit A/D converter. The selection of low noise components and careful

Figure V.1: MLSR Data Receiver

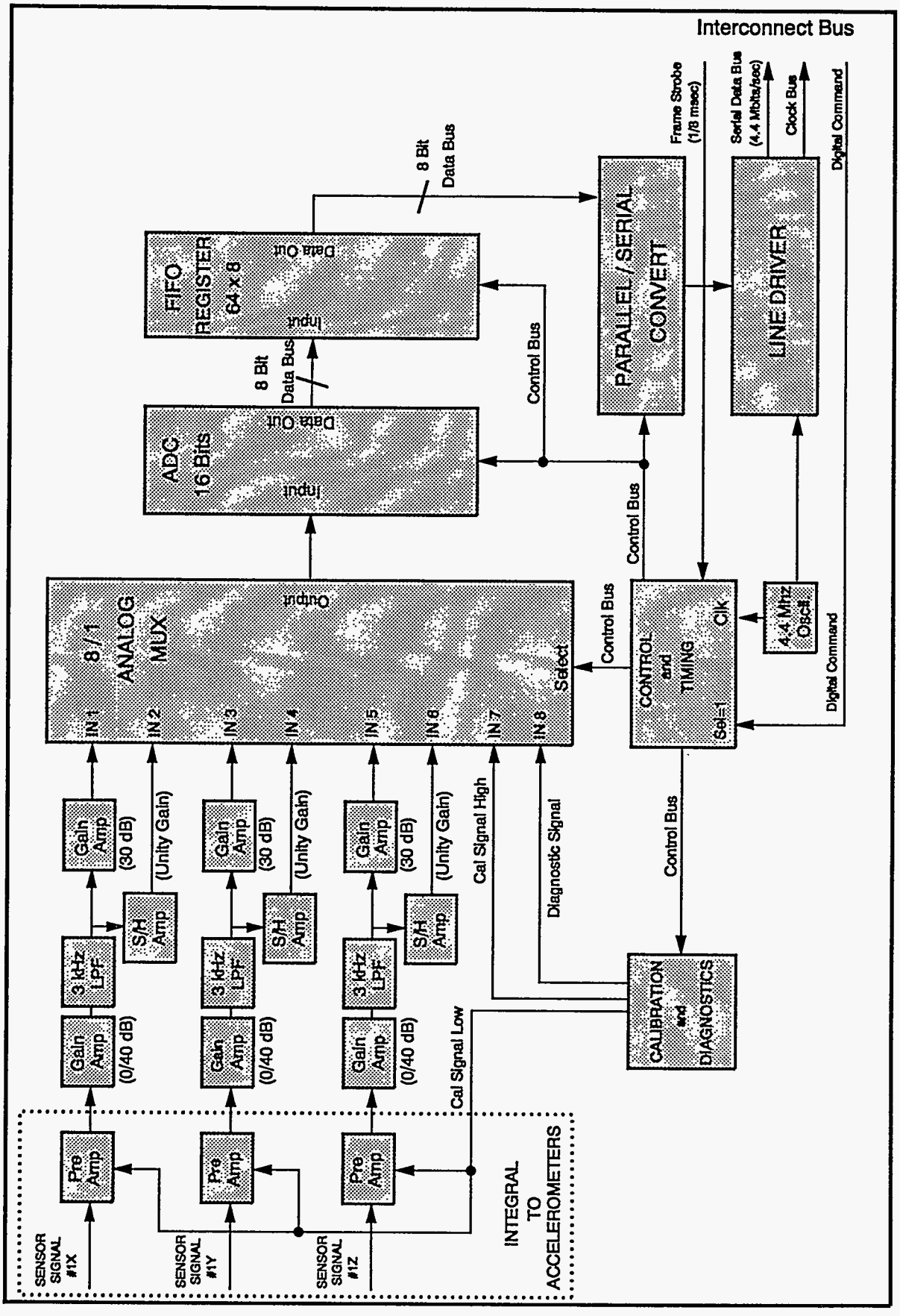

Figure V.2: MLSR Data Receiver Wiring Diagram

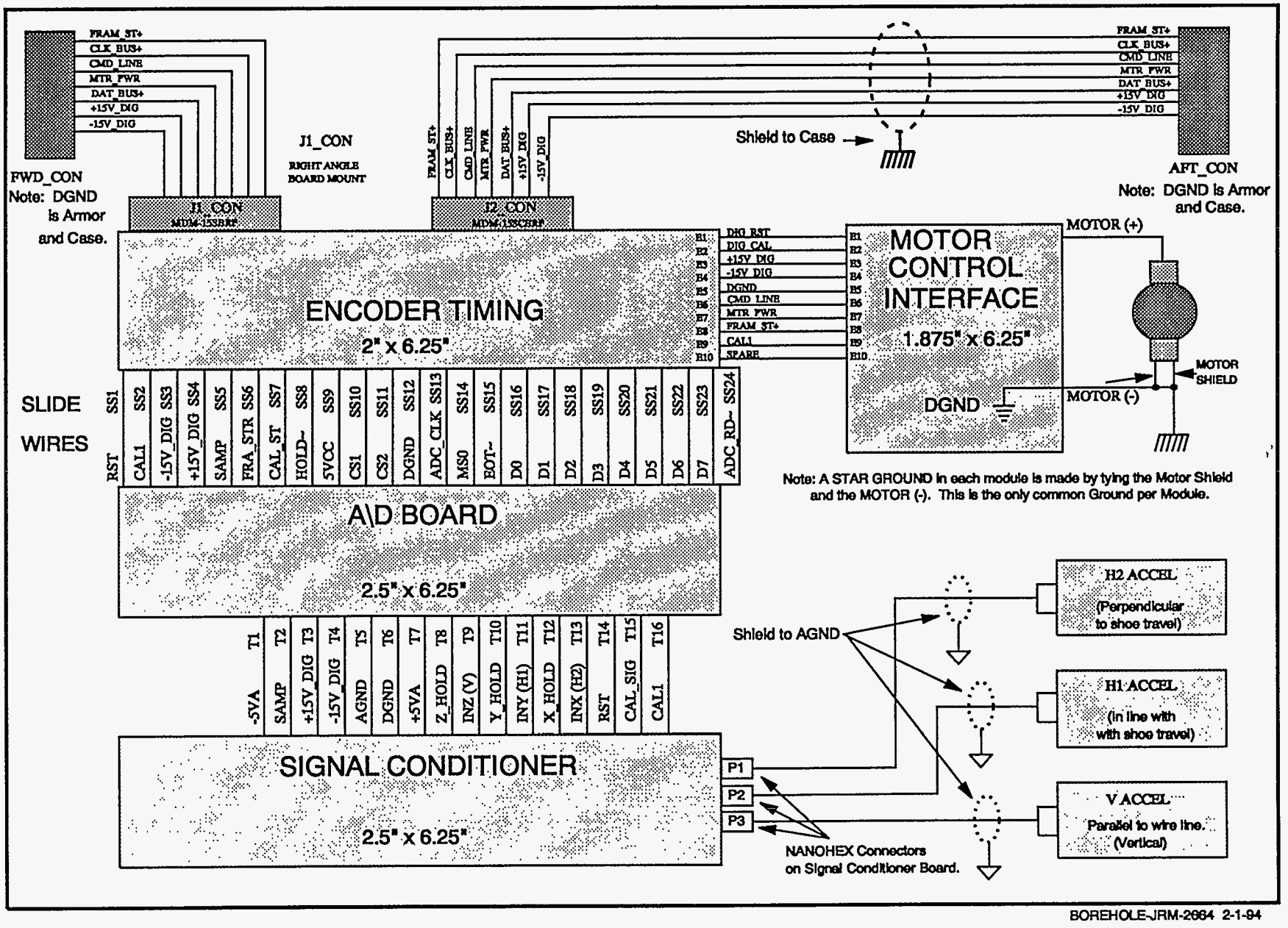

control of component layout and trace routing on the Digitizer A/D board was of critical importance. The A/D output is buffered into a FIFO register to be clocked onto the serial interconnect bus in sequence.

The digital output from the Data Receivers share a single serial data wire in the interconnect bus. Each unit must clock its data onto the bus during its prescribed bus period within the frame (See Figure V.3.). This requires that the receiver must have a full set of six words ready to be clocked onto the bus when its bus period opens up. Since the conversion of six words takes nearly all of the 125 μ sec period of the frame, at least one full sample must be available for data output at the same time that the next sample is being converted. This is the requirement which drives the use of a FIFO register. Thus, two asynchronous data operations are taking place. Data is being converted and written into the FIFO gradually throughout the sample window while the data is "bursted" out of the FIFO when the receiver has control of the bus. Bus control between the receivers is synchronized by a common strobe pulse to all receivers which triggers a timer in each unit. The EPLD (Erasable Programmable Logic Device) carries a unique time-out for each receiver. Thus, receiver #1 transmits from time = 0 to 20 μsec, #2 from 25 to 45 μsec and so on. Receiver #5 completes it bus period at time = 120 μsec leaving a 5 μsec gap at the end of the frame before the next frame starts. Note, that the receivers transmit a coherent clock on another interconnect bus so that the clock and data signals experience nearly identical transmission delay whether the receiver is at the top or bottom of the string. Circuit loading of the bus is avoided by the use of tristate line drivers, with each receiver enabling its output only during its bus period.

It should also be noted the Digitizer A/D board contains a local signal source to accommodate calibration of the receivers without retrieving them from the well. Also included is a series of diagnostic measurements to allow the receiver state-of-health to be checked without retrieving the unit. The schematics for the Encoder Timing, Digitizer A/D and Signal Conditioner are included in Appendix C.

V.3.b Signal Conditioning Design

The circuitry included on the Signal Conditioning Board can be identified in the upper left corner of Figure V.1. Three channels of identical circuitry processes each of the accelerometer inputs. Testing to date has utilized only the constant current inputs, but single-ended inputs are available. Each of the channels contains a 9-pole, Butterworth filter to minimize aliasing. The filters are fixed frequency and based on Sallen-Key operational amplifier topology. The amplifier chosen for this design is the Burr Brown OPA-2111, which is a low-noise, dual amplifier. The calibration signal is incorporated in a series of three SPDT analog switches which are controlled to pass either the calibration signal or the filter outputs of the three channels. Each of the three switch outputs drive the input of a unity gain sample and hold amplifier (Crystal Semiconductor CS3112) and a 30 dB gain amplifier (OPA-627). These six outputs are connected to six multiplexer inputs to the digitizer (Figure V.1.)

The design of the signal conditioner circuits was followed by careful laboratory evaluation of the performance characteristics of this portion of the Data Receiver as a subsystem. Detailed testing of the noise floor on the signal conditioner outputs was critical to insure the integrity of the digitized data to be produced by the units. Testing of the noise floor, spectral purity, harmonic distortion and cross

Figure V.3: MLSR Telemetry Data Timing

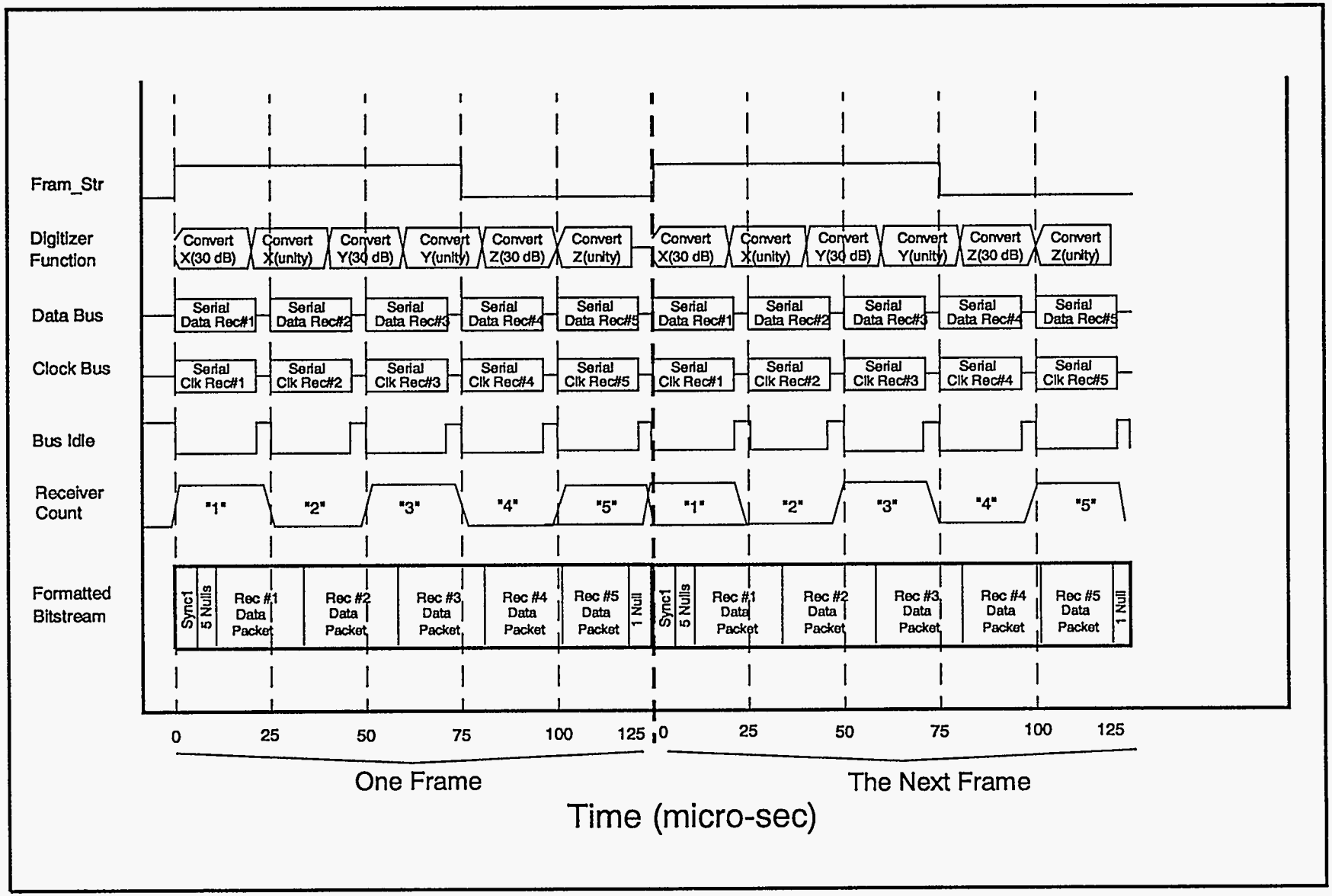

R. J. Franco, 2664
1/28/94
File: sande3

talk were performed to insure that overall system specifications in these areas could be met. The geophone preamplifier was of greatest concern since this input requires the more stringent noise performance than the accelerometer input. Testing on this preamplifier input indicates that geophones can be used with this receiver with confidence of good results. The other area of careful testing in this design was to verify the amplitude response of the 9-pole Butterworth filter. The flatness of the amplitude in the passband and adequate roll off to control aliasing was studied and the design found to be quite suitable. An amplitude response curve for the design is included as Figure V.4.

V.3.c Motor Control Design

The clamping motors in the receivers must be controlled individually to insure the reliability of the clamping operation and to minimize voltage drop on the motor current wire. Each receiver contains a motor control board which is, effectively an RS232 receiver and decoder. This controller also provides command signal decoding for the receivers. The RS232 interface detects the transmitted command byte, checks parity, and decodes the command. If a parity error is detected the command is not executed. Addressing the motor in a selected receiver is accomplished as follows. First, the motor enable command for the selected receiver is generated at the control panel and detected at the Command Interface board in the Wireline Interface Unit at the top of the string. Second, the Command Interface completes the echo and verify handshake and transmits the command to the interconnect bus (down hole) for the Data Receivers. All of the receivers detect the command and decode it, but only the addressed motor control board will execute the command. Finally, the single motor control board addressed in the command will enable its bidirectional MOSFET (Metal On Silicon Field Effect Transistor) switch, connecting its Motor + wire to the common motor control wire in the interconnect bus. The MOSFETs used in this design must be rated to 200V, because the motor voltage requirement is for 150V typical.

This Motor Control circuit also implements a panic mode of operation in the event of digital control failure. When an analog signal is placed on the Fram_Str line, rather than the 0 to 15V strobe which is normally there, the circuit recognizes a panic condition. This condition is actually detected in the Command Interface Board in the Wireline Interface unit at the top of the downhole string. When the analog voltage on Fram_Str line falls inside this illegal range, voltage comparators on the motor control board drive the MOSFET switches and the digital control line is ignored. Each of the motor control circuits in the Data Receivers has a unique signal range for which it is enabled. Since these voltage ranges do not overlap, each Data Receiver has a unique "Analog Address" for which its motor is enabled in a panic condition. The panic voltage ranges for each Data Receiver are defined in Table V.4. Note, this is a failure recovery design in the circuit which should not be used except in the event of failure in the digital control. The digital control has proven very robust to this date.

Figure V.4 Amplitude Response of MLSR Lowpass Filters

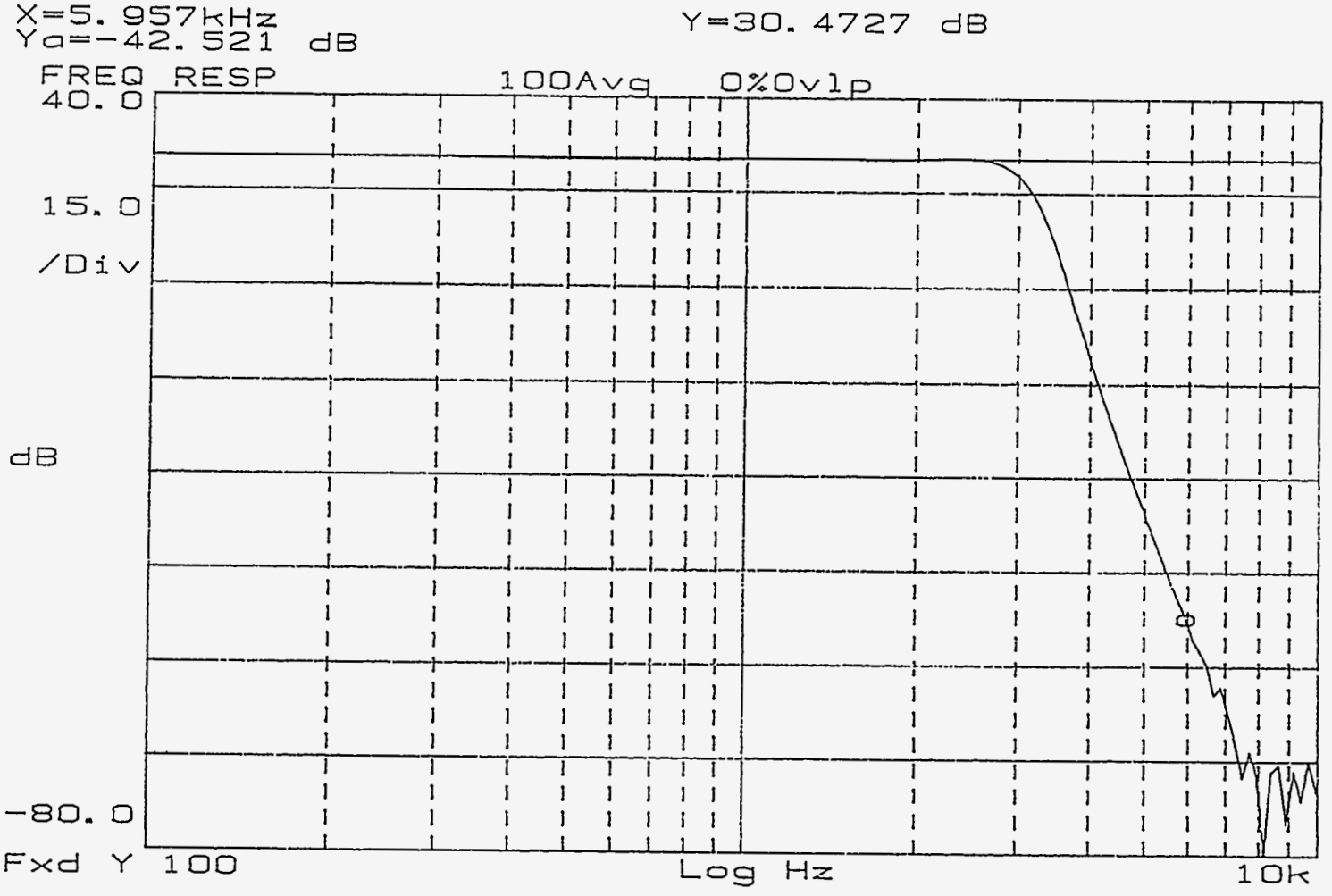

Table V.4. Panic Mode Voltage Ranges		
Data Receiver #	Panic Voltage Range (Volts)	Panic Voltage Setting, Nom (V)
1	1.7 to 3.0	2.4
2	3.4 to 4.6	4.0
3	5.0 to 6.3	5.7
4	6.9 to 8.2	7.6
5	8.6 to 9.3	9.0

V.3.d Wireline Interface Unit Design

The Data Formatter and Command Interface boards are physically located in the Wireline Interface Unit (WIU). A block diagram of the Wireline Interface Unit is provided as Figure V.5. As mentioned earlier, the Wireline Interface Unit provides electrical and mechanical interface functions for the Command Link and the Data Link. The wiring diagram for the Wireline Interface Unit is provided in Figure V.6. Note that the up hole end of the WIU is terminated in a Western Head Connector to allow it to be connected to the wireline termination package of the Chevron fiber optic wireline. The down hole end terminates into a standard 7-conductor wireline connector (Gearhardt-Owens). This down hole end is the termination point for the Receiver Interconnect Bus. The discussion of the electronics design for the Data Formatter and Command Interface Boards follow in the next two sections.

V.3.e Data Formatter Design

The basic system function provided on the Data Formatter PC Board is to convert the "bursted data from the Data Receiver units into a single, continuous, formatted data stream. The data timing and strobing functions originate in the Data Formatter unit which generates the master 1/8 msec. timing strobe and controls all data transfers. This "Fram_Str" (1/8 msec) signal is used in the Data Receivers to sample the current frame and synchronize the time sharing of the Interconnect Bus. Fram_Str is based on the 4.992 MHz oscillator in the Data Formatter (Figure V.5). The Fram_Str signal also controls the rate at which data is clocked out of the formatter to the surface. Thus, on average, bits are clocked into formatter at exactly the rate at which they are clocked out.

Data flow though the Formatter occurs as follows. The Fram_Str signal initiates the frame with the injection of a "Station ID" tag into the FIFO input, which begins with "F0" for the first Data Receiver packet. Data Receiver #1 then controls the Interconnect Bus for that first period and places its serial data and local clock onto the bus (Recall Figure V.3). The two signals are used to clock the 12 bytes of data into the serial to parallel converter. The parallel output is strobed into a FIFO input as well as an 8-bit wide sumcheck generator, where the sum is accumulated for the 12 byte packet originating from Data Receiver #1. The 8-bit sum is then strobed into the FIFO and the summing circuit is then

Figure V.5: MLSR Wireline Interface Unit

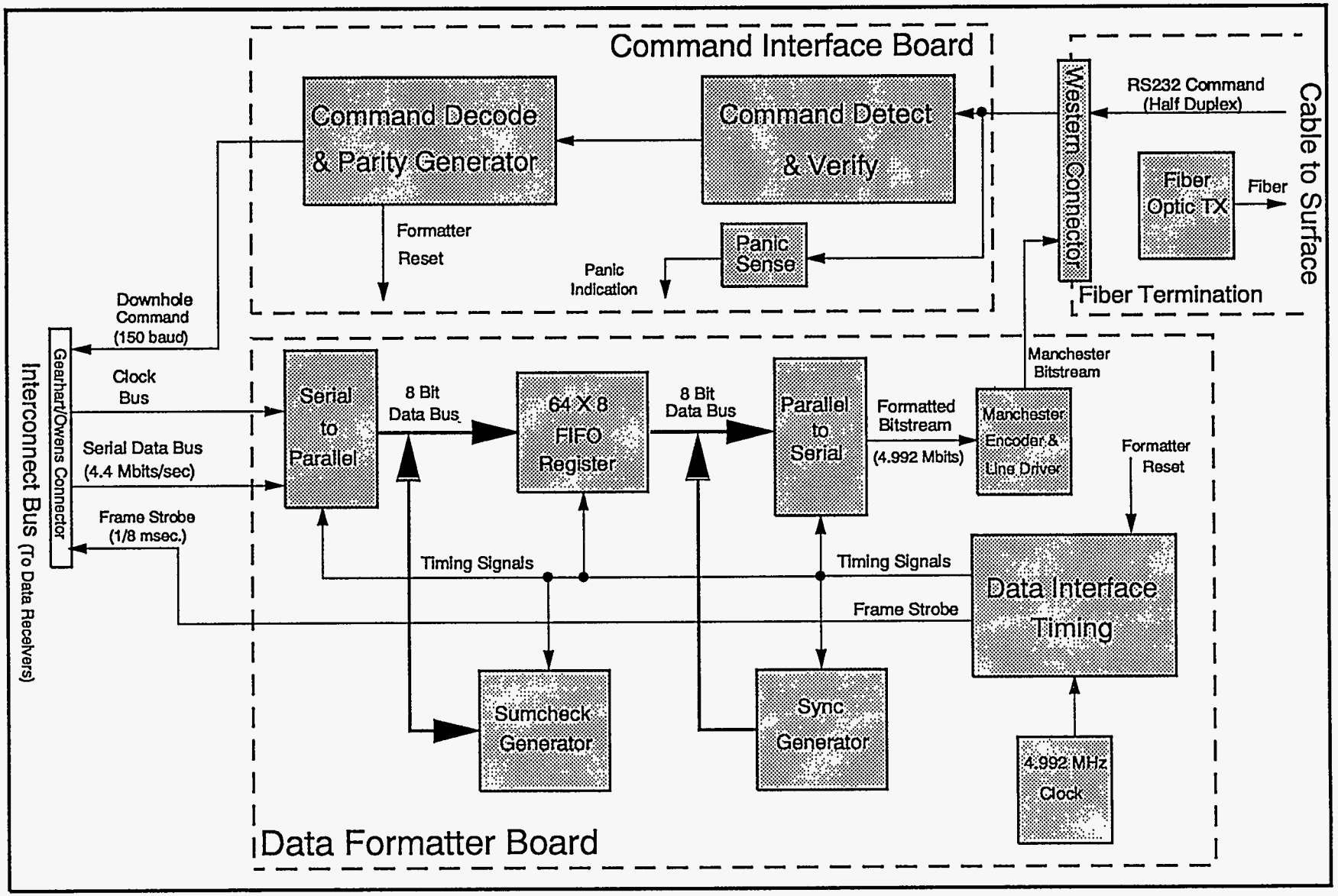

R. J. Franco
1-28-94
File: sande5

Figure V.6: Wireline Interface Unit Wiring Diagram

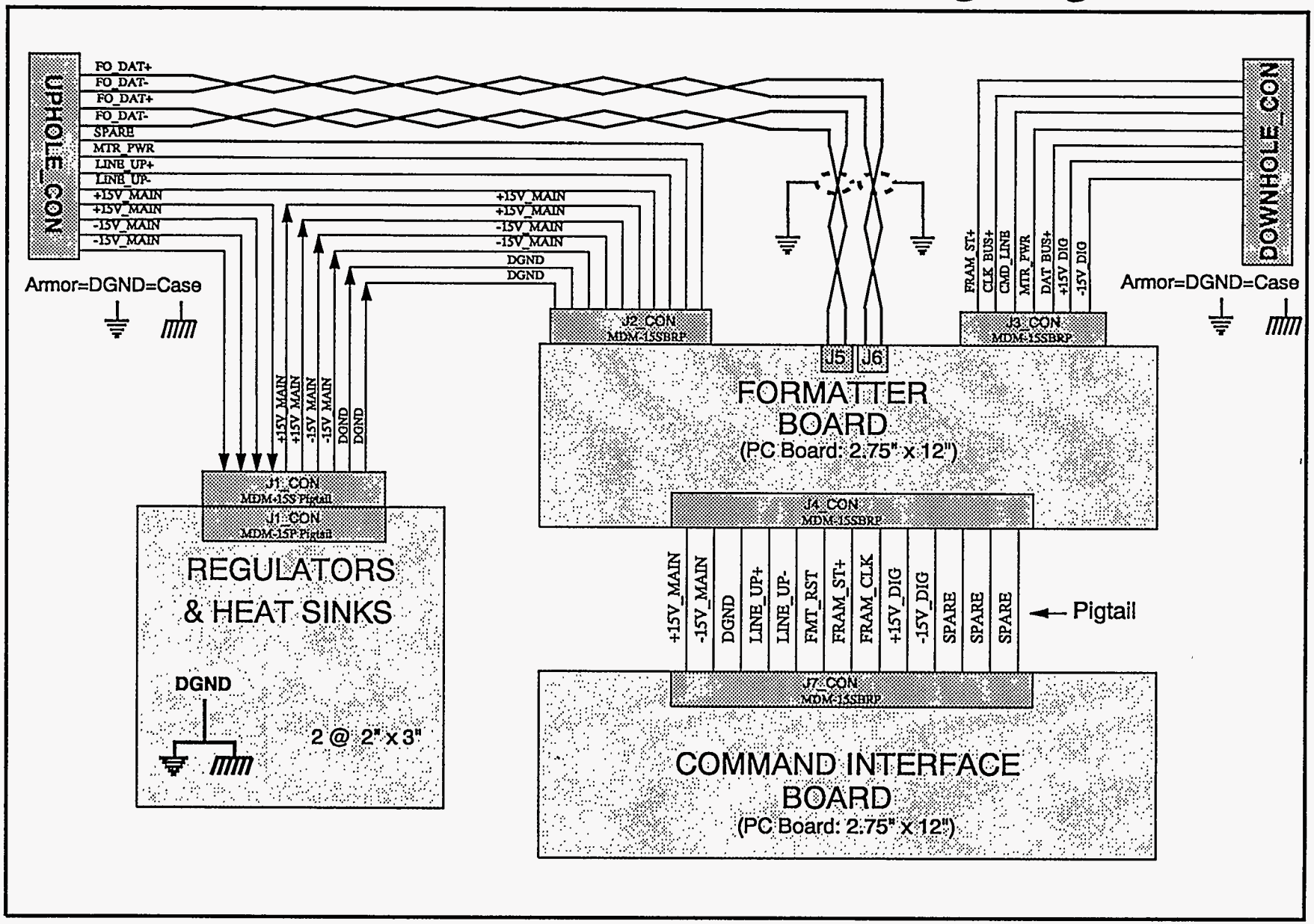

cleared to begin the sum for the next Data Receiver to report on the bus. In this manner, a packet of 14 bytes for each Data Receiver on line is accumulated into the FIFO. Any Data Receiver not connected will be represented as nulls in the output frame. Thus, exactly 70 bytes of data are clocked into the FIFO during each 1/8 msec. period of Fram_Str. Fram_Str is also the key timing signal in creating the formatted bitstream which is telemetered to the surface. This strobe is used to clock a 16 bit sync word into the data output buffer which is the identifying word in a "frame" of 78 bytes length (Figure V.7). The output frame consists of two bytes of sync, five packets of station data (14 bytes/packet) and six nulls. The nulls were added to provide the needed "extra" bytes to allow 1/8 msec. sampling with a total 4.992 Mbit/sec data rate. The FIFO data transfer was designed such that the last byte clocked out of the FIFO for a normal frame empties the FIFO. Any words remaining in the FIFO as the Fram_Str activates, are indication that the frame was bad. This allows the FIFO to be cleared at the end of each frame and forces any "byte-slippage" to be corrected on frame boundaries. It should also be pointed out that each 78 byte frame represents a single three axis sample from each of the five Data Receivers.

The output of the FIFO is clocked continuously to the input of a parallel to serial converter, which has as its output a continuous, formatted bitstream. The Manchester code was chosen for transmission over the fiber link to allow reconstruction of the clock at the up hole receiver. The output of the Formatter is a differential line driver of the Manchester data signal. This signal connects to the fiber optic LEDs housed in Chevron's wireline cable head.

V.3.f Command Interface Design

The functions provided on the Command Interface Board center around providing the down hole logic for the command signal handshake described in section B.4. and decoding the commands for execution. As mentioned before, the host computer initiates each command and transmits it in RS232 code down the wireline. The Command Interface circuit receives each command and echoes it back up hole. If the command is echoed correctly, the Host Computer issues a verify code and the Command Interface circuit will execute the command. The commands in current use are defined in Table V.5. Note that all Formatter commands have high in the MSB. These codes are used only in the Data Formatter and are decoded on the Command Interface Board for local use. These commands are not relayed down the Interconnect Bus since they are not decoded in the Data Receivers. Any commands with MSB of "0" are echoed down the Interconnect Bus with parity to be decoded in the Data Receivers. Note, only the Motor On command is decoded to address each Data Receiver individually. All other commands are global and are executed in all Data Receivers each time they are issued.

The other function provided in the Command Interface circuit is the detection of panic condition for motor control. The Control Panel on the surface has a switch allowing the RS232 control line to be switched with an Analog Panic Voltage. If digital control to the motor fails, this analog voltage can be used to address each motor as discussed before. The function in the Interface Control Unit is simply to detect the condition and switch the analog panic voltage onto the Fram_Str signal so that it will be detected in the Data Receivers.

Figure V.7: MLSR Data Format

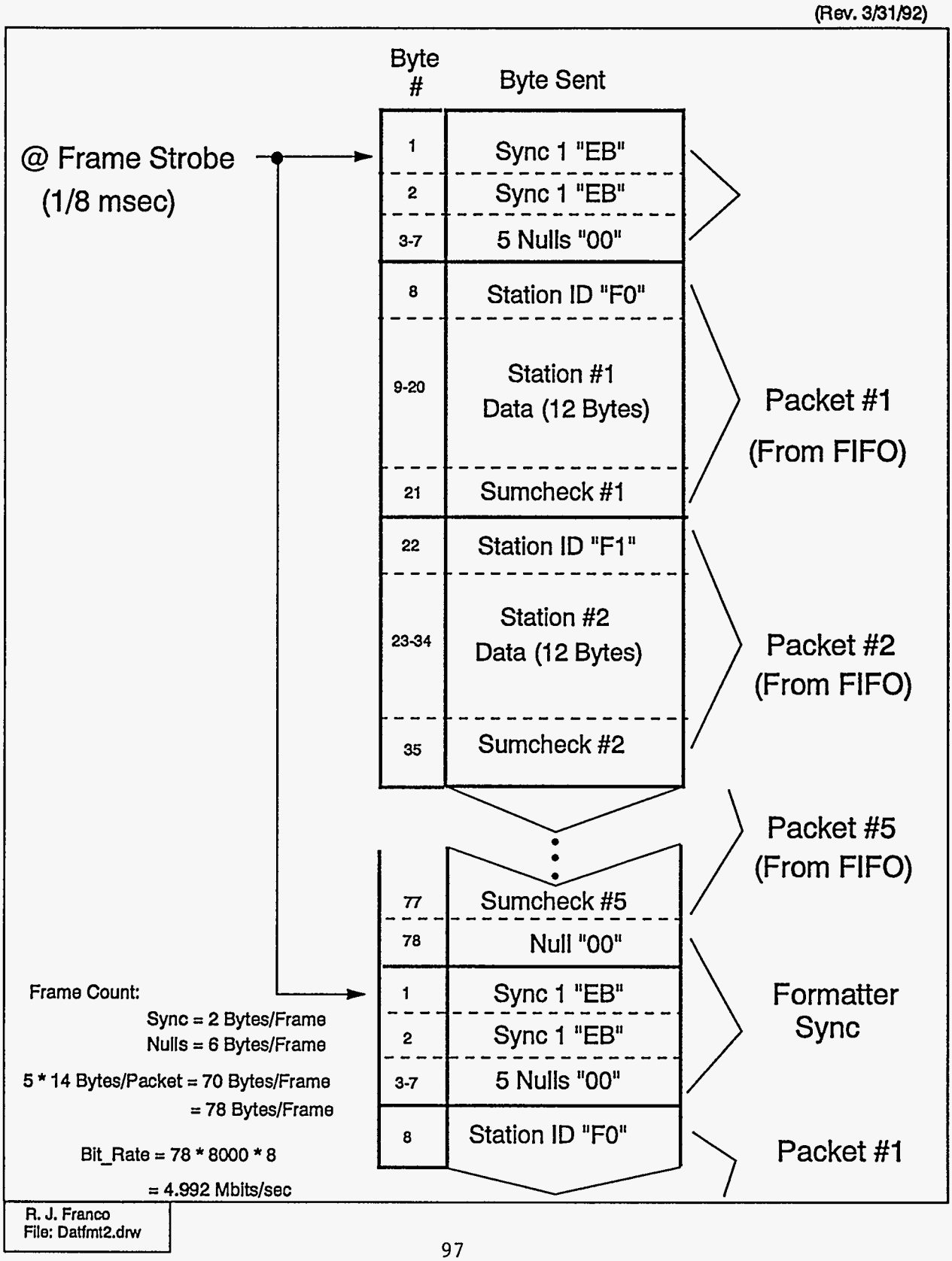

Table V.5. Digital Command Codes								
Formatter Function	MSB	B6	B5	B4	B3	B2	B1	B0
FMT_Reset	1	0	1	0	Don't Care			
FMT On	1	0	1	1				
Verify	1	1	0	0				
Data Receiver Function								
Motor On	0	0	1	0	(Unit Address, Start @ 0)			
Calibrate (Cal 1)	0	0	1	1	Don't Care			
Motor Off	0	1	0	0				
Diagnostic (Cal On)	0	1	0	1				
Dig Reset	0	1	1	1				

V.3.g Fiber Optic Data Detection

As mentioned previously, the data modulated onto the optical fiber for transmission up hole is encoded with Manchester format at 4.992 Mbits/sec. The up hole end of the fiber is terminated into the reeling drum on the Chevron wireline truck. The fiber optic receivers of Chevron's original design are deployed in the truck and are in current field test use. This design allows the fibers to be terminated before the signal passes through the slip rings. The fiber optic receiver boards include 50Ω driver devices which buffer the receiver output onto coax which is then passed through the slip ring and up to the control panel in the truck. The fiber optic receivers are powered through the slip rings with AC/DC converters residing inside the drum. The Chevron wireline actually carries three fibers and has drivers and receivers for each. The receiver circuit also provides DC status voltages to indicate the automatic gain control (AGC) setting in the receivers. These AGC voltage readings offer an indication of the optical signal strength at the optical receiver inputs and are valuable diagnostics. The detected Manchester data is then connected by coax into the Control Panel (Figure V.8) for further processing. Schematics for the fiber optic transmitter and receiver circuitry are not included because the design is proprietary. The design was used as a matter of convenience and has been reliable. However, the design is based on 1970's technology and should probably not be applied in future applications.

Figure V.8: MLSR Control Panel and Equipment Interface

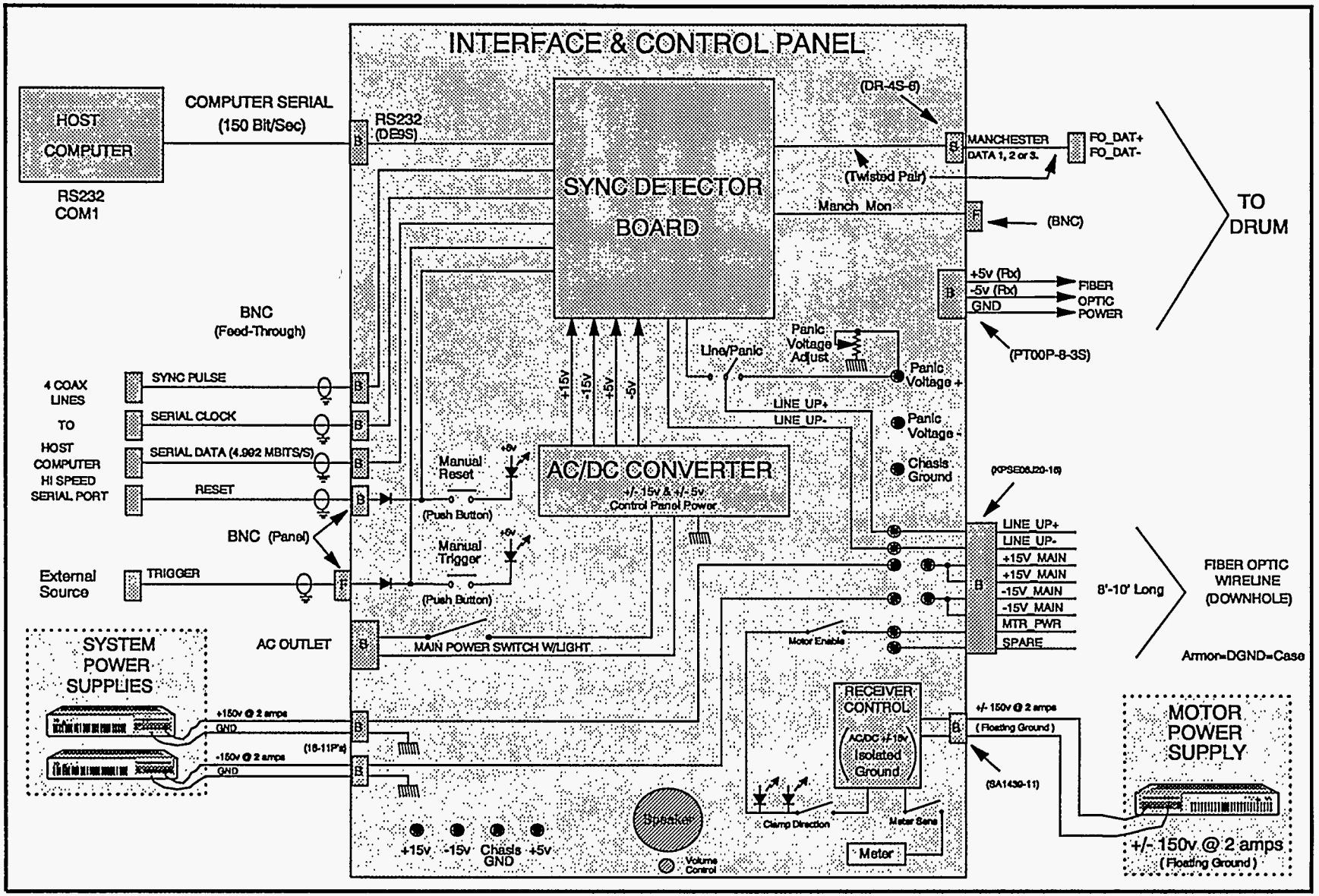

File: Sande8, 1-28-94

V.3.h Up Hole Clock and Sync Detection

The Manchester data recovered from the fiber must be converted into a serial format suitable for the interface included in the DSP (digital signal processing) card in the Host Computer. This interface requires serial data, coherent clock, and a sync pulse marking the MSB of the first sixteen bit word in the frame. This function is provided by the Sync Detector Board in the Control Panel (Schematic included in Appendix C). Since only one fiber is used, all three of these signals are embedded in the Manchester coded signal. The first operation required is to decode the Manchester signal and recover the clock. The outputs of the Manchester decoder (MAD-85) include the serial data and coherent clock. Recovering the sync pulse is accomplished by searching the serial data for the "EBEB" pattern which marks the beginning of each data frame. This is accomplished with a sixteen bit digital magnitude comparator running against the recovered Manchester data as it clocks through. When a sync match is found, a sync pulse one bit wide is activated to mark the MSB of the first word in the frame. This sync pulse is also used as a synchronous strobe to sample the up hole sweep channels. It is quite adequate for this purpose, since it is synchronous to the same clock which controls sampling in the Data Receivers down hole.

V.3.i Up Hole Command Interface Design

Two control functions are also included in the Sync Detector Board in the Control Panel. The RS232 command signal (150 baud) is connected to the wireline for half duplex communication. The Host Computer initiates all commands, and the communication proceeds. A line driver is included in the Sync Detector Board to buffer the computer from the long wireline cable. The "panic" condition, mentioned before, is also controlled from the Control Panel. There is a switch on the panel which determines whether the digital computer command signal is sent down hole or the analog panic voltage signal. The panic voltage can be set to the desired voltage by controlling a potentiometer on the front of the panel.

The other function implemented in the panel is the control and monitoring of the clamping motors in the Data Receivers. As has been mentioned, the digital control interface allows each motor to be individually addressed. The power supply which drives the motor current is patched into the Control Panel, which includes switches to connect motor current and control it's direction (i.e. clamp or unclamp). Another feature useful in monitoring the clamping process is an audio amplifier and speaker which is modulated by the motor current. Vibrations and motor sticking can be detected through this audio signal.

V.4. HIGH TEMPERATURE DESIGN AND TESTING

V.4.a High Temperature Electronics Design Approach

The temperature issue was addressed in the design phase by first identifying the basic circuit functions required and testing components individually to verify their performance at temperature. Having determined the need for logic devices, temperature tests were run on several FACT logic devices

(54ACXXX) to determine power stability, propagation delay, and other key specifications. These devices were found to function very well at 200° C and were used extensively in the design. A similar approach was used to determine the suitability of Altera EPLD devices, crystal oscillators and other digital devices. The end result of the investigation was to conclude that most CMOS devices work very well in this environment. Analog to Digital Converters (ADC), sample and hold, amplifiers, operational amplifiers, and analog multiplexers were chosen and tested with a similar approach. The Harris and Burr Brown devices based on dielectrically insulated field effect transistors (DiFET) processes were found to work very well and used in the design. Bipolar devices of any sort shut down at about 130° C. It was discovered that commercial temperature devices made from the "high temperature" processes mentioned above work well at temperature. Therefore, it is not necessary to purchase military temperature part unless commercial parts are not available in ceramic or hermetic can type packages. Commercial temperature parts in ceramic or hermetic packages can be used, plastic should be avoided. A more detailed discussion of high temperature electronic design rules is provided in Appendix D.

V.4.b Laboratory Temperature Testing

Early in the design stage of this program, temperature tests were performed on an analog prototype of the signal conditioner and ADC front end of the Data Receivers. These tests proved the functionality of all the critical analog circuits up to 200° C. Dynamic range, linearity, and cross talk were all found to meet the desired specifications, so the design was continued based on these devices. As mentioned above, all of the digital devices used in the design were also tested individually to 200° C and found to be functional. The design of the rest of the electronics was subsequently completed and the units have been field tested extensively at lower temperatures. Temperature testing of the entire system at 200° C has not been possible to date, because the accelerometers purchased for the early development are only rated to 130° C (Although they are available at higher price to operate to 175° C.). Temperature tests of all down hole circuitry have been completed to 130° C and the unit is fully functional to that temperature.

V.5. FURTHER DEVELOPMENT NEEDS IN TELEMETRY AND INSTRUMENTATION

There are several development needs in the area of Telemetry and Instrumentation of the MLSR system which would expand its range of applications. As mentioned above, full unit testing to 200° C has not been done and would be a useful exercise to insure the systems performance in that arena. The other approach to this concern is to simply broaden the application of the unit to deeper wells to determine the upper limit of the system. This approach is fine, as long as, the clients requiring these tests are made aware of the risk in testing beyond the unit's known operational limits. Full unit temperature testing is certainly feasible at Sandia National Labs (SNL) and is advised to minimize client risk.

A design enhancement of potential interest is to allow longer interconnect runs between the Data Receivers. Spacings of up to 50 feet between Data Receivers has been suggested as desirable. Because of the high bandwidth required in the interconnect lines, it is likely that custom interconnects with twisted pair for high frequency signals will be required. This issue has been addressed already and testing is likely to continue in this area. A second design enhancement that has been proposed is to increase the number of Data Receivers in the string to ten. The design of the Data Receivers

doesn't change at all for this upgrade, but reprogramming of EPLD devices controlling the data format would be required. This design upgrade would also require evaluation and testing of the fiber optic link to handle the increased bandwidth in transmission to the surface.

A third design feature which has been raised is that of using geophones as the Data Receiver sensors. The electronics in the Data Receivers are designed to accept geophone inputs and noise performance is suitable for this application. However, mechanical mounting of the geophones would need to be investigated, as well as, further system level testing with the geophones installed.

VI. UP-HOLE COMPUTER AND DATA ACQUISITION

As stated in the previous chapter, the Multi-Level Seismic Receiver (MLSR) utilizes real-time digital seismic data telemetry. The down-hole receivers transmit digital seismic data to the surface, which must, in turn, be received by a digital data acquisition system. The digital data acquisition system must perform the functions of front-end signal processing and seismic data storage. This chapter describes the real-time digital data acquisition system developed for this purpose.

VI.1. UP-HOLE COMPUTER HARDWARE DESCRIPTION

The up-hole computer accepts data from the real-time digital telemetry system described in the previous chapter. The up-hole computer is actually a parallel processing system which consists of two main processors. The front-end processor, based around a Texas Instruments TMS320C30 DSP chip, accepts and processes data from the telemetry system in real-time. The user-interface processor, based around an Intel 80486 CPU chip, performs the tasks which are not time-critical: the user interface and data input/output to/from various peripheral devices. A block diagram of this parallel processing architecture is depicted in Figure V1.1.

The front-end processor is a commercial AT-style plug-in board from Spectrum Signal Processing, model "TMS320C30 DEVELOPMENT BOARD". It consists of a 33 MHZ TMS320C30 digital signal processor, 128kwords of 0-wait-state static RAM, 4MWords of Dynamic RAM, and two channels of analog data acquisition. The C30 processor executes 32-bit floating point instructions in a single cycle time of 60 ns. Due to parallel multiply and add circuitry, it is capable of a throughput of 33 MFLOPS. The C30 has extensive I/O capability which provides an interface to both the telemetry system and on-board A/D converters. The telemetry data is delivered to the C30 directly through its high-speed synchronous serial port. This serial port is capable of data rates up to 8 MBits/sec. Since the telemetry system data rate is 1 Mbit/sec/sonde, real-time reception from a 5-sonde receiver is easily handled. The on-board A/D converters on the Spectrum board are memory mapped to the C30 processor and provide two channels of 16 bit analog-to-digital data conversion. These A/D converters are used for auxiliary up-hole data acquisition, such as the recording of pilot sweeps and fiducial signals. A unique feature of this system is that the auxiliary A/D converters are synchronized to the down-hole A/D converter clock. This feature is implemented by utilizing the 8 KHz frame strobe generated by the telemetry system to trigger auxiliary A/D conversions.

The user-interface processor system is an 80486 PC/AT compatible computer. It is housed in a field-rugged enclosure, commercially known as the OYO Geospace DFM-480. The DFM-480 contains 16 Mbytes of RAM, and has extensive expansion capability through its EISA bus slots. The DFM-480 houses a built-in VGA monochrome monitor and a built-in high-resolution thermal plotter. Other features include an interface to 9-track seismic tape devices, an Ethernet port, and the Micro-Max array processor. The system is therefore a stand-alone field-rugged seismic data acquisition system for digital seismic borehole receivers.

Figure VI.1 Block Diagram of the Borehole Data Acquisition surface hardware.

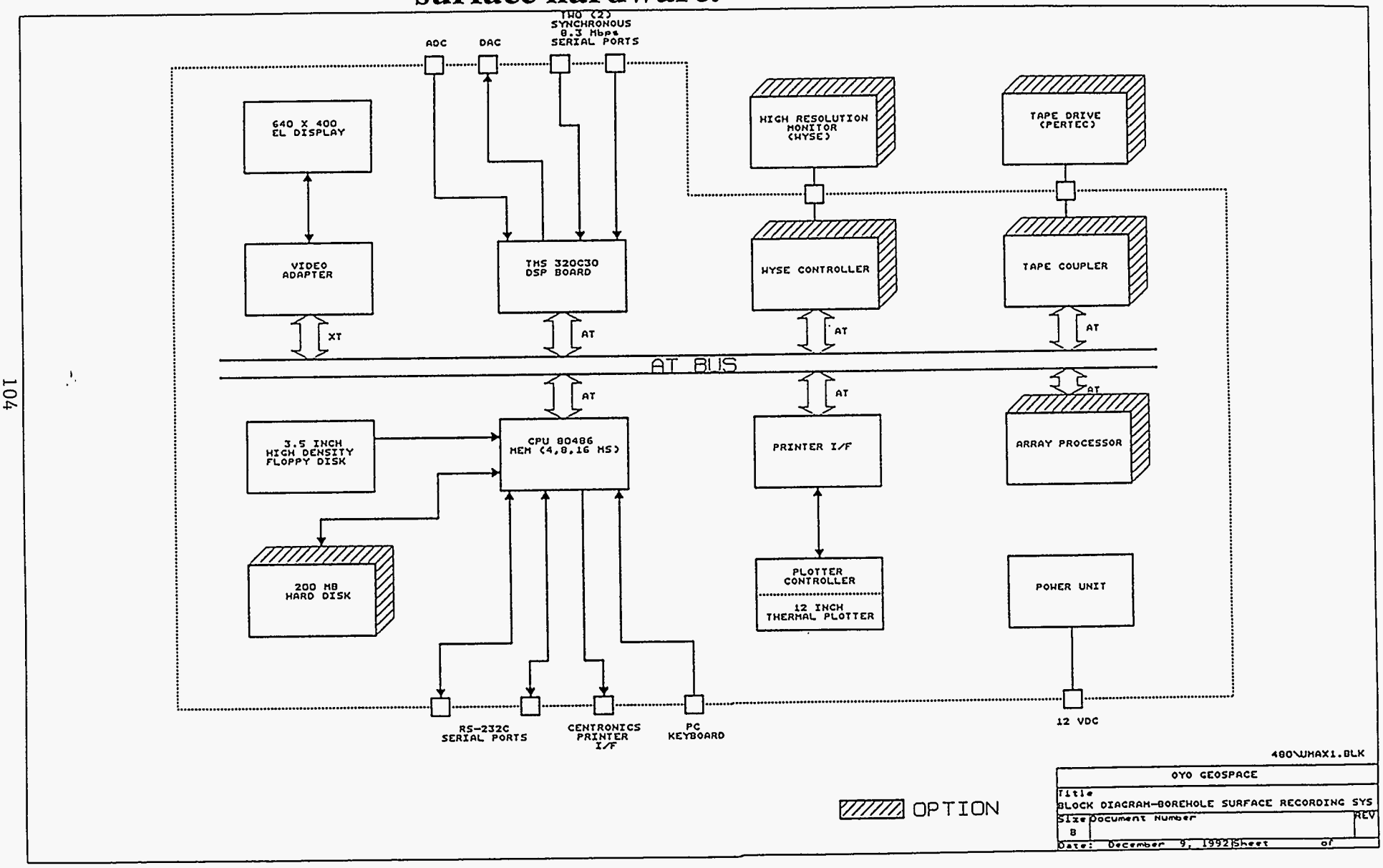

VI.2. UP-HOLE COMPUTER REAL-TIME SOFTWARE DESCRIPTION

As the serial data is clocked into the C30, real-time digital signal processing routines are performed. The C30 serial port is reset each time a start-of-frame strobe signal is received. In between frame strobes, the C30 serial port buffers each 16-bit packet to form a data word. The software polls the serial port until a 16 bit data word is available. Once a 16-bit data word is available, the data word is operated upon. Recall from the previous chapter that the telemetry data frame consists of 78 bytes. This represents 39 unique 16-bit words that must be processed. Each 16-bit word is processed differently depending upon whether it is a synch word, a station id/ checksum word, or seismic data. The real-time software keeps track of the current word's location within the data frame and processes it accordingly. Since there are 39 words which must be processed in 1/8 of a millisecond (the telemetry frame rate), the real-time operations must be limited to 3.2 micro-microsecs of computations per 16-bit word. This corresponds to a maximum of 54 cycles of the 60-ns C30 clock. This means that the C30 can execute up to 54 single-cycle instructions for each data word input to the C30 serial port. However, memory read/write wait states must be accounted for, and the total number of available instructions is somewhat less than 54.

The real-time operations performed on the input serial data stream are as follows:

- checksum calculation and comparison with transmitted checksum

- data correction when a checksum error occurs

- station i.d. checking

- correction of gain and offsets for each channel's x1 and x32 amplifiers

- Instantaneous floating-point calculations (combination of each channel's x1 and x32 16-bit words into a 21 bit word)

- demultiplexing of multi-channel data

- data stacking to memory (signal averaging)

- statistics calculations (mean and rms for each data channel)

- miscellaneous "book-keeping" operations, and data integrity checks.

The real-time software stores this processed data into the large on-board DRAM memory. The data stored to memory is a trace-sequential 32-bit floating-point format. Once the desired amount of data is acquired, the real-time software sets a memory-mapped flag which alerts the 486 processor that the real-time task is done. The real-time software will then wait for the 486 processor to reset the flags, indicating that the system should arm and record another set of seismic data.

The software running on the C30 also can be commanded by the 486 to perform various non-real-time operations on the seismic data in its DRAM memory buffer. These operations execute extremely rapidly and include: digital filtering, decimation, cross-correlation, fast Fourier transformations, and the generation of test data. All of these operations are transparent to the user: the user simply selects the desired acquisition/processing parameters, and the 486 commands the C30 to execute the required flow of operations.

VI.3. UP-HOLE COMPUTER USER INTERFACE SOFTWARE DESCRIPTION

The user-interface software executes on the 486 processor and runs in parallel with the real-time operations. The user interface software is based on the very popular DAS-1 program developed and marketed by OYO Geospace Corp. Basically, the user-interface software, referred to as BHDAS, is a menu-driven program which allows the user to set acquisition, processing, and I/O parameters. It takes the user-desired parameters, converts them as required, downloads this information to the C30, and commands the C30 to begin its tasks. Once the C30 completes its tasks, the BHDAS software uploads the seismic data and performs a variety of functions. (Actually, the BHDAS software performs some of its functions while the C30 is acquiring/processing data, so that it is really a parallel processing arrangement). The tasks performed by the BHDAS software include:

- conversion of seismic data to standard seismic format (e.g. SEG-D)
- storage of standard seismic data to tape/disk/or network
- display of seismic traces on CRT
- printing of seismic traces on thermal plotter
- all user interfacing and conversion of user entries into processing parameters
- monitoring and display of seismic acquisition status
- full control of down-hole systems including motor control, diagnostics generation, and calibration
- a variety of quality assurance routines including FFT display, correlation display, and statistics tabulation

The full set of features and user interface functions of this software package are too extensive to list in this document. Figures VI.2 and VI.3 are provided to give the reader a feel for the features and menu structure of the software.

System Acquisition Menu

Figure VI.2

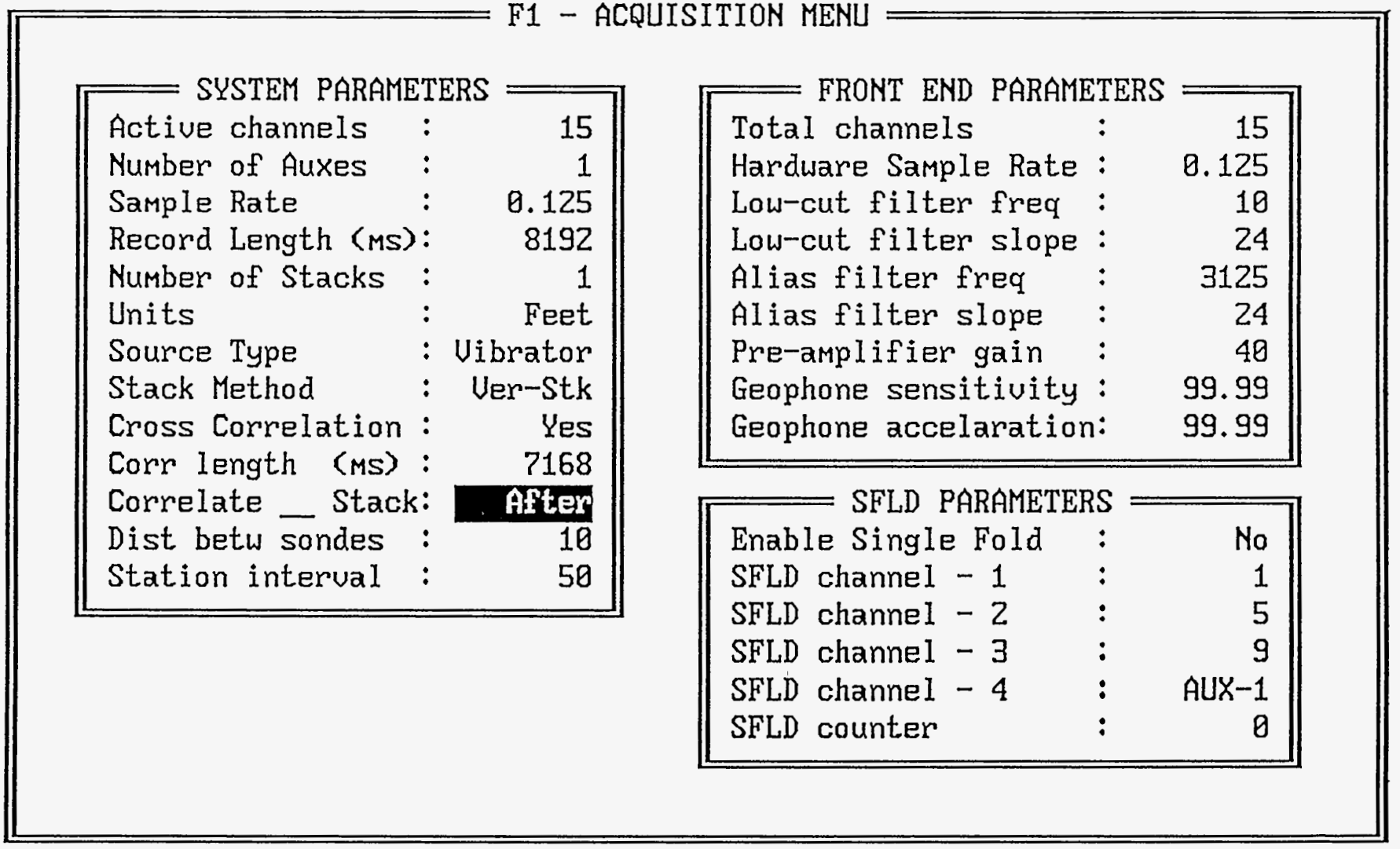

Seismic Display Screen

Figure VI.3

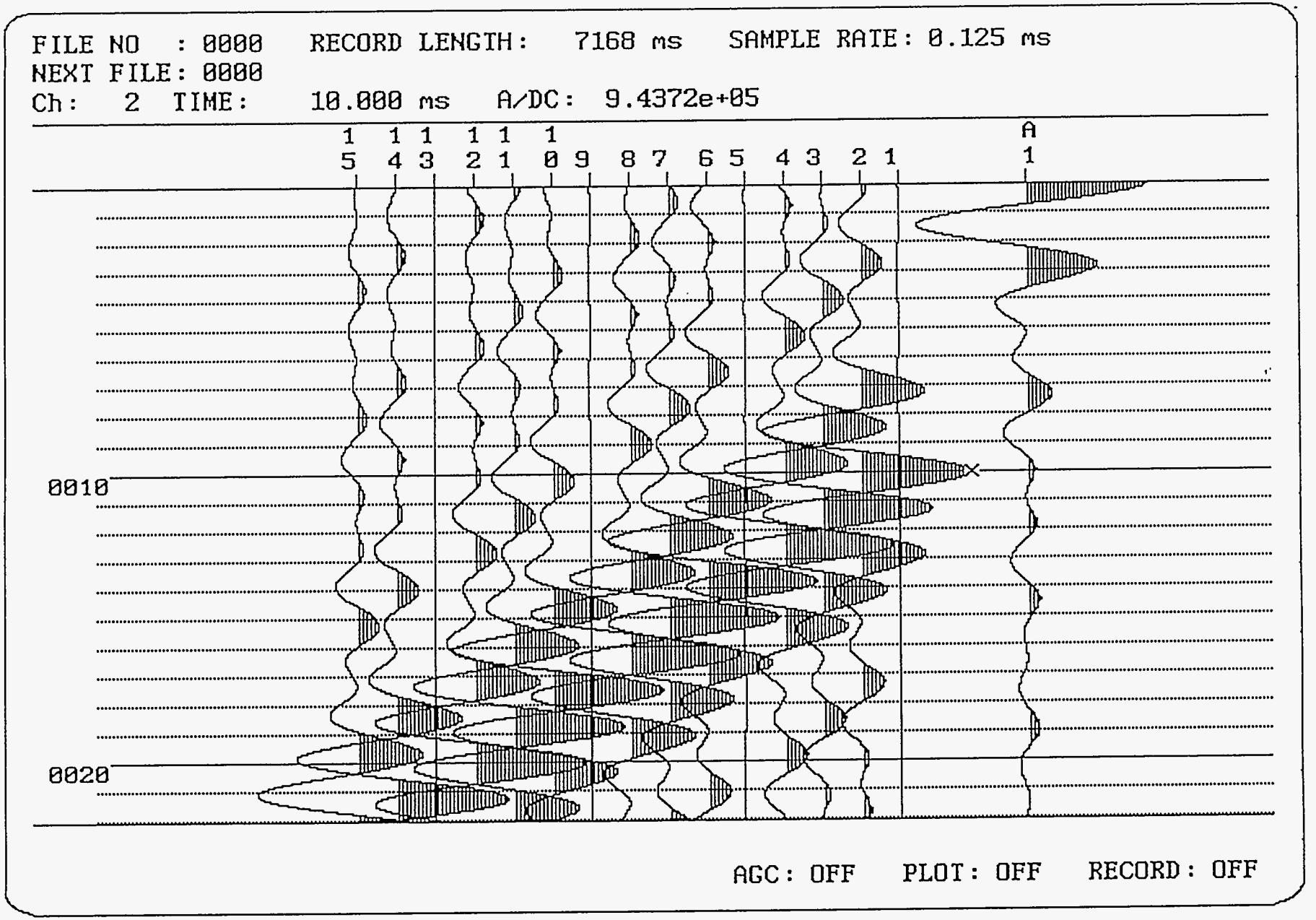

VII. WIRELINE CABLES

The seismic receivers can be operated in two modes: as a single analog receiver; or as a multi-level seismic receiver system. In the single analog receiver mode, a standard 7-conductor wireline is used to transmit analog data from the receiver to the surface. In the multi-level configuration, a fiber optic wireline is used to transmit digital data to the surface, with short lengths of 7-conductor wireline serving as a digital data bus between seismic receiver modules. The following sections describe these connecting cables in more detail.

VII.1. ANALOG OPERATION - 7 CONDUCTOR WIRELINE

VII.1.a Clamp Controller For Single Sonde Analog Operation

In analog mode, a long length of standard 7-conductor wireline is used to connect the sonde to an uphole standard seismograph recorder. Accelerometer signals are carried on the 6 outer conductors of the wireline. The 7th conductor (central conductor) and the cable armor are used to carry power to the d.c. clamping motor.

The schematic for the clamp controller for the analog receiver is shown in Figure VII.1. It consists of a voltage and current regulated DC power supply, a current measuring resistor with a dual range meter and an audio amplifier for verification of clamp operation, a double pole double throw clamp direction control switch, and a double pole double throw motor enable switch. The motor in the sonde is connected to the wireline by pin 7 and the armor of the Gearhart-Owens connector. For safety the armor is always connected to earth ground while pin 7 is at earth ground potential through the motor enable switch when the clamp motor is inactive. To operate the clamp, power is applied to the motor via the motor enable switch with the clamp direction switch determining the proper voltage polarity for the clamp to extend or retract. The variable power supply was chosen so that compensation could be made for the voltage drop from different wireline units used to lower the tool into the well bore. This capability allows the motor to have full voltage applied while safely limiting the current available to the motor. The current that the motor is drawing is measured by observing the voltage drop across a 10 ohm resistor in series with the motor. This measurement is made with a switch selectable dual range meter, one range is for the motor free run current measurement, while the other is for the motor stall current measurement. Also connected to the current measuring resistor is an audio amplifier that while the motor is running amplifies pulses in the audible range that are generated by the motor armature. This signal can be used by the operator as a diagnostic to determine if the motor is functioning properly.

When used in analog mode, an important limitation must be considered. First, due to line resistance in the cable, the voltage delivered to the motor is less than the voltage at the surface power supply. Therefore, the power supply voltage must be increased in order to compensate for the line drop. This compensation is simple to perform using the following procedure:

1.) attach receiver to the end of the wireline via the Gearhart-Owens 7-conductor connector.

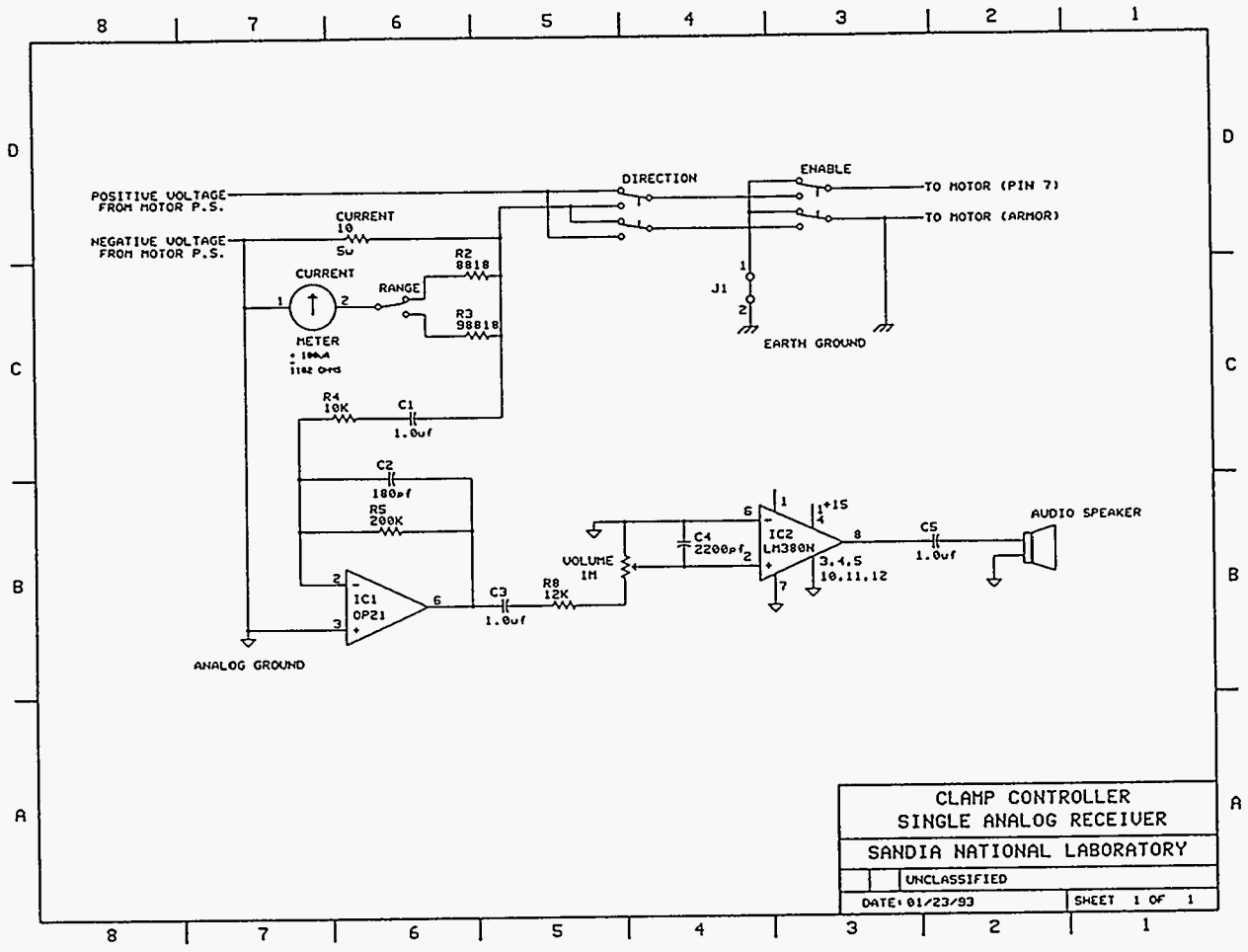

Figure VII.1 Clamp Controller for Single Analog Seismic Receiver

2.) set the power supply voltage at 115 volts (the rated voltage of the d.c. motor)

3.) push the clamp button, and allow the shoe to run to full stall

4.) the stall current must be between 0.65 and 0.7 amps in order to achieve full clamp force. Any readings lower than this indicate a voltage line drop, resulting in less than 115 volts delivered to the motor. Slowly increase the power supply voltage until the stall current reaches the 0.65-0.7 ma range. At that point, adequate line drop compensation is provided.

5.) It is not recommended that the power supply be set to voltages above 210 volts d.c. Only very long cables would require such a high voltage. In general, 7-conductor cable lengths (using #20 wire) up to 20,000 ft can be handled in this manner.

VII.1.b Data Acquisition and Monitoring For Analog Receivers

Data acquisition for all analog testing was done using an EG&G model 2401 seismograph. The sonde is connected to the data acquisition system through the wireline, the control unit, a Wilcoxen model PR710-3 power unit/amplifier, and an attenuator before entering the seismograph. The signals were attenuated because the input to the seismograph is set up for non amplified geophones with a maximum output of +/-24 millivolts. The output from the amplified accelerometers are +/-5 volts. The attenuators used were Kay Elemetrics model 437A switch selectable attenuators. The seismic signals were recorded with a sample rate of 250 microseconds per point and suitable record lengths determined by the various sources used and site characteristics. Monitoring was done using a Rockland model 9040 dual channel signal analysis unit in place of, or in parallel with the seismograph. The monitoring generally consisted of setting the Rockland up for spectral analysis and observing the signals for noise or resonances.

The analog sonde is connected to the wireline via a Gearhart-Owens 1-1/2 inch 7 conductor cable head. The sonde is suspended in or over the well by a tripod. The armored cable route being from the winch unit to a sheave wheel anchored to the well head up to and over a sheave wheel suspended from the tripod and then down into the well. The signals from the pass sonde, through the armored cable to a set of slip rings. The signals are then cabled to a patch panel and routed to the appropriate connections on the control box (the motor drive line to the motor control section and the accelerometer lines to the power supply/amplifier unit). This arrangement allows the operator to move the tool in the well in a safe manner without making and breaking any connections. The general operating sequence once all the connections are made is to first zero the tool at ground level then lower the tool to a depth of interest, clamp the tool in place, put some slack in the cable to eliminate surface noise that would travel on a taught cable, install a foam plug at the well head to eliminate wind noise, and then begin diagnostic testing of the sonde for performance verification. This testing consists of making noise measurements, firing test shots for signal adjustments and clamp verification. At this time if all systems are operational the test may begin as required by the test plan developed by the project leader. It is important to note that when using the analog 7-conductor wireline method, excessively long cables can result in reduced seismic bandwidth. This results from the line capacitance and the limited drive capabilities of the accelerometers. It has been determined that a 13,000 ft 7-conductor cable (with #20 AWG wires) provides a -3 dB bandwidth of approximately 800 Hz when using a 9 ma constant current

diode. Longer cable lengths, or smaller gauge wire would result in a lower bandwidth. High constant current diodes can be used to increase the bandwidth when driving long cables.

VII.2. DIGITAL OPERATION - FIBER OPTIC WIRELINE

When operated in the multi-station mode, a special fiber optic wireline is used to transmit digital seismic data from the tool string to the surface. The wireline used in the testing of the MLSR was developed by Chevron Corp. in the early 1980's and is described in detail in [VII.1]. Figure VII.2 shows the geometry of this cable. As shown in Figure VII.2, it consists of a central tube containing 3 stress-relieved multi-mode optical fibers. The central tube core is surrounded by 8 electrical conductors. The MLSR uses only one of the three fibers for data transmission to the surface. The MLSR uses the electrical conductors for electrical power to the tool string and to transmit/receive low-speed telemetry commands.

The fiber optic wireline is supported on the up-hole end by a standard Gearhard Owens logging truck. This truck provides the winch for deploying the wireline, and also has dog-house space for housing the up-hole components of the MLSR. The fiber-optic wireline is terminated up-hole inside the rotating winch drum. Inside the drum are opto-electric converter circuits (developed/provided by Chevron) for conditioning the high-speed data signals. The high-speed signals and 8 conventional conductor signals are brought to the dog-house through high-bandwidth electrical slip-rings.

The down-hole end of the cable is terminated in a modified Western logging head. This head terminates the fiber and contains electro-optic converters. This logging head directly mates to the MLSR Wireline Interface Unit. Further information on the wireline cable and the termination methods are provided in [VII.1].

VIII. LABORATORY AND FIELD TESTING

Numerous laboratory and field tests were undertaken to evaluate the performance of the receiver system and its components. All field tests were performed at industry-owned sites to help foster feedback from industry to the National Laboratory. Several of the laboratory and field tests are described in this chapter.

VIII.1. SINGLE SONDE TEST (ANALOG)

VIII.1.a Laboratory Testing and Quality Assurance

A significant series of laboratory tests were performed on the sonde in order to verify that the prototype meets the design requirements. These tests also served as a quality assurance measure prior to testing the prototype in a oil field situation. Below is a list of some of the tests that were performed.

High Data Rate Fiber Optic Cable

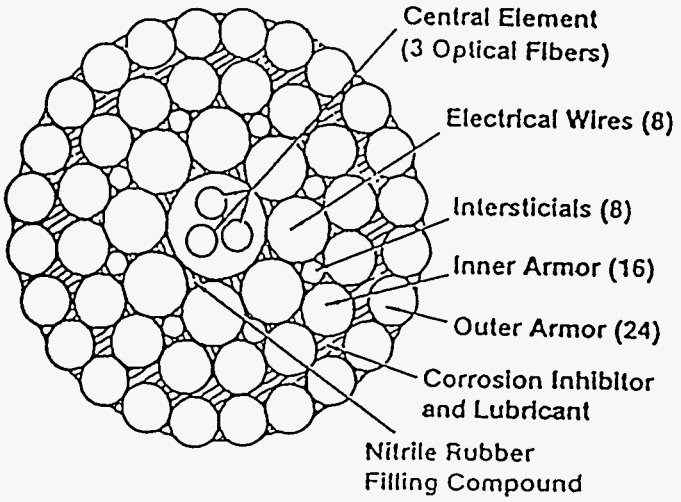

Figure 1: Cross section of cable.

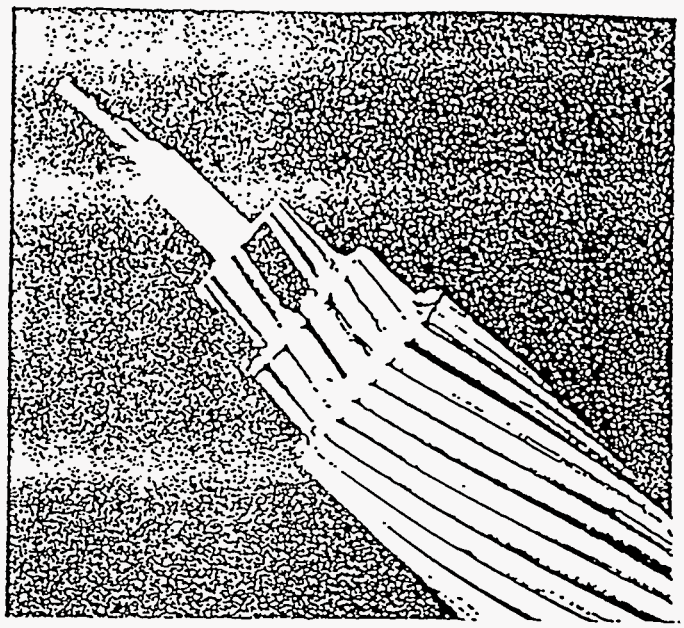

Figure VII.2 Fiber Optic Wireline Construction

1.) Pressure Testing: The sonde was pressure tested to 3000 psi. This assured that the sonde and its internal components would survive borehole pressures.

2.) Clamp Arm Testing: Clamping force was measured and the resulting clamp-force-to-weight ratio is in excess of 5:1. Clamp reliability and repeatability tests were run by sequential tool clamping/unclamping in a dry steel casing.

3.) Accelerometer Testing: Each accelerometer in the tool underwent laboratory calibration and verification. Noise floor of the accelerometers was measured and found to conform with the specifications that Sandia required Wilcoxon Research to meet(-158 dB re 1 g @ 100 Hz and -163 dB re 1 g @ 1000 Hz). The accelerometers were tested for operation on a long wireline and proved effective for wirelines up to 13000 ft length. Grounding configurations for the tool/wireline configuration were established and tested.

4.) Sonde Free-body Frequency Response: The tool was placed on a shake table in its unclamped mode. Reference accelerometers were placed on different portions of the sonde and compared with the internal accelerometers. No internal tool resonances were found within the range of the experimental apparatus (10 Hz to 1000 Hz).

5.) Sonde Clamped-in-tube Frequency Response: This test turned out to be more difficult than initially anticipated; all the shake table fixtures at Sandia exhibit resonances below 1000 Hz. The best fixture was found to be a solid cube of granite (36 inches to a side) with a water-filled 5" borehole. This fixture is a reasonably fair simulation of the borehole environment. Due to the finite size of the block, however, modes were excited in the block at frequencies above 800 Hz. Below 800 Hz, a reaction-type shaker was used to excite the block, and the clamped accelerometer response was compared with accelerometers cemented to the walls of the water-filled borehole. The results of these tests showed that the clamped tool exhibits a flat response to at least 800 Hz.

4.) Uphole Electronics Testing: The uphole electronics used to condition the accelerometers and clamp the tool were fully evaluated prior to the field experiments.

VIII.1.b Humble Field Seismic Receiver Tests

The prototype sonde and its uphole electronics were taken to the Texaco Humble Field Site in Houston, Texas. This was the first in-hole testing of the receiver. This site is an active oil producing field which has numerous wells available for running cross-well seismic tests. The objectives of these tests were; verify operation of tool in the actual borehole environment, confirm that the tool meets the design specifications, and to perform a limited comparison of the prototype sonde with other (non-Sandia) borehole receivers. Texaco provided the field site, operated the data recording system, and operated the Vibroseis truck for the VSP test. Exxon operated its borehole explosive source for cross-well testing of the receivers. The fielding of the Sandia/OYO sonde was performed by Pat Drozda, Bruce Engler, and Gerry Sleefe, all of Sandia.

In addition to the extensive pre-field tests described above, the prototype sonde was further tested in the actual borehole environment. These tests included verification of grounding configuration, electrical/mechanical interface with wireline truck, and clamping procedure in different size well

field which has numerous wells available for running cross-well seismic tests. The objectives of these tests were; verify operation of tool in the actual borehole environment, confirm that the tool meets the design specifications, and to perform a limited comparison of the prototype sonde with other (non-Sandia) borehole receivers. Texaco provided the field site, operated the data recording system, and operated the Vibroseis truck for the VSP test. Exxon operated its borehole explosive source for cross-well testing of the receivers. The fielding of the Sandia/OYO sonde was performed by Pat Drozda, Bruce Engler, and Gerry Sleefe, all of Sandia.

In addition to the extensive pre-field tests described above, the prototype sonde was further tested in the actual borehole environment. These tests included verification of grounding configuration, electrical/mechanical interface with wireline truck, and clamping procedure in different size well casings. The outcome of these tests proved the prototype sonde to be "field capable" and as a result, a large number of cross-well and VSP seismic tests were performed to evaluate the sonde's characteristics. A cross section of the field geometry is shown in Figure VIII.1. Table VIII.1 summarizes the seismic field tests.

Table VIII.1 indicates that a reasonable data base was established for comparing, at 800 ft nominal cross-well spacing, the Sandia accelerometer sonde with the following seismic receivers; Sandia sonde with geophones, Texaco buried geophone string, Exxon 32-level hydrophone array, Texaco 3-level hydrophone array, Texaco geophone VSP sonde, and the Geosource (Halliburton) geophone VSP sonde. Additionally, a small VSP data set is available which allows direct comparison between the Sandia accelerometer sonde and the buried geophones.

Since this test represents the first true cross-well data set using accelerometers, we wanted to determine the signal resolving capabilities of the accelerometers. While clamped at 1200 ft depths in Wells C30 and K74, calibrated noise spectra were measured from the accelerometers. The noise spectra are shown in Figure VIII.2. Note that Well C30 is considerably noisier than K74. This was found to be the result of oil well pump-jacks operating in the vicinity of C30. For the measured noise spectra, the seismic noise is generally above the electronic noise limit of the accelerometers. The only exception to this is that the noise in K74 is at or below the accelerometer noise floor at frequencies above 200 Hz. Also note in Figure 1 that the geophone absolute theoretical noise floor is indicated. Clearly, the accelerometers can provide substantial signal to noise enhancement at frequencies above 150 Hz.

Figure VIII.3 is a representative data set obtained from the advanced sonde in the cross-well configuration. Figure 3 is a common-receiver gather (receiver depth of 1200 ft.) obtained in a cross-well configuration of 815 ft well-to-well spacing. The seismic source was a 10 gram explosive p-wave source which generates wide-bandwidth signals. Figure VIII.4 illustrates a common receiver gather for the same exact shots as used for Figure 3, but recorded by nearby cemented and buried geophones. The offset of the buried geophones from the source well was 1015 ft. Figures VIII.5 - VIII.7 show near-trace common receiver gathers for the advanced sonde, the buried geophones, and the VSP respectively.

Texaco Reservoir Geophysics Test Facility

Well Location

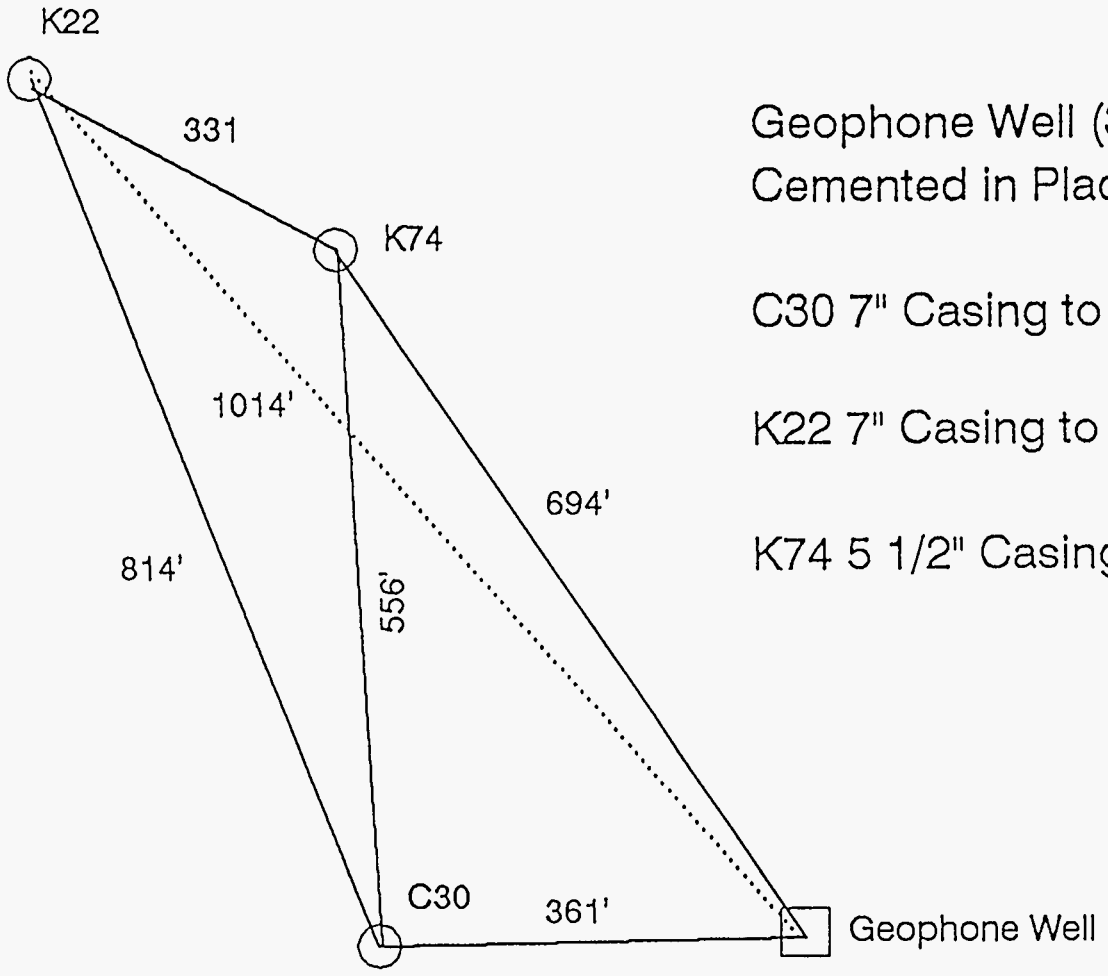

Geophone Well (30) 3-Component Geophones
Cemented in Place Top 37 ft. Bottom 1487 ft

C30 7" Casing to 2495' 5 1/2' to 2880'

K22 7" Casing to 2419' 5 1/2" to 3165'

K74 5 1/2" Casing to 2930'

Figure VIII.1

TEXACO-HUMBLE RECEIVER FIELD TESTS

PARTICIPANTS: SANDIA, OYO, TEXACO, EXXON

Well Spacing	Source	Receivers	Comments
814 ft	Explosive	Sandia/OYO 3-component	Good comparative data
		Commercial VSP 3-component	"
		Exxon 32-level hydrophones	"
		Texaco 3-level hydrophone	"
		Buried geophones (1014 ft offset)	"
331 ft	Explosive	Sandia/OYO	Used for initial sonde Q/A. First data set low clamp force
VSP	Vibrosis	Sandia/OYO Buried Geophones	Good comparative data, limited shot locations

Table VIII.1

GES:6250:vcg:5

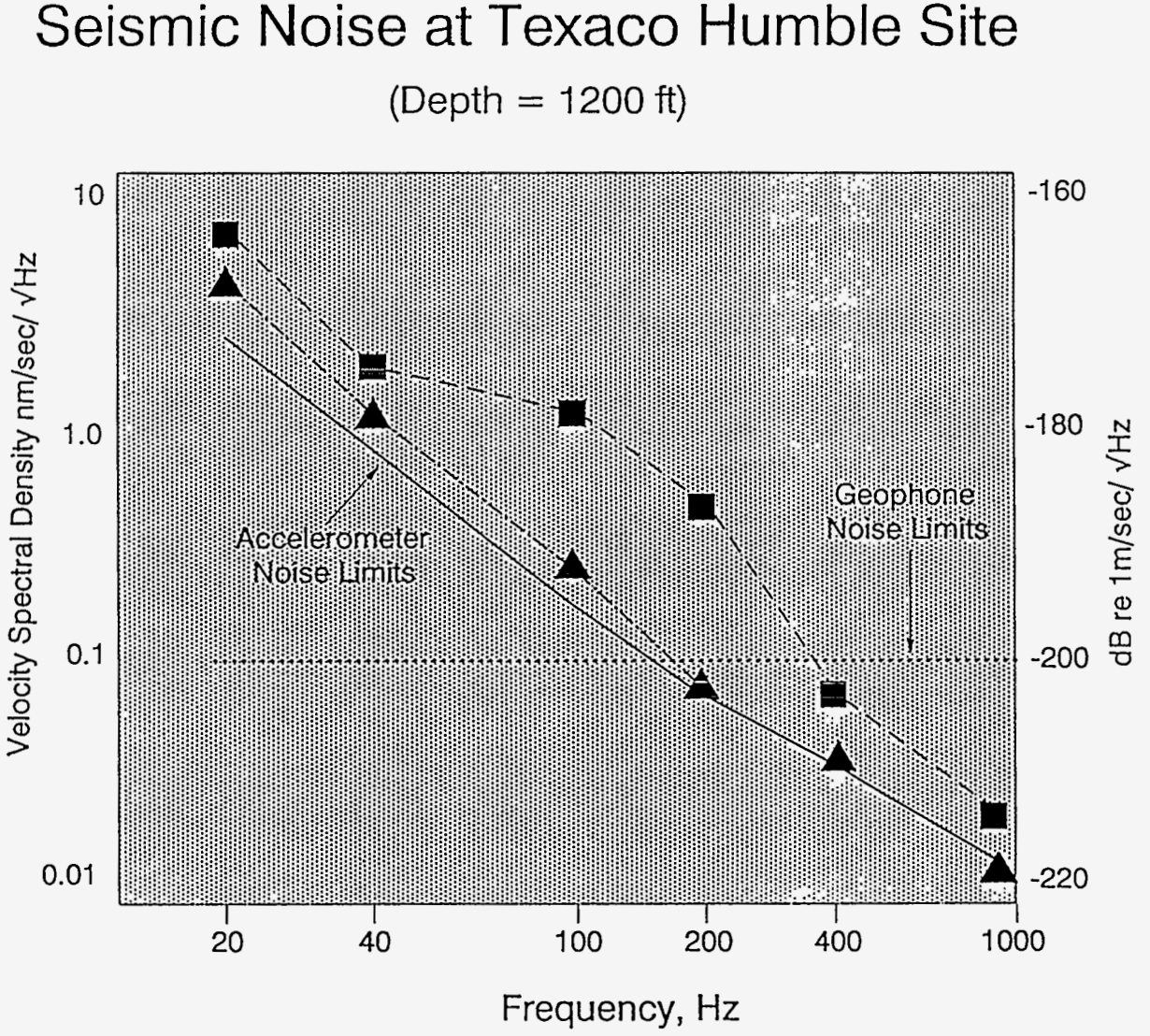

Figure VIII.2

noise

ADVANCED SONDE (ACCELEROMETER)
COMMON RECEIVER GATHER
DEPTH = 1200 FT.
WELL-TO-WELL SPACING = 814 FT.

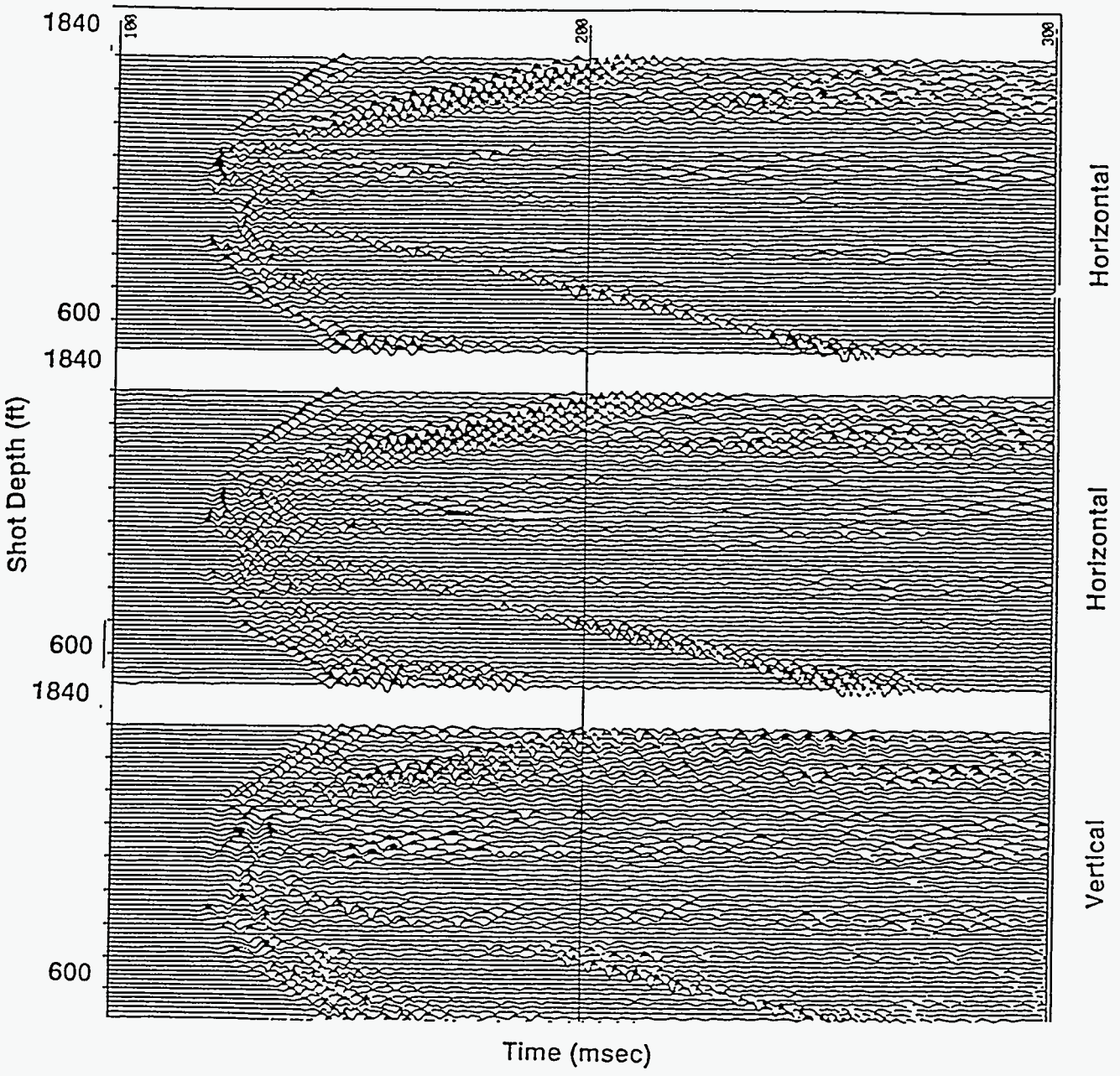

Figure VIII.3

BURIED GEOPHONES
COMMON RECEIVER GATHER
DEPTH = 1187 FT.
WELL-TO-WELL SPACING = 1014 FT.

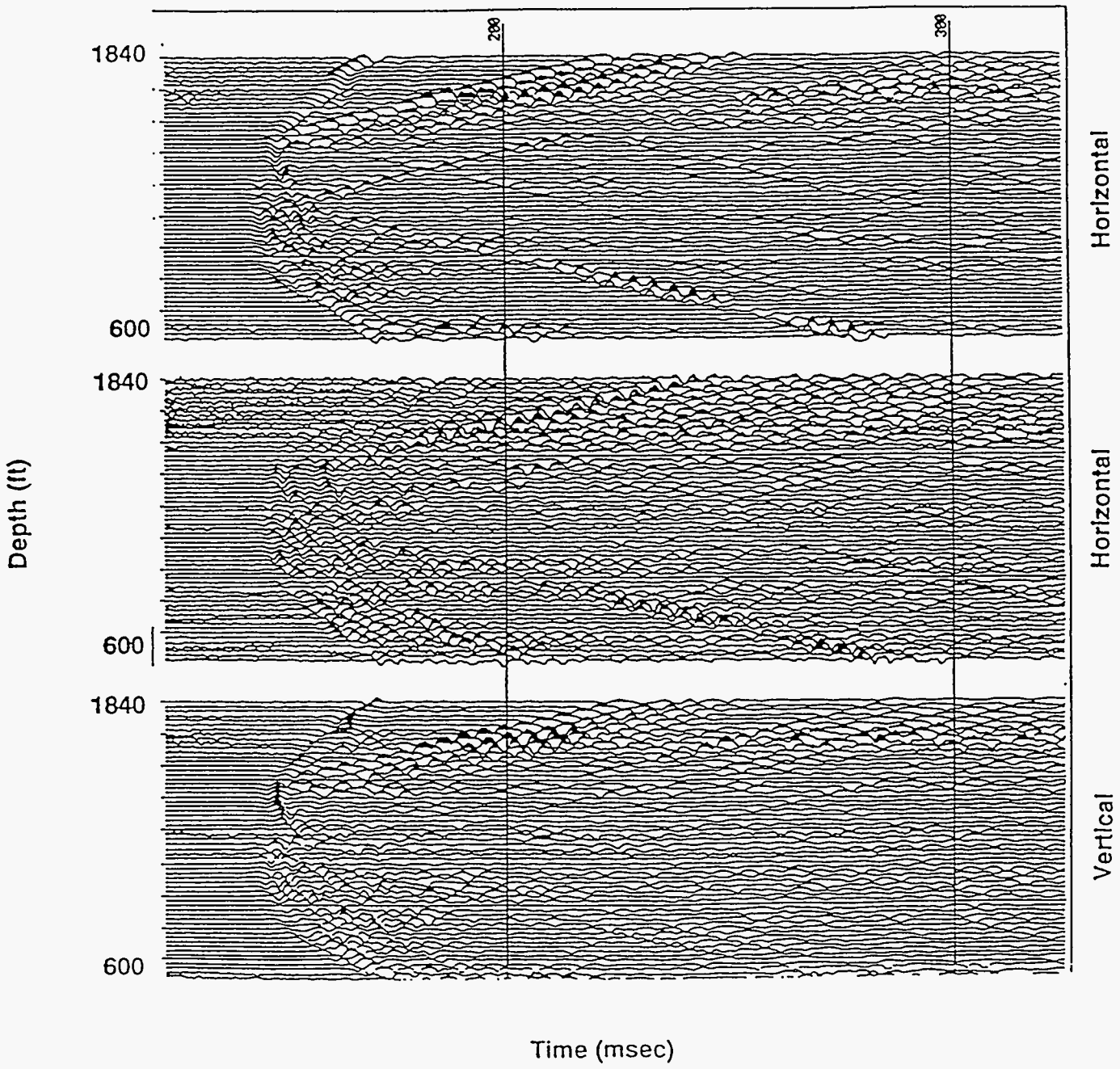

Figure VIII.4

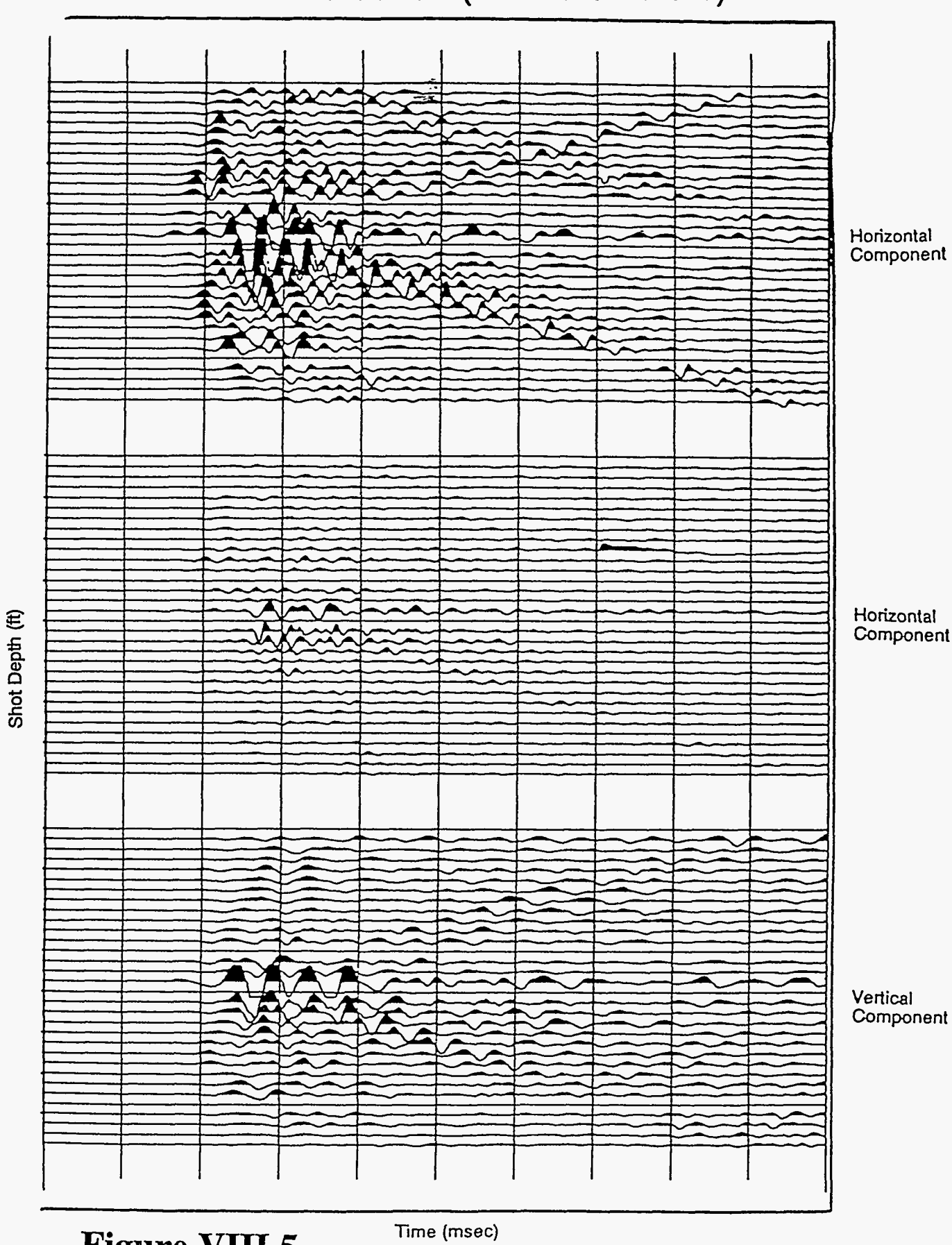

Figure VIII.5

Figure 3: Common-receiver gather obtained from Advanced Borehole Receiver (Accelerometer-Based). Receiver depth is 1200 ft, well-to-well spacing is 815 ft, and fixed display gain is used.

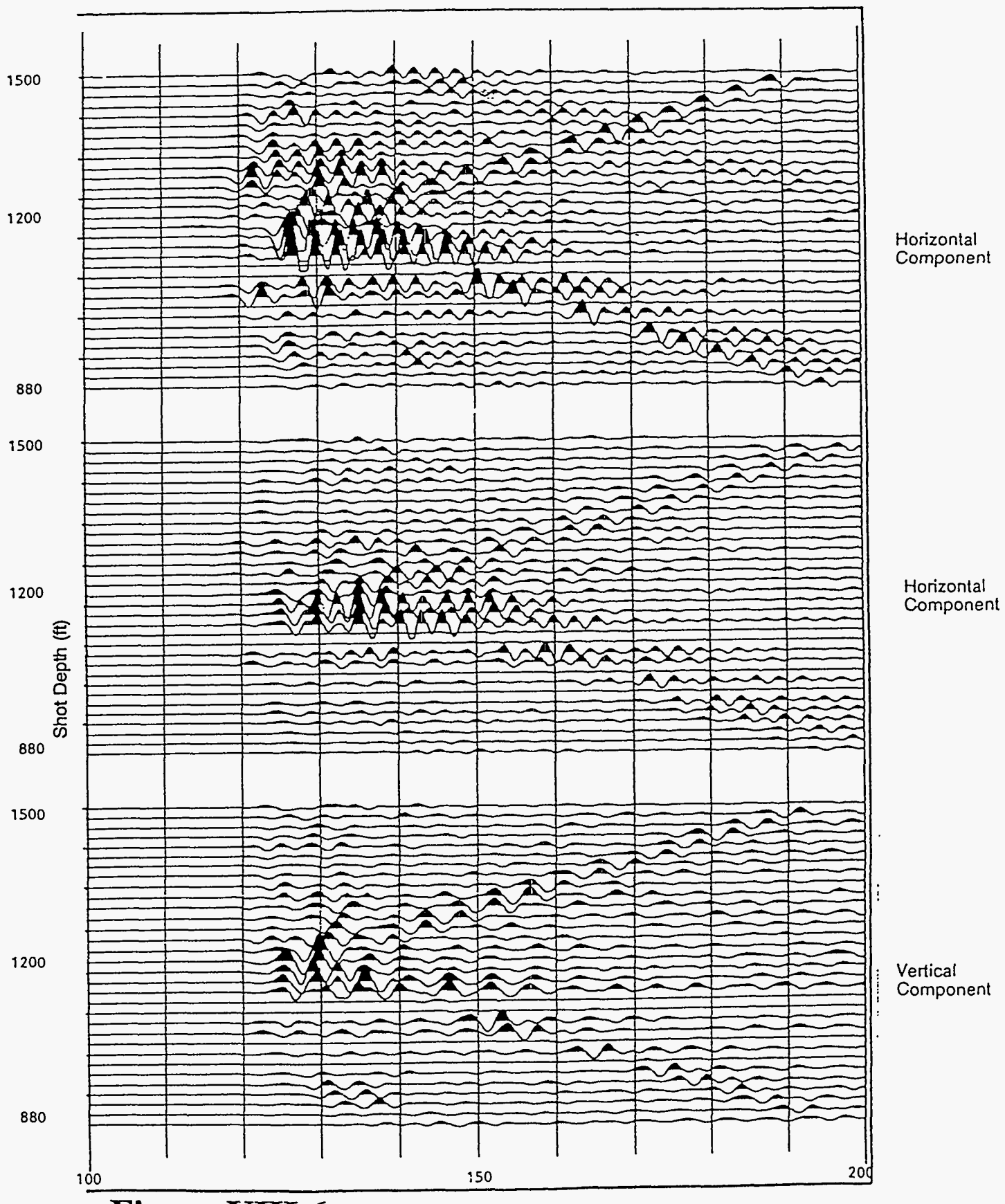

Figure VIII.6

Figure 5: Common-receiver gather obtained from commercial VSP geophone sonde. Sonde depth is 1200 ft, well-to-well spacing is 815 ft, and fixed display gain is used.

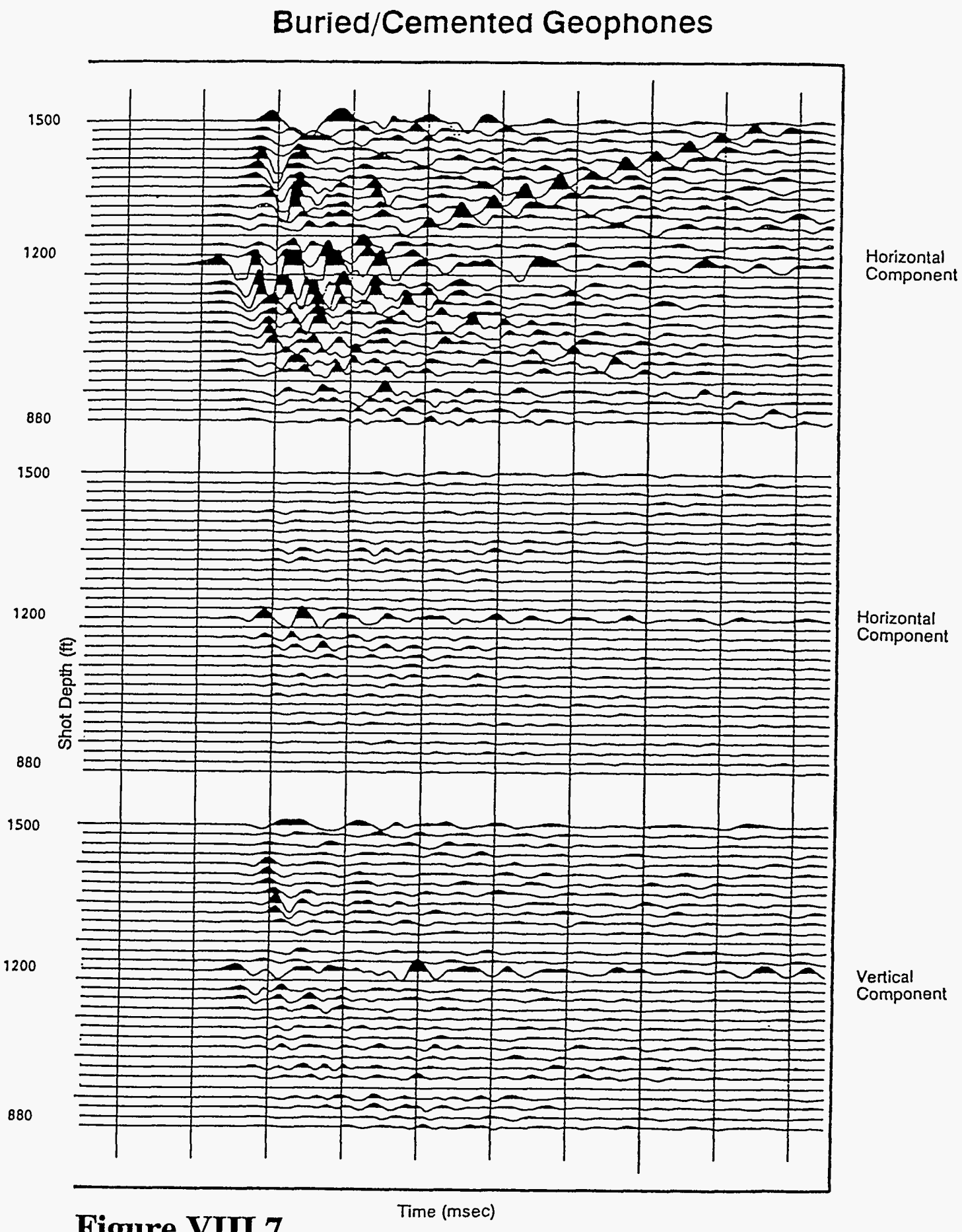

Figure VIII.7

Figure 4: Common-receiver gather obtained from buried and cemented geophones. Geophone depth is 1187 ft, well-to-well spacing is 1015 ft, and fixed display gain is used.

Comparing Figures 5 and 6, it is clear that the basic character of the seismic sections is the same for both the buried geophones and the accelerometer-based sonde. In other words, the Advanced Borehole Receiver appears to couple adequately to the casing and is free from significant resonances in the pass-band (10 Hz to 1400 Hz). On the other hand, the commercial VSP tool, as indicated in Figure 7, produces "ringy" first arrivals indicative of resonances in the pass-band. Thus the advanced sonde provides for better coupling than the VSP tool at the cross-well seismic frequencies.

In order to quantify the signal-enhancement characteristics of the accelerometer-based sonde, spectral analysis of the p-wave arrivals from Figures 5, 6, and 7 was performed. Both average p-wave spectra and average noise spectra were computed for each section, thereby allowing a determination of the signal-to-noise ratio versus frequency. Figure VIII.8 displays the results from this spectral analysis and clearly indicates the increased bandwidth and signal-to-noise enhancement of the accelerometer-based sonde. Specifically, note that the accelerometers offer an approximately 25 dB signal-to-noise enhancement at 1000 Hz relative to the buried geophones.

VIII.1.c Mounds Field Tests

A second test of the single analog receiver prototype took place at the Amoco Mounds Field Test near Tulsa, OK. The objectives of this test were to determine the very-high frequency response of the receiver to perform an absolute comparison between geophone and accelerometer sensors. Figure VIII.9 shows the lay-out of the Mounds site. Table VIII.2 summarizes the tests performed at this site. A unique feature of this experiment is that a tri-axial accelerometer package using Wilcoxon Model 731-20 was grouted in the vicinity of the receiver well. This enabled us to compare potential borehole/cement/receiver coupling differences.

Figure VIII.10 shows the measured seismic noise in the well-bore when using accelerometers and geophones. The data shown in Figure 10 was taken under exact comparison conditions. Measurements were taken at a depth of 200 ft with the advanced receiver clamped into the borehole. For the data labelled "accelerometer", the 731-20 accelerometer was installed in the sonde. For the data labelled "geophone", an OYO Geospace 14Hz phone was used with a very-low noise down-hole pre-amp. The figure clearly indicates that the accelerometer achieves lower absolute noise floor than the geophone above 100 Hz. Again, this confirms the theory that an accelerometer can provide improved signal to noise ratios at higher seismic frequencies.

Figure VIII.11 shows a common receiver fan for the grouted receiver, Figure VIII.12 shows the same fan geometry for the advanced receiver using accelerometers, and Figure VIII.13 shows the same fan geometry for the advanced receiver with a geophone package. Figures VIII.14 - VIII.16 show spectral analysis plots for figures VIII.11-VIII.13 respectively.

The data set obtained from the Mounds experiment led to some interesting observations. First, the buried accelerometer is somewhat larger bandwidth than the advanced-sonde-with accelerometer data. The potential causes of this phenomena are additional wave modes in the borehole/casing structure and/or inaccurate sonde coupling over the entire frequency band. Further study of this phenomena

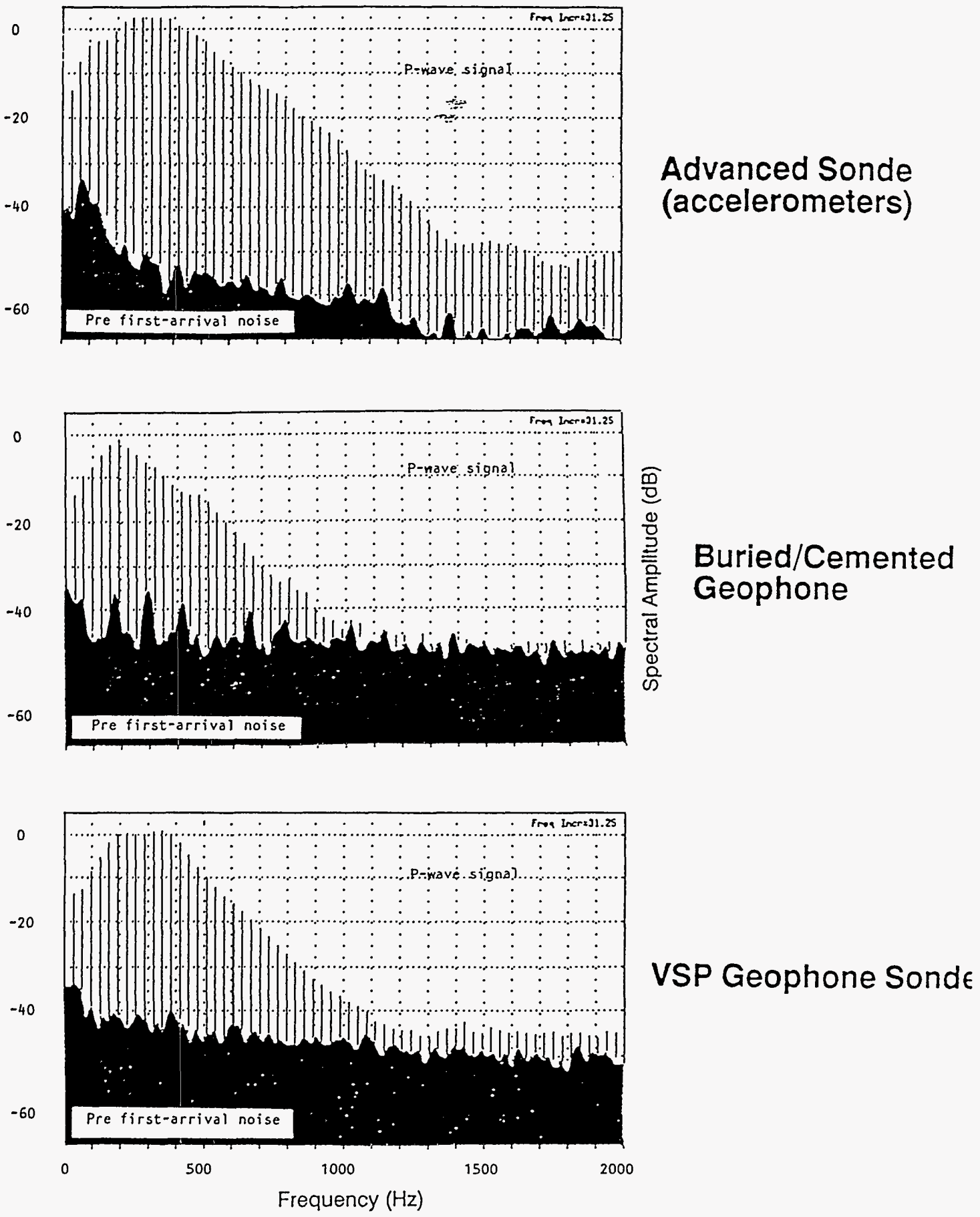

Figure VIII.8

Spectral analysis of common receiver gathers. Both average horizontal-component p-wave spectra and pre-first-arrival noise spectra are shown.

Mounds Site Test Well Locations

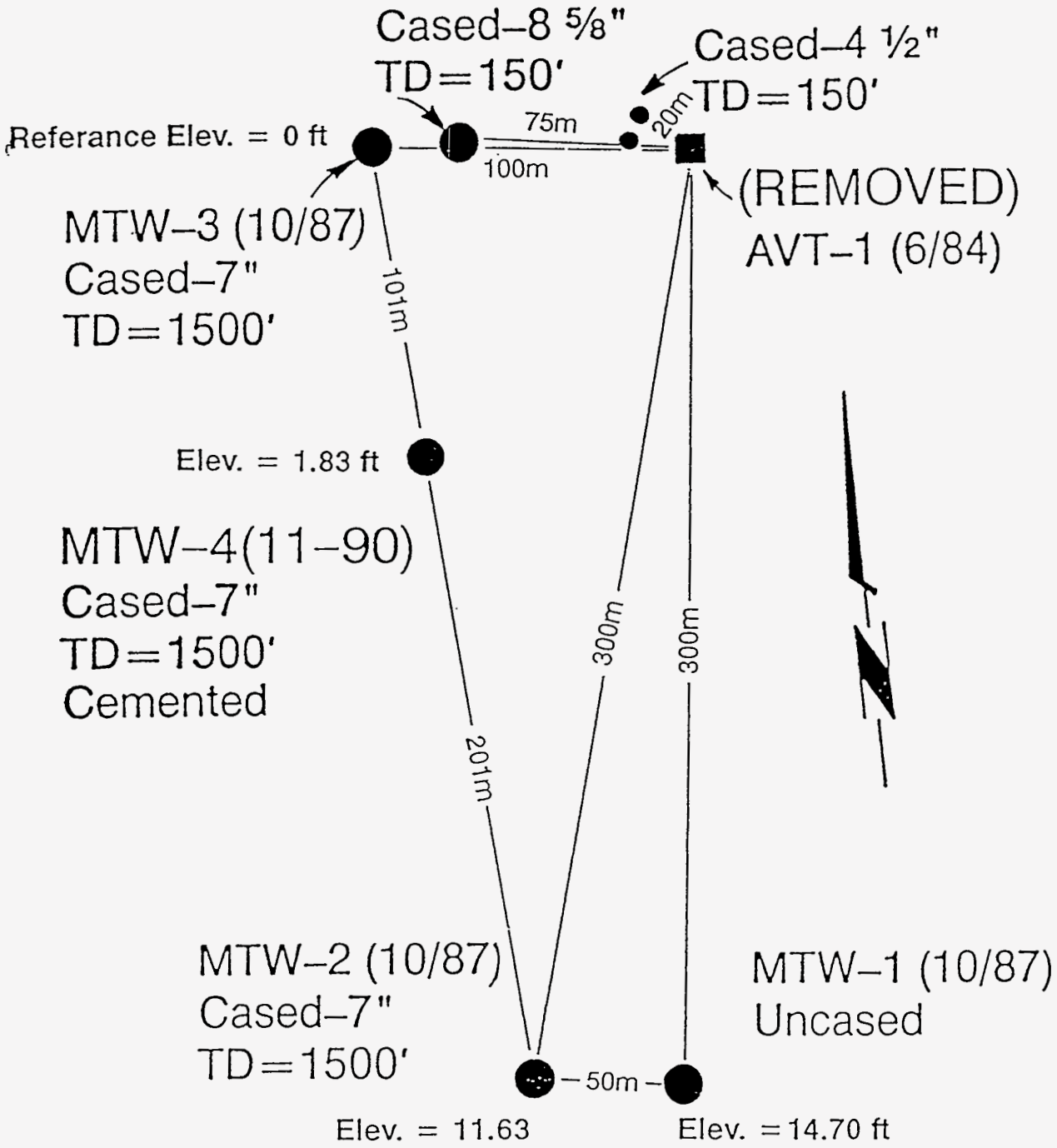

Figure VIII.9

Revised 7–26–91

AMOCO-MOUNDS RECEIVER FIELD TESTS

PARTICIPANTS: SANDIA, OYO, GEOVIEW, AMOCO, CONOCO, PHILLIPS, STANFORD / SWRI

Well Spacing	Source	Receivers	Comments
330 ft	Explosive	Sandia/Oyo Accelerometers	Common source fan
		Buried Accelerometers	One depth only, indicated variability in shots
330 ft	Piezo-electric	Sandia/OYO 3 Accelerometers	Common source fan
			Common receiver fan
		Buried Accelerometers	Common receiver fan
		Sandia/OYO Geophones	Common receiver fan
		Sandia/OYO Cheap Accel. Mount	1 sensor rings
		Sandia - OYO/Geoview	Common receiver, no stacking
330 ft	Rotary	Sandia/OYO Accelerometer	Abbreviated common receiver
		Buried Accelerometer	

Table VIII.2

GES:6250:vcg:4

Well Noise at Amoco Mounds Site
Sonde Clamped at 200 ft, Vertical Sensor Noise

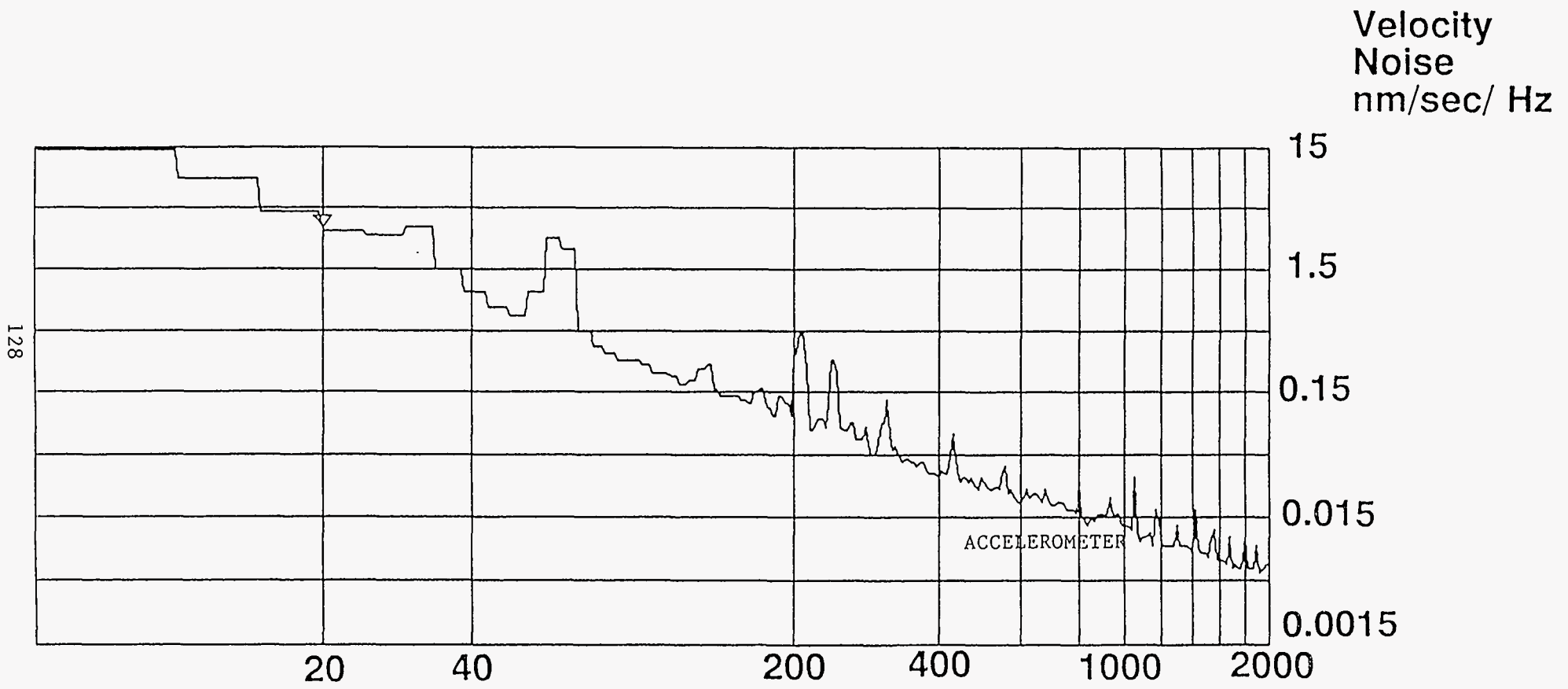

Figure VIII.10

Frequency, Hz

Buried Accelerometers 200 ft Depth Common Receiver
Piezo Electric Source

Figure VIII.11

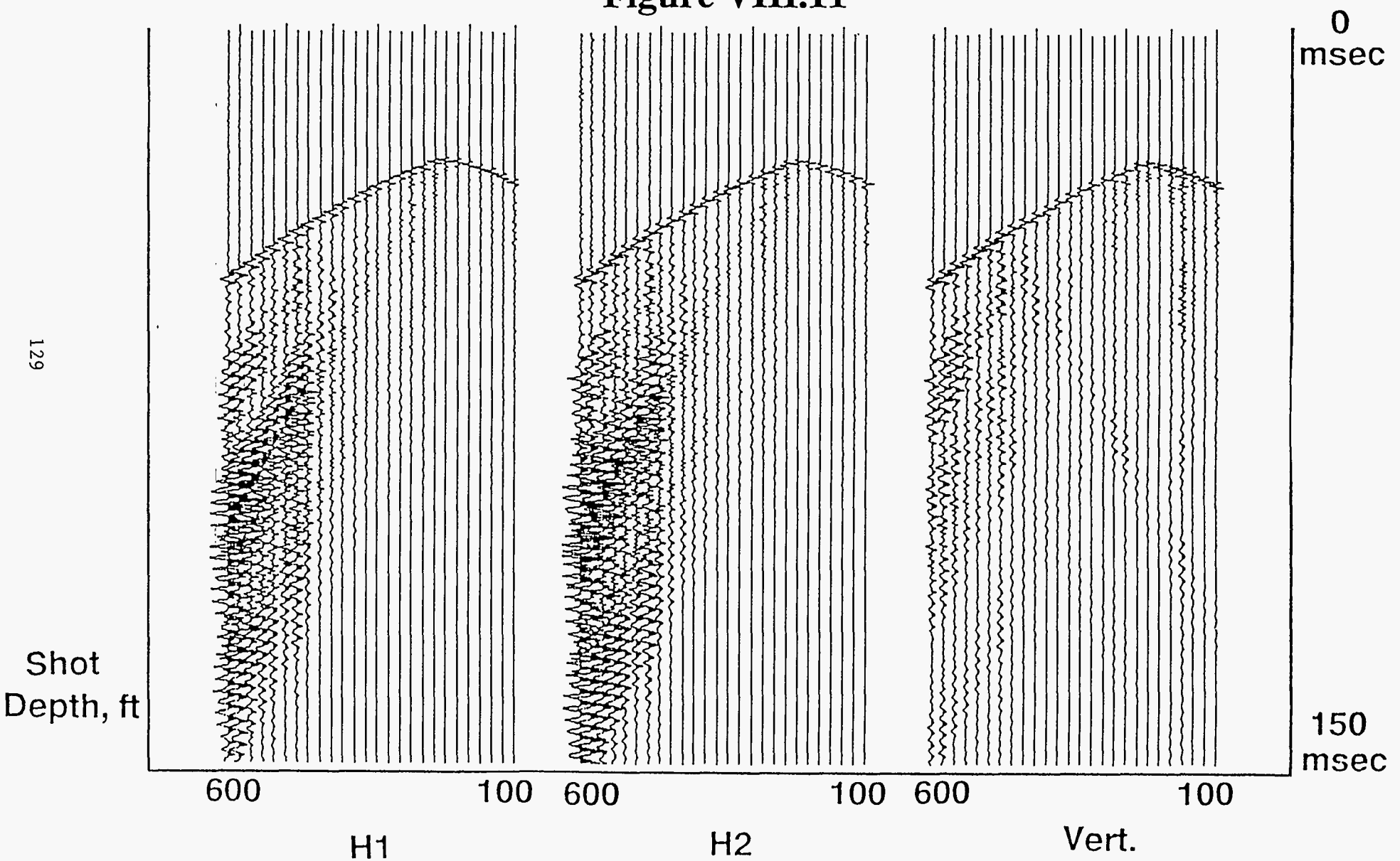

Accelerometer Sonde, 200 ft Depth Common Receiver
Piezo Electric Source

Figure VIII.12

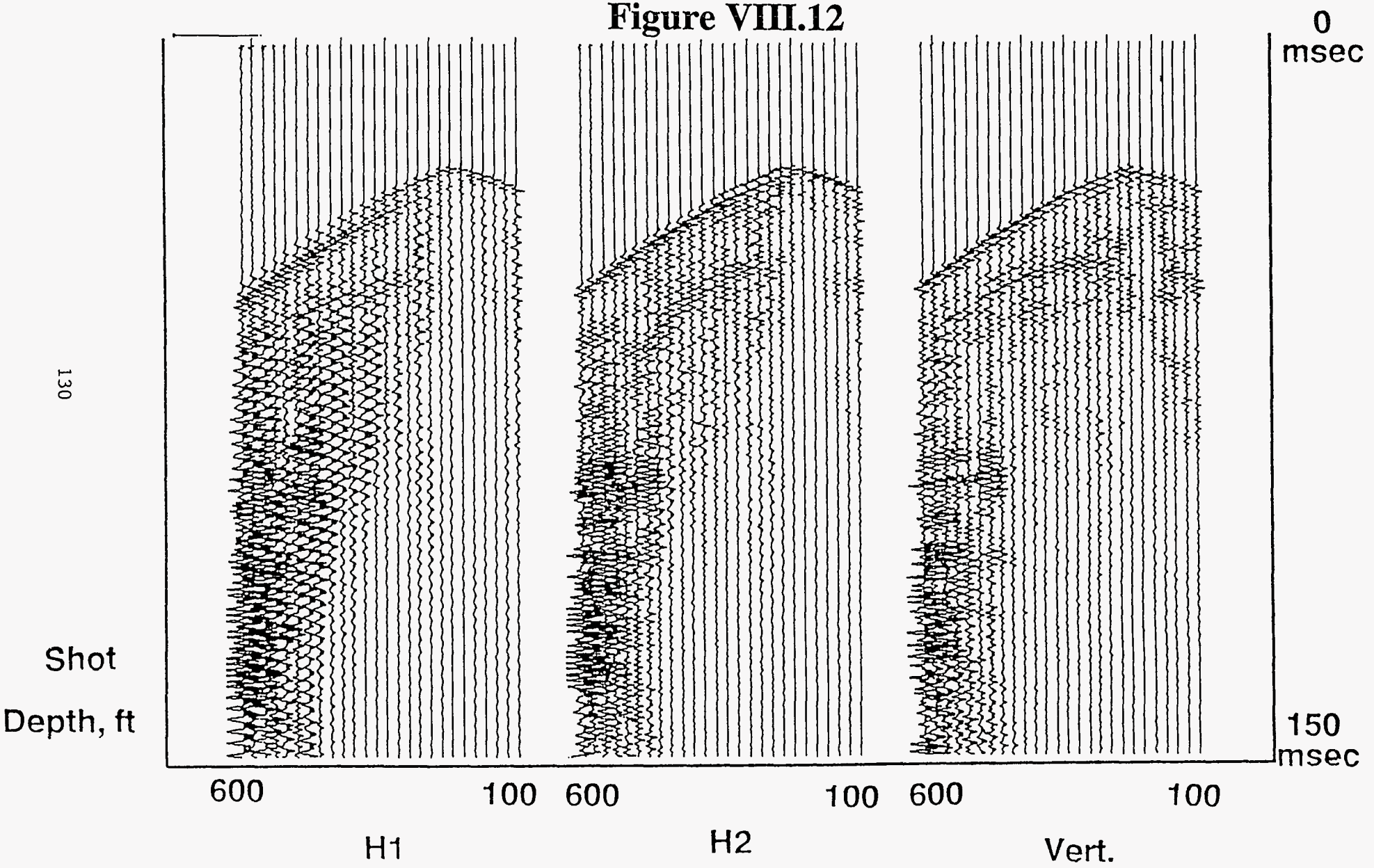

Geophones in Advanced Sonde, 200 ft Depth Common Receiver
Piezo Source

Figure VIII.13

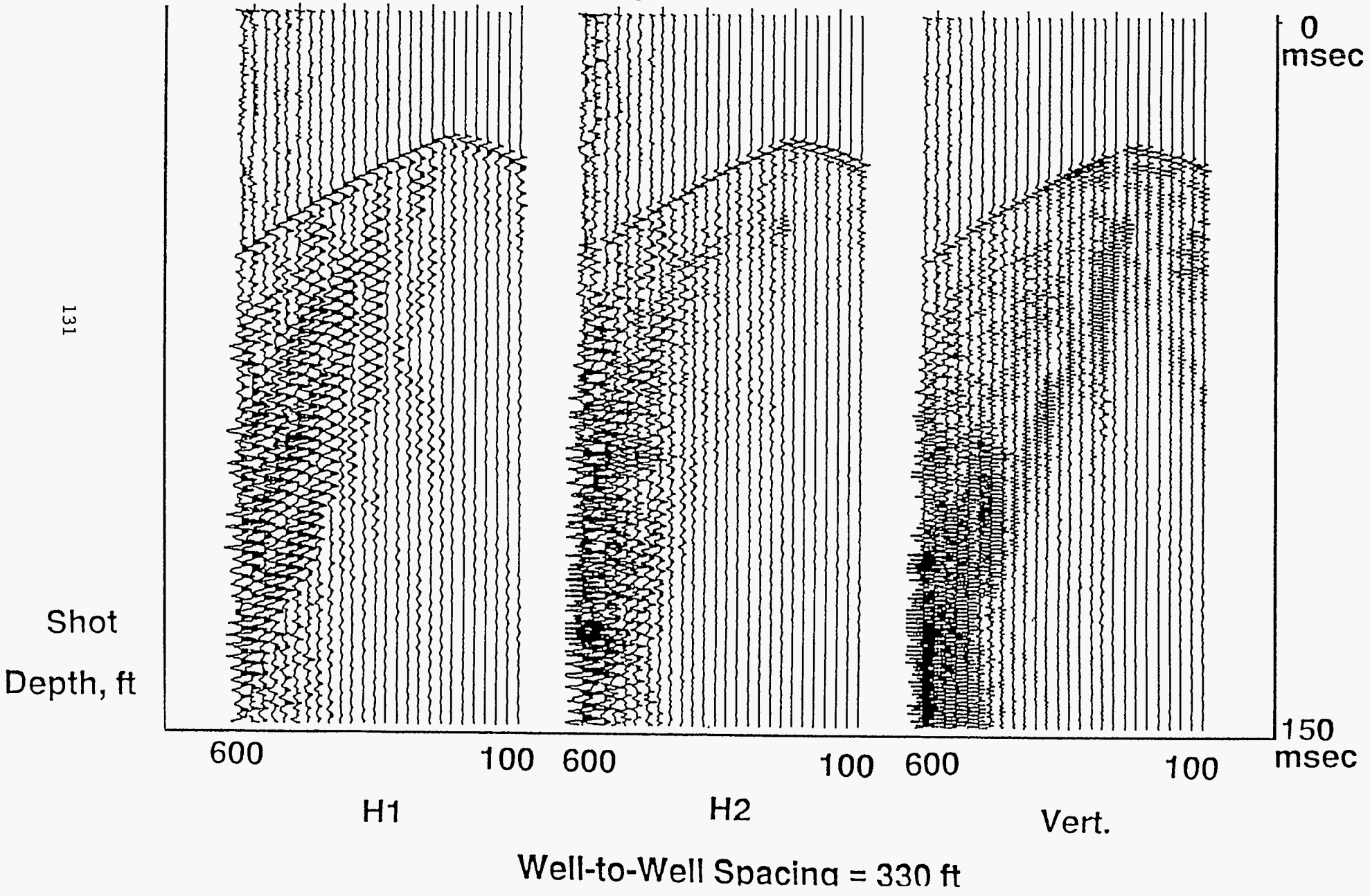

Buried Accelerometers

Figure VIII.14

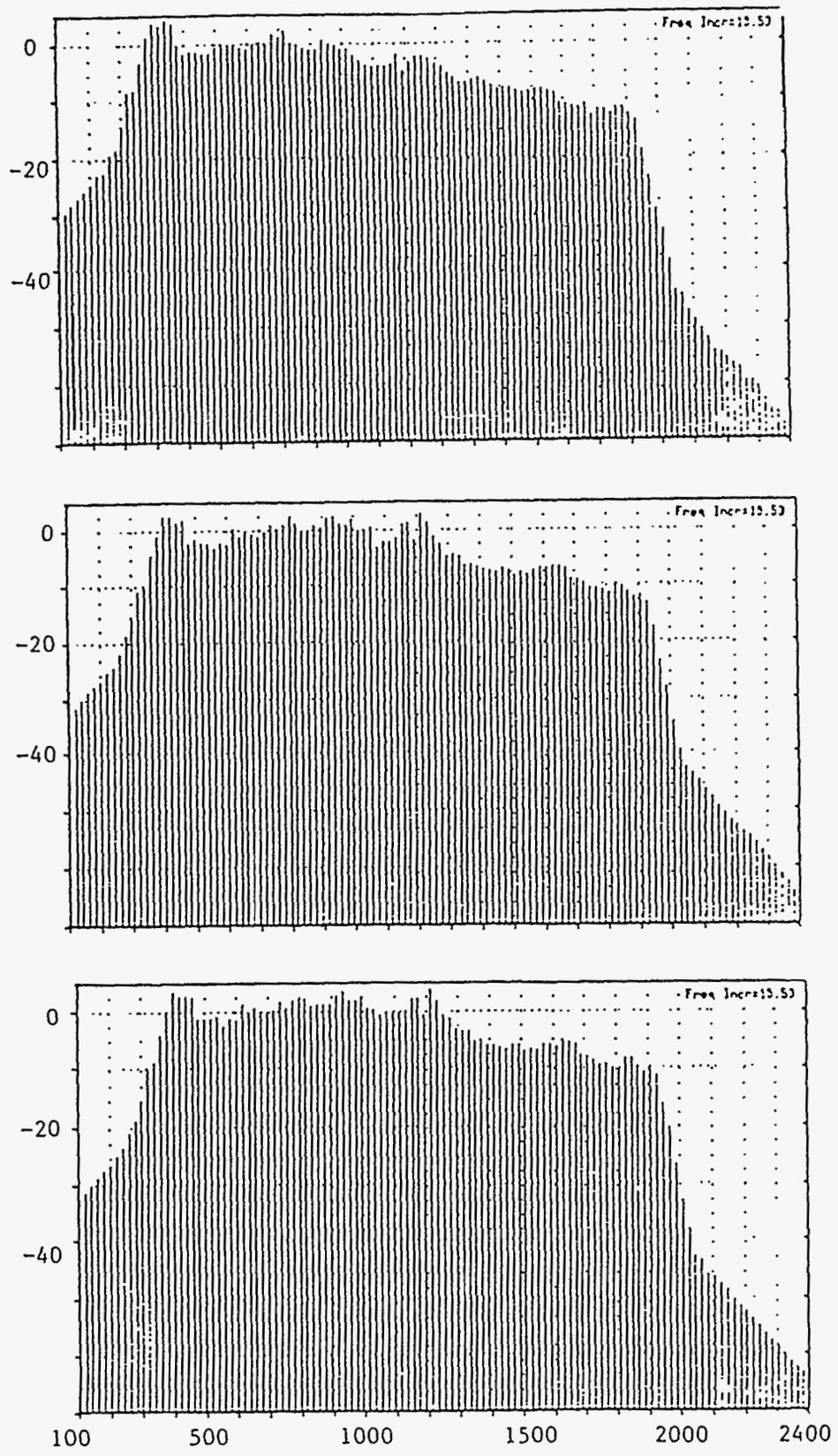

Advanced Sonde, Accelerometers

Figure VIII.15

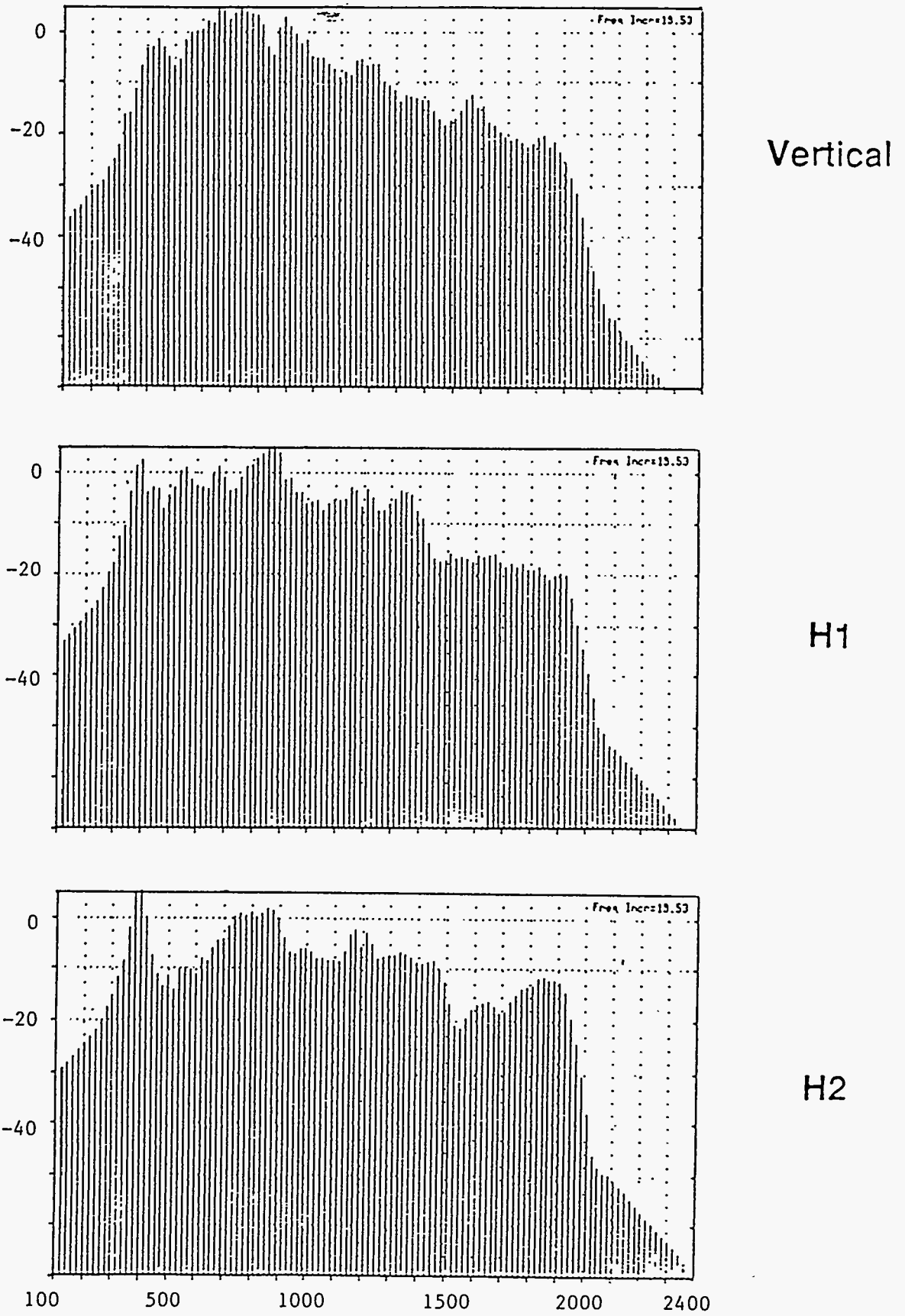

Advanced Sonde, With Geophones

Figure VIII.16

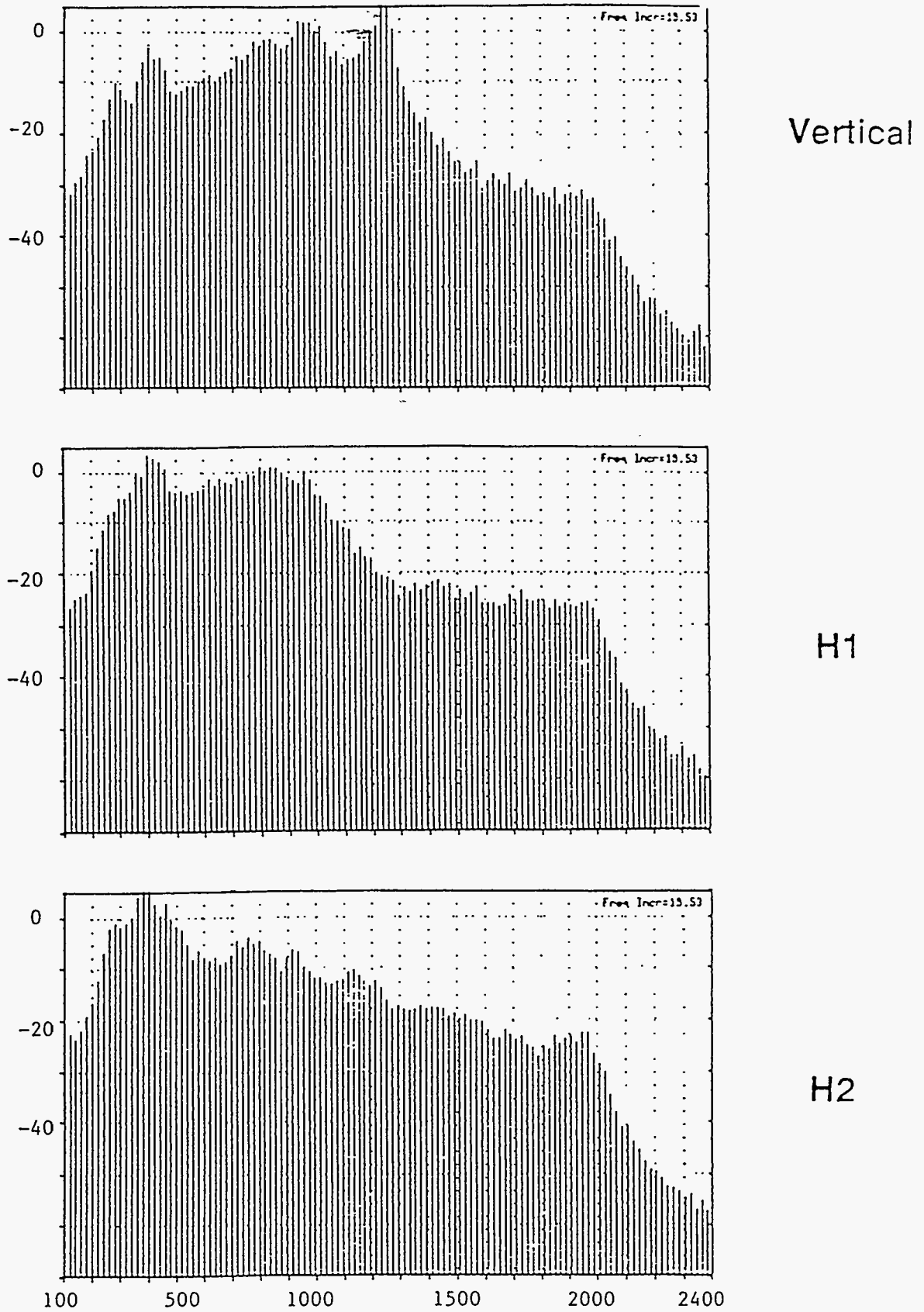

indicated that both situations can occur. Future versions of the sonde contained additional stabilizing rails to improve very high frequency coupling.

The data from this test also confirm the superiority of accelerometers when used for broad-band cross-well operations. The data sets were obtained using the same clamping sonde, but different internal sensor elements. The geophone data has lower signal-to-noise and contains sensor distortions due to geophone spurious modes.

VIII.2. MULTI-LEVEL RECEIVER TESTS AT CHEVRON LA HABRA FIELD

The first in-hole test of the multi-level seismic receiver occurred at the Chevron La Habra Field Facility near Los Angeles CA. During this field test, four seismic receivers were deployed in a single well using the real-time fiber optic link. Data were acquired four times faster than was possible with a single-level receiver using analog data transmission (also a real-time link, but in an analog fashion which is limited to three downhole channels). The acquisition cycle, which includes clamping of receivers, acquisition of 8-sec. swept data, and unclamping was less than 60 seconds. Each acquisition cycle represents the simultaneous collection of four receiver depths, separated by 10 ft. By moving the multi-level receiver system and the seismic source, data for a tomographic survey can be collected in a very rapid fashion.

In the Chevron La Habra Test Site field experiment, two separate data sets were acquired from one pair of test holes for the purpose of comparison: one data set was recorded using the MLSR, the other with the Wuenschel single-station three-component geophone receiver described in [VIII.1]. The objective of the experiment was to compare the bandwidth, sensitivity, and signal-to-noise characteristics of the two receiver packages, using identical acquisition parameters.

The geology at the Chevron La Habra test site consists of relatively young (Mio-Pliocene) poorly-consolidated clastic rocks, characterized by relatively low seismic velocities (5000 - 7000 ft/sec for P-waves) and low Q values. The apparent dip of beds between wells is about 17 degrees, with the source well structurally high. The ground surface at the site is flat, with the water table at a depth of about 50 feet. The distance between the source and receiver wells is 400 ft. Both the source and receiver wells are about 2000 feet in depth, and are cased and cemented with 13 3/8" casing to about 80 ft., and 7" casing to total depth. Full waveform sonic, density, gamma ray, and caliper logs were run in each well.

Cross-well seismic data were recorded with the receivers located at 10 foot vertical intervals from 100 to 1190 feet. The receiver well was fluid-filled so that the response to receiver-well tube waves could be observed. The seismic source used in the experiment was Chevron's downhole axial vibrator. The vibrator was held fixed at a depth of 500 feet, sweeping from 10 to 640 Hz in 7 seconds. No vertical stacking of individual sweep records was employed. The source well was dry during the experiment.

The common receiver gather of vertical component data using the multi-station receiver is shown in Figure VIII.17. The common source gather of vertical component data using the Wuenschel receiver is shown in Figure VIII.18. The raw data for each gather were muted prior to the first breaks, and a

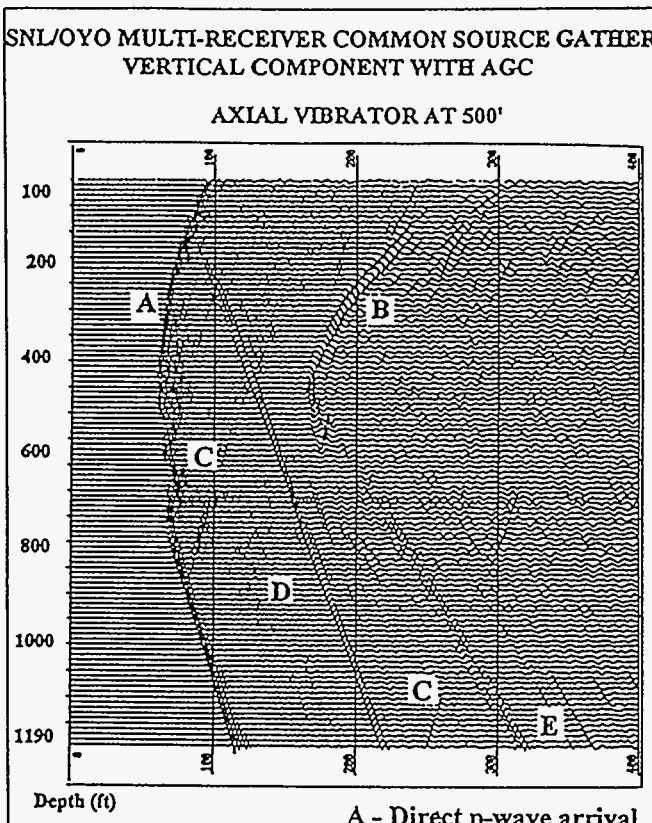

A - Direct p-wave arrival
B - Direct s-wave arrival
C - Upgoing refelections
D - Downgoing reflection
E - Tube waves

Figure VIII.17

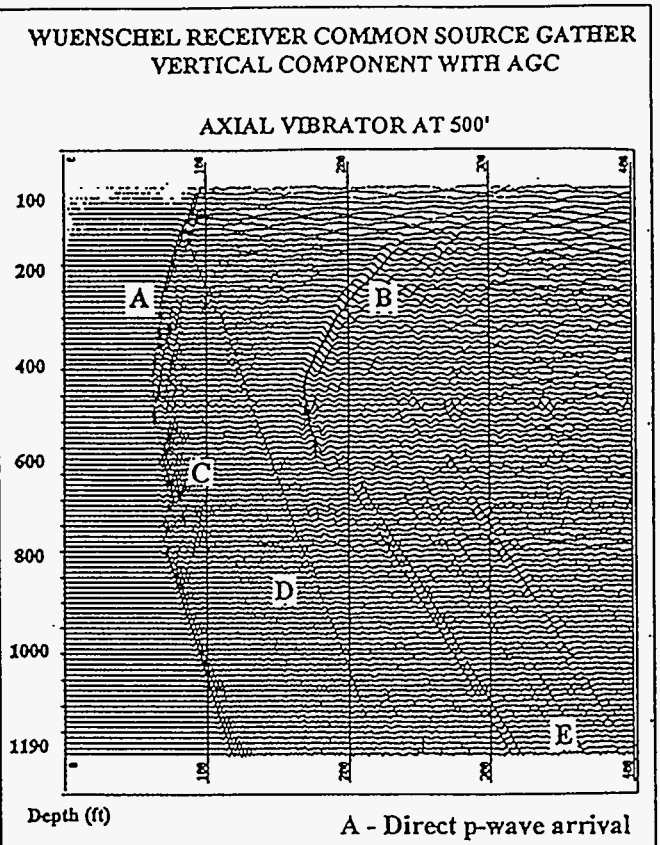

A - Direct p-wave arrival
B - Direct s-wave arrival
C - Upgoing refelections
D - Downgoing reflection
E - Tube waves

Figure VIII.18

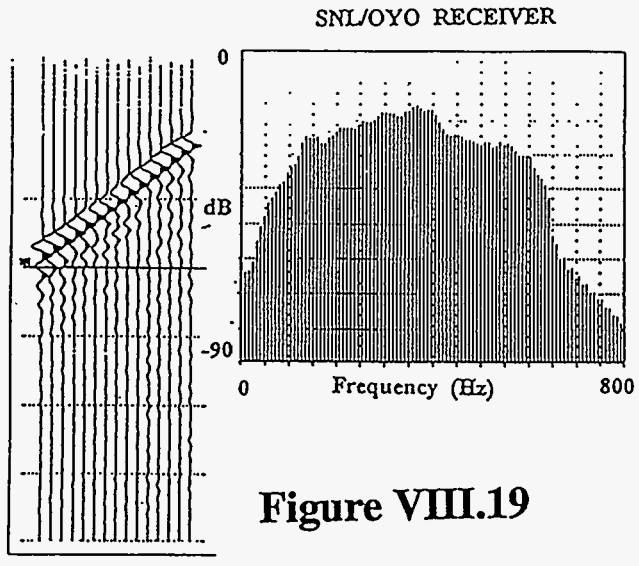

Figure VIII.19

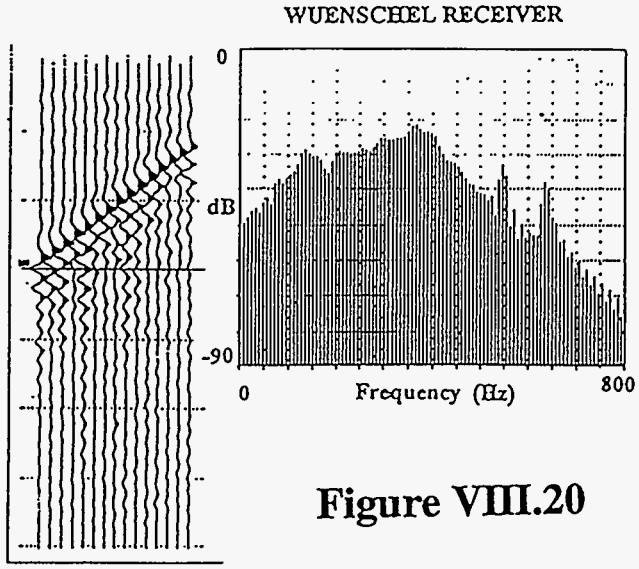

Figure VIII.20

60 millisecond AGC was applied to enhance the visibility of events arriving after the first breaks. Both gathers clearly show P and S wave direct arrivals as well as later-arriving events. Vertical component amplitudes of the P wave direct arrivals on both data sets are diminished when receiver depths are approximately equal to the source depth of 500 ft. This effect is expected due to the vertical polarization and directivity of the seismic vibratory source.

Of particular interest is the higher signal-to-noise ratio of reflected P wave events on the multi-station receiver. It is expected, given the source directivity, that the P wave reflections are more prevalent than S wave reflections in these data. Note for example, the strong down-going reflection event which originates from a tight sand/shale interface at a receiver well depth of 200 ft. On the multi-level receiver data, this event show excellent signal-to-noise ratio, with variations in event amplitude and phase easily discernible across the full aperture of receiver stations. At the deeper Wuenschel receiver stations, this event is almost completely lost in the noise. Also note in the MLSR data the upgoing event originating at about 900 ft, which is barely detected by the Wuenschel receiver. Perhaps most noteworthy, is the deeper upgoing reflection event on the multi-station receiver gather evident from 250 to 300 milliseconds at receiver levels from 1190 to 800 ft, which is not present at all in the Wuenschel data. Sonic and density log data indicate that this event is probably a reflection from a high-impedance highly-cemented sandstone bed at a depth of 1800 ft in the receiver well, which is 610 feet below the deepest receiver level.

Both gathers show S wave direct arrivals whose amplitudes decrease below a receiver depth of about 600 ft. This depth in the receiver well corresponds to the base of a low velocity shale bed which appears to have channeled the direct shear wave energy away from the deeper receiver levels, creating a shadow effect. Note also the down-going tube waves in the receiver well, apparently generated by the shear wave energy propagating inside a shale bed waveguide, as well as by incident shear wave arrivals at shallower levels in the well. In general, tube waves are more prominent in the multi-station receiver data.

Spectral amplitude plots for portions of the two gathers are illustrated in Figures VIII.19 and VIII.20. The analyses were performed on traces from 890 to 1030 feet, over a 70 millisec time window which includes the P wave direct arrivals. In comparing the amplitude spectra it is immediately apparent that the MLSR data amplitude spectrum is nearly flat for all frequencies output by the source (up to 640 Hz), while the Wuenschel tool response rolls off markedly beginning around 400 Hz. Given the flat response of the MLSR over the entire spectrum of swept frequencies, it seems likely that higher frequencies could have been recorded had they been generated by the source. At 600 Hz the response of the Wuenschel tool is down 30 dB from the response at 400 Hz, while the multi-station receiver is down only 10 dB, a difference of 20 dB.

When comparing the response of the MLSR, which contains accelerometers, to geophone-type receivers like the Wuenschel tool, recall that accelerometer measurements include a built-in 6 dB/octave high-frequency pre-emphasis relative to geophone (velocity sensor) measurements. Thus, the actual improvement of the MLSR relative to the Wuenschel tool is approximately 17 dB for the half-octave from 400 to 600 Hz. In this regard, it is also important to note that the accelerometers have an intrinsically lower noise floor over this frequency range so that more high-frequency information can be recovered from the accelerometer data. Furthermore, the Wuenschel tool displays

mechanical resonances and/or spurious modes at 550 and 650 Hz, characteristics which are common in conventional geophone-based receivers.

VIII.3 MISCELLANEOUS FIELD TESTS

The previous sections discussed the results from initial testing of both a single-level advanced receiver and the Multi-Level Seismic Receiver. Since these initial tests, numerous field acquisitions using these systems have occurred. The tests have ranged from in-well system checkout tests (for improving the reliability of the system) to full commercial cross-well seismic surveys. Currently, Bolt Technologies Inc., Houston Texas, is providing the MLSR on a commercial service basis. Information on the performance of the MLSR under a variety of field conditions can be obtained directly from Bolt Technologies.

XIV. DIRECTION OF FUTURE WORK AND RECOMMENDATIONS

The Multi-Level Seismic Receiver developed under the D.O.E's Oil Recovery Technology Partnership represents a significant advancement in borehole seismic data acquisition. The system has proved itself in a variety of oil well conditions and is now a commercially available technology. However, due to limited funding and limited scope of the project, several important areas warrant future investigation. The following are areas where future work could be focused:

1.) Development of very-long term reliability of the system
2.) Analysis/Study of formation/grout/borehole/fluid/tool coupling at high frequencies
3.) Complete system implementation, evaluation and extended operation at very high temperatures
4.) Modifications to the system to allow more than 5 sondes and variable interconnect length
5.) The development of low-cost off-the-shelf fiber optic wirelines

Some of these issues are under investigation as part of new seismic projects at Sandia National Laboratories. Sandia welcomes the opportunity to team with the Oil and Gas Industry in solving these and other technically challenging tasks.

X. CONCLUSIONS AND CLOSING SUMMARY

An advanced technology Multi-Level Borehole Seismic Receiver (MLSR) has been designed, developed, and field tested. The MLSR represents a significant advancement over prior borehole receiver systems. These advancements are the result of improved sensor, data acquisition/telemetry, and mechanical technologies. The MLSR is currently commercially available from OYO Geospace Corporation and is available as a service of Bolt Technologies Inc. The system is currently undergoing commercial field trials, and future enhancements will be provided both by industry and new Sandia/Industry partnerships.

XI. REFERENCES

[I.1] Hardage, B.A., "Crosswell Seismology and Reverse VSP,", Geophysical Press, 1992.

[I.2] Harris., J.M., et. al.,"High Resolution Cross-Well Imaging of a West Texas Carbonate Reservoir: Part 1. Data Acquisition and Project Overview," Proceedings of 62nd Annual International SEG Meeting, New Orleans, LA, pp. 35-39, 1992.

[I.3] Kawahara, H., et. al., "Engineering Design and Field Performance of an Array-Type Downhole Seismic Tool for Cased Hole VSP Surveys," Proceedings of 60th Annual International SEG Meeting, San Francisco, CA, pp. 144-147, 1990.

[I.4] Krohn, C.E., "Comparisons of Downhole Geophones and Hydrophones," Geophysics, Vol. 6, p. 841, June 1992.

[I.5] Coffeen, J.A., Seismic exploration fundamentals, Second Edition, Penwell Publishing, Tulsa, Ok., 1986.

[I.6] Bloch, M., Borehole Seismic Techniques: Review and Outlook, Institut Francais Du Petrole, Report No. 37915, 1990.

[I.7] Galperin, E.I., Vertical seismic profiling and its exploration potential, D. Reidel Publ. Co., Boston, MA. pp. 25-26, 1985.

[I.8] Stanley, P.J., The geophone and front-end fidelity, First Break, Vol. 4, No. 12, pp. 11-14, 1986.

[I.9] Sleefe, G.E., and Engler, B.P., "Experimental Study of an Advanced Three-Component Borehole Seismic Receiver," Proceedings of 61st Annual SEG Meeting, Houston, TX, pp. 30-33, 1991.

[III.1] Berger, J., et al, "Studies of High-Frequency Seismic Noise in Eastern Kazakhstan," Bulletin of the Seismological Soc. Amer., Vol. 78, No. 5, pp. 1744-1758, October, 1988.

[III.2] Li, T.M.C., et al, "High Frequency Seismic Noise at Lajitas, Texas," Bul. Seism. Soc. Amer., Vol. 74, No. 5, PP. 2015-2033, October, 1984.

[IV.1] Dynamic Analysis of Downhole Receiver Tool, memo to P.J. Hommert, 6258, from K.W. Gwinn, 1524, dated November 28, 1989.

[IV.2] Patran Plus User's Manual, PDA Engineering, Costa Mesa, CA., 1987.

[IV.3] MSC/Nastran User's Manual, Version 66, MacNeal-Schwendler Corp., Los Angeles, CA., 1988.

XI. REFERENCES (Continued)

[IV.4] Phelan, Richard M., Fundamentals of Mechanical Design, 3rd Edition, McGraw-Hill Book Company, Chapter 10, pp. 222-229., 1970

[IV.5] Young, Warren C., Roark's Formulas for Stress and Strain, 6th Edition, McGraw-Hill Book Company, Chapter 9, pp. 345-385, 1989

[IV.6] Oberg,E., Jones,F.D., Horton,H.L., Machinery's Handbook, 22nd Edition, Edited by Ryffel,H.H., Industrial Press Inc., pp.340-352.

[VII.1] Anghern, J.A. and Sie, S.A., "A High Data Rate Fiber Optic Well Logging Cable," The Log Analyst, March 1987, pp. 184-189.

[VIII.1] Wuenschel, P.C., "The Vertical Array in Reflection Seismology - Some Experimental Results," Geophysics, Vol. 41, p 219-232.

Appendix A: List of Personnel Involved in Development of the MLSR

The development of the MLSR involved a substantial project team. Summarized below are the names of the team members and their contribution to the development efforts.

Name	Company	Contribution
G.E. Sleefe	Sandia	Project Leader; major technical efforts in sensor design, data acquisition, design of BHDAS software, and design/development of BHDSP software.
R.J. Franco	Sandia	Electronic Engineering; major technical efforts in digital electronics design, telemetry design and system testing
B.P. Engler	Sandia	Mechanical Engineering; major technical efforts in clamp package design, housings, connectors, and CAD
J.R. Morgan	Sandia	Electronics; electronics assembly, test, and PCB schematics and Layout
P.M. Drozda	Sandia	Field Test; system assembly, checkout, and field implementation
K.T. Gwinn	Sandia	Mechanical Modeling; finite element analysis of clamp subsystem
W.T. Davis	OYO	Industry Liaison; commercialization and industry needs identification
S. Thane	OYO	Software Engineering; software design/development of BHDAS software
P. Jezek	OYO	Mechanical Fabrication; mechanical drafting, parts manufacturing and assembly
J.A. Anghern	Chev	Fiber Optic Wireline Liaison

Appendix B. MLSR Mechanical Drawings

NOTES:
1) BREAK SHARP EDGES .03 x 45°
2) MATL: 6061 ALUM.
3) QTY: 1 REQD.
4) ⌀.900 DIA. BORES TO BE FINISHED TO GIVE .001"-.002" DIAMETRICAL CLEARANCE AND ⌀.002" PERPENDICULARITY WITH ACCELEROMETERS INSTALLED.

REVISIONS			
REV	DESCRIPTION	DATE	APPROVED

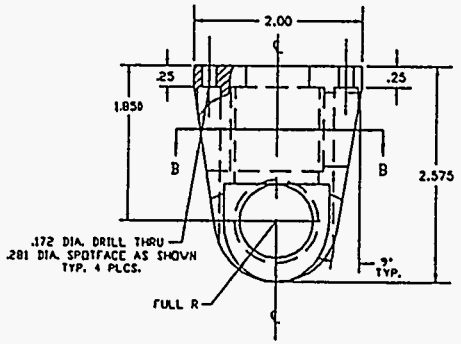

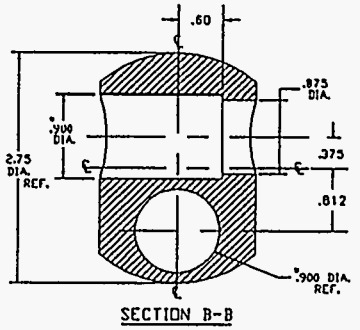

SECTION B-B

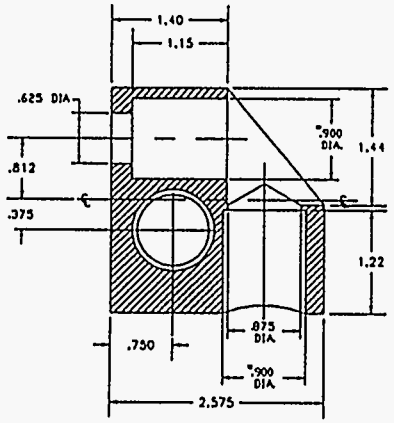

SECTION A-A

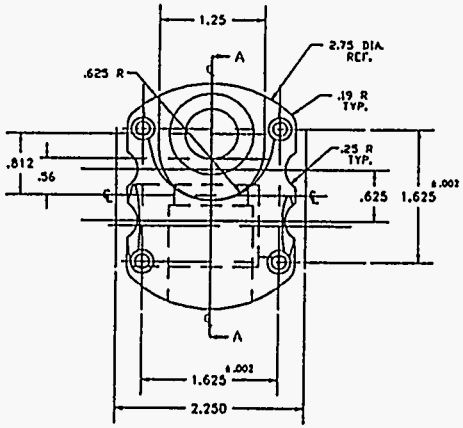

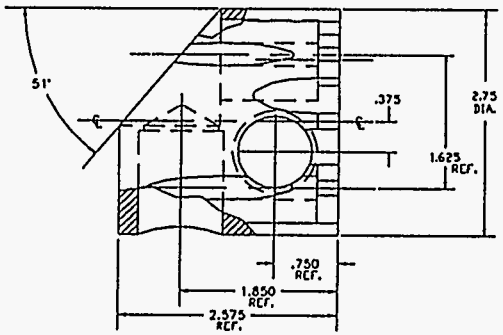

	SANDIA NATIONAL LAB.		
	BOREHOLE RECEIVER ACCELEROMETER MOUNT		
ENGR. BY: B. ENGLER	SIZE C	FSCM NO	DWG NO 1001-4A REV
DRAWN BY: B. ENGLER	SCALE 1X		SHEET 1 OF 1

DWG NO 1001-4A REV 1

B.1

REVISIONS			
REV	DESCRIPTION	DATE	APPROVED
A	8-32 TO 10-32 TAP	11/91	B.E.
B	10-32 TO 1/4-28 TAP .250 In. TO .201 In.	11/91	B.E.
C	.375 TO .31 AND .026 TO .000	11/91	B.E.

NOTES:
1) BREAK EDGES .03 X 45°
2) MATL: 17-4 OR 15-5 S.S.
3) QTY: 1 REQD.

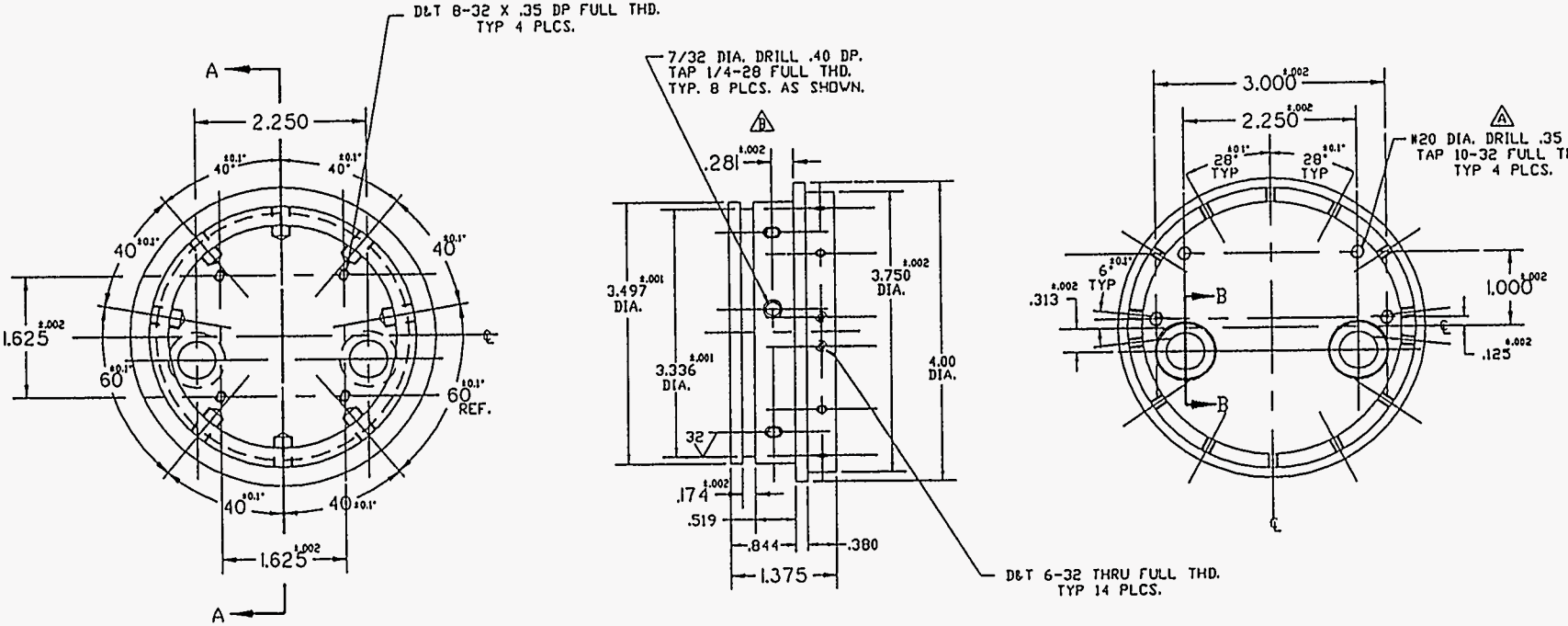

B.2

	SANDIA NATIONAL LAB.		
	BOREHOLE RECEIVER SENSOR BULKHEAD		
ENGR. BY: B. ENGLER	SIZE C	FSCM NO	DWG NO 1002-4A REV C
DRAWN BY: B. ENGLER	SCALE 1X		SHEET 1 OF 2

DWG 1002-4A

REVISIONS			
REV	DESCRIPTION	DATE	APPROVED

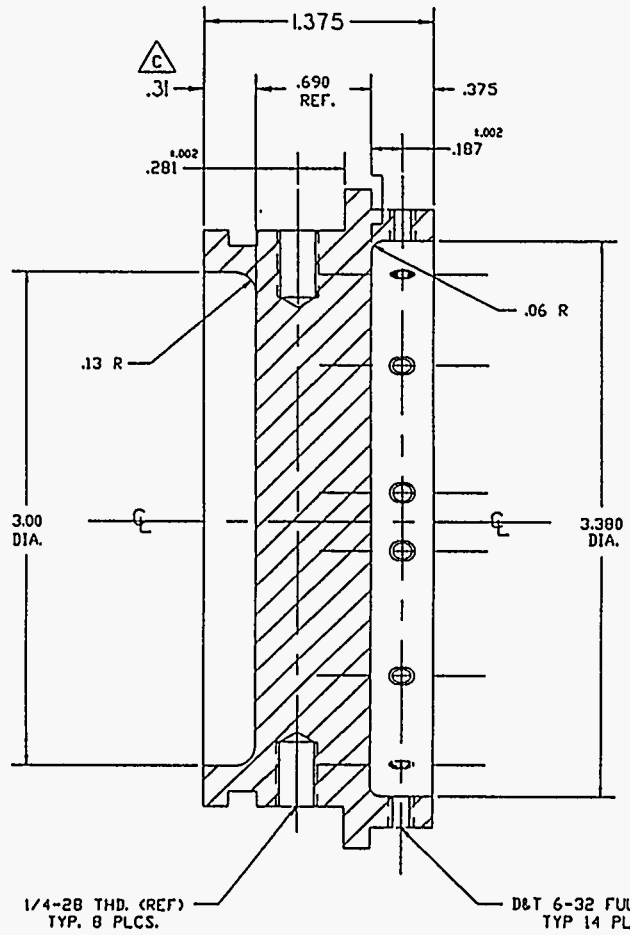

SECTION A-A
(SCALE: 2X)

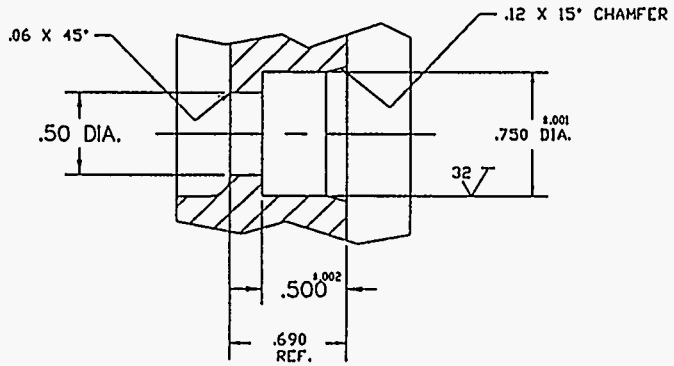

SECTION B-B
(SCALE: 2X)

B.3

	SANDIA NATIONAL LAB.		
	BOREHOLE RECEIVER SENSOR BULKHEAD		
ENGR. BY: B. ENGLER	SIZE C	FSCM NO	DWG NO 1002-4B REV C
DRAWN BY: B. ENGLER	SCALE 2X		SHEET 2 OF 2

DWG NO 1002-4B SH 2

147

NOTES:
1) BREAK EDGES .03 X 45°
2) MATL: 304 S.S.
3) QTY: 1 REQD.

REVISIONS			
REV	DESCRIPTION	DATE	APPROVED
A	PISTON HEIGHT CHANGED FROM 2.188 TO 2.000 (SHOE RETRIEVAL SYSTEM)	3/91	B.E.

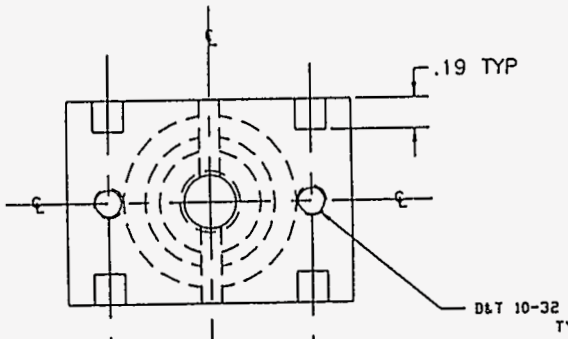

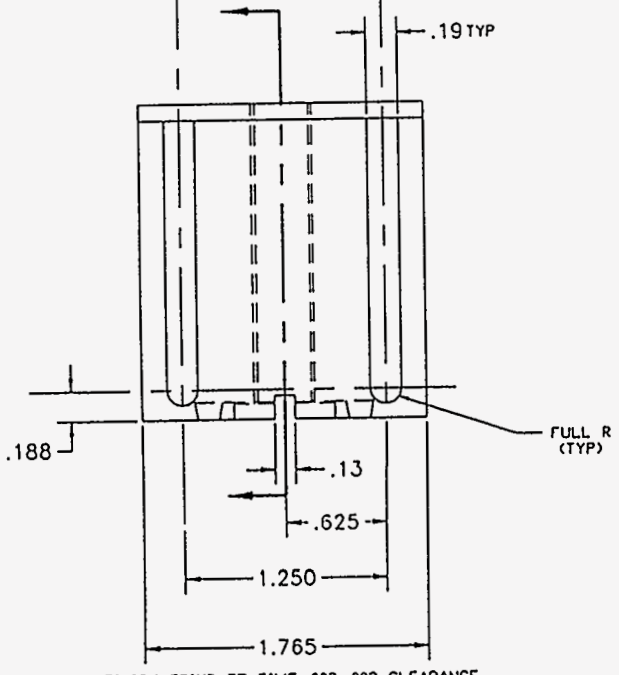

(FINISH GRIND TO GIVE .002-.003 CLEARANCE TO 1.755 DIM OF FINISHED PART NO. 1007-4)

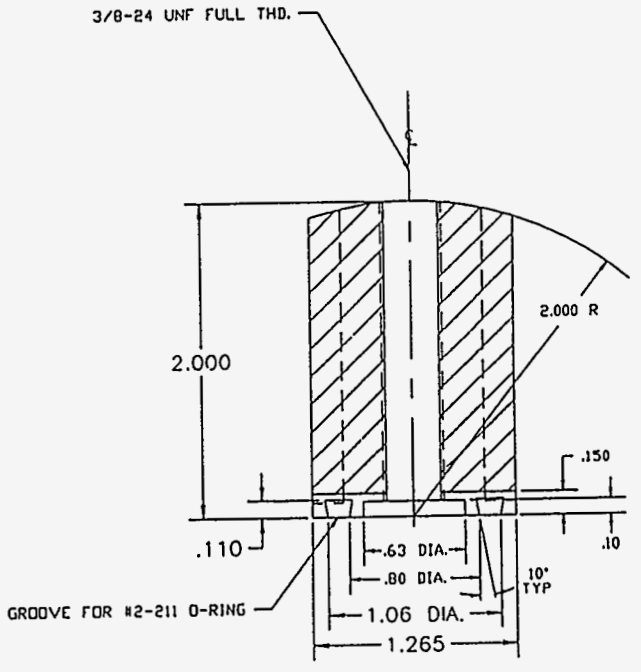

(FINISH GRIND TO GIVE .002-.003 CLEARANCE TO 1.255 DIM OF FINISHED PART NO. 1007-4)

	SANDIA NATIONAL LAB.			
	BOREHOLE RECEIVER CLAMP PISTON			
ENGR. BY: B. ENGLER	SIZE C	FSCM NO	DWG NO 1006-4	REV A
DRAWN BY: B. ENGLER	SCALE 2X		SHEET 1 OF 1	

NOTES:
1) BREAK EDGES .03 X 45°
2) MATL: 17-4 OR 13-8 S.S.
3) QTY: 1 REQD.

REV	DESCRIPTION	DATE	APPROVED

DWG NO 1007-4 SH 1

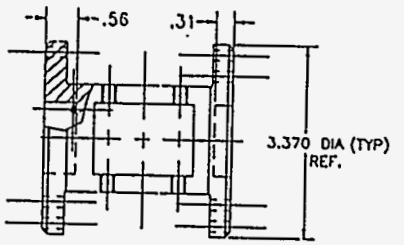

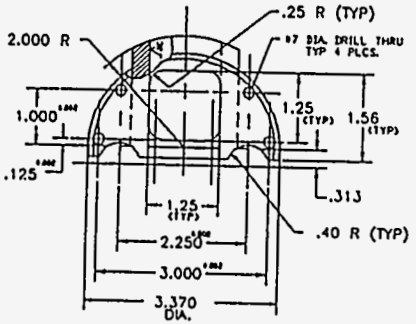

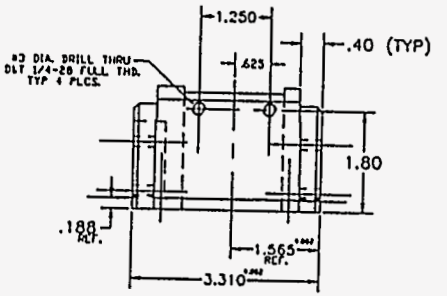

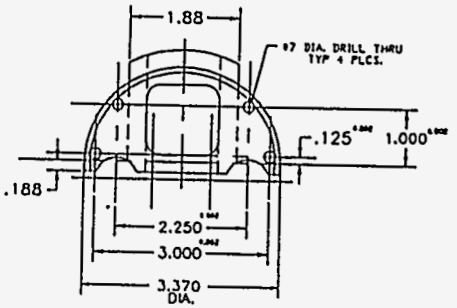

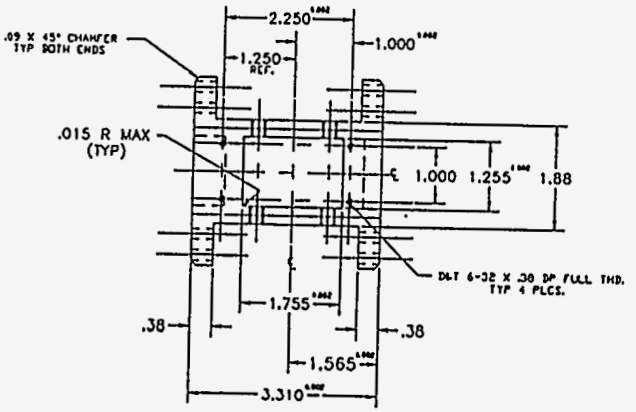

B.5

	SANDIA NATIONAL LAB.	
	BOREHOLE RECEIVER CLAMP PISTON HOUSING	
ENGR. BY: B. ENGLER	REV 0	DWG NO 1007-4
DRAWN BY: B. ENGLER	WGHT 1X	SHEET 1 OF 1

NOTES:
1) BREAK EDGES .03 X 45°
2) MATL: 15-5 S.S.
3) QTY: 1 REQD.

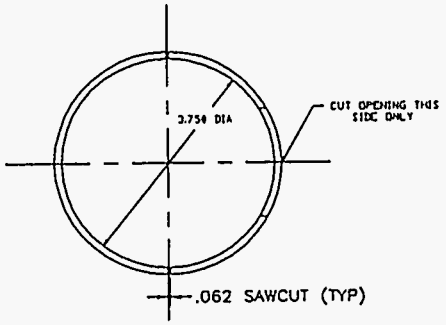

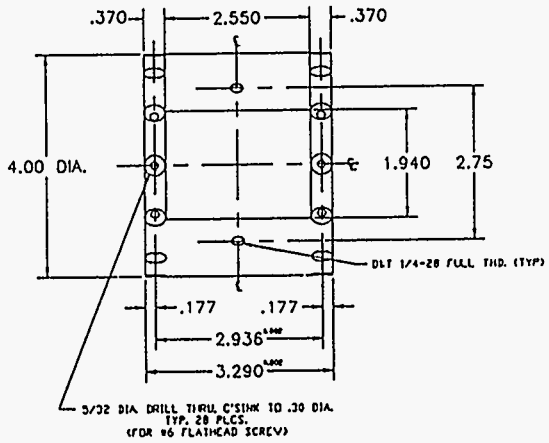

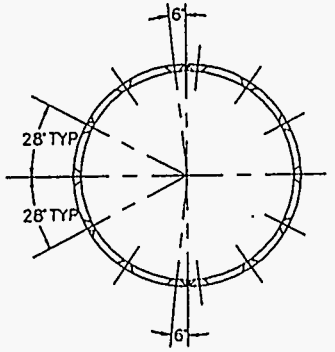

	SANDIA NATIONAL LAB.
	BOREHOLE RECEIVER MID-SECTION CLAM SHELL 2-PC.
ENGR. BY: B. ENGLER	SIZE D — DWG NO 1008-4 — REV
DRAWN BY: B ENGLER	SCALE 1X — SHEET 1 OF 1

DWG NO 1010-4 SH 1

REVISIONS			
REV	DESCRIPTION	DATE	APPROVED
A	CHANGE LENGTH FROM 2.25 TO 2.13	12/91	B.E.

NOTES:
1) BREAK CORNERS .03 X 45°
2) QTY: 1 REQD.
3) MATERIAL: 303 S.S.

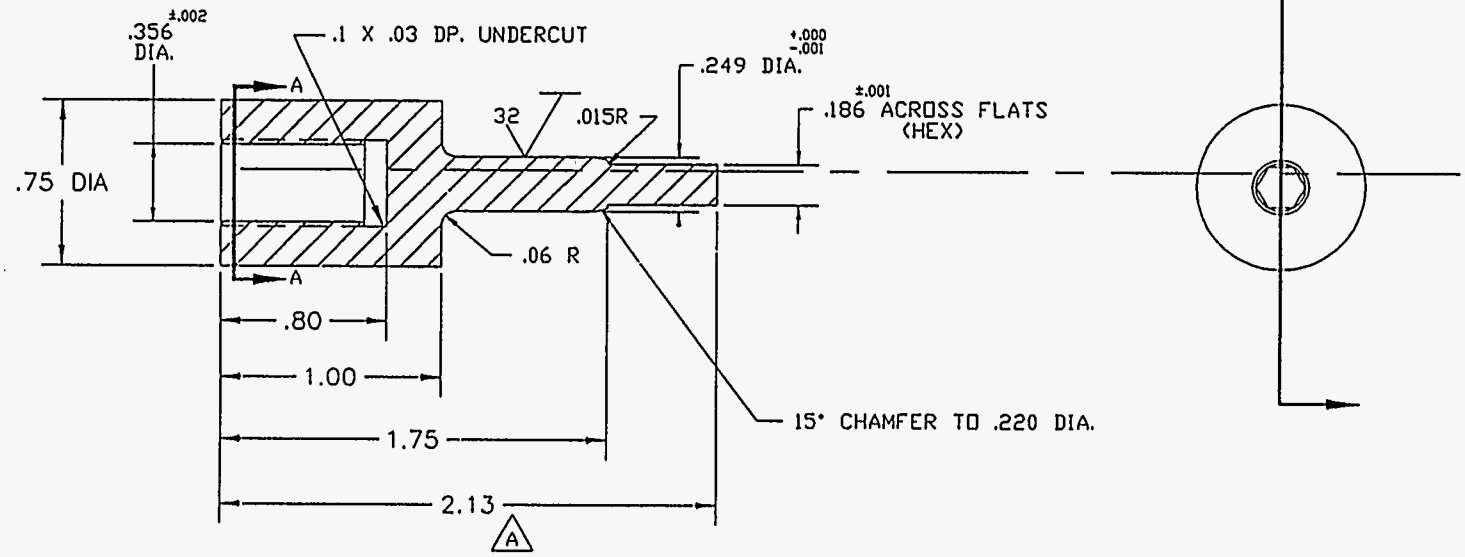

B.7

	SANDIA NATIONAL LAB.			
	BOREHOLE RECEIVER MOTOR DRIVE CONNECTING SHAFT			
ENGR. BY: B. ENGLER	SIZE B	FSCM NO	DWG NO 1010-4	REV A
DRAWN BY: B. ENGLER	SCALE 2X		SHEET 1 OF 2	

DWG NO 1010-4B SH 2

REVISIONS			
REV	DESCRIPTION	DATE	APPROVED

SECTION A–A

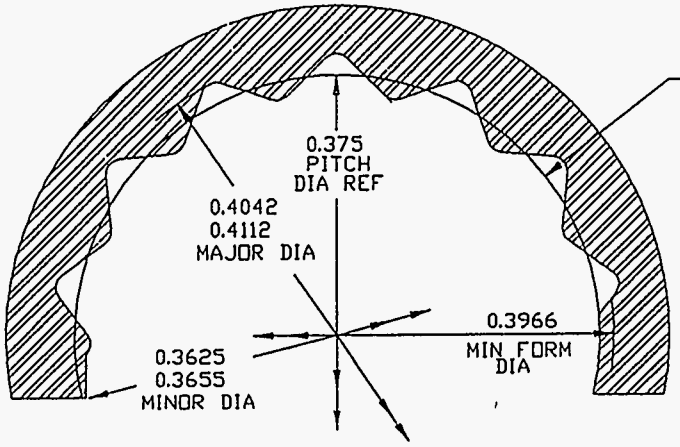

INVOLUTE SPLINE PER ANSI B92.1 - 1970
18 TEETH
48/96 PITCH
45° PRESSURE ANGLE

B.8

	SANDIA NATIONAL LAB.			
	BOREHOLE RECEIVER MOTOR DRIVE SHAFT SPLINE			
ENGR. BY: B. ENGLER	SIZE B	FSCM NO	DWG NO 1010-4B	REV
DRAWN BY: B. ENGLER	SCALE 1X		SHEET 2 OF 2	

NOTES:
1) BREAK EDGES .03 X 45°
2) MATL: 15-5 S.S.
3) QTY: 2 REQD.

REVISIONS			
REV	DESCRIPTION	DATE	APPROVED

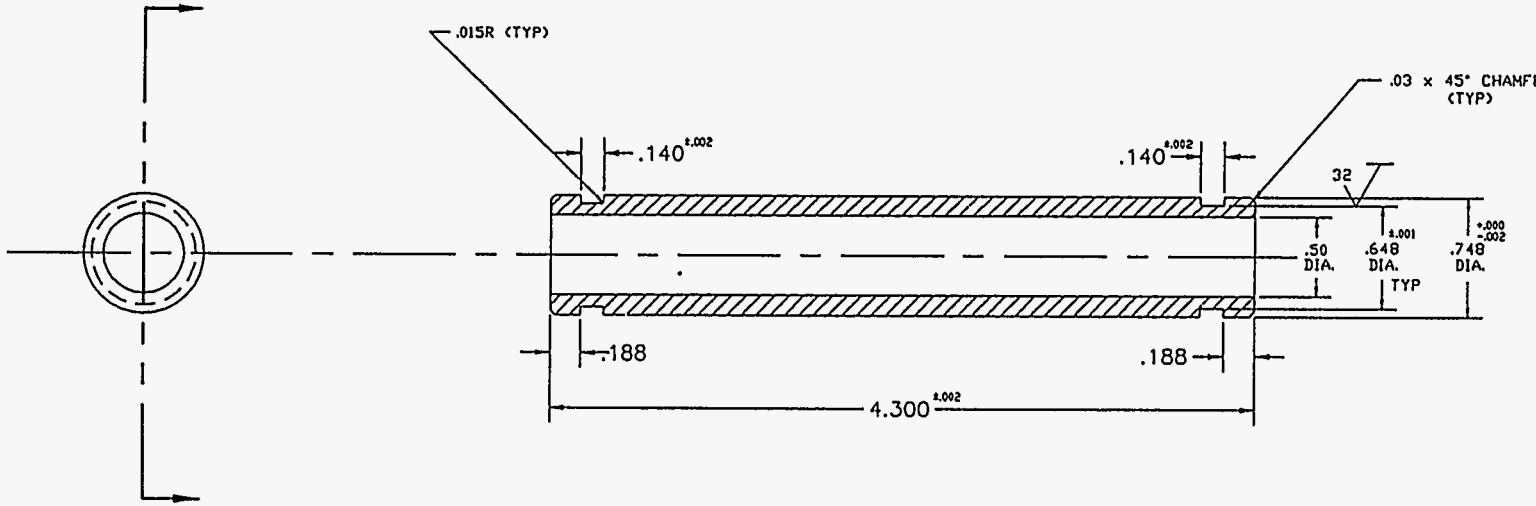

B.9

	SANDIA NATIONAL LAB.
	BOREHOLE RECEIVER MID-SECTION FEED THRU
ENGR. BY: B. ENGLER	SIZE C · FSCM NO · DWG NO 1011-4 · REV
DRAWN BY: B. ENGLER	SCALE 2X · SHEET 1 OF 1

DWG NO 1011-4

DWG NO 1013-4 SH 1

REVISIONS			
REV	DESCRIPTION	DATE	APPROVED

NOTES:

1) BREAK EDGES .015 X 45°
2) QTY: 1 REQD.
3) MATERIAL: 304 S.S.

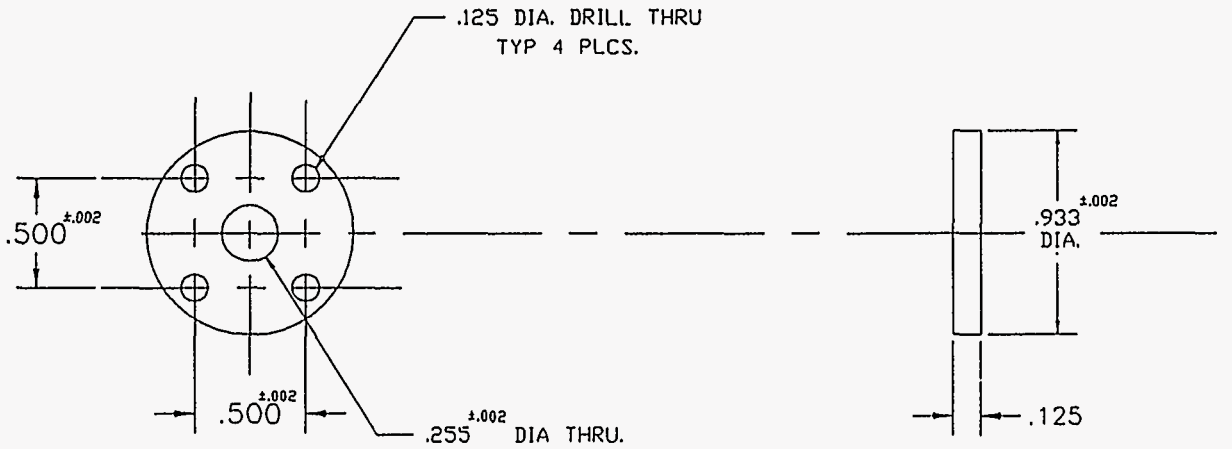

B.10

	SANDIA NATIONAL LAB.			
	BOREHOLE RECEIVER ROTARY SEAL RETAINER			
ENGR. BY: B. ENGLER	SIZE B	FSCM NO	DWG NO 1013-4	REV
DRAWN BY: B. ENGLER	SCALE 2X		SHEET 1 OF 1	

DWG NO 1014-4 | SH 1

REVISIONS			
REV	DESCRIPTION	DATE	APPROVED

NOTES:
1) BREAK EDGES .015 X 45°
2) QTY: 3 REQD.
3) MATERIAL: 304. S.S.

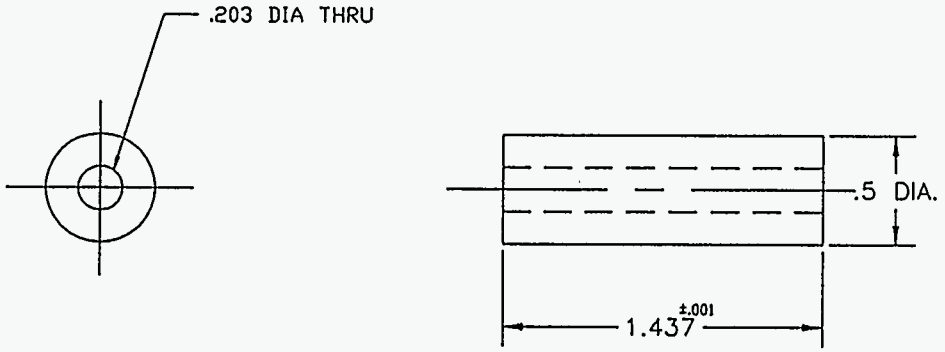

B.11

	SANDIA NATIONAL LAB.		
	BOREHOLE RECEIVER MOTOR MOUNT SPACER		
ENGR. BY: B. ENGLER	SIZE B	I SCH NO	DWG NO 1014-4 REV
DRAWN BY: B. ENGLER	SCALE 2X		SHEET 1 OF 1

DWG NO 1015-4 | SH 1

REVISIONS			
REV	DESCRIPTION	DATE	APPROVED

NOTES:
1) BREAK EDGES .015 X 45°
2) QTY: 1 REQD.

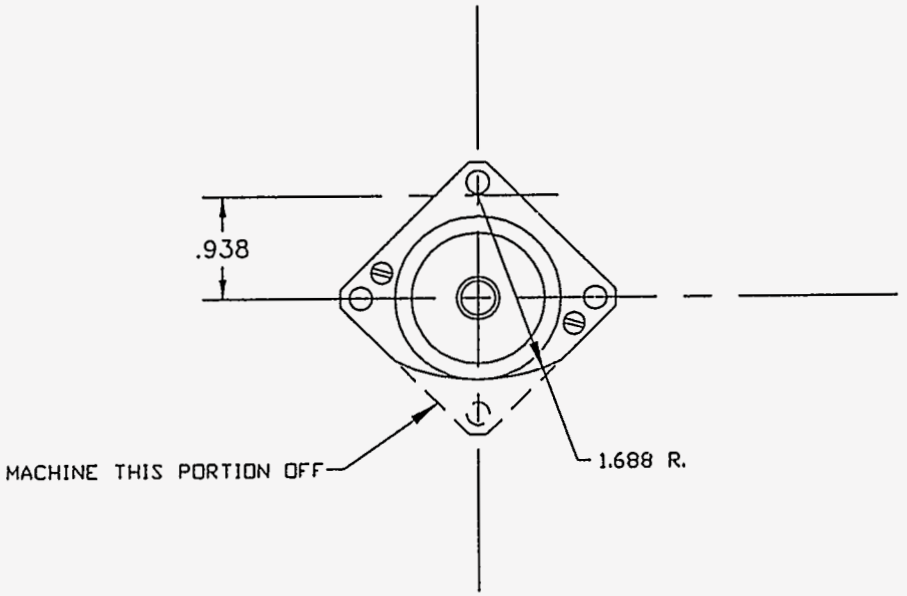

B.12

	SANDIA NATIONAL LAB.		
	BOREHOLE RECEIVER MOTOR MODIFICATION		
ENGR. BY: B. ENGLER	SIZE B	DWG NO 1015-4	REV
DRAWN BY: B. ENGLER	SCALE 1X	SHEET 1 OF 1	

REVISIONS			
REV	DESCRIPTION	DATE	APPROVED

NOTES:

1) MATERIAL: 1.000 DIAM 6061 T6 ALUM.
2) TOLERANCE: PLUS/MINUS .010"
3) DRAWING TO SCALE UNLESS NOTED
4) QUANTITY: 2 EACH

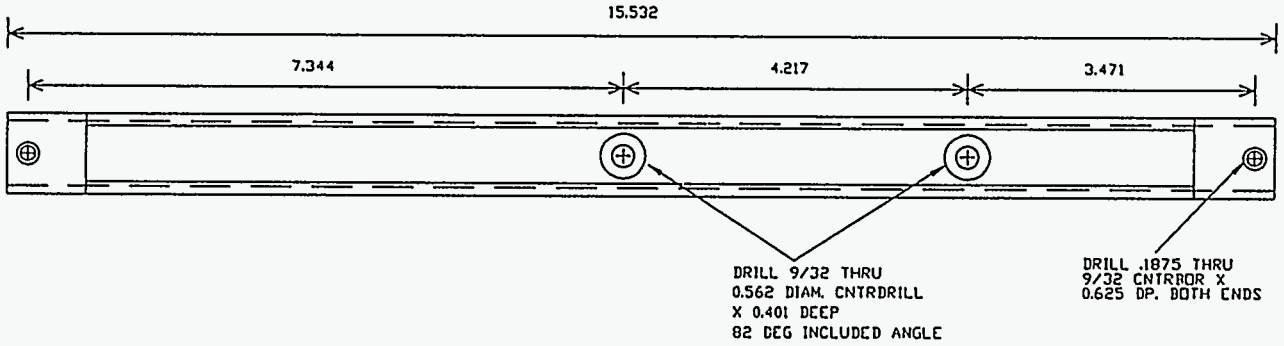

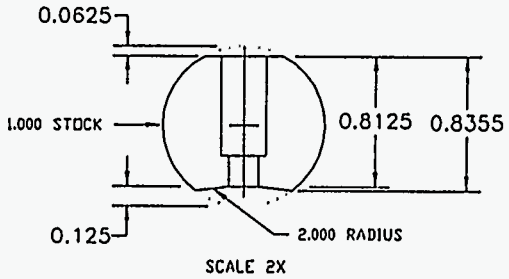

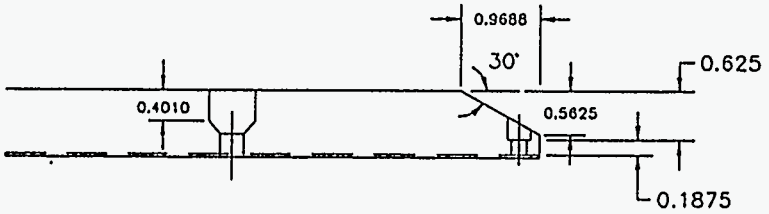

B.13

	SANDIA NATIONAL LAB.	
	BOREHOLE RECEIVER RAILS FOR 6-INCH I.D.	
ENGR. BY: B. ENGLER	SIZE C / FSCM NO / DWG NO 1016-4	REV
DRAWN BY: B. ENGLER	SCALE 1X	SHEET 1 OF 1

REVISIONS			
REV	DESCRIPTION	DATE	APPROVED

NOTES:

1) MATERIAL: 2.000 DIAM 6061 T6 ALUM.
2) TOLERANCE: PLUS/MINUS .010"
3) DRAWING TO SCALE UNLESS NOTED
4) QUANTITY: 2 EACH

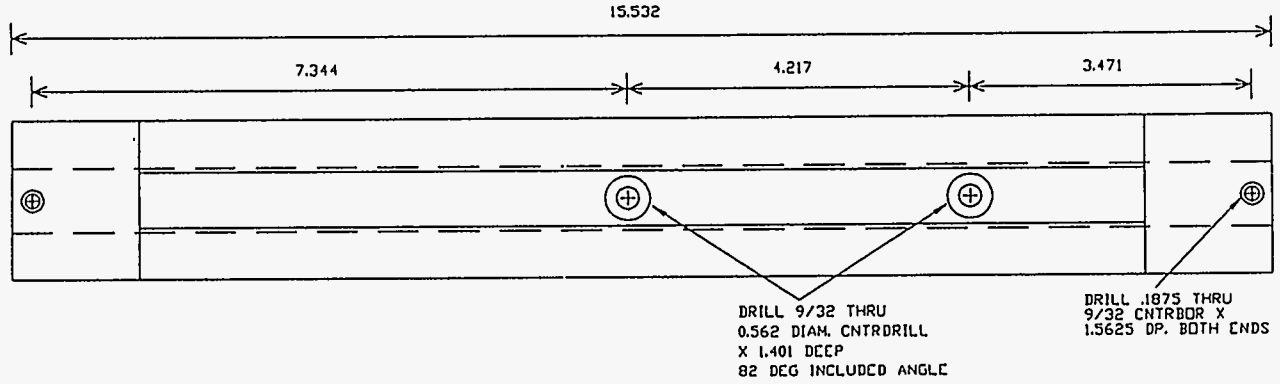

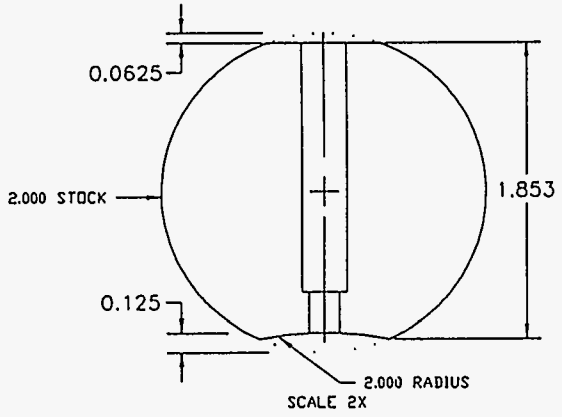

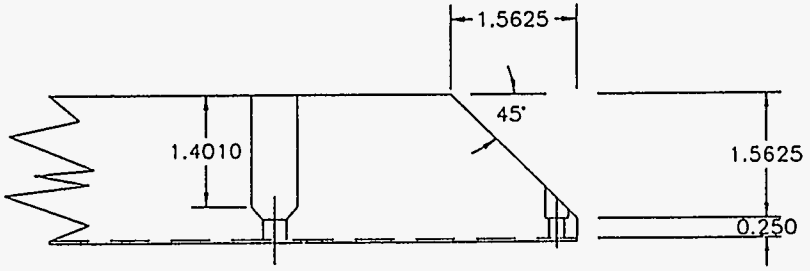

B.14

	SANDIA NATIONAL LAB.	
	BOREHOLE RECEIVER RAILS FOR 8-INCH I.D.	
ENGR. BY: B. ENGLER	SIZE C / DWG NO 1017-4	REV
DRAWN BY: B. ENGLER	SCALE 1X	SHEET 1 OF 1

DWG NO 1017-4 REV

NOTES:

1) MATERIAL: 1.000 DIAM 6061 T6 ALUM.
2) TOLERANCE: PLUS/MINUS .010"
3) QUANTITY: 2 EACH PER RECEIVER

REVISIONS			
REV	DESCRIPTION	DATE	APPROVED
A	CHANGE CNTR'BORE DEPTH FROM 0.23 TO 0.22 ON END HOLES.	3/26/94	B.E.

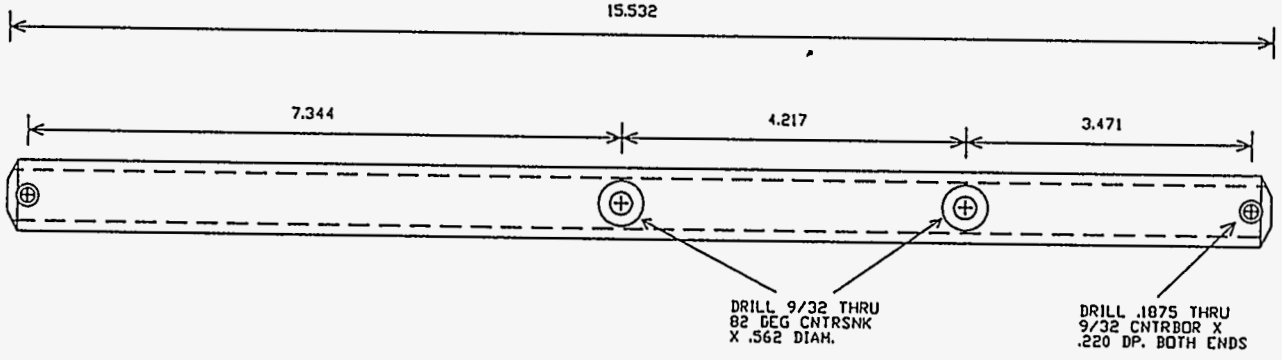

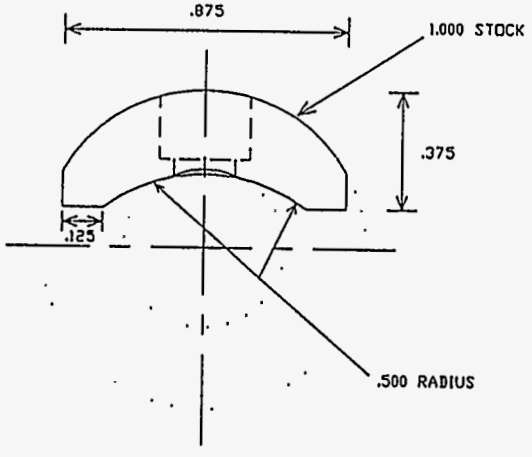

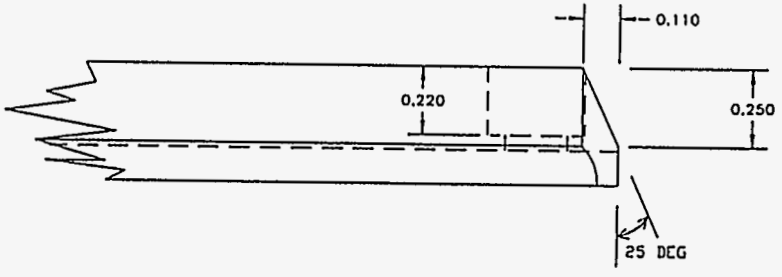

B.15

	SANDIA NATIONAL LAB.	
	BOREHOLE RECEIVER RAILS FOR 4.5-5.5 I.D.	
ENGR. BY: B. ENGLER	SIZE C / FSCM NO / DWG NO 1018-4	REV
DRAWN BY: B. ENGLER	SCALE 1X	SHEET 1 OF 1

REVISIONS			
REV	DESCRIPTION	DATE	APPROVED

NOTES:
1) BREAK EDGES .03 X 45°
2) MATL: MILD STEEL OR ALUMINUM

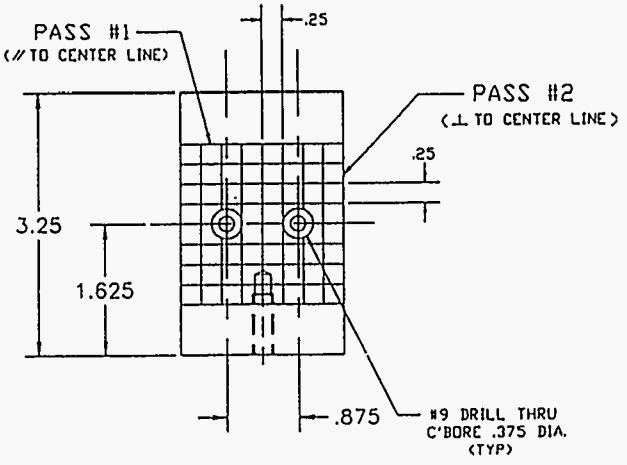

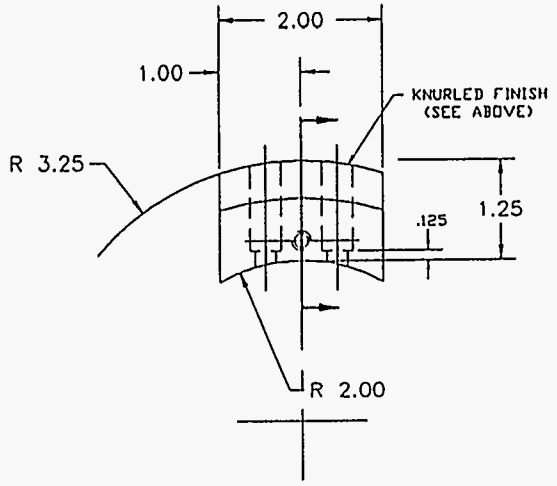

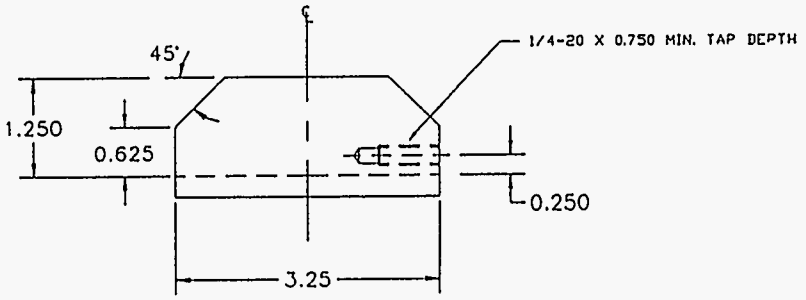

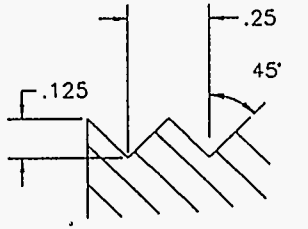

KNURLED FINISH DETAIL
PASSES MADE ON 0.25 IN CENTERS AT 45°
AND A DEPTH OF 0.125 IN.

KNURLING DETAIL

DWG NO 1021-5A REV

	SANDIA NATIONAL LAB.	
	BOREHOLE RECEIVER SHOE ADAPTER - SMALL	
ENGR. BY: D. ENGLER	SIZE C / DWG NO 1021-5A	REV
DRAWN BY: D. ENGLER	SCALE 1X	SHEET 1 OF 1

NOTES:
1) BREAK EDGES .03 X 45°
2) MATL: MILD STEEL OR ALUMINUM

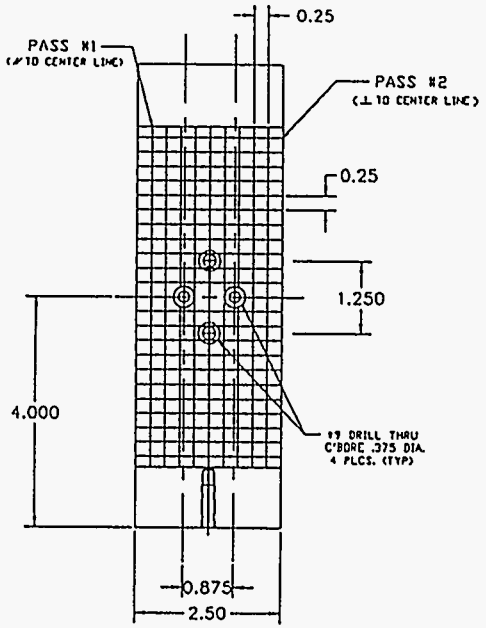

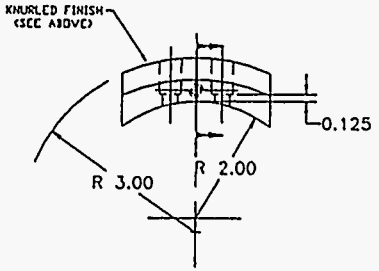

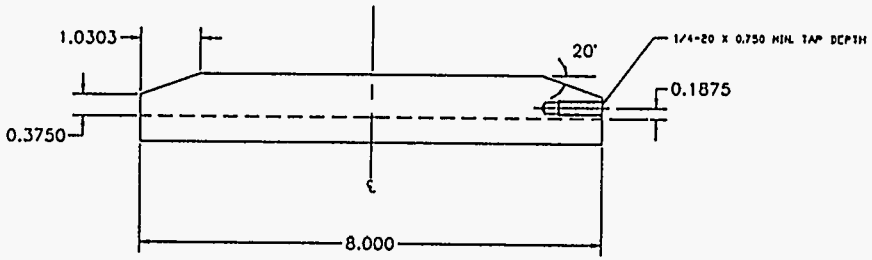

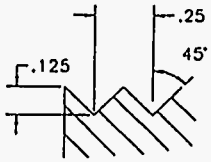

KNURLED FINISH DETAIL
PASSES MADE ON 0.25 IN CENTERS AT 45°
AND A DEPTH OF 0.125 IN.

KNURLING DETAIL

	SANDIA NATIONAL LAB.
	BOREHOLE RECEIVER
	SHOE ADAPTER – LARGE
ENGR. BY: B. ENGLER	SIZE D / DWG NO. 1021-5B / REV
DRAWN BY: B. ENGLER	SCALE 1X / SHEET 1 OF 1

REVISIONS			
REV	DESCRIPTION	DATE	APPROVED
A	ADD NOTE	6/92	B.E.

NOTES:
1) BREAK CORNERS .03 X 45°.
2) REF. O-RING #2-127
3) MACHINE FROM MINERAL LOGGING SERVICES OR VIDCO LOGGERS UNIVERSAL ADAPTER, 2 1/2 OD X 3/4 ID.
4) MATERIAL: 15-5 S.S.

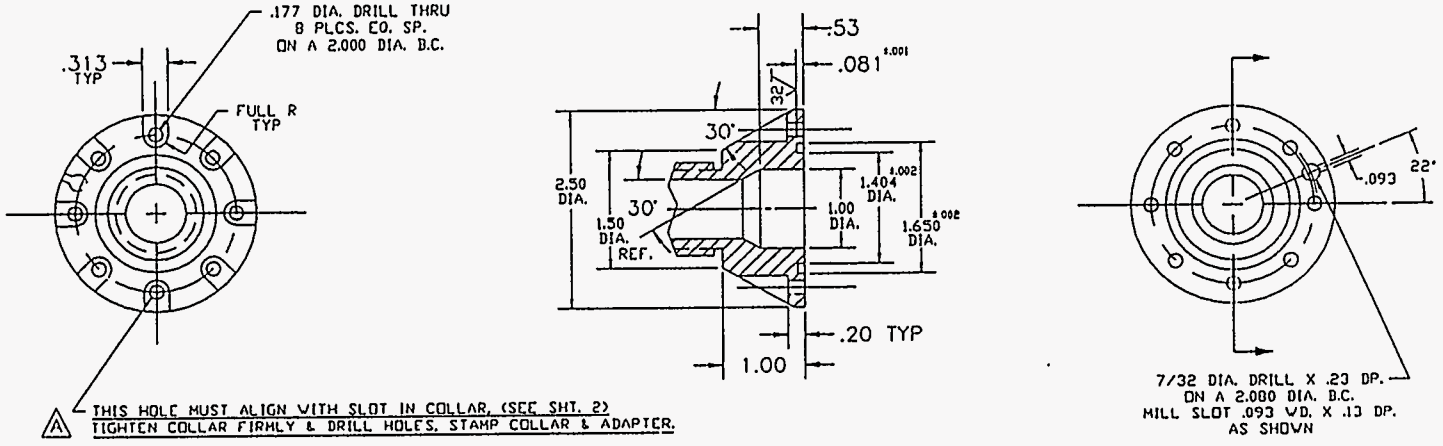

	SANDIA NATIONAL LAB.	
	BOREHOLE RECEIVER G.O. CONNECTOR FLANGE	
ENGR. BY: D. ENGLER	WT: G / DWG NO: 1023-4	REV: A
DRAWN BY: D. ENGLER	SCALE: 1X	SHEET 1 OF 2

DWG NO 1023-4 SH 1

REVISIONS			
REV	DESCRIPTION	DATE	APPROVED
A	ADD NOTE	6/92	B.E.

NOTES:
1) BREAK CORNERS .03 X 45°.
2) MACHINE FROM M.L.S. GEARHART-OWENS ADAPTER COLLAR.
3) MATERIAL: 304 S.S.

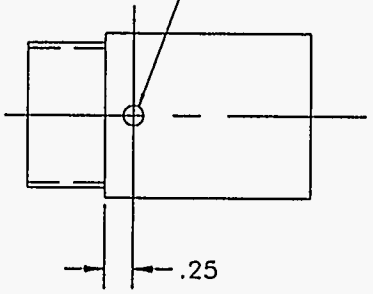

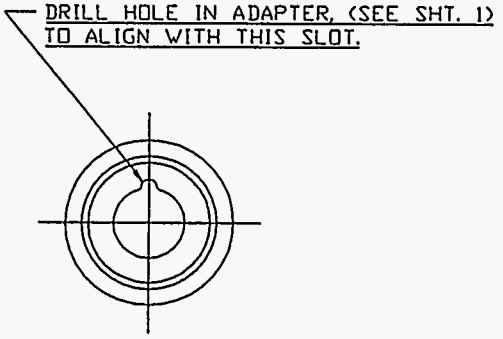

B.19

	SANDIA NATIONAL LAB.			
	BOREHOLE RECEIVER G.O. CONNECTOR COLLAR			
ENGR. BY: B. ENGLER	SIZE B	FSCM NO	DWG NO 1023-4	REV A
DRAWN BY: B. ENGLER	SCALE 1X			SHEET 2 OF 2

REVISIONS			
REV	DESCRIPTION	DATE	APPROVED

NOTES:
1) BREAK CORNERS .03 X 45°.
2) REF. O-RING #2-127
3) MATERIAL: 15-5 S.S.

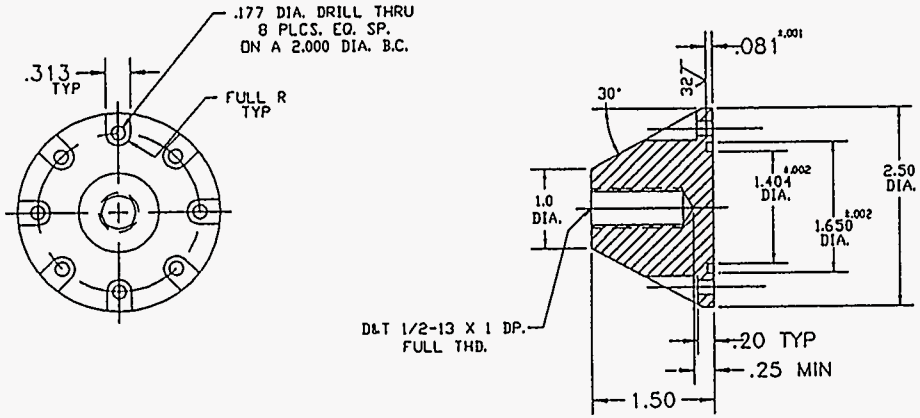

B.20

	SANDIA NATIONAL LAB.
	BOREHOLE RECEIVER SINKER BAR / PLUG ADAPTER
ENGR. BY: B. ENGLER	SIZE C | F SCM NO | DWG NO 1024-4 | REV
DRAWN BY: B. ENGLER	SCALE 1X | SHEET 1 OF 1

DWG 1024-4 REV

REVISIONS			
REV	DESCRIPTION	DATE	APPROVED

NOTES:
1) BREAK CORNERS .03 X 45°
2) MATL: 304 S.S.
3) QTY: 1 REQD.
4) REFER TO DWG. 1036-4 SWAG BALL AFTER CABLE IS THREADED
5) DIMENSIONS CAN BE ADJUSTED RELATIVE TO SHOE IF NECESSARY

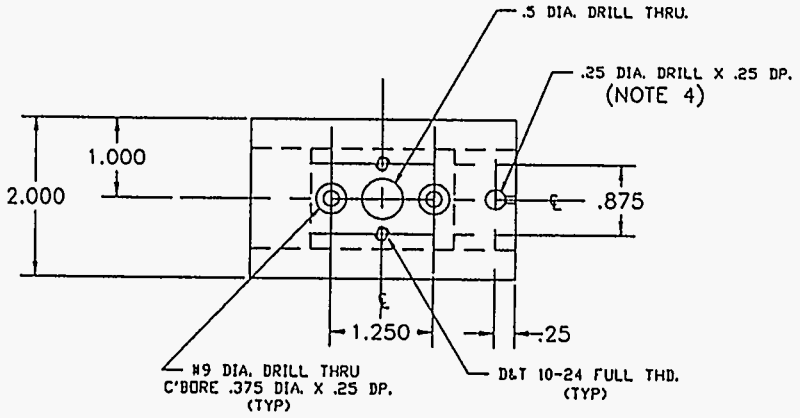

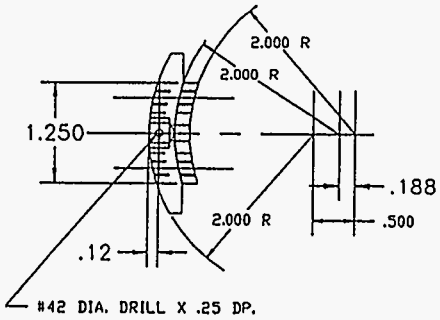

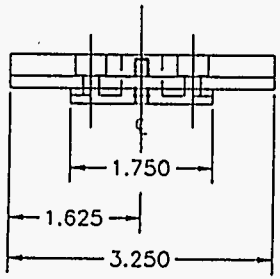

B.21

	SANDIA NATIONAL LAB.	
	BOREHOLE RECEIVER CLAMP MUSHROOM PLATE	
ENGR. BY: B. ENGLER	SIZE C / FSCM NO / DWG NO 1026-4	REV
DRAWN BY: B. ENGLER	SCALE 1X	SHEET 1 OF 1

DWG NO 1026-4 REV

REVISIONS			
REV	DESCRIPTION	DATE	APPROVED

NOTES:
1) BREAK CORNERS .03 X 45°
2) MATL: 304 S.S.
3) QTY: 1 REQD.
4) REFER TO DWG. 1036-4 BALL CAN BE SWAGGED PRIOR TO ASSEMBLY.
5) DIMENSIONS CAN BE ADJUSTED RELATIVE TO SHOE IF NECESSARY.

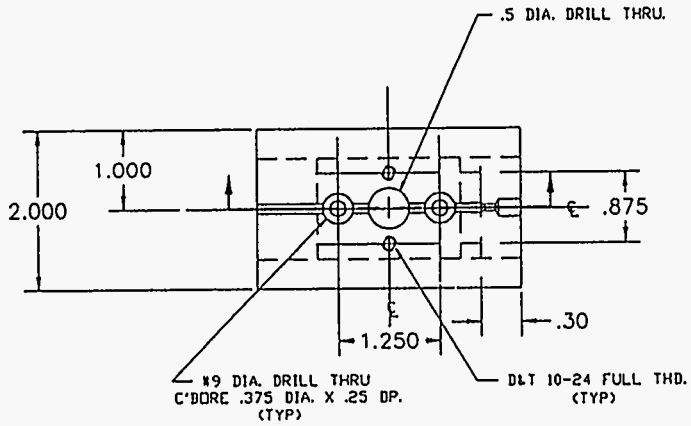

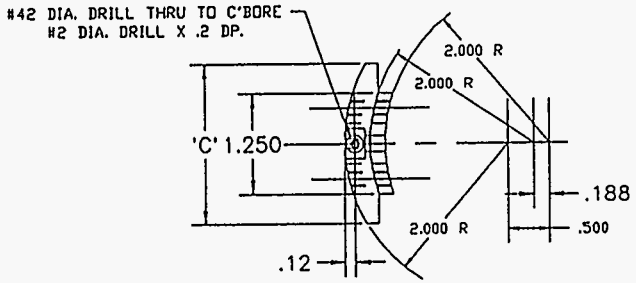

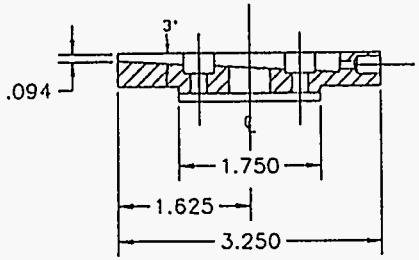

	SANDIA NATIONAL LAB.		
	BOREHOLE RECEIVER CLAMP MUSHROOM PLATE-2		
ENGR. BY: B. ENGLER	SIZE C	FSCM NO	DWG NO 1027-4 REV
DRAWN BY: B. ENGLER	SCALE 1X		SHEET 1 OF 1

DWG NO 1027-4 SH 1

B.22

NOTES:
1) BREAK CORNERS .03 X 45°
2) MATL: 303 S.S.
3) QTY: 1 REQD.
4) SCALE: 2X

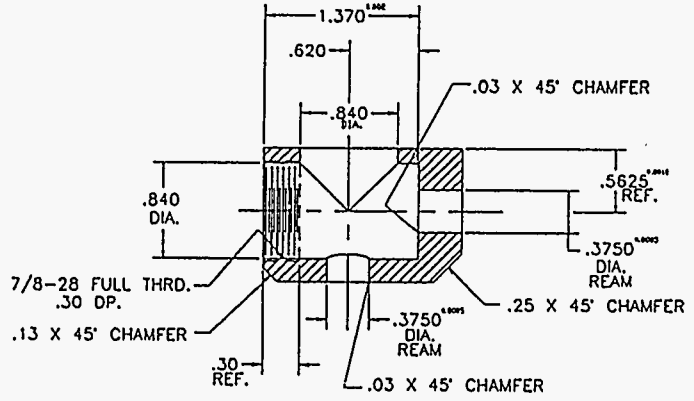

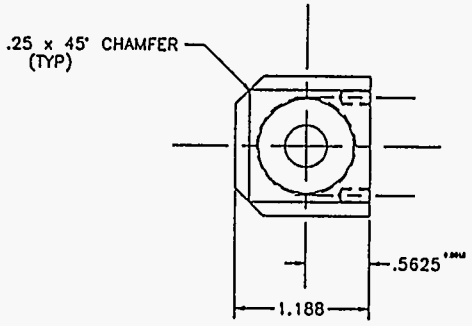

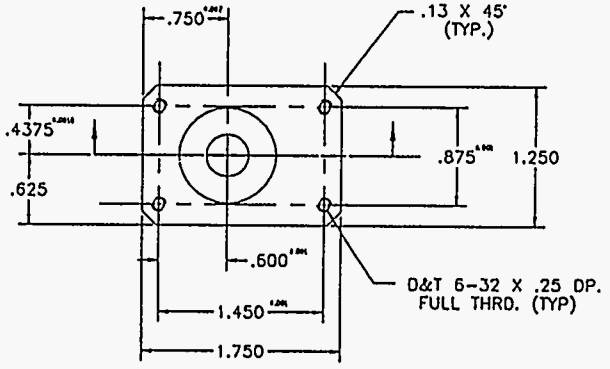

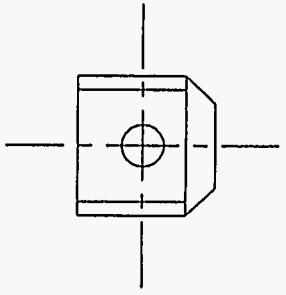

	SANDIA NATIONAL LAB.
	BOREHOLE RECEIVER RIGHT ANGLE GEARBOX
ENGR. BY: B. ENGLER	SIZE D — DWG NO. 1028-4 — REV
DRAWN BY: CAD GEOSPACE	SCALE 1X — SHEET 1 OF 1

B.23

REVISIONS			
REV	DESCRIPTION	DATE	APPROVED

NOTES:
1) BREAK EDGES .03 X 45°
2) QTY: 1 REQD.
3) MATL: 304 S.S.

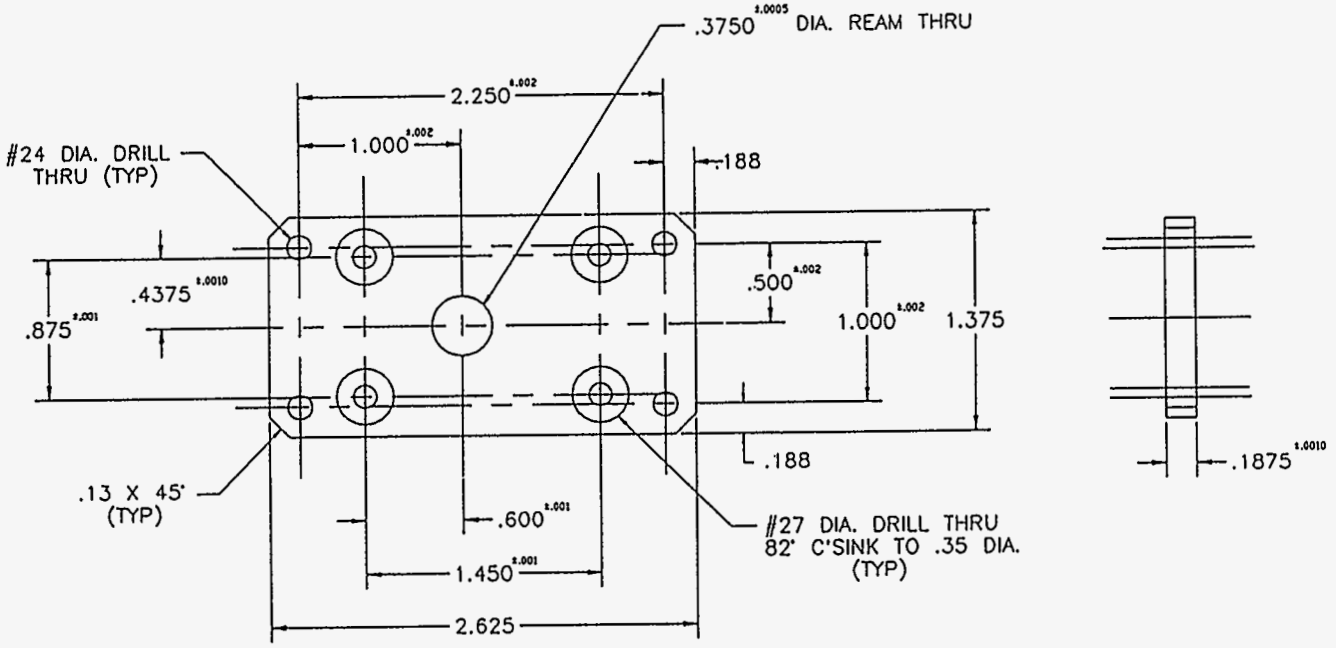

B.24

	SANDIA NATIONAL LAB.	
	BOREHOLE RECEIVER PLATE, GEARBOX	
ENGR. BY: B. ENGLER	SIZE C / FSCM NO / DWG NO 1029-4	REV
DRAWN BY: GYD GEOSPACE	SCALE 1X	SHEET 1 OF 1

DWG NO 1029-4 REV

DWG NO 1031-4 | SH 1

REVISIONS			
REV	DESCRIPTION	DATE	APPROVED

NOTES:
1) BREAK EDGES .03 X 45°
2) QTY: 1 REQD.
3) SCALE: 4X
4) MATERIAL: 316 S.S.

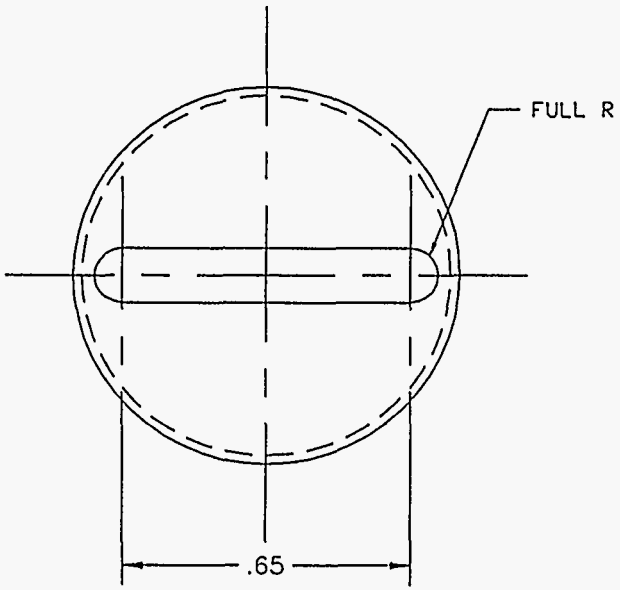

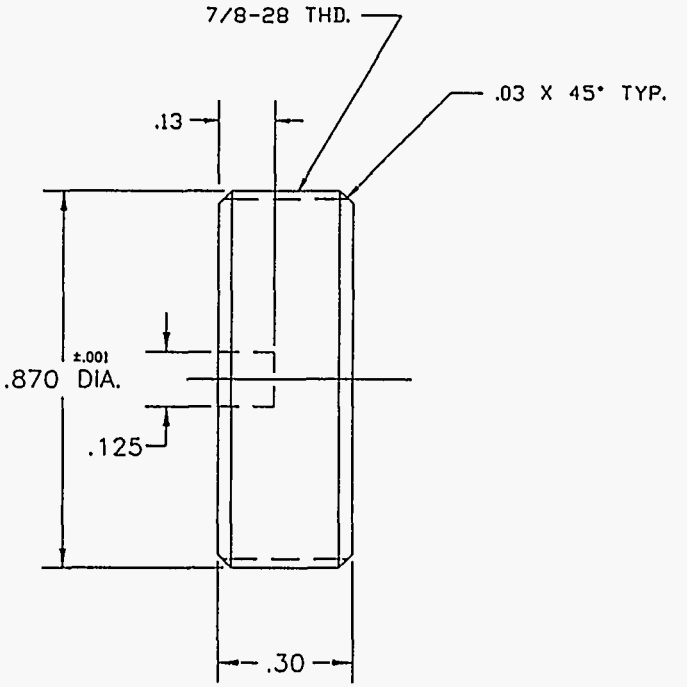

B.25

	SANDIA NATIONAL LAB.			
	BOREHOLE RECEIVER GEARBOX INSPECTION COVER			
ENGR. BY: OYO GEOSPACE	SIZE B	FSCM NO	DWG NO 1031-4	REV
DRAWN BY: OYO GEOSPACE	SCALE 4X		SHEET 1 OF 1	

DWG NO 1032-4 | SH 1

REVISIONS			
REV	DESCRIPTION	DATE	APPROVED

NOTES:
1) BREAK EDGES .03 X 45°
2) QTY: 1 REQD.
3) MATERIAL: 304 S.S.

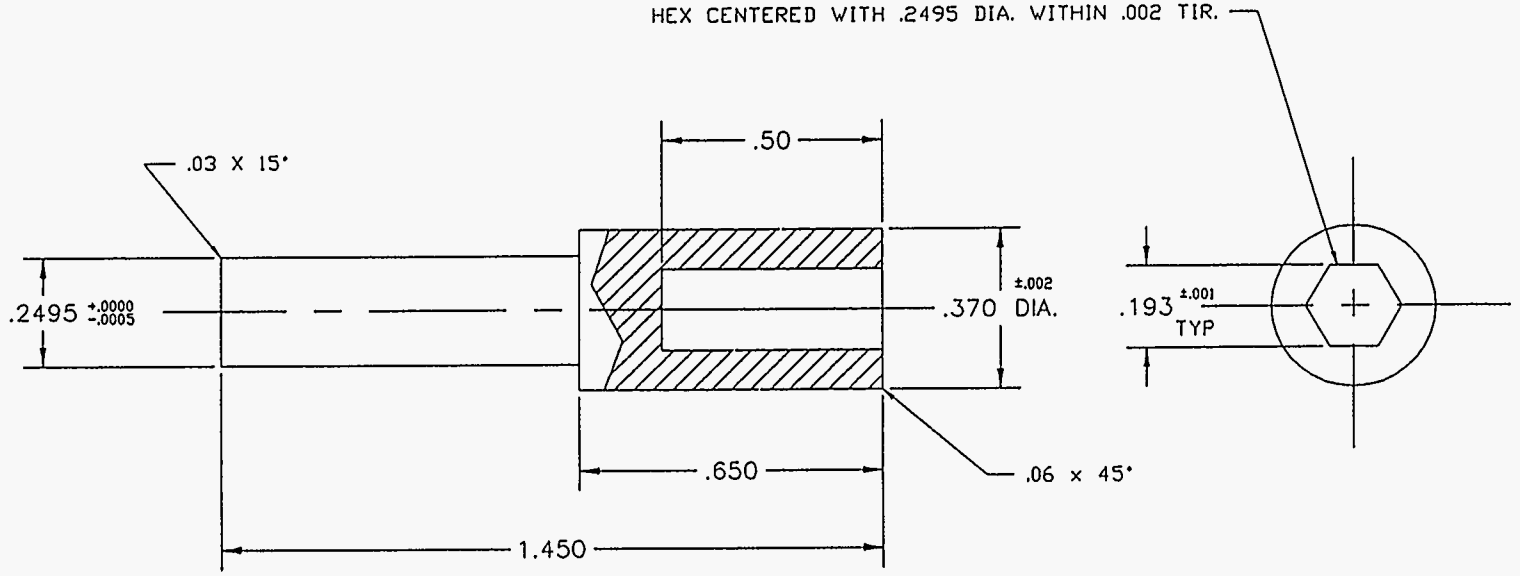

B.26

	SANDIA NATIONAL LAB.			
	BOREHOLE RECEIVER INPUT COUPLING SHAFT			
ENGR. BY: B. ENGLER	SIZE B	FSCM NO	DWG NO 1032-4	REV
DRAWN BY: B. ENGLER	SCALE 4X		SHEET 1 OF 1	

DWG NO 1033-4 | SH 1

REVISIONS			
REV	DESCRIPTION	DATE	APPROVED

NOTES:
1) BREAK SHARP EDGES .03 X 45°
2) STOCK DRIVE PRODUCTS PART #1C4-Y32024

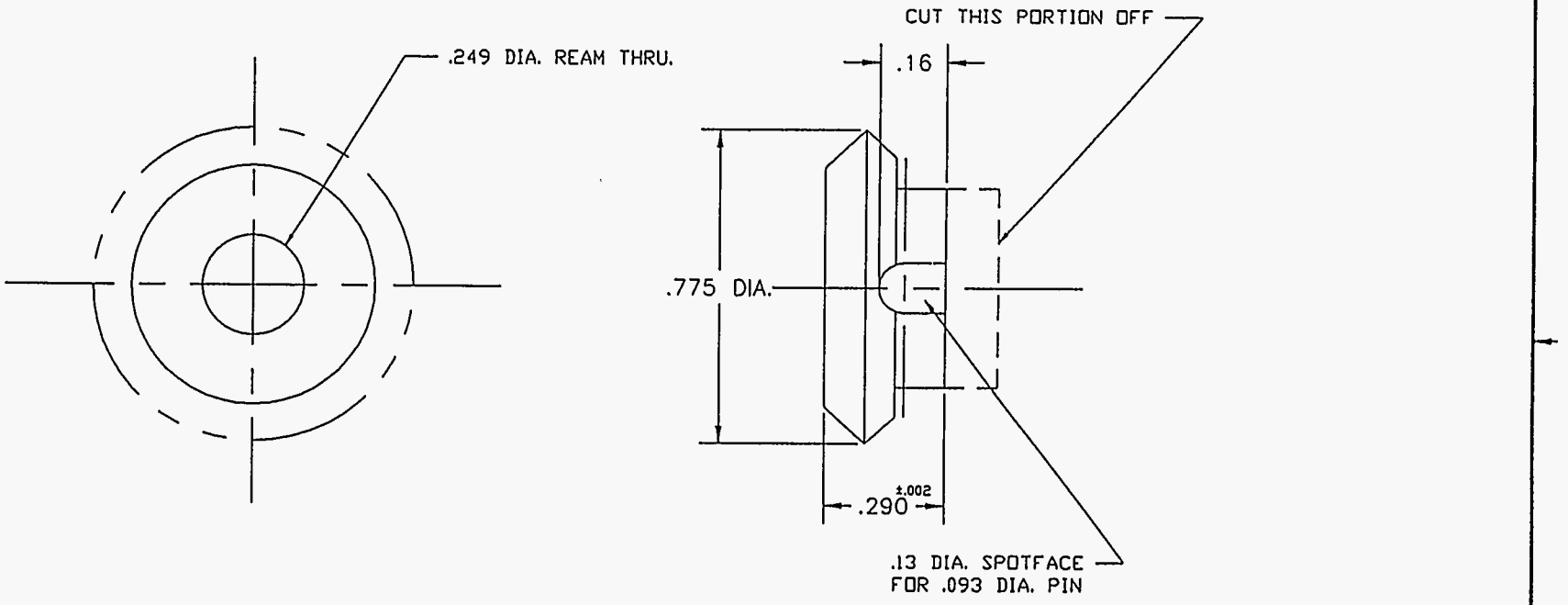

B.27

	SANDIA NATIONAL LAB.		
	BOREHOLE RECEIVER GEAR MODIFICATION		
ENGR. BY: OYO GEOSPACE	SIZE B	FSCM NO	DWG NO 1033-4	REV
DRAWN BY: OYO GEOSPACE	SCALE 4X		SHEET 1 OF 1

DWG NO 1034-4 | SH 1

REVISIONS			
REV	DESCRIPTION	DATE	APPROVED

NOTES:
1) BREAK EDGES .015 X 45°
2) QTY: 1 REQD PER TOOL
3) SAND ENDS SMOOTH
4) MATERIAL: 17-4 S.S.

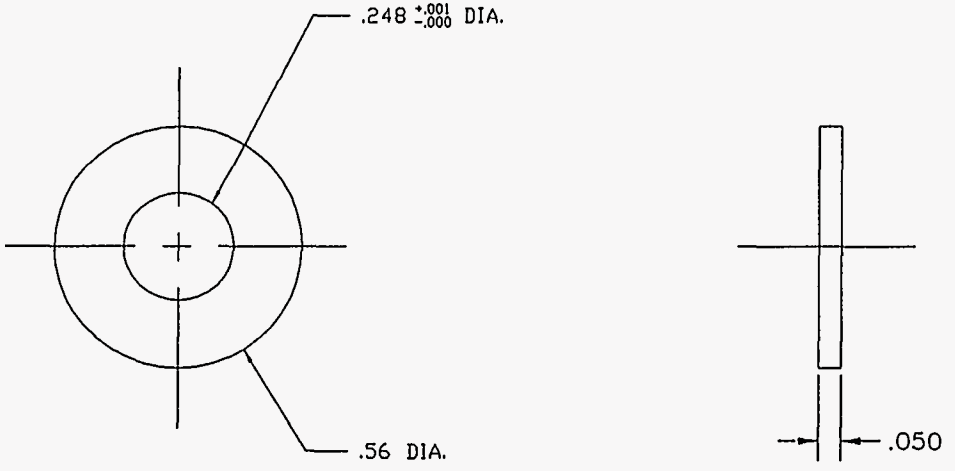

B.28

	SANDIA NATIONAL LAB.		
	BOREHOLE RECEIVER GEARBOX WASHER		
ENGR. BY: OYO GEOSPACE	SIZE B	FSCM NO	DWG NO 1034-4 REV
DRAWN BY: OYO GEOSPACE	SCALE 4X		SHEET 1 OF 1

DWG NO 1035-4 | SH 1

REVISIONS			
REV	DESCRIPTION	DATE	APPROVED

NOTES:

1) 3/8-24 LEAD SCREW
2) MATERIAL: 316 S.S.
3) FOR USE WITH THRUST WASHER #B5-3-SS

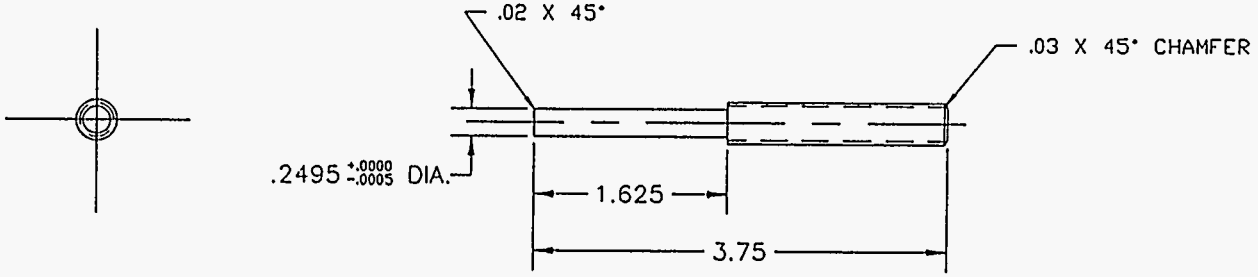

B.29

	SANDIA NATIONAL LAB.			
	BOREHOLE RECEIVER CLAMP LEAD SCREW			
ENGR. BY: B. ENGLER	SIZE B	FSCM NO	DWG NO 1035-4	REV
DRAWN BY: B. ENGLER	SCALE 1X		SHEET 1 OF 1	

DWG NO 1036-4 | SH 1

REVISIONS			
REV	DESCRIPTION	DATE	APPROVED

NOTES:
1) SAVA PART #565-S
2) MATL: STAINLESS STEEL
3) CHECK LENGTH

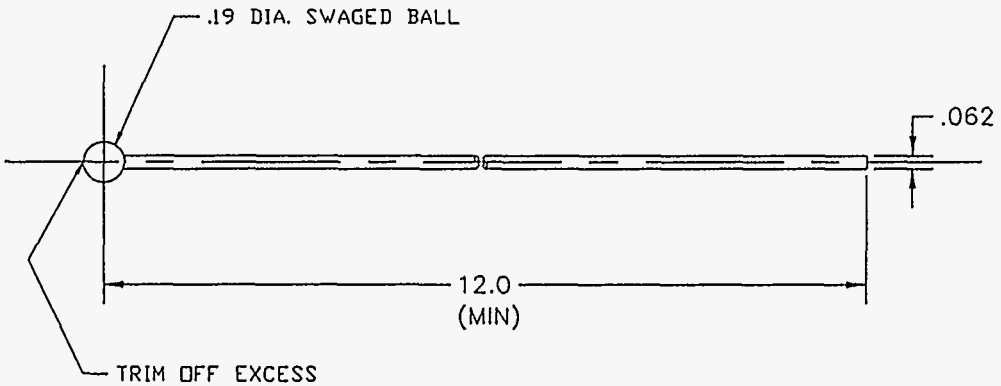

B.30

	SANDIA NATIONAL LAB.		
	BOREHOLE RECEIVER SWAGGED BALL ASSEMBLY		
ENGR. BY: B. ENGLER	SIZE B	FSCM NO	DWG NO 1036-4	REV
DRAWN BY: B. ENGLER	SCALE 1X		SHEET 1 OF 1

NOTES
1) MATERIAL 316 S.S.
2) QUANTITY 1 EACH
3) TOLERANCES ±0.005

REVISIONS			
REV	DESCRIPTION	DATE	APPROVED

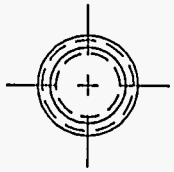

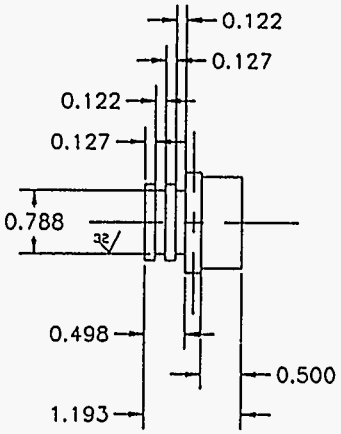

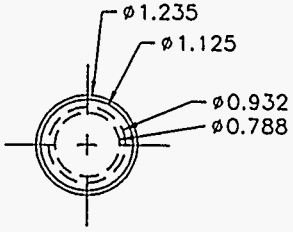

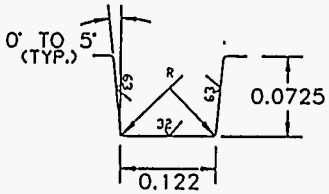

R= 0.005 TO 0.015

NOT TO SCALE

	SANDIA NATIONAL LAB.		
	BOREHOLE RECEIVER G.O. HEAD PLUG ADAPTER		
ENGR. BY: B. ENGLER	SIZE C	FSCM NO	DWG NO 1037-4 REV
DRAWN BY: B. ENGLER	SCALE 1X		SHEET 1 OF 1

B.31

DWG NO	SH
1038-4	1

REVISIONS			
REV	DESCRIPTION	DATE	APPROVED

NOTES:
1) MATERIAL: 6061 ALUMINUM
2) QUANTITY: 6 EACH PER RECEIVER TOOL

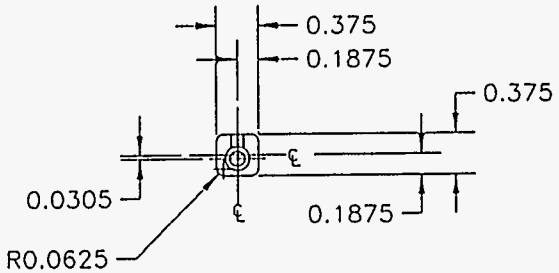

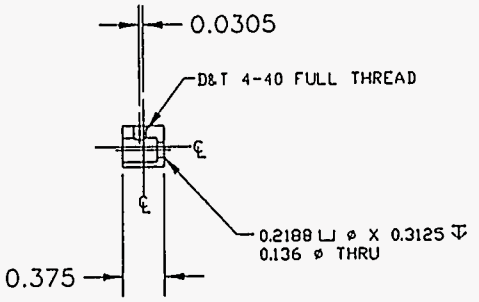

B.32

	SANDIA NATIONAL LAB.			
	BOREHOLE RECEIVER PC BOARD / BULKHEAD MOUNTS			
ENGR. BY: B. ENGLER	SIZE B	FSCM NO	DWG NO 1038-4	REV
DRAWN BY: B. ENGLER	SCALE 1X		SHEET 1 OF 1	

DWG NO 1040-4 | SH 1

REVISIONS			
REV	DESCRIPTION	DATE	APPROVED

NOTES:
1) LUBRICATE BEARING BEFORE ASSEMBLY WITH MOBIL SYNTHETIC GREASE.

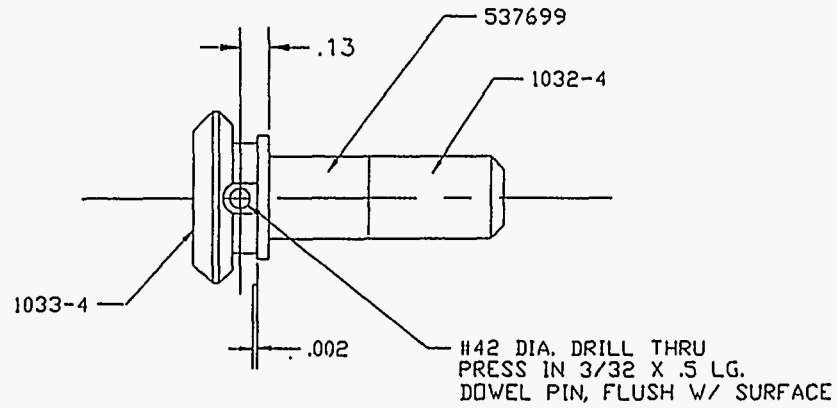

	SANDIA NATIONAL LAB.			
	BOREHOLE RECEIVER GEARBOX INPUT DRIVE ASSEMBLY			
ENGR. BY: OYO GEOSPACE	SIZE B	FSCM NO	DWG NO 1040-4	REV
DRAWN BY: OYO GEOSPACE	SCALE 2X		SHEET 1 OF 1	

DWG NO 1041-4	SH 1

REVISIONS			
REV	DESCRIPTION	DATE	APPROVED

NOTES:
1) LUBRICATE THRUST BEARING WITH MOBIL SYNTHETIC GREASE PRIOR TO ASSEMBLY.

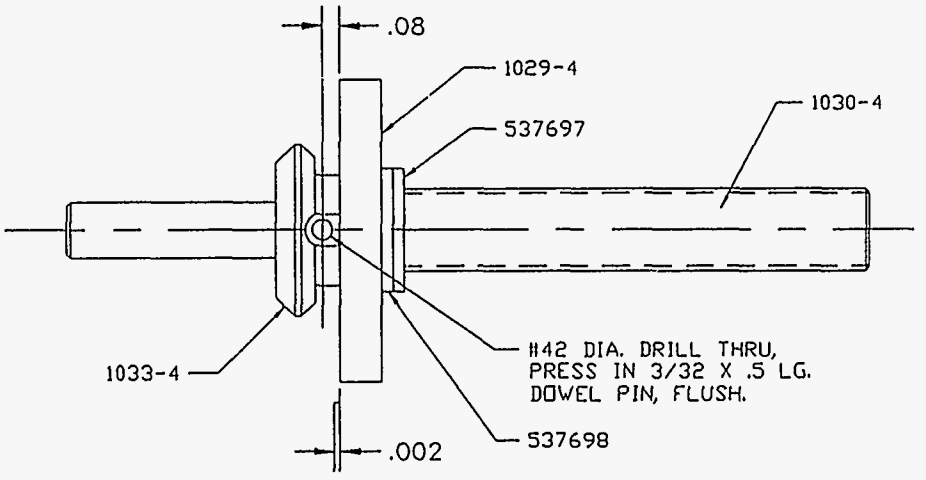

	SANDIA NATIONAL LAB.			
	BOREHOLE RECEIVER GEARBOX LEADSCREW ASSEMBLY			
ENGR. BY: OYO GEOSPACE	SIZE B	FSCM NO	DWG NO 1041-4	REV
DRAWN BY: OYO GEOSPACE	SCALE 2X		SHEET 1 OF 1	

178

NOTES:
1) BREAK EDGES .03 X 45°
2) MATL: ALUMINUM
3) QTY: 1 REQD. PER TOOL

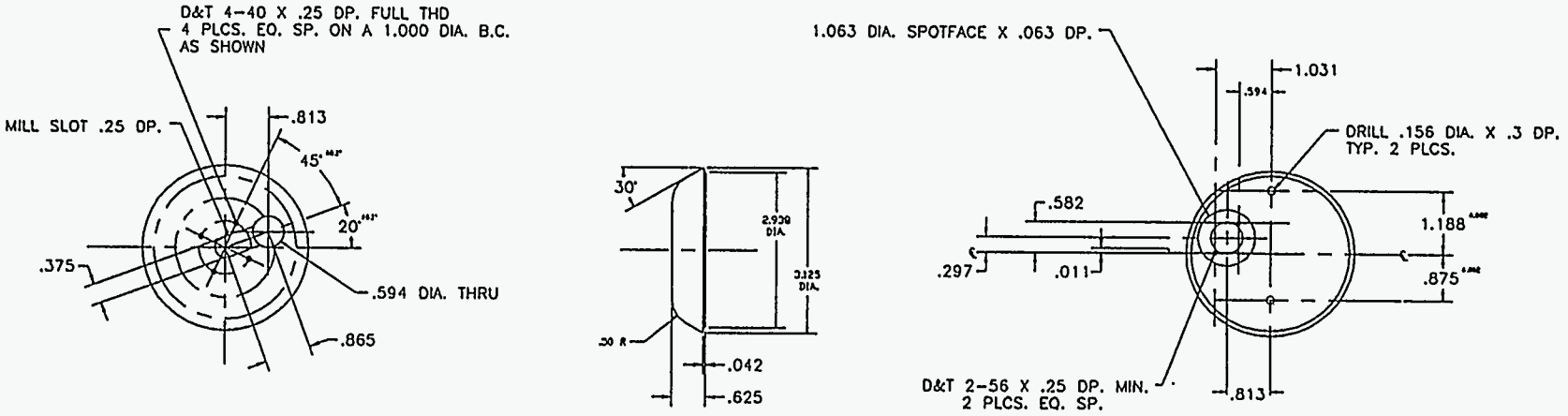

REV	DESCRIPTION	DATE	APPROVED
	2000-4		

	SANDIA NATIONAL LAB.
	BOREHOLE RECEIVER
	P.C. BOARD CONNECTOR/HOUSING ADAPTER
ENGR. BY: B. ENGLER	SIZE D — DWG NO 2000-4 — REV
DRAWN BY: B. ENGLER	SCALE 1X — SHEET 1 OF 1

DWG NO	REV
2001-4	1

REV	DESCRIPTION	DATE	APPROVED

NOTES:
1) BREAK EDGES .03 X 45°
2) MATL: ALUMINUM
3) QTY: 1 REQD. PER TOOL.

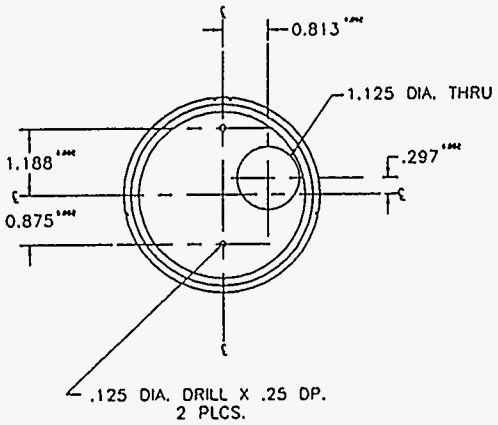

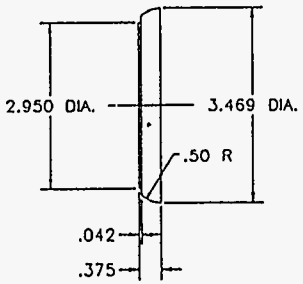

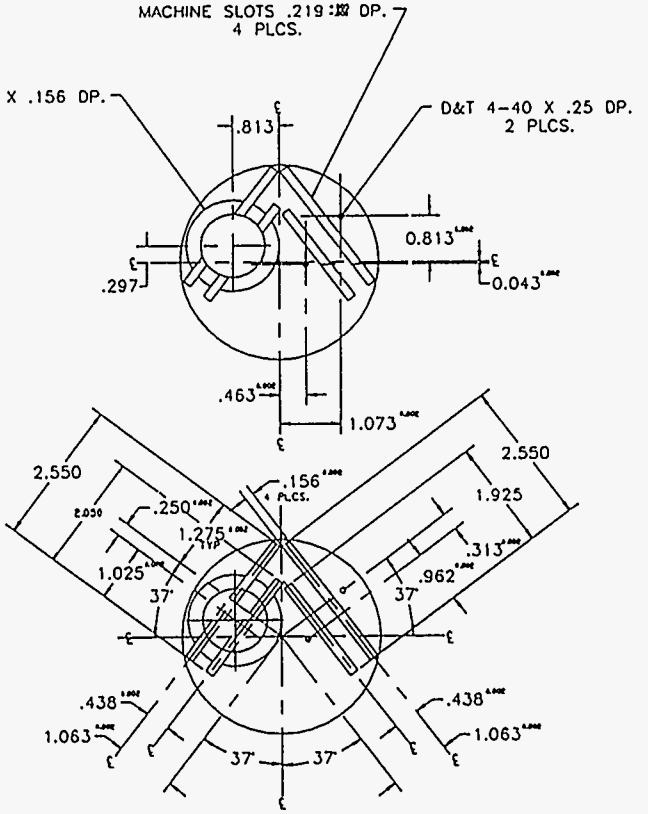

180

	SANDIA NATIONAL LAB.
	BOREHOLE RECEIVER
	P.C. BOARD ENDCAP
ENGR. BY: B. ENGLER	SIZE: D; FSCM NO; DWG NO: 2001-4; REV
DRAWN BY: B. ENGLER	SCALE: 1X; SHEET 1 OF 1

NOTES:
1) BREAK EDGES .03 X 45°
2) MATL: 17-4 OR 15-5 S.S.
3) QTY: 1 REQD.

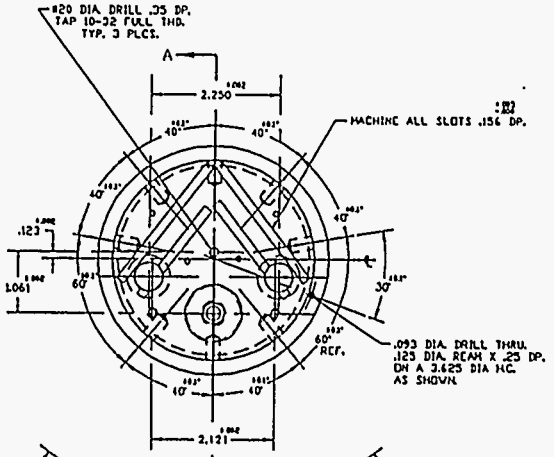

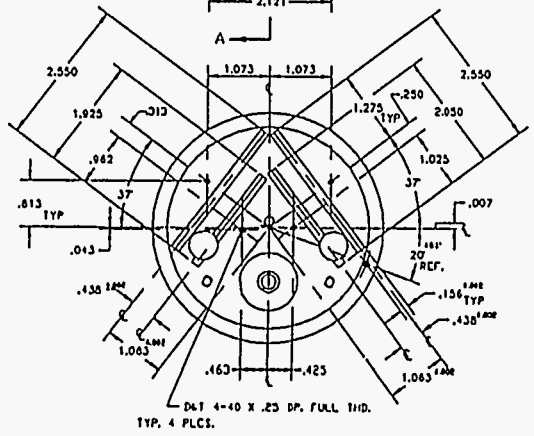

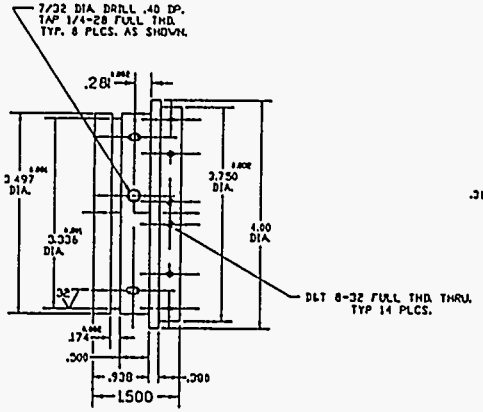

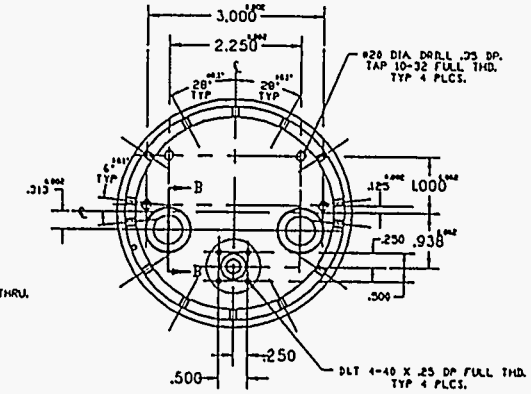

REVISIONS			
REV	DESCRIPTION	DATE	APPROVED

SANDIA NATIONAL LAB.

BOREHOLE RECEIVER
MOTOR BULKHEAD

ENGR. BY: B. ENGLER
DRAWN BY: B. ENGLER
SIZE D | FSCM NO | DWG NO 2002-4A | REV
SCALE 1X | SHEET 1 OF 2

DWG NO 2002-4B | SH 2 | REV

REV	DESCRIPTION	DATE	APPROVED

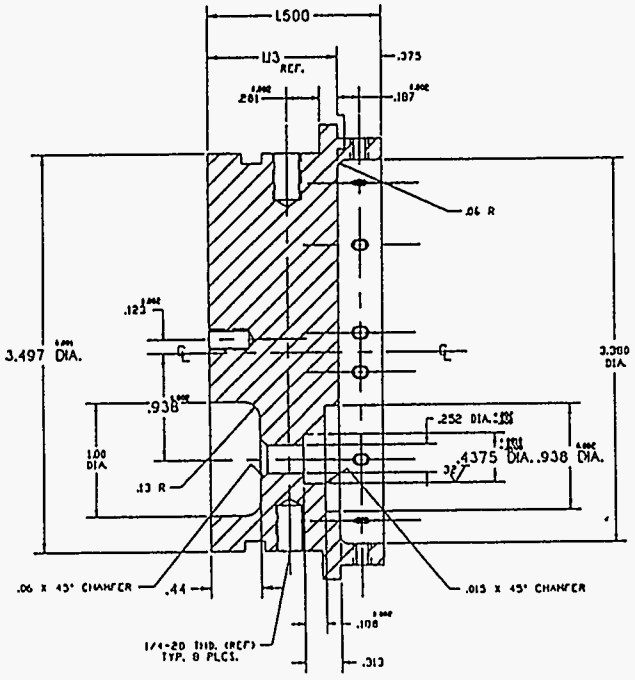

SECTION A-A
(SCALE: 2X)

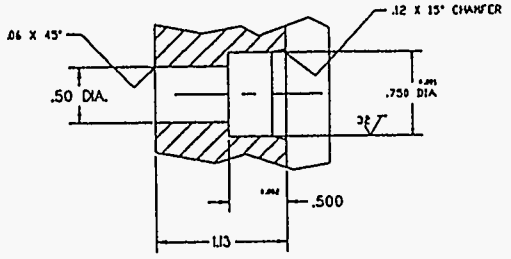

SECTION B-B
(SCALE: 2X)

	SANDIA NATIONAL LAB.
	BOREHOLE RECEIVER MOTOR BULKHEAD
ENGR. BY: B. ENGLER	SIZE D · DWG NO 2002-4B · REV
DRAWN BY: B. ENGLER	SCALE 1X · SHEET 2 OF 2

NOTES:
1) BREAK EDGES .03 x 45°
2) # HOLE TOLERANCE AND FINISH OVER THIS LENGTH ONLY.
3) MATL: 17-4 OR 15-5 S.S.
4) QTY: 1 REQD.

REVISIONS			
LTR	DESCRIPTION	DATE	APPROVED
A	#6 DIA. DRILL THRU TO H DIA. DRILL THRU (CHANGE TO 1/4-28)	3/92	B.E.
B	.136 X .375 DP. TO #30 (.1285) X .3 DP.	5/92	B.E.

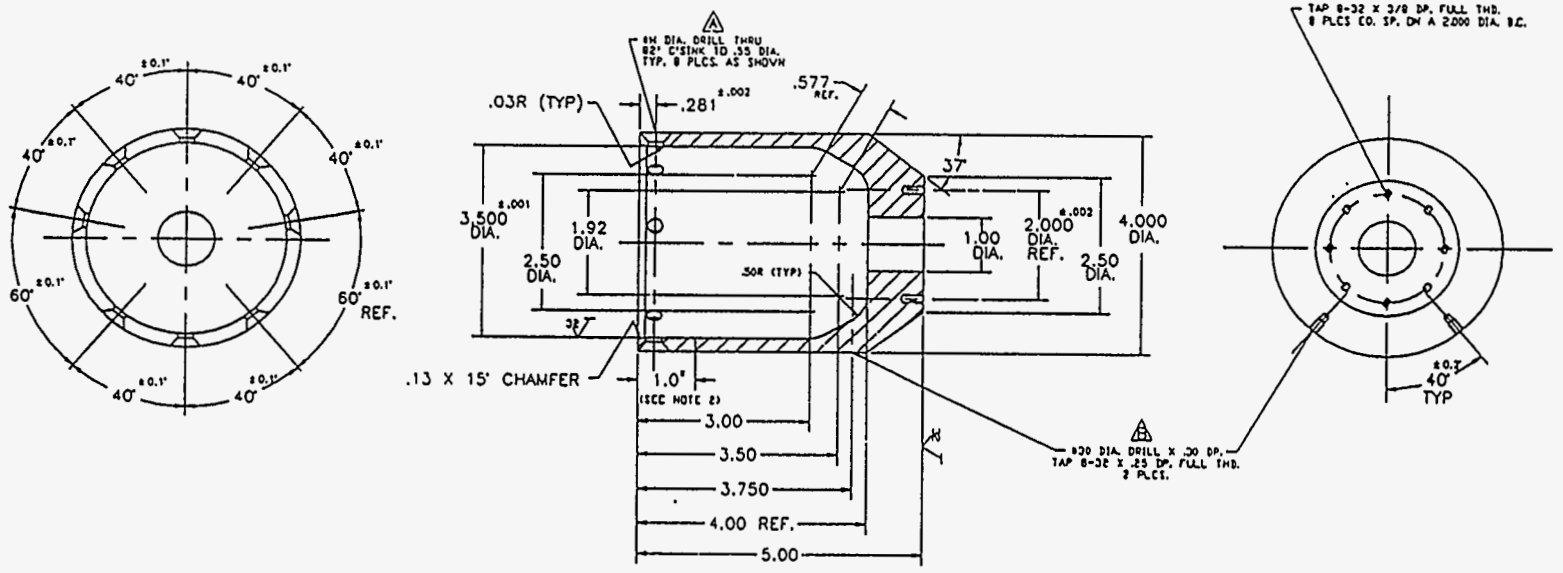

	SANDIA NATIONAL LAB.	
	BOREHOLE RECEIVER SENSOR HOUSING	
ENGR. BY: B. ENGLER	SIZE D	DWG NO. 2004-4
DRAWN BY: B. ENGLER	SCALE: NONE X	SHEET 1 OF 1

DWG NO 3005-4 | SH 1

REVISIONS			
REV	DESCRIPTION	DATE	APPROVED

NOTES:
1) BREAK EDGES .015 X 45°
2) QTY: 3 REQD.
3) MATERIAL: 304 S.S.

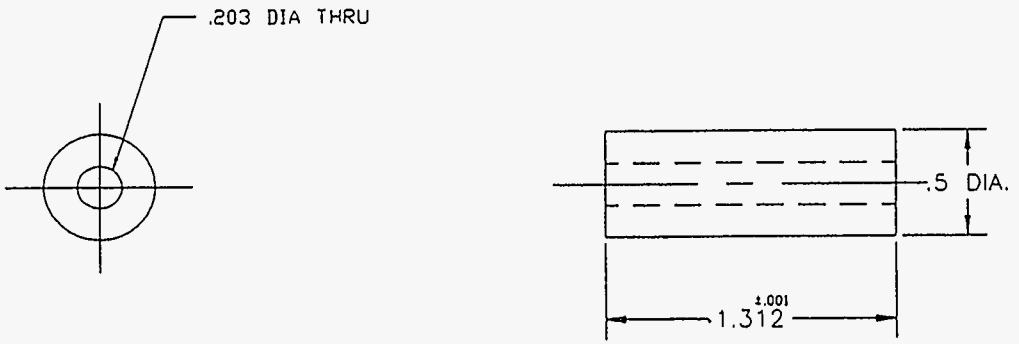

B.41

	SANDIA NATIONAL LAB.		
	BOREHOLE RECEIVER FIBER-OPTIC MOTOR MOUNT SPACER		
ENGR BY B. ENGLER	SIZE B	DWG NO 3005-4	REV
DRAWN BY B. ENGLER	SCALE 2X	SHEET 1 OF 1	

NOTES:
1) BREAK EDGES .03 X 45°
2) Ø HOLD TOLERANCE AND FINISH OVER THIS LENGTH ONLY.
3) MATL: 17-4 OR 15-5 S.S.
4) QTY: 1 REQD

REV	DESCRIPTION	DATE	APPROVED
A	#6 DIA. DRILL THRU TO #H DIA. DRILL THRU (CHANGE TO 1/4-28)	3/92	B.E.
B	.136 X .375 DP. TO #30(.1285) X .3 DP.	5/92	B.E.
C	.129 TO .125 DRILL THRU C'BORE .219 TO .189 DIA C'BORE DEPTH .188 TO .13 .875 TO 1.0 DIA B.C.	5/92	B.E.

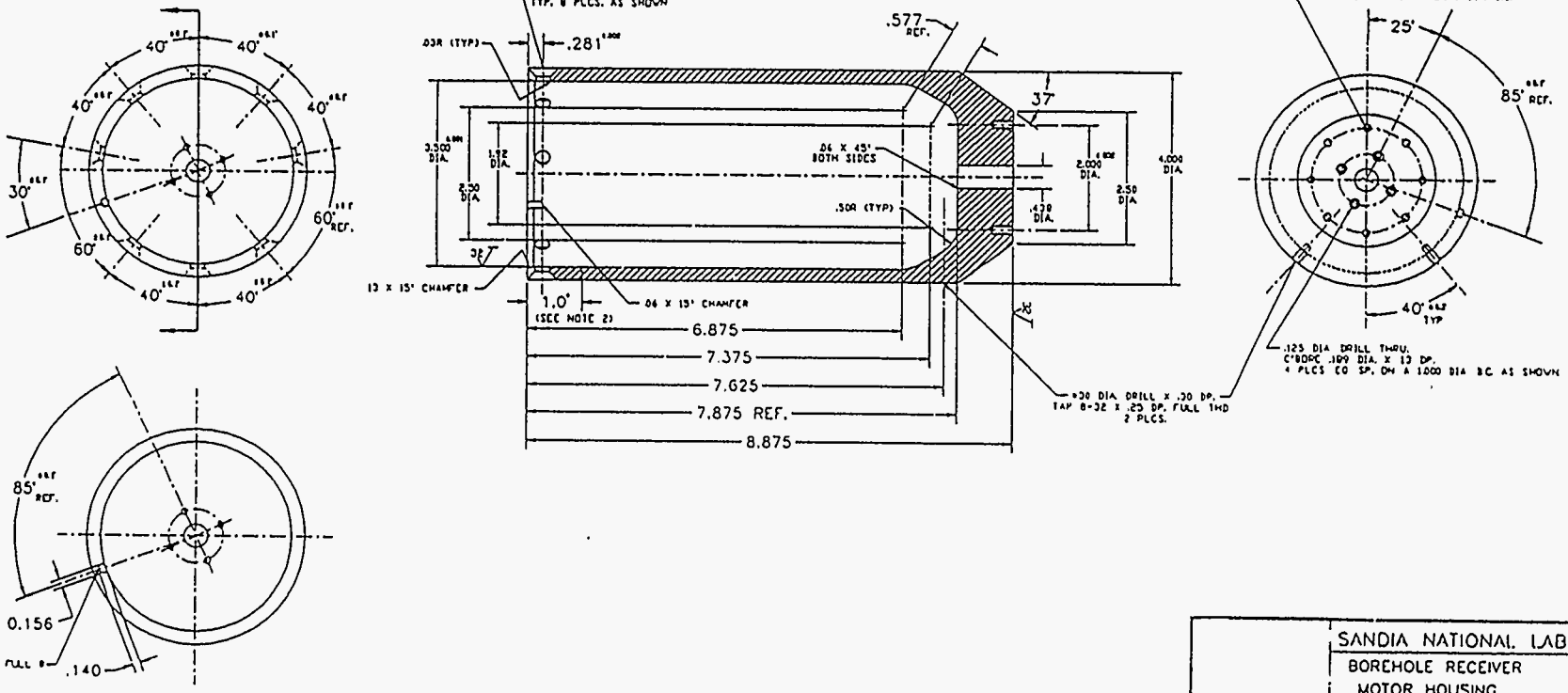

B.39

SANDIA NATIONAL LAB.
BOREHOLE RECEIVER
MOTOR HOUSING

ENGR BY: B. ENGLER
DRAWN BY: B. ENGLER
SIZE D
DWG NO 2003-4
SCALE 1X
SHEET 1 OF 1

185

Appendix C. MLSR Electronics Schematics

The following pages include the MLSR electronics schematics. Included are all schematics for the Data Receivers, Data Formatter, Command Interface, and Sync Detector. Each Figure # corresponds to a single PC Board with the designations "a,b, or c" used to designate the multiple drawing pages required for each PC board design. A system level cabling diagram is also included.

Altera EPLD devices are used extensively in this design and careful attention should be directed to insuring that the devices be programmed with the correct revision date. Since the devices are programmable, inputs and outputs are programmed according to circuit function needs and are NOT the same in every case in this design. This means that programming an EPLD for use in the Motor Control Board and using in another board could cause failure of the EPLD or other devices on the board. Using the proper revision date in the devices is also critical. The file names, file revision dates and target location in the system are included in Table C.1.

Table C.1: MLSR Altera Programming File Names

Unit #	PC Board Name	Component #	File Name (XXXX.JED)	Revision Date	File Size (bytes)
Data Rec (All)	Motor Cnt	U1	MCU1	1/16/92	7481
Data Rec 1	Encoder	U1	ENC1U1	7/16/93	7486
	Encoder	U2	ENC1U2	7/27/93	7514
	Encoder	U11	ENC1U11	7/14/93	7538
Data Rec (2-5)	Encoder	U1	ENC25U1	5/15/92	7485
	Encoder	U11	ENC25U11	10/28/91	7529
Data Rec 2	Encoder	U2	ENC2U2	6/8/92	7517
Data Rec 3	Encoder	U2	ENC3U2	6/8/92	7517
Data Rec 4	Encoder	U2	ENC4U2	7/30/92	7519
Data Rec 5	Encoder	U2	ENC5U2	7/31/92	7519
Wireline Interface Unit	Formatter	U13	FMTU13	8/2/93	7527
	Formatter	U14	FMTU14	8/12/93	18759
	Formatter	U15	FMTU15	7/28/93	7500
	CMDIface	U2	CMIU2	5/27/92	7523
	CMDIface	U20	CMIU20	6/1/92	18732
Sync Detec	Sync Det	U2	SYNDU2	7/10/92	7475

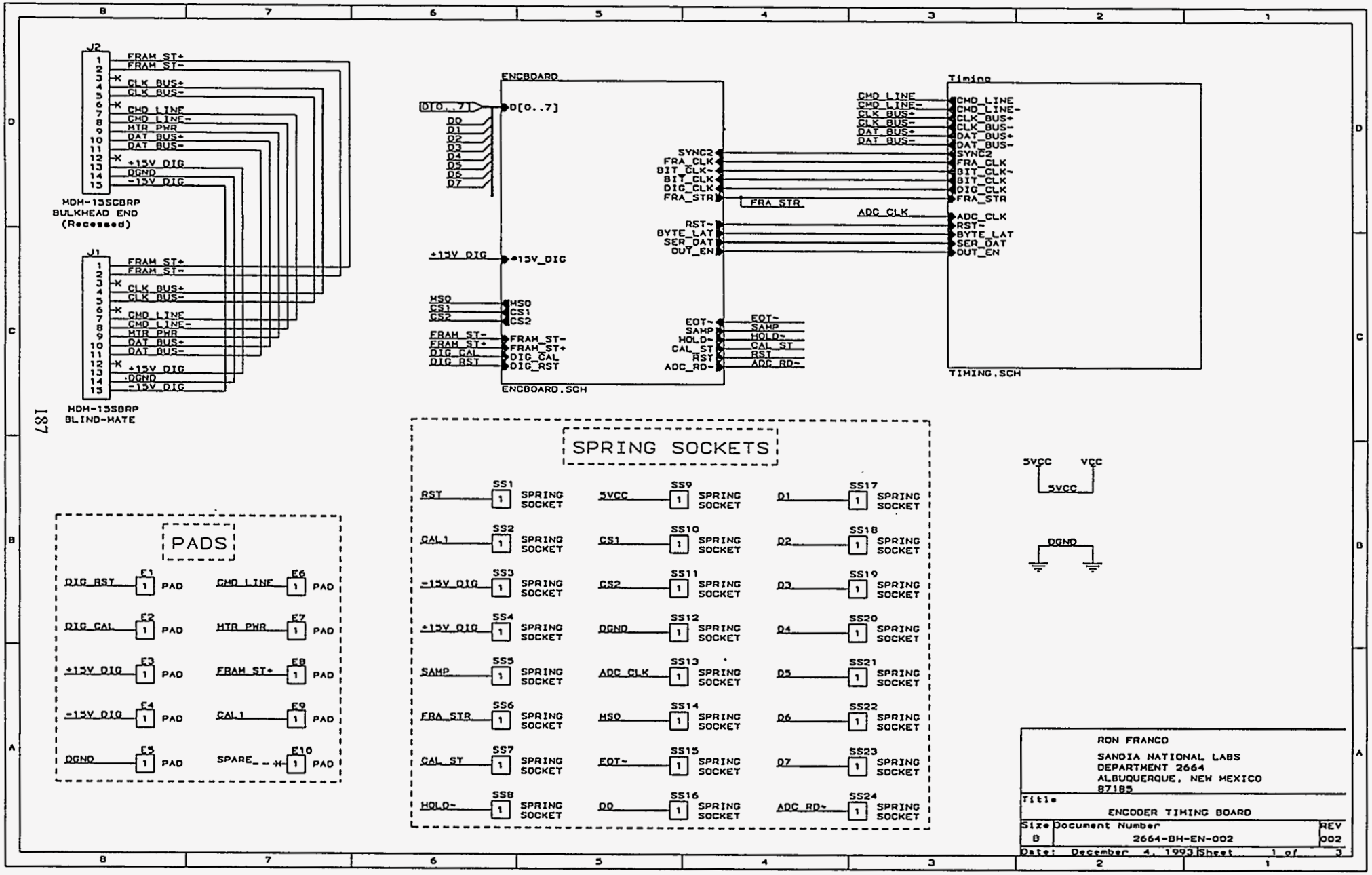

Figure C1a: Encoder Timing Board

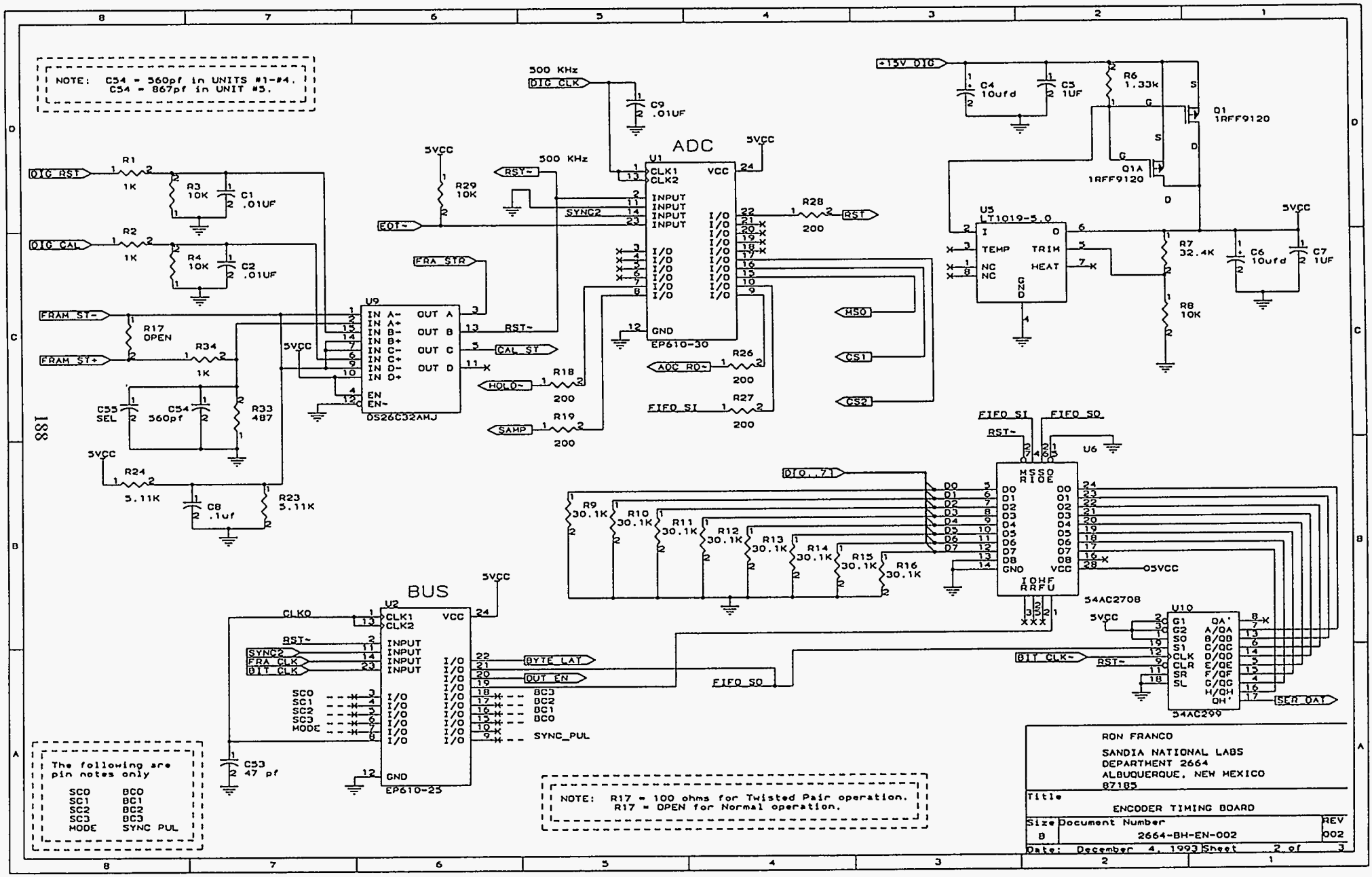

Figure C1.b Encoder Timing Board

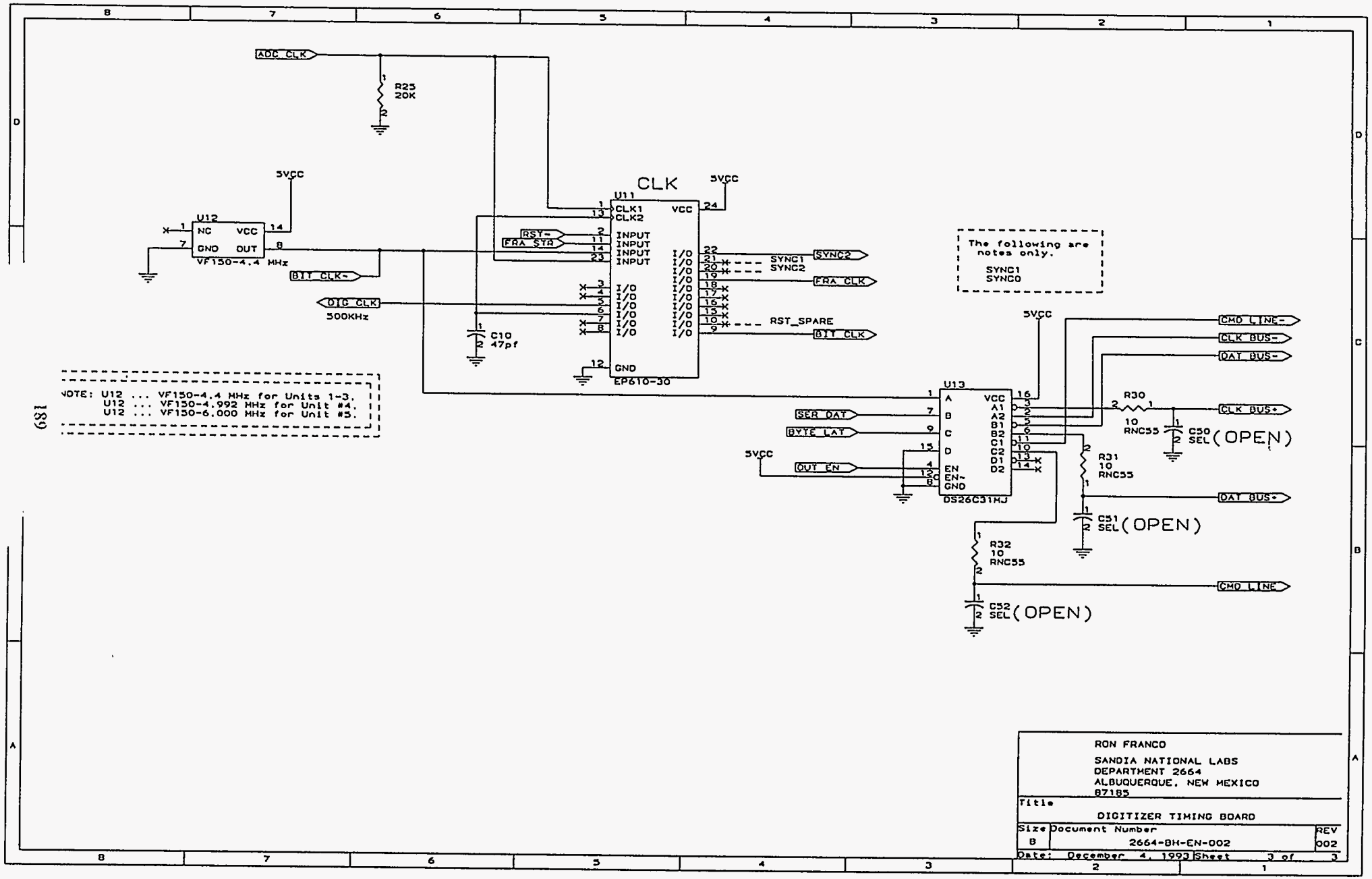

Figure C1c: Encoder Timing Board

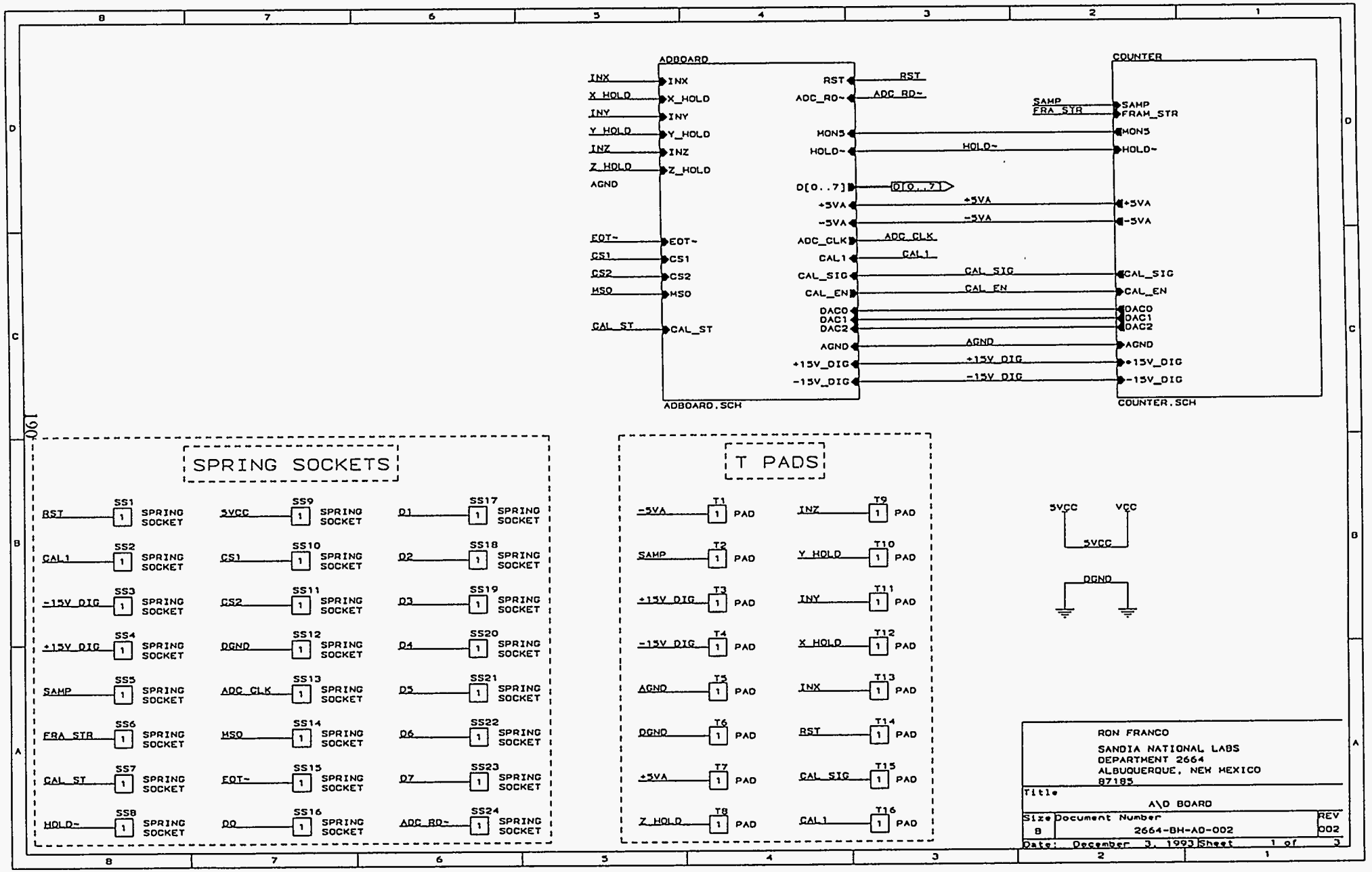

Figure C2.a Digitizer A/D Board

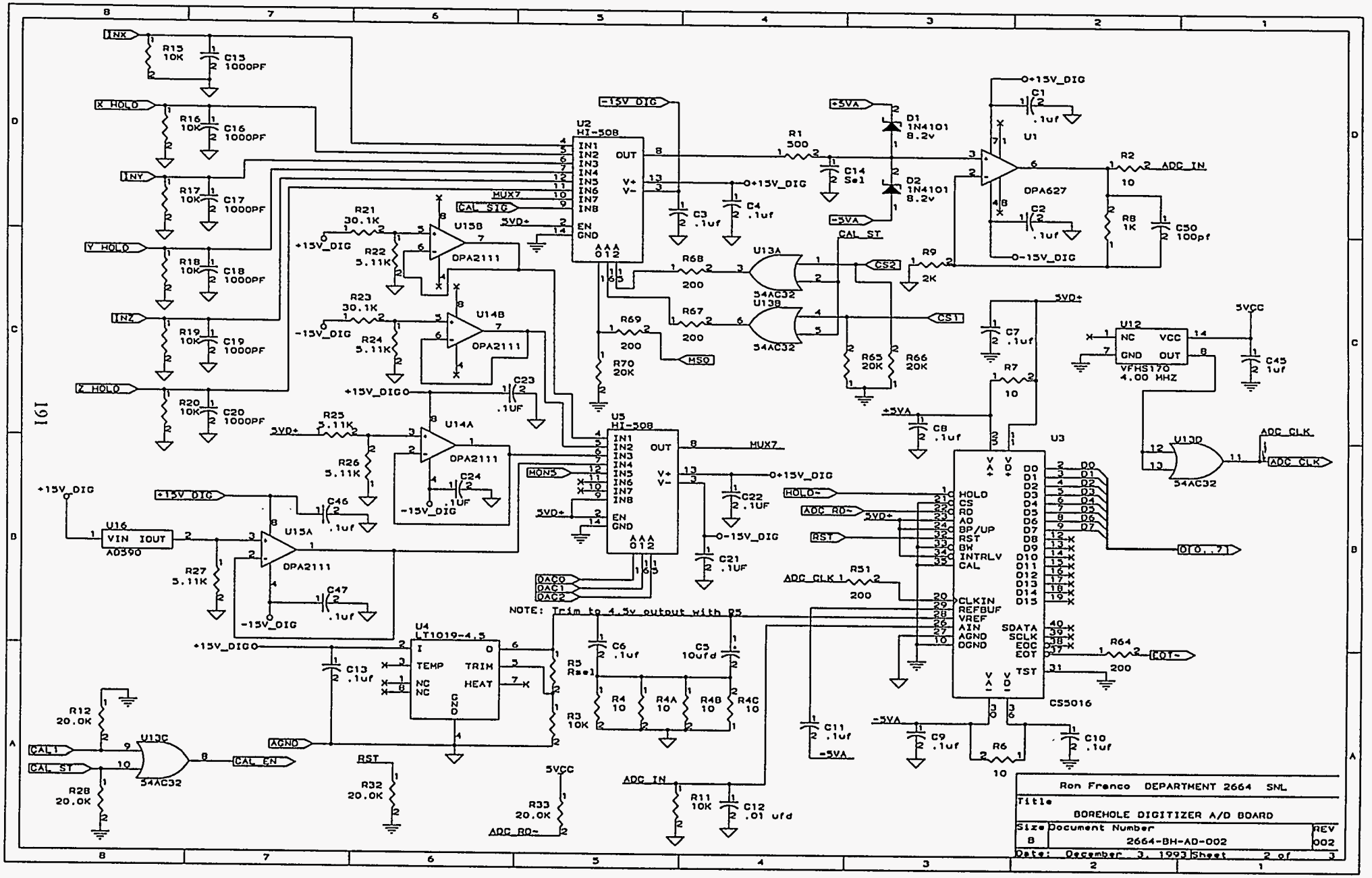

Figure C2b: Digitizer A/D Board

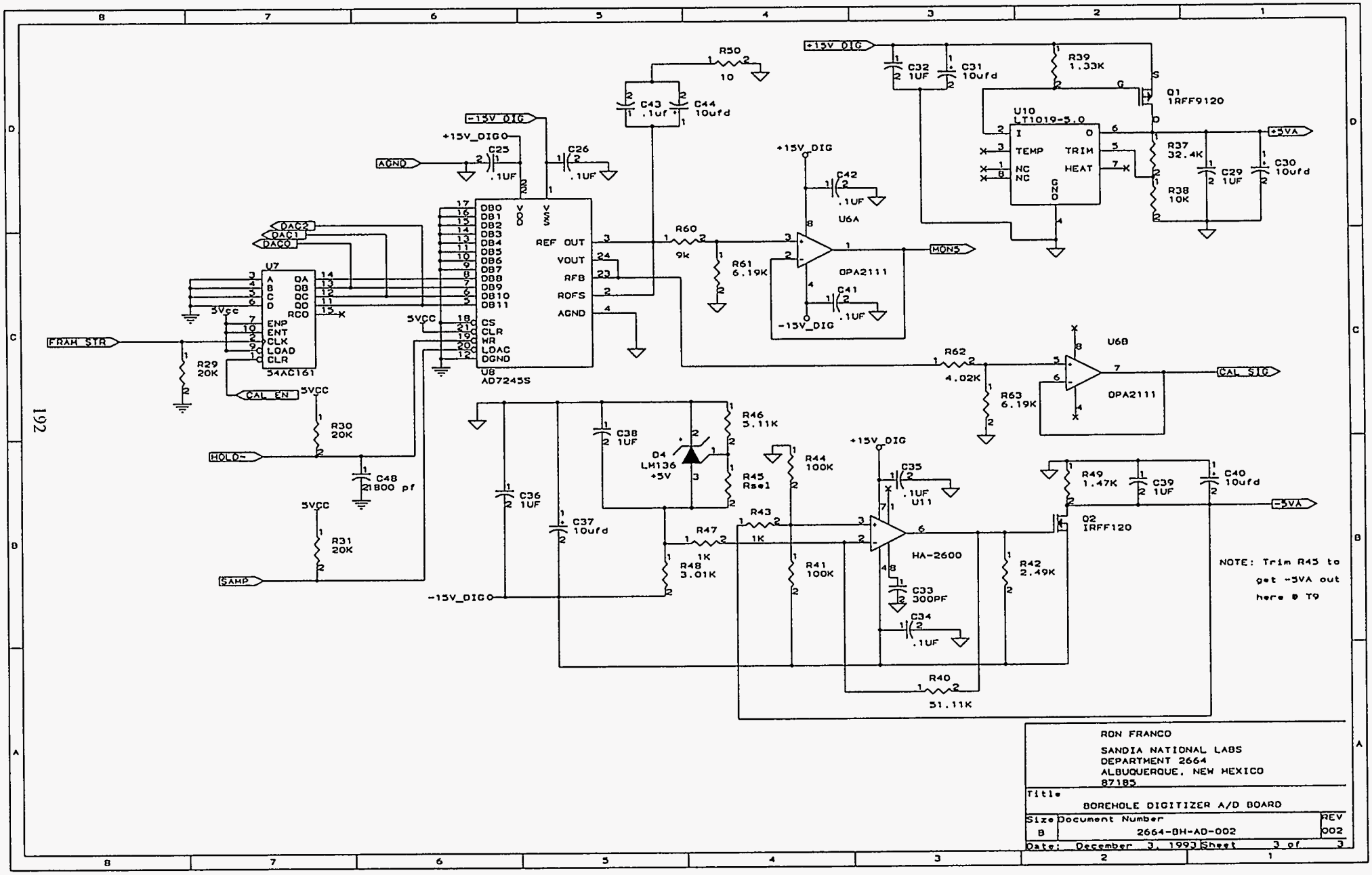

Figure C2c: Digitizer A/D Board

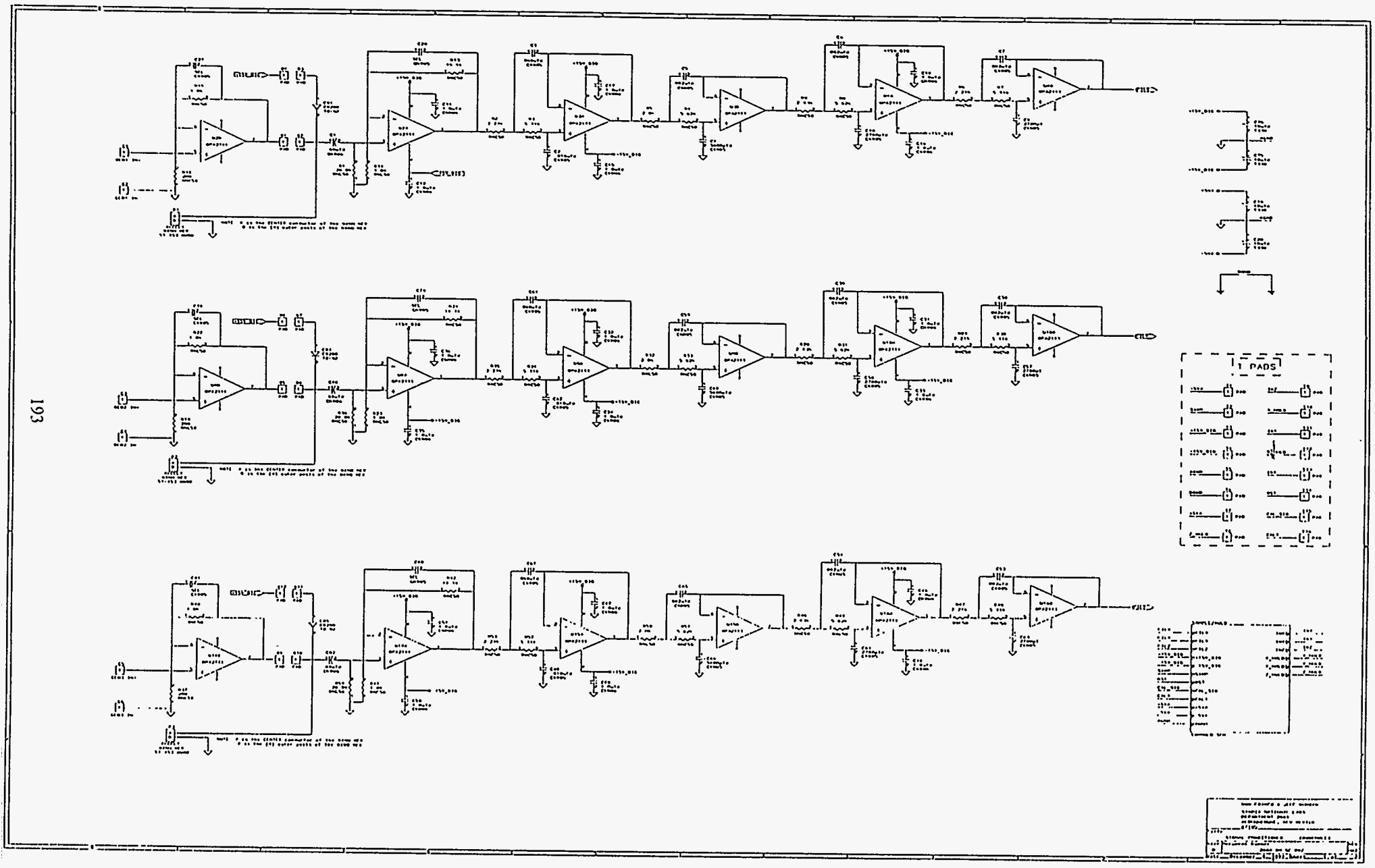

Figure C3a: Signal Conditioner Board

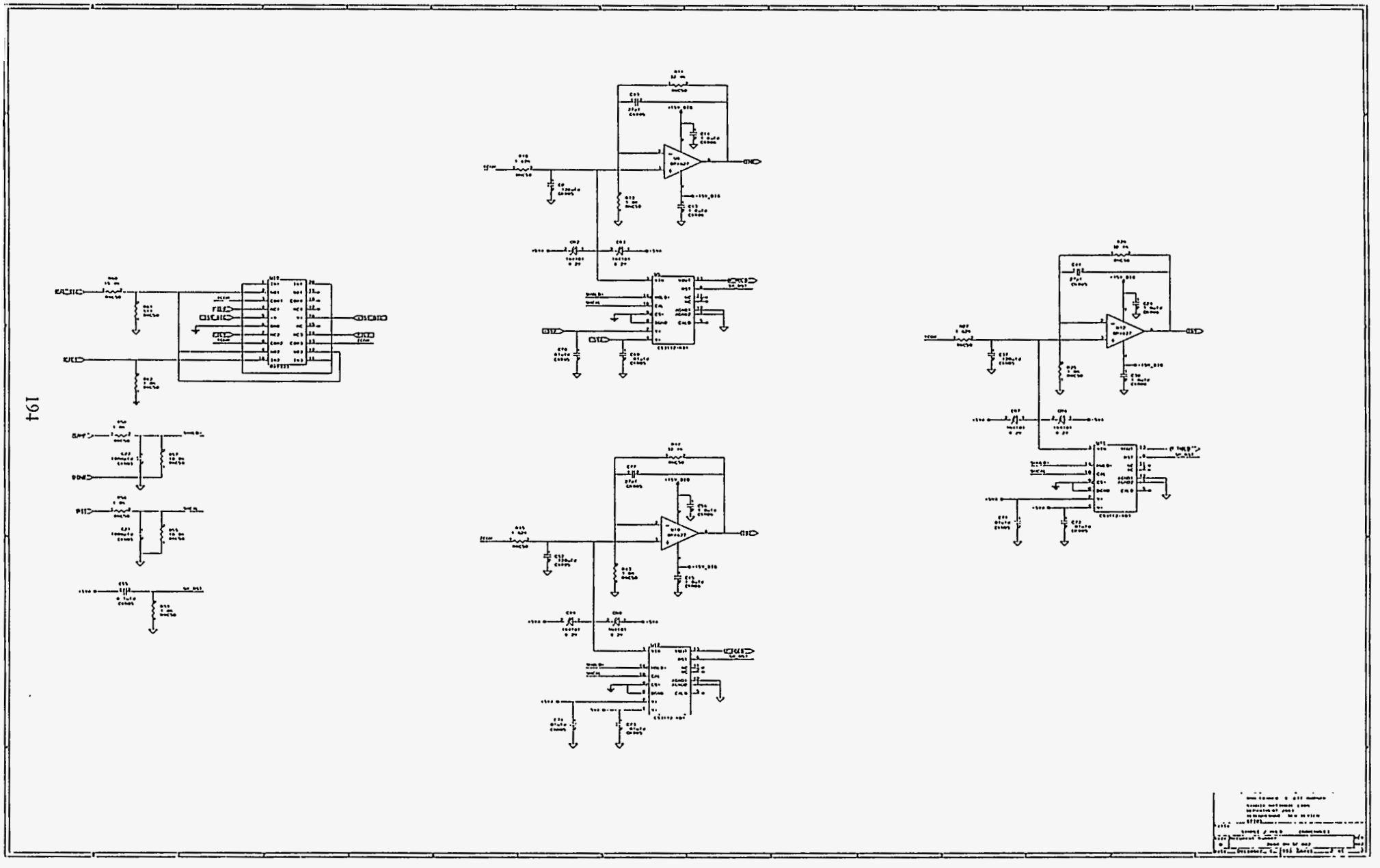

Figure C3b: Signal Conditioner Board

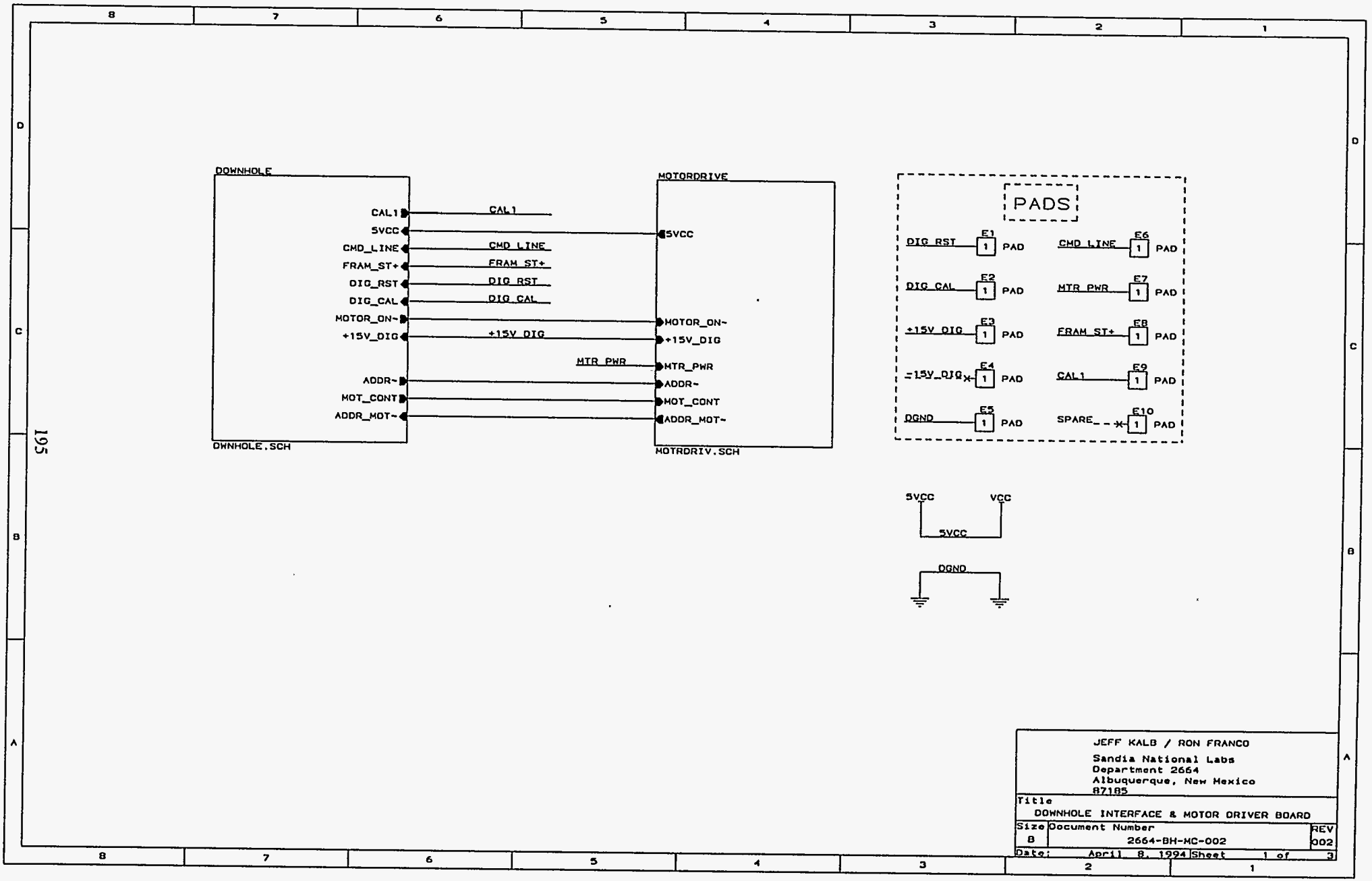

Figure C4a: Motor Control Board

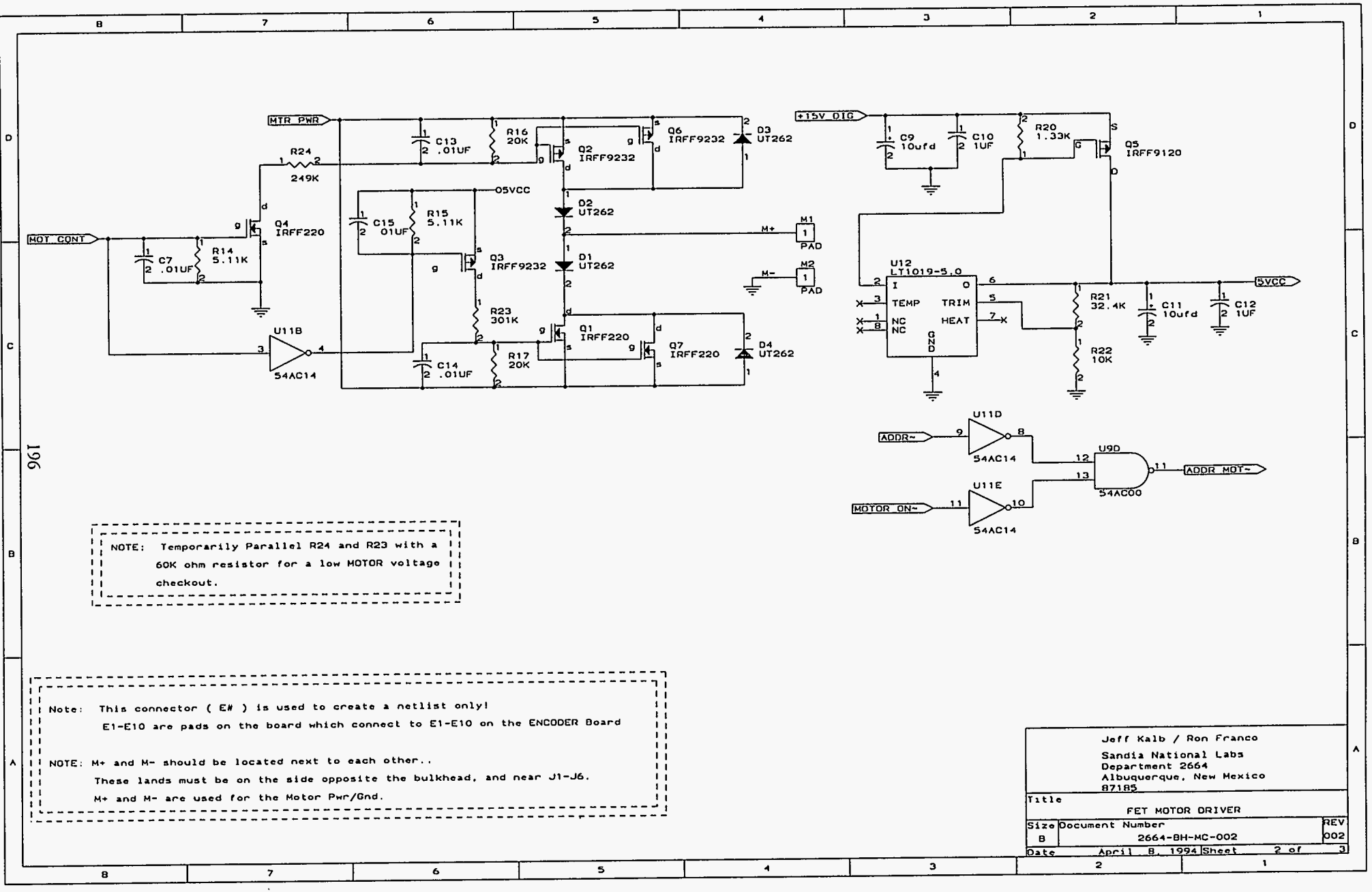

Figure C4b: Motor Control Board

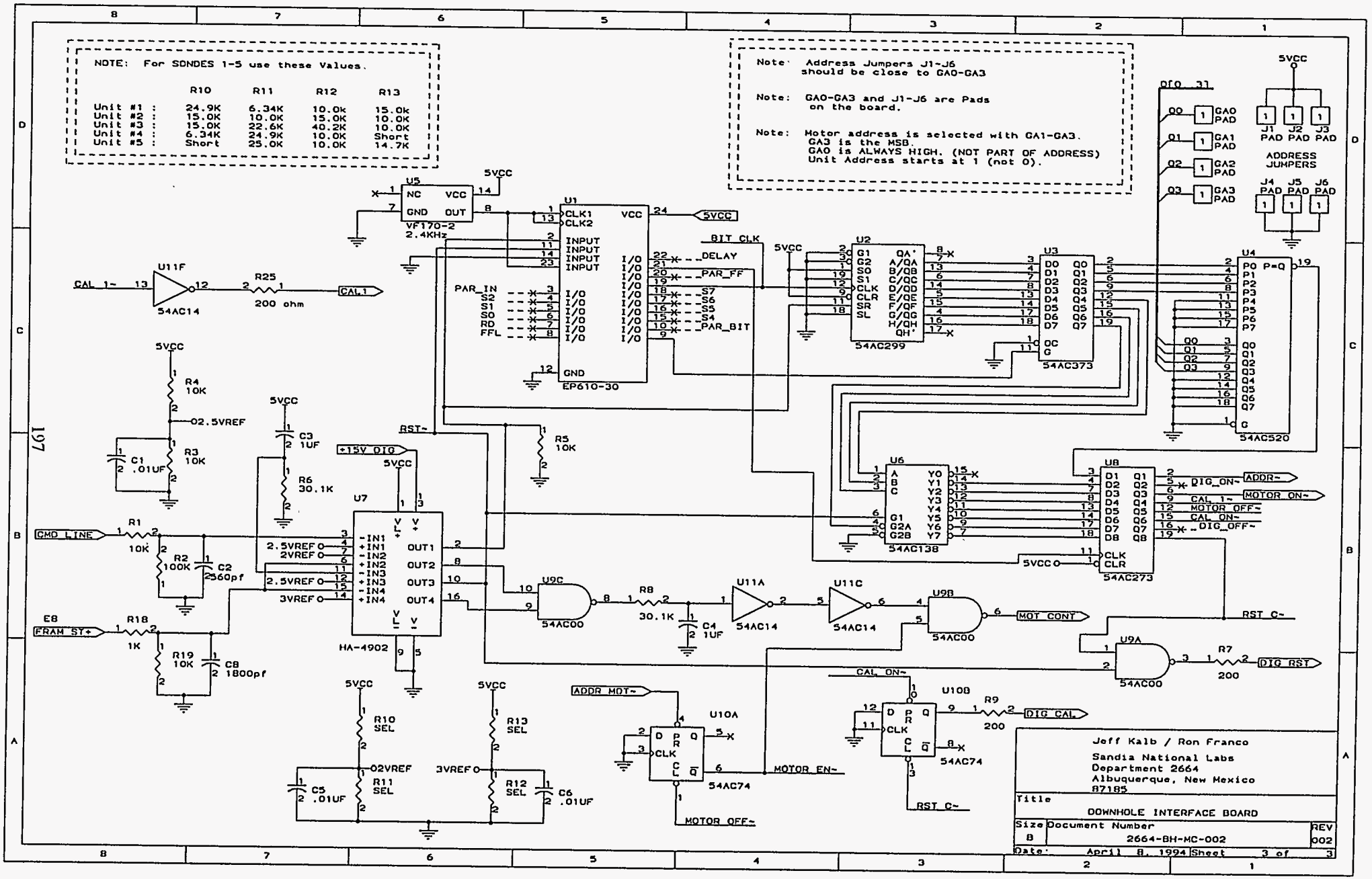

Figure C4c: Motor Control Board

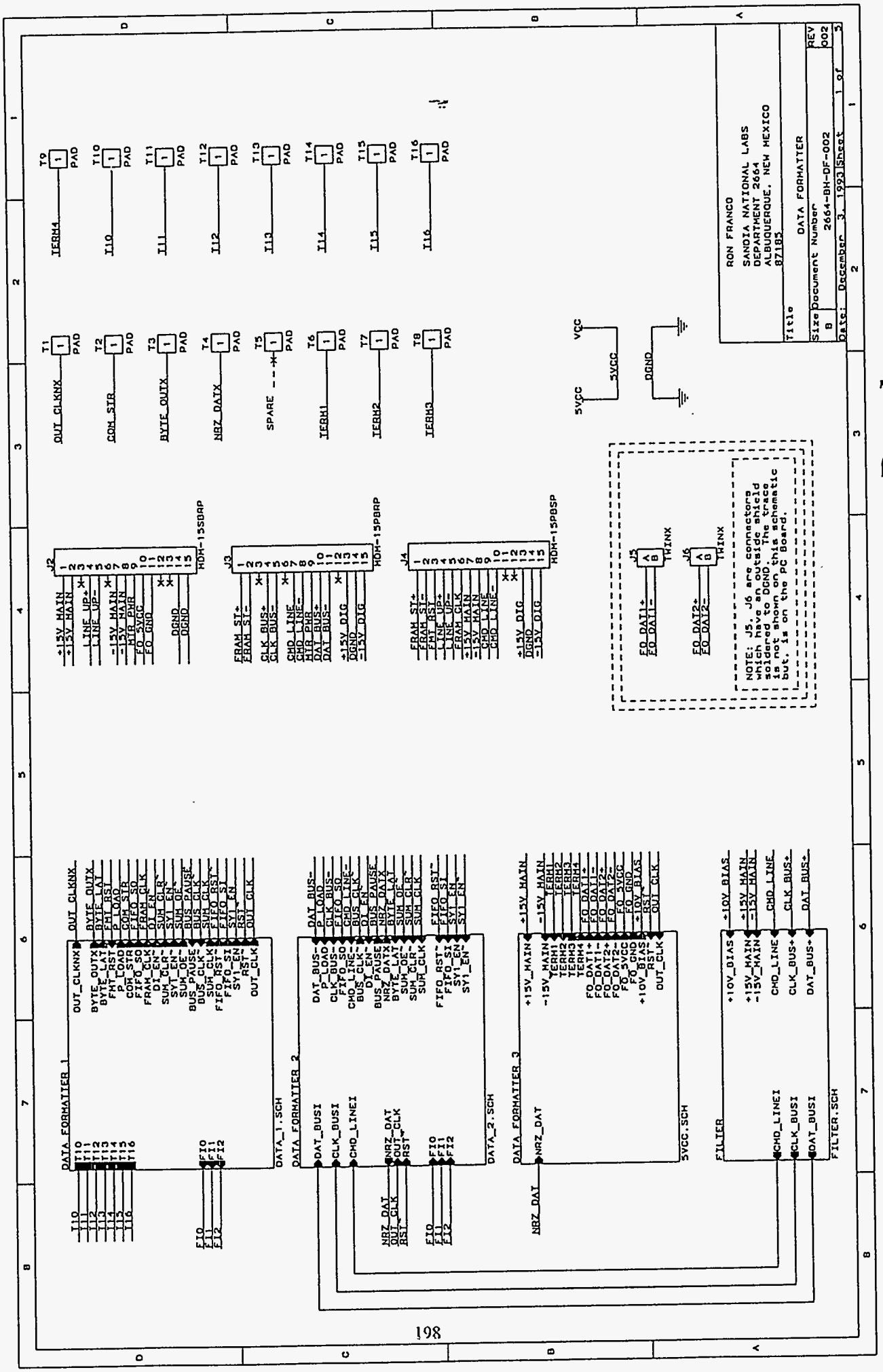

Figure C5a: Data Formatter Board

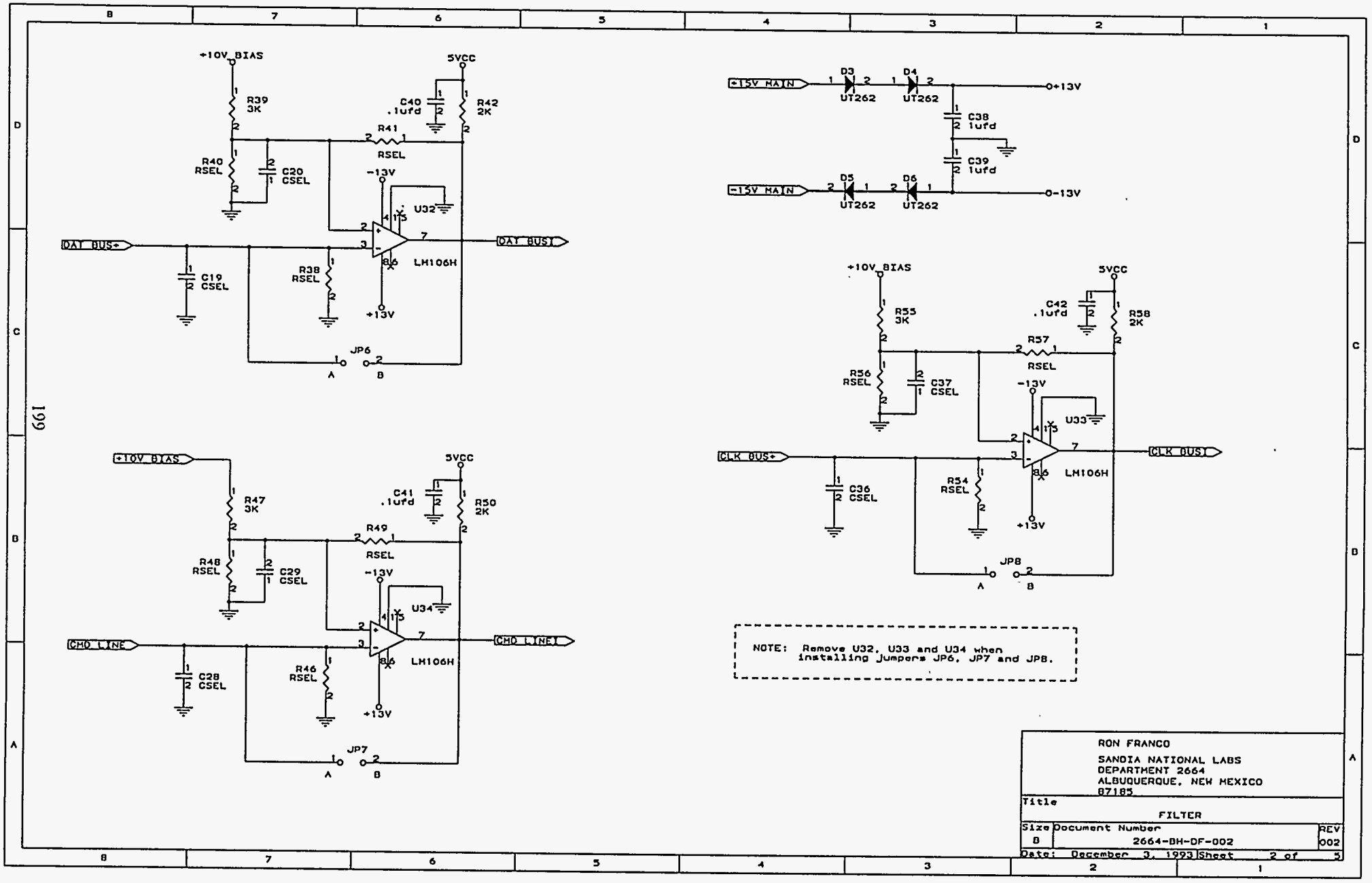

Figure C5b: Data Formatter Board

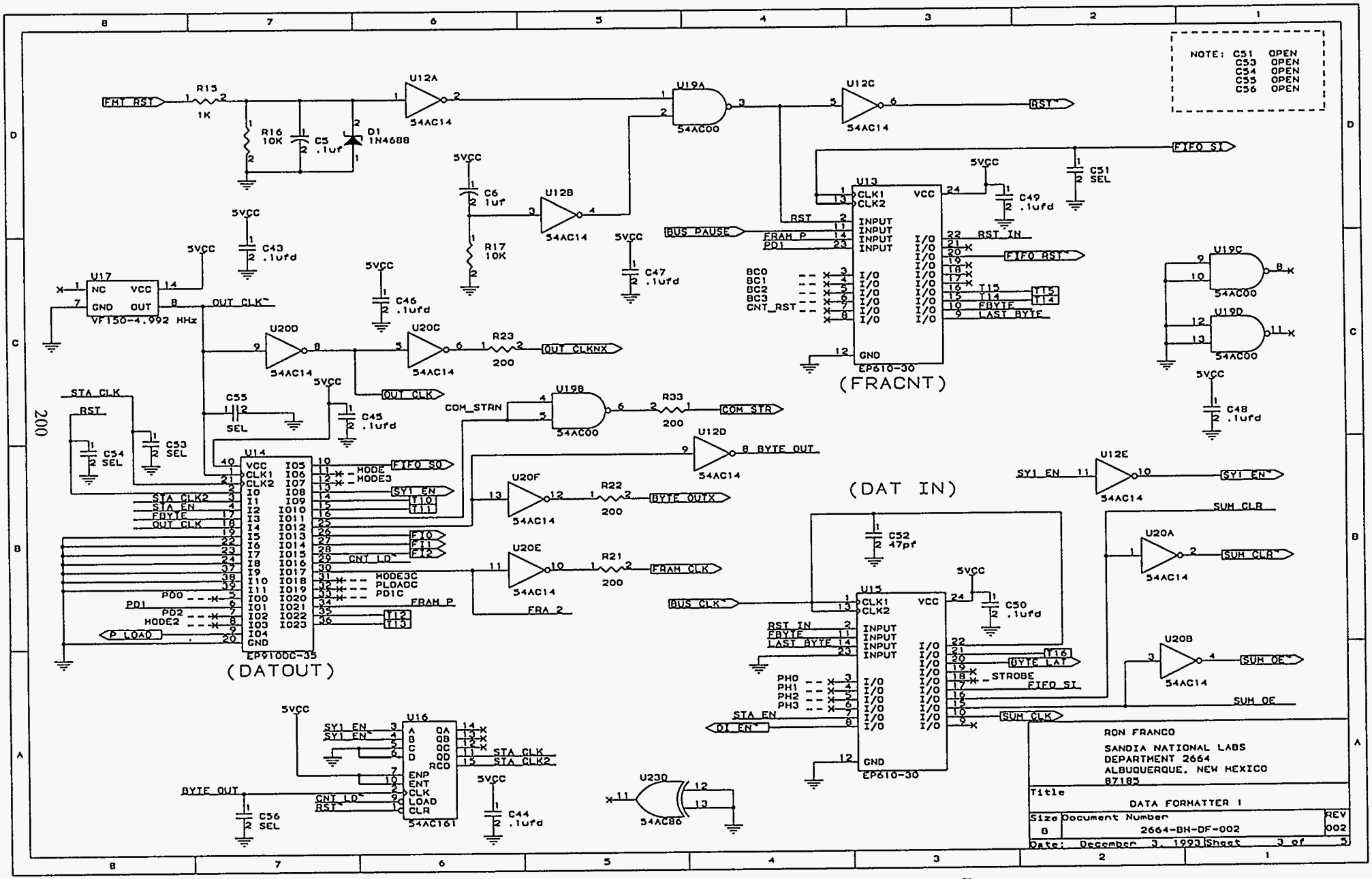

Figure C5c: Data Formatter Board

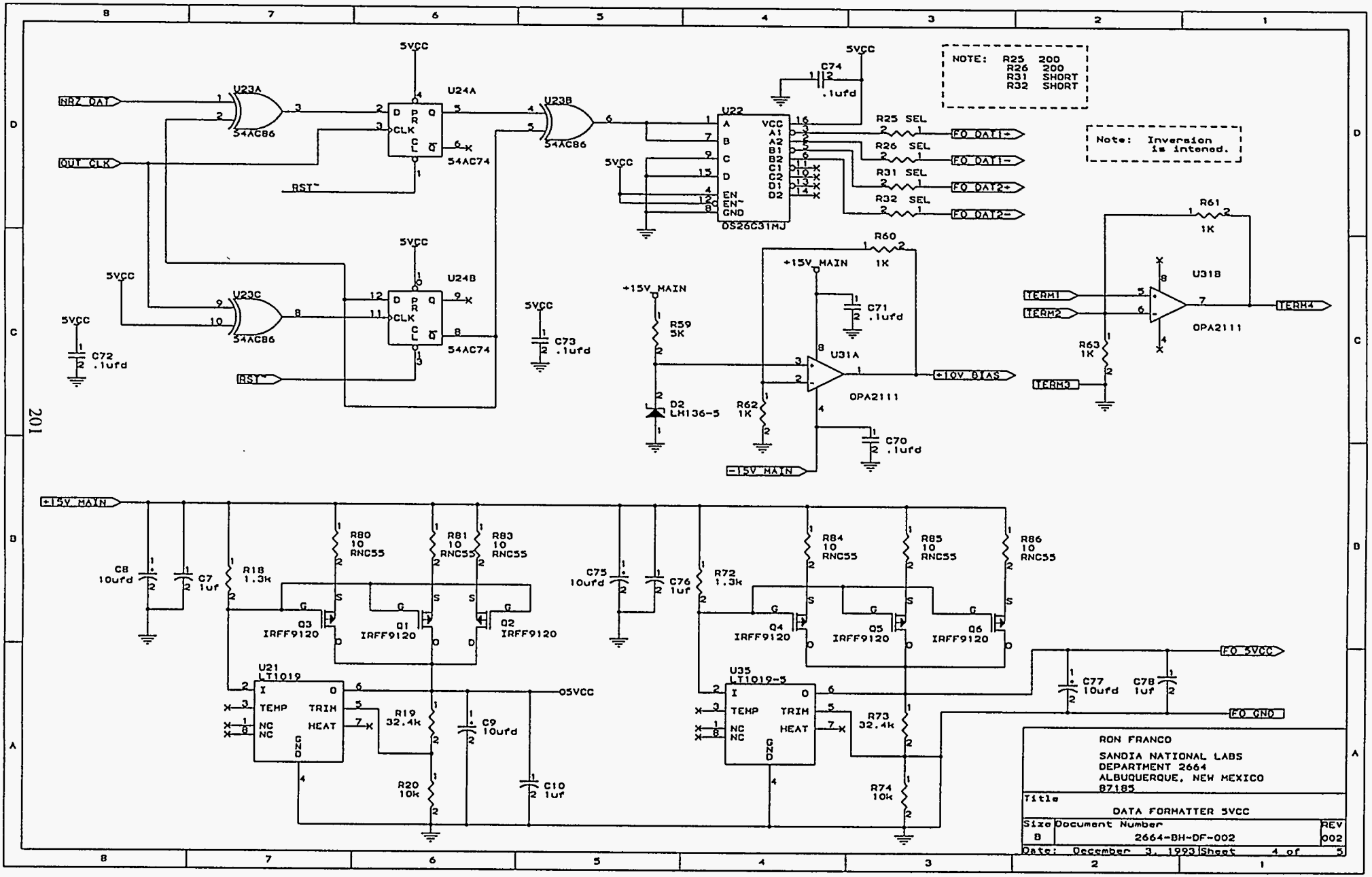

Figure C5d: Data Formatter Board

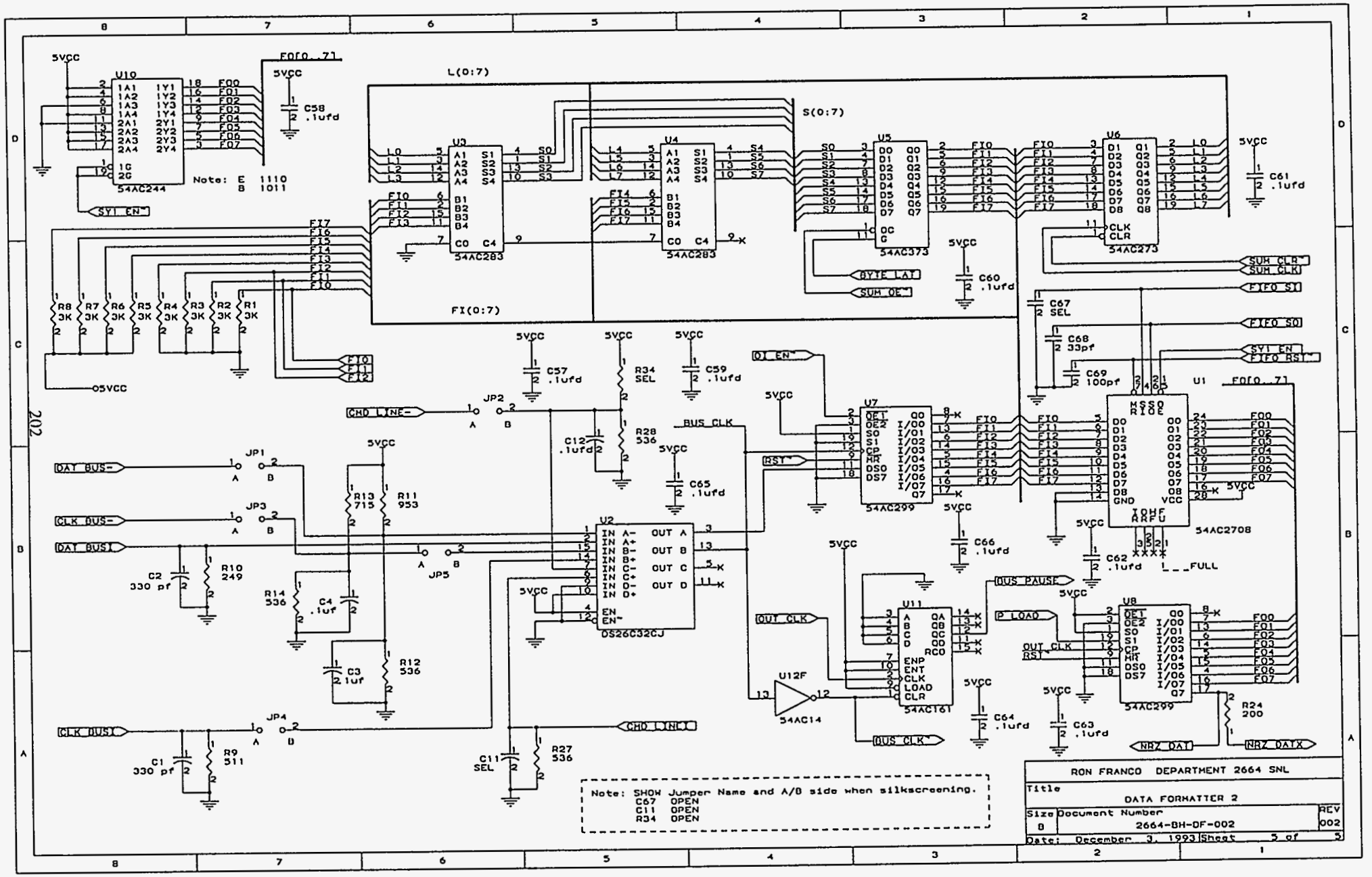

Figure C5e: Data Formatter Board

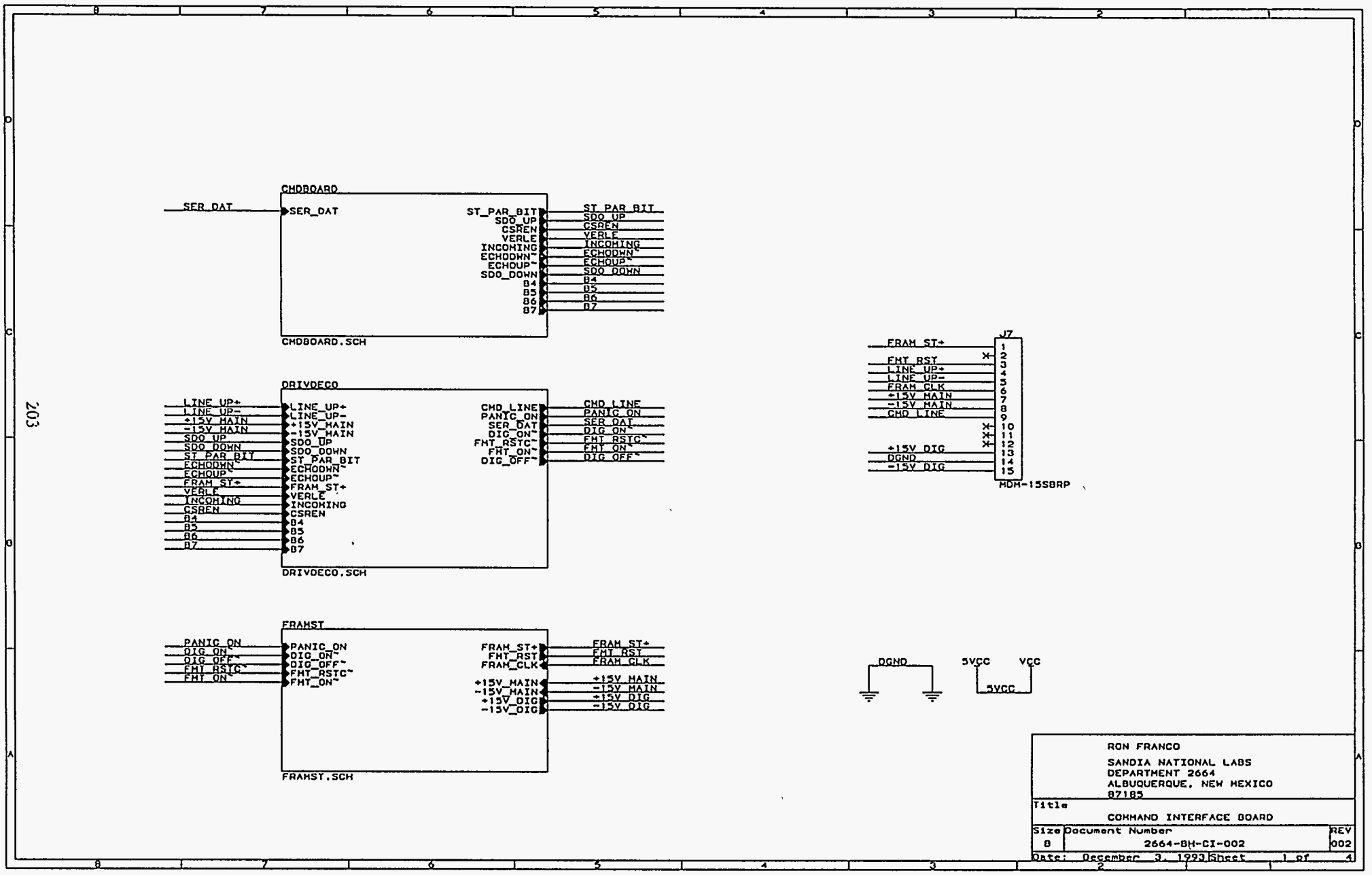

Figure C6.a Command Interface Board

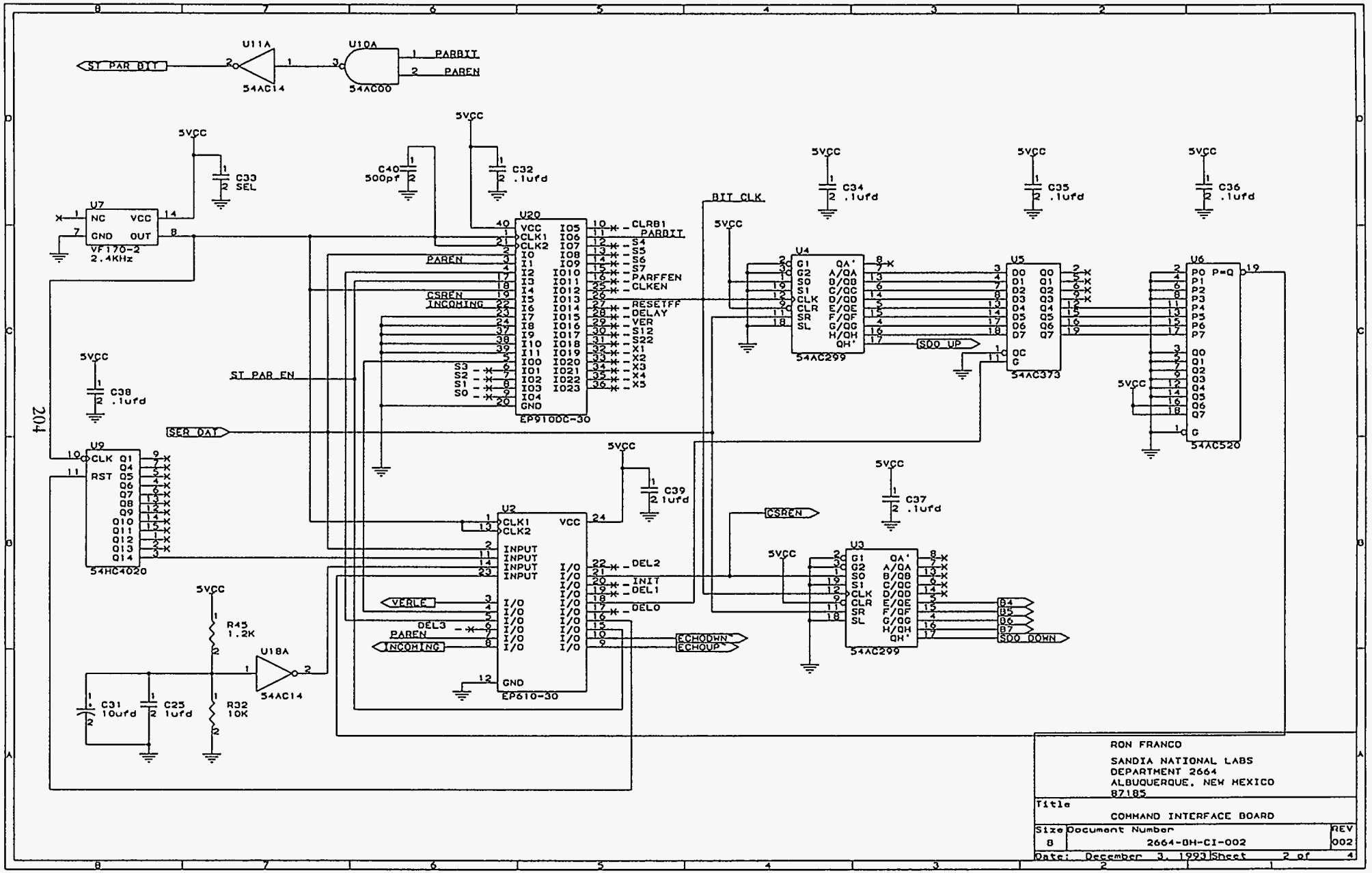

Figure C6b: Command Interface Board

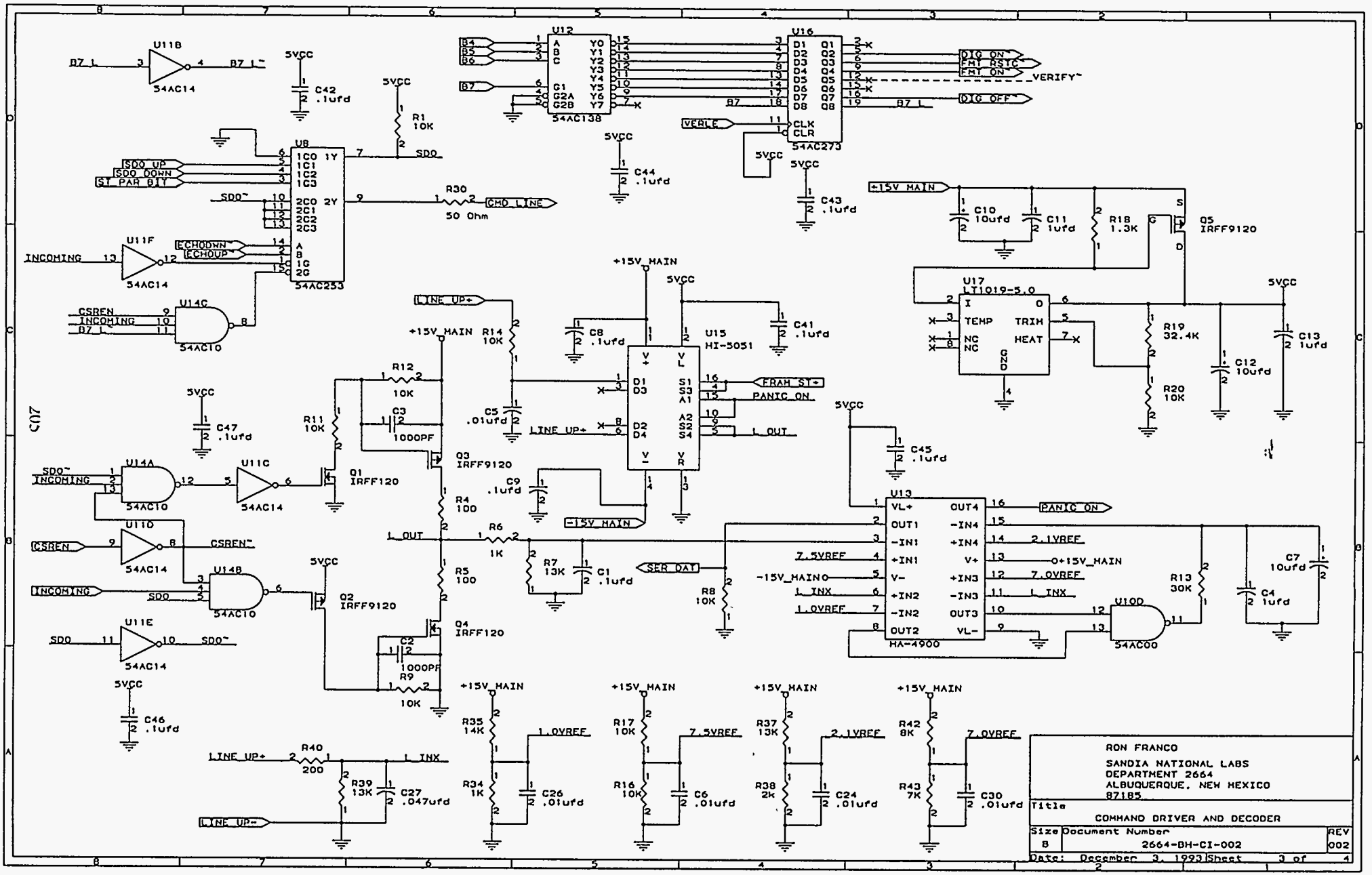

Figure C6c: Command Interface Board

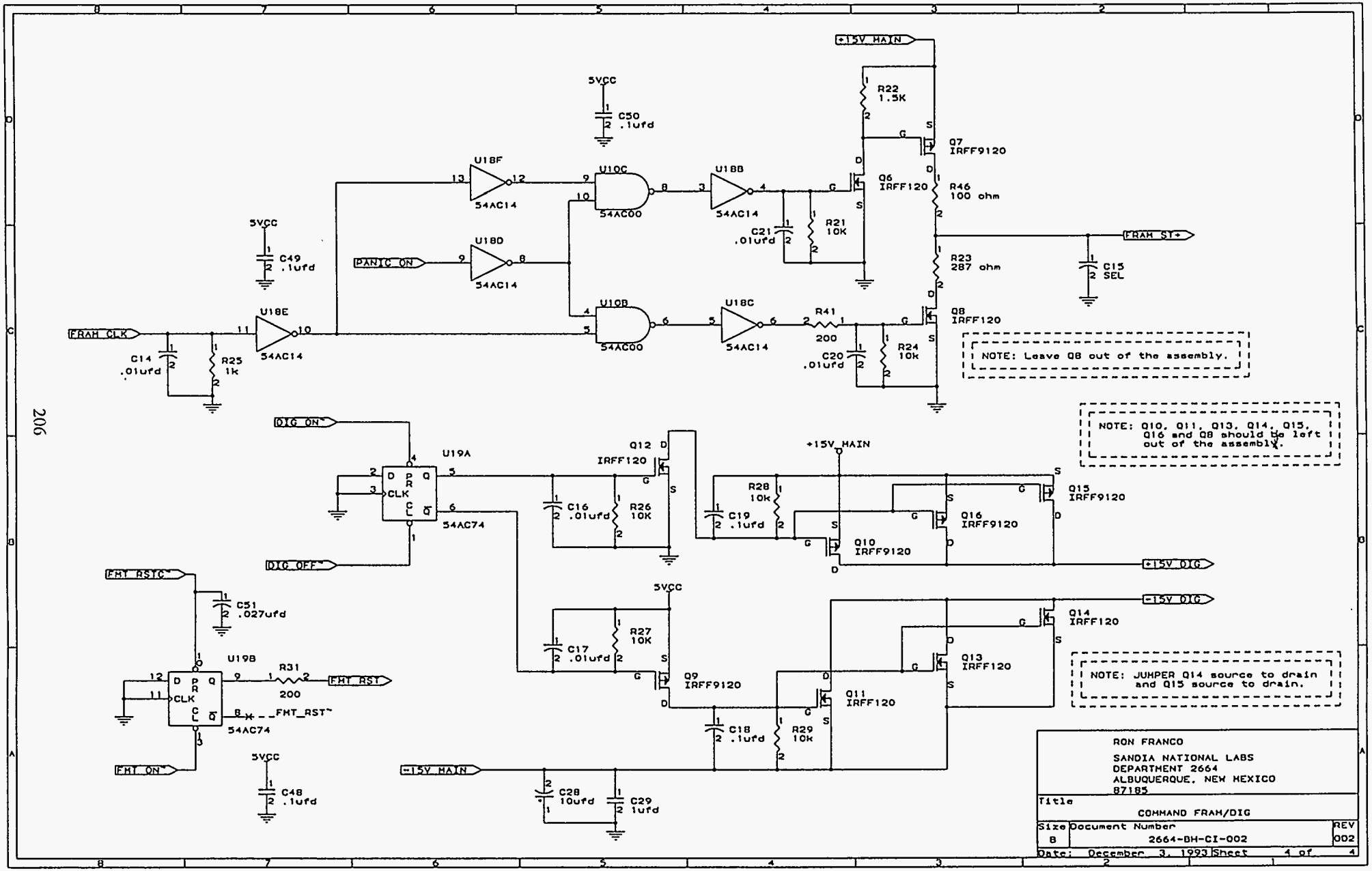

Figure C6d: Command Interface Board

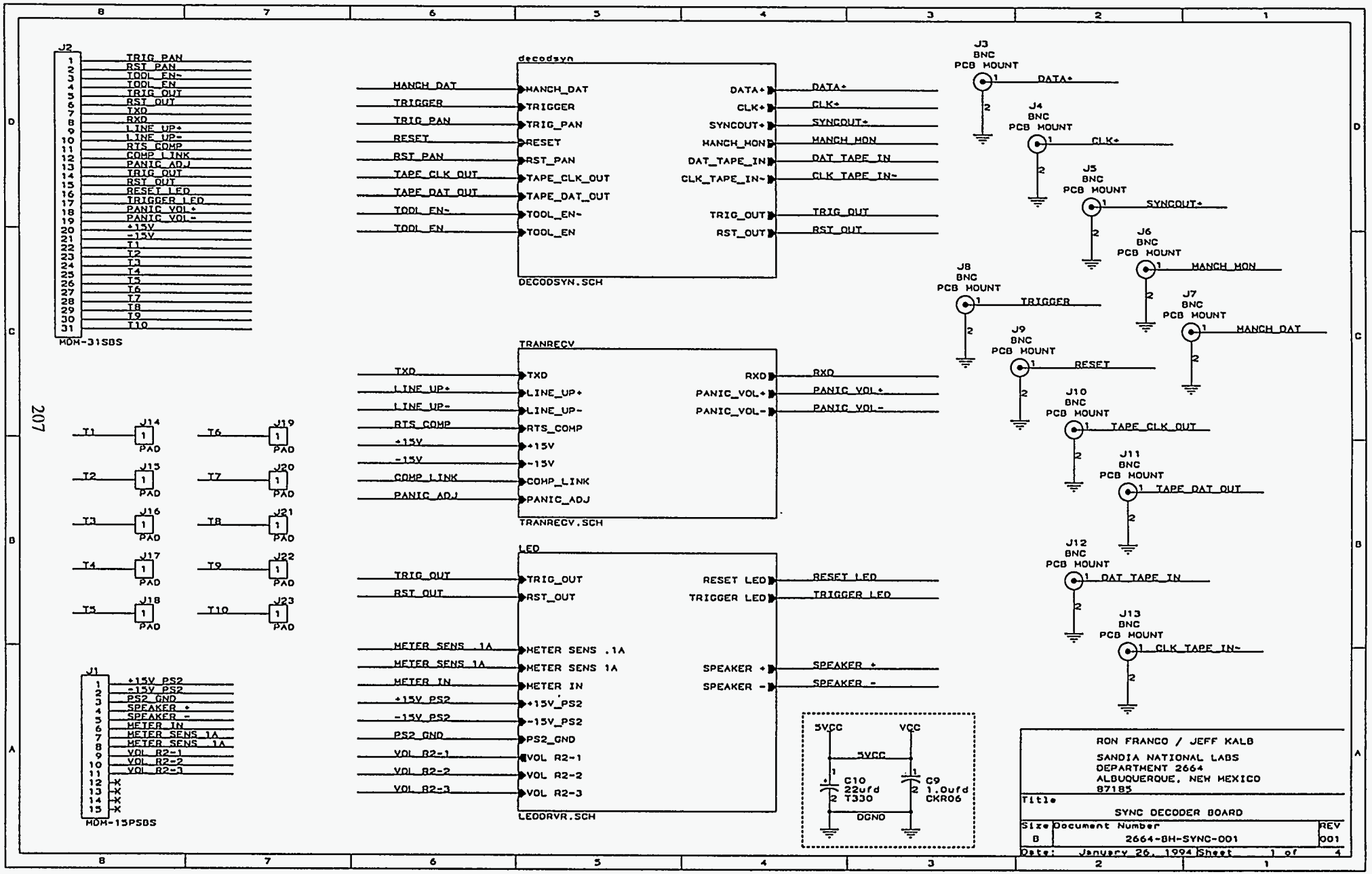

207

Figure C7a: Sync Detector Board

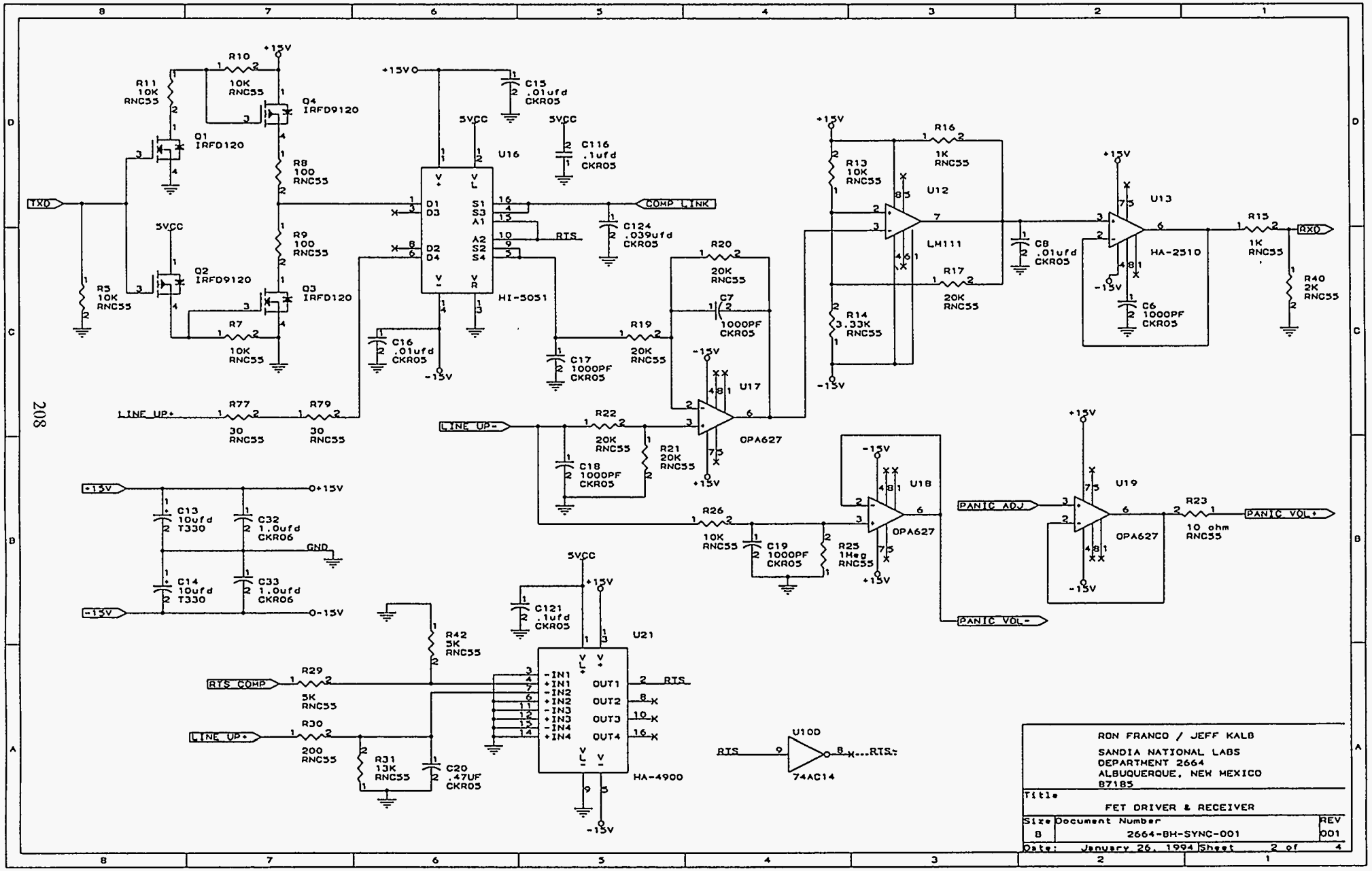

Figure C7b: Sync Detector Board

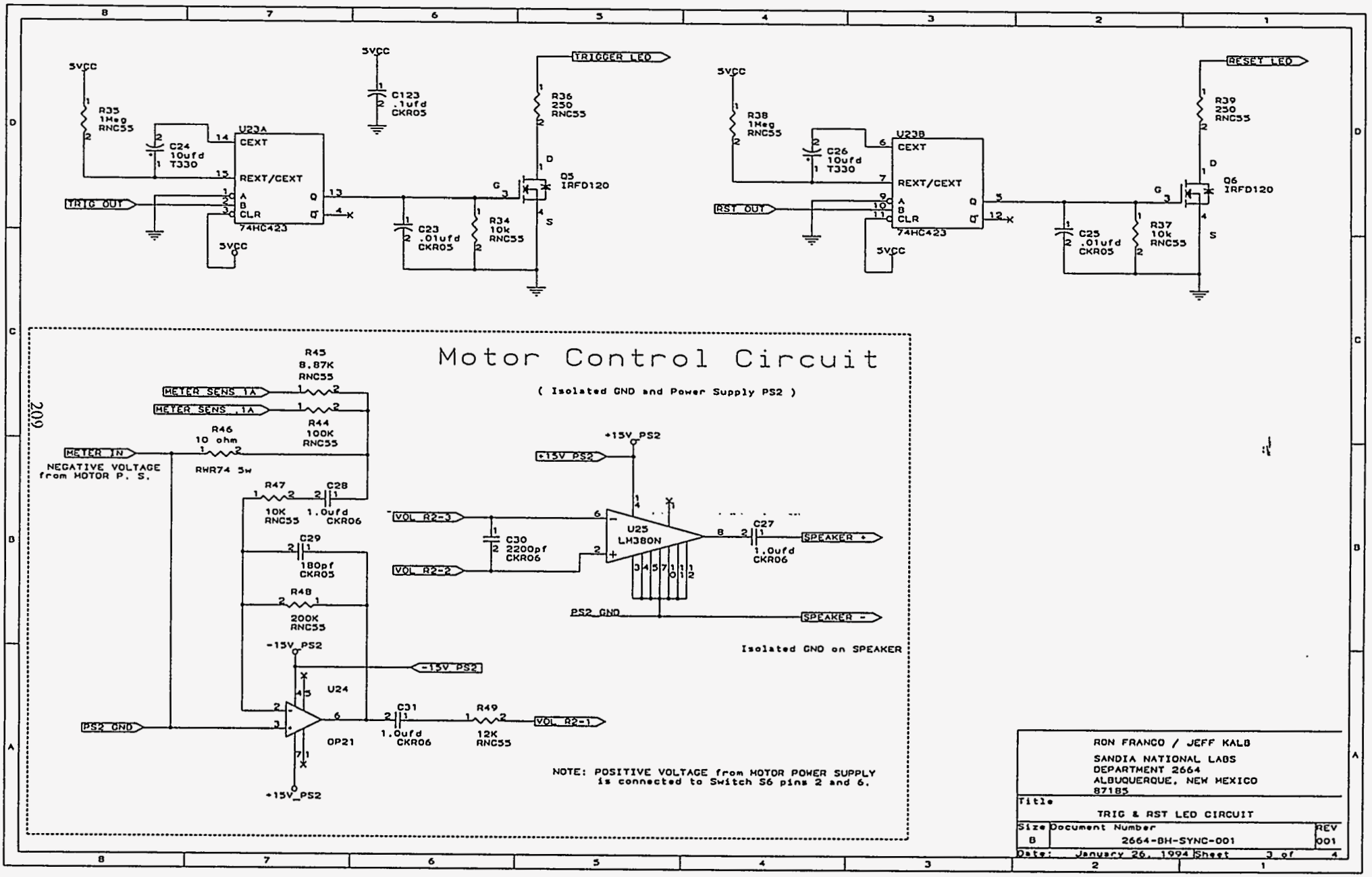

Figure C7c: Sync Detector Board

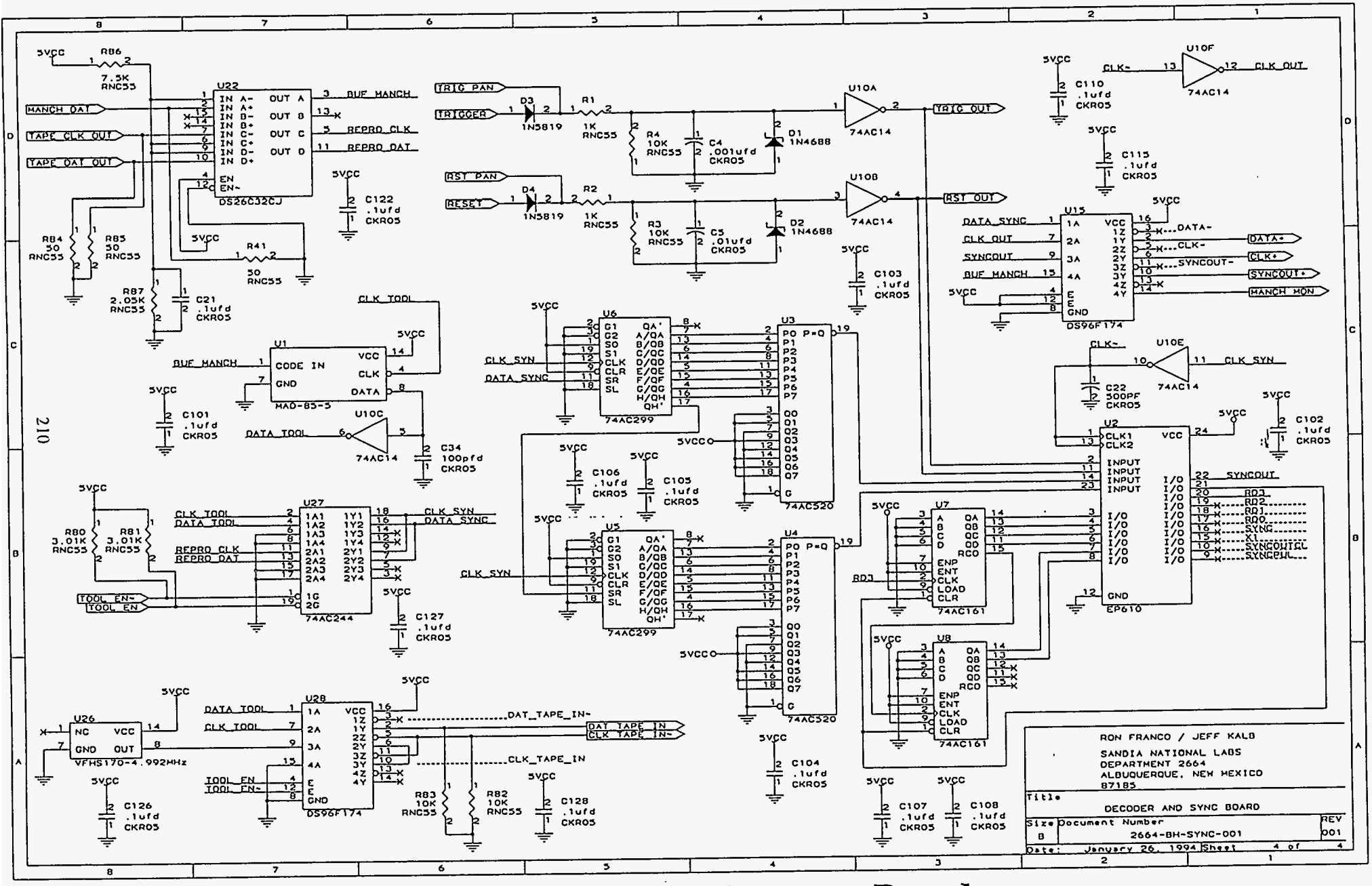

Figure C7d: Sync Detector Board

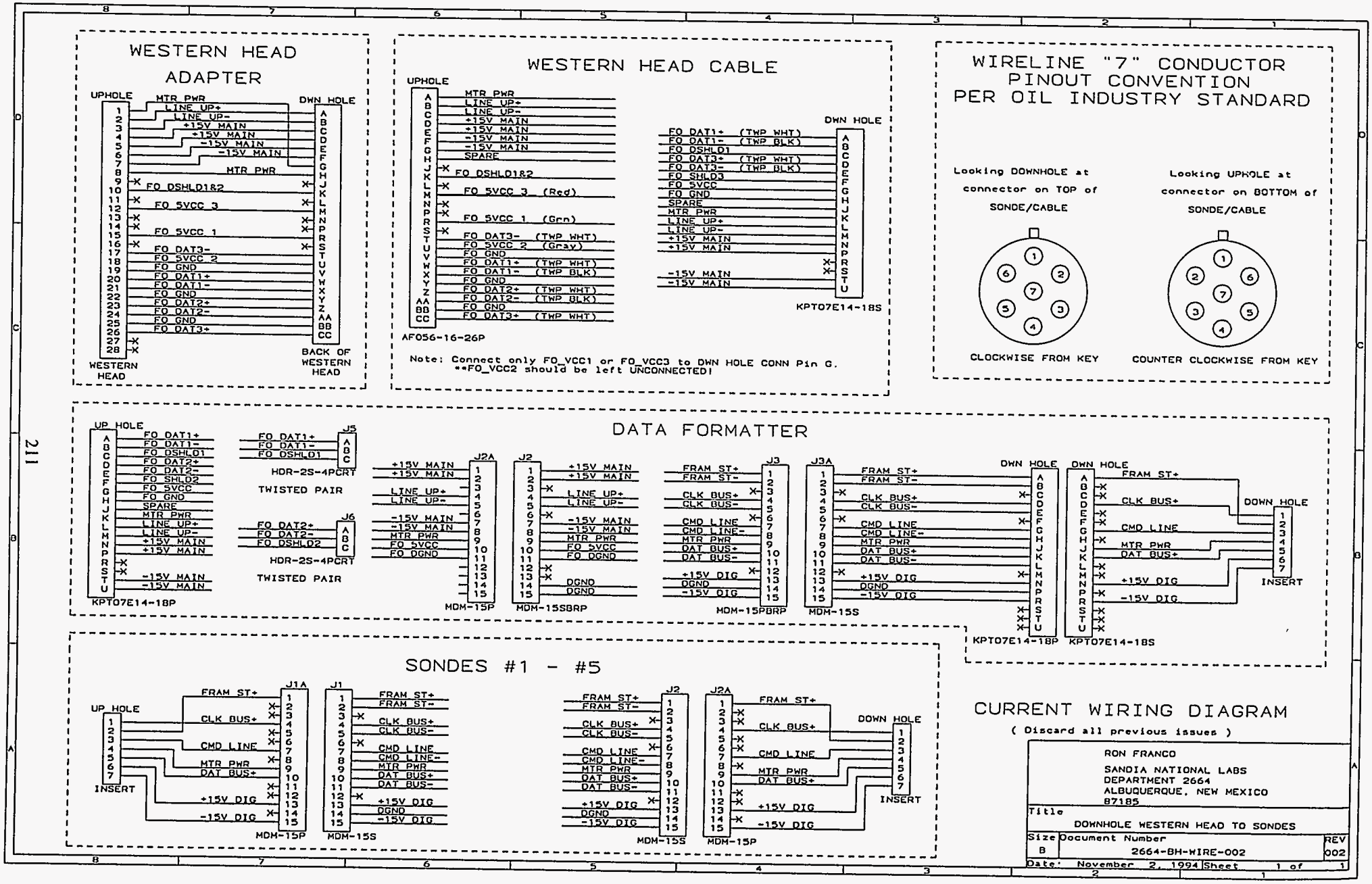

Figure C8: System Cabling Diagram for MLSR

Appendix D. High Temperature Electronics Design Rules

D.1. Digital Logic Devices

a. All CMOS Logic Families function well up to 200° C with modest increase in propagation time being the only notable performance change.

b. The "AC" logic families (called "FACT" by National Semiconductor) are the devices of choice. This family was developed by Fairchild under ownership of Schlumberger for high temperature applications.

c. Bipolar technologies of any sort shut down at about 125° C. Shut down means outputs totally stop responding. This would include "LS" and "ALS" Logic families and any LSI devices (gate arrays, microprocessors, memories) which are bipolar or hybrid bipolar-CMOS technologies.

d. The Altera CMOS EPLD logic devices function well with modest propagation delay increase to 200° C. These devices rely on UV erasable EPROM technology and they suffered no loss of programmed information in the EPROM section.

e. Crystal Oscillators based on HCMOS technology provided excellent frequency stability to 200° C.

f. We did not find it necessary to purchase mil-spec devices to operate at 200° C. We purchased mil-spec devices only when commercial or industrial grade parts were NOT available in ceramic or hermetic can packages.

g. Choosing devices of proper technology is critical and much more important than purchasing temperature screened devices.

h. Beware of devices which claim "short circuit" protection. Most of these devices sense high junction temperature as the shut down stimulus. Operation at 200° C shut down every such device evaluated.

D.2. Analog Devices

a. Again CMOS type devices must be used. Bipolar analog technologies are unacceptable for reasons cited below (part D.2.e).

b. We used CMOS ADCs, DACs and track-and-hold amps with excellent results to 160° C, and only modest degradation to 200° C.

c. Operational Amplifiers and Analog Multiplexers with "isolated gate" inputs work well with modest degradation to 200° C. Burr Brown calls its process "DiFET", Harris calls its

process "Dielectric Isolation", DI (see notes for HI-508/509). We used these Harris and Burr Brown devices soley.

d. Note that both Harris and Burr Brown make many devices that aren't of this (isolated gate) technology type. They both make bipolar and FET amplifiers which operate only poorly at 200° C.

e. The Bipolar and FET amplifiers suffer from excessive leakage at the input junctions. The primary performance penalties are excessive offset voltage and current, and gain and bandwidth degradation. The output drive capability doesn't suffer much, so the devices do work reasonably well at low gains and low speed.

D.3. Discretes

a. MOSFET devices have an "isolated-gate" type construction and work very well. We used these for power switches.

b. Bipolar transistors are unacceptable for the same reasons cited previously.

c. Linear Voltage regulators are generally based on bipolar technology and we had no luck with the ones we tried.

d. Zener diodes worked well to 200° C with modest change in regulation voltage.

e. Ceramic and solid tantalum capacitors, metal film resistors, and silicon diodes worked very well to 200° C.

D.4. PC Boards and Electronic Assembly

a. The PC board process we used is bare copper on Polyamide glass.

b. Since most commercial components have low temperature solder on the leads a direct high temperature solder joint is not practical. We inserted gold plated spring sockets in each hole and relied on the mechanical spring to maintain the contact. This works well although the low temperature solder on the leads tends to flow over the socket at 200° C operation.

c. A caution should be raised about the vibration/handling environment associated with seismic field survey operation. Our first units were not conformal coated and relied on the spring socket tension to hold parts in. Several of them vibrated loose on the road trip in the back of the wireline truck. We recommend that all boards have components either soldered (as practical with temperature) or coated with high temperature silicon sealant. Dow Corning, RTV-3145 is rated to 250° C. This process holds the devices very well.

d. Another approach would be to tin the PC boards with high temperature solder and purchase electronic devices with untinned leads. These devices would have to be special ordered and would be considerably more expensive.

Appendix E. MLSR Data Acquisition Checkout Procedures

MLSR Digitizer & Sig. Conditioner Checkout

A. Documentary Information:

1. Date: _____ 2. Time (of Day): _____

3. Test Name: _____ 4. Receiver SN: _____

5. Checker's Name: _____

B. Individual Board Checkouts:

Encoder Timing Board, SN: _____.

Configured for Data Receiver Station # _____. (1 through 5)

1. Assembly Notes:

a. EPLD Revisions:

U1(ADC) Filename:_____, Date: _____, Device Spd? _____ (ns)

U2(Bus) Filename:_____, Date: _____, Device Spd? _____ (ns)

U11(ClkG) Filename:_____, Date: _____, Device Spd? _____ (ns)

b. Bit Clock Oscillator:

U12 Specified Frequency: _____ MHz

c. Select Components:

R17: _____ Ω (Nom = open)

C50, C51, C52 = Open? _____

2. Voltage & Current Checks for Encoder Timing Board:

a. Power the Board through J2 with +15V_Dig(p13) & DGND(p14).

b. Record Voltage and Currents:

+15V_Dig: _____ V, Current: _____ ma (Nom = 120 ma)

5VCC: _____ V. (Monitored on SS9)

3. Oscillator Check:

Bit_Clk: _____ MHz, (Measured @ U11 pin 14)

B. Individual Board Checkouts (Continued):

A/D Board, SN: _____.

1. Assembly Notes:

a. Bit Clock Oscillator:

U12 Specified Frequency: _____ MHz (Nom = 4.00 MHz)

b. Select Components:

R5: _____ Ω (Nom = 28.7 kΩ)

R45: _____ Ω (Nom = 5.49 kΩ)

C14: _____ pf (Nom = open)

c. Install Jumper AGND(T5) to DGND(T6) & Maintain open sockets. _____

2. Voltage & Current Checks for A/D Board:

a. Power the Board through Spring Sockets:

+15V_Dig @ SS4, -15V_Dig @ SS3, 5VCC @ SS9, DGND @ SS12

b. Record Voltage and Currents:

+15V_Dig: _____ V, Current: _____ ma (Nom = 49 ma)

-15V_Dig: _____ V, Current: _____ ma (Nom = 48 ma)

5VCC: _____ V, Current: _____ ma (Nom = 2 ma)

+5Va: _____ V. (Monitored on T7)

-5Va: _____ V. (Monitored on T1)

ADRef:_____ V. (Monitored on U3 pin 28)

3. Oscillator Check:

ADC_Clk: _____ MHz, (Measured @ SS13)

B. Individual Board Checkouts (Continued):

A/D Board

4. Monitor Voltage Checks:

+15V_Mon: _____ (V), (Nom = 2.2V, U5p4)

-15V_Mon: _____ (V), (Nom = -2.2V, U5p5)

5VD+_Mon: _____ (V), (Nom = 2.5V, U5p6)

Temp_Mon: _____ (V), (Nom = 1.6V, U5p7)

MON5: _____ (V), (Nom = 2.0V, U5p12)

B. Individual Board Checkouts (Continued):

Motor Control Board, SN: _____.

Configured for Data Receiver Station # _____. (1 through 5)

1. Assembly Notes:

a. EPLD Revisions:

U1(MC) Filename:_____, Date: _____, Device Spd? _____ (ns)

b. Bit Clock Oscillator:

U5 Specified Frequency: _____ kHz

c. Select Components:
(See notes on Schematic for Resistor Settings per Station #).

R10: _____ Ω (Nom = See Schematic Page 3 of 3)

R11: _____ Ω

R12: _____ Ω

R13: _____ Ω

d. Motor Address Jumpers:
(See notes on Schematic for Jumper Settings per Station #).

GA3: _____ (H or L) GA2: _____ (H or L)

GA1: _____ (H or L) GA0: _____ (H or L) (Should be High)

2. Voltage & Current Checks for Motor Control Board:

a. Power the Board with +15V_Dig(E3), -15V_Dig(E4) & DGND(E5).

b. Record Voltage and Currents:

+15V_Dig: _____ V, Current: _____ ma (Nom = 20 ma)

5VCC: _____ V. (Monitored on U1p24)

3. Oscillator Check:

Clk_Cntr: _____ kHz, (Measured @ U1 pin 1)

B. Individual Board Checkouts (Continued):

Signal Conditioner Board, SN: _____.

1. Assembly Notes:

a. Configured for Accelerometers or Geophones? _____

b. Jumper Configuration:

All Jumpers B1-B12 Open for this Test. Install Later. _____ (OK?)

Install Following Jumpers for this test:

G1/G2: _____ (Short) G3/G4: _____ (Short)

G5/G6: _____ (Short)

c. Install CR1, CR4, CR5 for Accel Operation, Remove for Geophone.

CR1,4,5 Installed? _____ (Y or N)

d. Select Components:

C27: _____ pf (Nom = open) C28: _____ pf (Nom = open)

C78: _____ pf (Nom = open) C79: _____ pf (Nom = open)

C81: _____ pf (Nom = open) C80: _____ pf (Nom = open)

2. Voltage & Current Checks for Signal Conditioning Board:

a. Power the Board:

+15V_Dig @ T3, -15V_Dig @ T4, -5VA @ T1, @ +5VA @ T7, GND @ T5 and T6

b. Record Voltage and Currents:

+15V_Dig: _____ V, Current: _____ ma (Nom = 64 ma)

-15V_Dig: _____ V, Current: _____ ma (Nom = 64 ma)

+5VA: _____ V, Current: _____ ma (Nom = 32 ma)

-5VA: _____ V, Current: _____ ma (Nom = 32 ma)

3. AC Gain Checks @ 100 Hz:

Channel #1:

Vix (@ P1): _____ mVrms (10 mv), Inx (T13) _____ mVrms, Gain = _____
(@B2)

XHold (T12) _____ mVrms, Gain = _____

Vix (@ P1): _____ mVrms (1 mv), Inx (T13) _____ mVrms, Gain = _____
(@B2)

XHold (T12) _____ mVrms, Gain = _____

Channel #2:

Viy (@ P2): _____ mVrms (10 mv), Iny (T11) _____ mVrms, Gain = _____
(@B6)

YHold (T10) _____ mVrms, Gain = _____

Viy (@ P2): _____ mVrms (1 mv), Iny (T11) _____ mVrms, Gain = _____
(@B6)

YHold (T10) _____ mVrms, Gain = _____

Channel #3:

Viz (@ P3): _____ mVrms (10 mv), Inz (T9) _____ mVrms, Gain = _____
(@B10)

ZHold (T8) _____ mVrms, Gain = _____

Viz (@ P3): _____ mVrms (1 mv), Inz (T9) _____ mVrms, Gain = _____
(@B10)

ZHold (T8) _____ mVrms, Gain = _____

4. Spectrum Checks: (Transfer Functions):

Inx/Vix(P1): Fhigh _____ kHz, (@10 db down) Plot Okay? _____

Inx/Viy(P2): Fhigh _____ kHz, (@10 db down) Plot Okay? _____

Inx/Viz(P3): Fhigh _____ kHz, (@10 db down) Plot Okay? _____

C. Full Receiver Test:

Setup Information:

1. Test Support Equipment

   Formatter Board SN: _____

   Command Iface Board SN: _____

   Control Panel SN: _____

2. Receiver Boards Under Test:

   Encoder Timing Board SN: _____

   A/D Board SN: _____

   Motor Control Board SN: _____

   Signal Conditioner Board SN: _____

Basic Functionality:

1. Cable the Formatter and Receiver Boards up to Panel and Boot the Computer.
2. Connect Sine Wave (10 mv @ 100 Hz) to P1, Short B6 and B10 to AGND.
3. Connect Metered Power Supplies to +15V_Main & -15V_Main. (On Panel)
4. Initialize and "ARM" the Computer

   Verify Sine on first Channel:_____ Others Quiet: _____

5. Check Power Voltage and Current:

   +15V_Main: _____ (V), Current: _____ (ma, Nom = 520 ma)

   -15V_Main: _____ (V). Current: _____ (ma, Nom = 160 ma)

Digital Bus Check:

1. Bus Window Time:
   (Clk_Bus+ (J1p1) measured relative to rising edge of Fram_St+)

   ON _____ (microsec), OFF _____ (microsec).

   Correct for Station # _____, OK? _____.

   Correct Bus Window Times:
   Station #1: 1 to 24 Microseconds
   Station #2: 25 to 48 Microseconds
   Station #3: 50 to 73 Microseconds
   Station #4: 75 to 97 Microseconds
   Station #5: 100 to 118 Microseconds

2. Clk_Bus+ (J1p4): Vlow _____V, Vhigh ____V, rise time ____ microseconds.

3. Dat_Bus+ (J1p10):Vlow _____V, Vhigh ____V, rise time ____ microseconds.

Calibration Functions Check:

1. Disconnect Signal Source and Connect AGND to B2, B6, B10.

2. Run "Calibrate Command": AC Calibrate Good? _____ (Y or N)

   DC Calibrate Good? _____ (Y or N)

3. Run "Diagnostic" Command: Waveforms Good? _____ (Y or N)

   Record Voltage Readings: +15V: _____ V -15V: _____V

   5V+: _____ V Temp: _____° C

   DAC Ref: _____ V

Digitizer Performance Checkout:

1. Arm and Collect a Frame of "Grounded Inputs" Data.

   ChanX: RMS(X32): _____ cnts (4.0 typ), RMS(X1) _____ cnts (1.5 typ)

   ChanY: RMS(X32): _____ cnts (4.0 typ), RMS(X1) _____ cnts (1.5 typ)

   ChanZ: RMS(X32): _____ cnts (4.0 typ), RMS(X1) _____ cnts (1.5 typ)

2. Inject 100 Hz Sine @ 130 mV (92mVrms) peak into P1 with others @ AGND.

   (Record Following from the "Peak Level" & "Trace Status" Screens on the Computer)

   Record Input Level: _____ mvrms (nom 92 mVrms)

   ChanX: Peak Lvl: _____ V (2.60V, nom)

   ChanY: RMS(X32): _____ cnts (4.0 typ), RMS(X1) _____ cnts (1.5 typ)

   ChanZ: RMS(X32): _____ cnts (4.0 typ), RMS(X1) _____ cnts (1.5 typ)

3. Inject 100 Hz Sine Wave @ 130 mV peak into P2 with others grounded.

   Record Input Level: _____ mvrms (nom 92 mVrms)

   ChanX: RMS(X32): _____ cnts (4.0 typ), RMS(X1) _____ cnts (1.5 typ)

   ChanY: Peak Lvl: _____ V (2.60V, nom)

   ChanZ: RMS(X32): _____ cnts (4.0 typ), RMS(X1) _____ cnts (1.5 typ)

4. Inject 100 Hz Sine Wave @ 130 mV peak into P3 with others grounded.

   Record Input Level: _____ mvrms (nom 92 mVrms)

   ChanX: RMS(X32): _____ cnts (4.0 typ), RMS(X1) _____ cnts (1.5 typ)

   ChanY: RMS(X32): _____ cnts (4.0 typ), RMS(X1) _____ cnts (1.5 typ)

   ChanZ: Peak Lvl: _____ V (2.60V, nom)

Final Pre-Assembly Checks

1. Jumpers installed For Accelerometer Operation of Signal Conditioner:

B4/B3: _____ (Short for Accel) B2/B1: _____ (Open for Accel)

B8/B7: _____ (Short for Accel) B5/B6: _____ (Open for Accel)

B12/B11: ____ (Short for Accel) B9/B10: _____ (Open for Accel)

2. Terminate Each Accel Input to AGND through 1 kΩ and Series Current Meter.

X Input (B2): Current: _____ ma (2 ma, typ) Volt: _____ V, (2.0V, typ)

Y Input (B6): Current: _____ ma (2 ma, typ) Volt: _____ V, (2.0V, typ)

Z Input (B10): Current: _____ ma (2 ma, typ) Volt: _____ V, (2.0V, typ)

DISTRIBUTION:

1 Tim Anderson
Unocal Corporation
P.O. Box 76
Brea, CA 92821

1 Pierre Benichou
CGG American Services, Inc.
2500 Wilcrest
Houston, TX 77042

1 Rod Boade
Phillips Petroleum Company
137 Geoscience Building
Phillips Research Center
Bartlesville, OK 74004

1 Alan Burnham
Lawrence Livermore National Lab
P.O. Box 808, L-644
Livermore, CA 94550

1 Jack Caldwell
Market Development Manager
Schlumberger/GECO-PRAKLA
1325 South Dairy Ashford
Houston, TX 77077

1 Dale Cox
Conoco, Inc.
P.O. Box 1267
Ponca City, OK 74602-1267

1 Gary Crawford
BP Exploration
P.O. Box 4587
Houston, TX 77210

1 Alex Crawley
U.S. DOE
P.O. box 1398
Bartlesville, OK 74005

1 Paul Cunningham
Mobil Exploration & Producing
Tech Center
Mobil Place
P.O. Box 650232
Dallas, TX 75265-0232

1 W.T. "Bill" Davis
Geospace Corporation
7334 N. Gessner Road
Houston, TX 77040

1 Dave DeMartini
Shell Development Corporation
P.O. Box 481
Houston, TX 77001-0481

1 William P. Diffin
Kerr-McGee Corporation
P.O. Box 25861
Technology Center
Oklahoma City, OK 73125

1 Tim Fasnacht
Gas Research Institute
8600 West Bryn Mawr Ave.
Chicago, IL 60631

1 Roger Flanagan
Oak Ridge National Laboratory
P.O. Box 2009, Bldg. 9111
Martin Marietta Energy Systems
Y-12 Plant
Bear Creek Road
Oak Ridge, TN 37831-8201

1 Bob Fleming
Oryx Energy Company
P.O. Box 2880
Dallas, TX 75221-2880

1 Joseph Gallagher
Phillips Petroleum Company
1110C Plaza Office Bldg.
Bartlesville, OK 74004

1 Allen Goland
Brookhaven National Laboratory
75 Rutherford Drive, Bldg. 815
Upton, NY 11973-5000

1 Norman Goldstein
Lawrence Berkeley Laboratory
Earth Sciences Division, B-50E
1 Cyclotron Road
Berkeley, CA 94720

1 Bob Hanold
Los Alamos National Laboratory
MS D446, P.O. Box 1663
Los Alamos, NM 87545

1 Bob A. Hardage
Bureau of Economic Geology
University Station, Box X
Austin, TX 78713

1 Dr. Jerry M. Harris
Department of Geophysics
Stanford University
Mitchell Building, MS-2215
Stanford, CA 94305

1 Robert Heming
Chevron Petroleum Technology
2811 Hayes Road
Houston, TX 77082

1 Donald L. Howlett
Texaco, Inc.
3901 Briarpark
Houston, TX 77042

1 Rob Huggins
Geometrics, Inc.
395 Java Drive
Sunnyvale, CA 94089

1 Frank van Humback
Canadian Hunter Exploration, Inc.
Suite 2000, 605 5th Avenue, SW
Calgary, Alberta,
CANADA T2P 3H5

1 Scott Jacobsen
Schlumberger, MS-1D3
5000 Gulf Freeway
Houston, TX 77252-2175

1 Frank Kissinger
Teledyne Geotech
P.O. Box 469007
Garland, TX 75046-9007

1 Christine Krohn
Exxon Production Research Co.
P.O. Box 2189
Houston, TX 77252

1 Gary Latham
U.S. DOE
FE-60, FORS
Washington, DC 20585

1 Bob Lemmon
U.S. DOE
Bartlesville Project Office
P.O. Box 1398
Bartlesville, OK 74005

1 Bailey Lindsey
Geospace Corporation
7334 North Gessner Road
Houston, TX 77040

1 Craig Lippus
Geometrics, Inc.
395 Java Drive
Sunnyvale, CA 94089

1 Kenneth D. Mahrer
Rimtech
9056 Marshall Court
Westminster, CO 80030

1 Wulf Massell
Exploration & Prod. Imaging Corp
1221 Lamar, Suite 605
Houston, TX 77010-3037

1 Mark Mathisen
Mobil Research & Development
P.O. Box 819047
Dallas, TX 75381-9047

1 Larry Matthews
Canadian Hunter
Suite 2000, 605 5th Ave. SW
Calgary, Alberta,
CANADA T2P-3H5

1 John A. McDonald
University of Houston
Allied Geophysics Lab
AGL Building
Houston, TX 77204-4231

1 Randy McKnight
Marathon Oil Company
P.O. Box 3128
Houston, TX 77253-3128

1 Danny R. Melton
Texaco Inc.
P.O. Box 770070
Houston, TX 77215-0070

1 John Minear
Halliburton Logging Serv.
P.O. box 42800
Houston, TX 77242

1 James Minto
Western Atlas International
10205 Westheimer, Bldg. 1
Houston, TX 77042

1 Bjorn N.P. Paulsson
Chevron Petroleum Tech. Co.
1300 Beach Blvd
La Habra, CA 90633-0446

1 Wayne D. Pennington
Michigan Technical Univ.
1400 Townsend Drive
Houghton, MI 49931-1295

1 Steve Peterson
Marathon Oil Company
P.O. Box 3128
Houston, TX 77253-3128

1 William E. Preeg
Schlumberger
8311 North RR 620
Austin, TX 78726

1 Maynard Redeker
Oryx Energy Company
P.O. Box 830936
Richardson, TX 75083-0936

1 Dick Rice
Idaho National Engineering Lab
2525 Freemont Avenue
Idaho Falls, ID 83415-3710

1 Salvadore Rodriguez
CGG American Services, Inc.
2500 Wilcrest
Houston, TX 77042

1 Iraj Salehi
Gas Research Institute
8600 Bryn Mawr Avenue
Chicago, IL 60631

1 Dave Schmalzer
Argonne National Lab
955 L'Enfant Plaza SW
Suite 6000
Washington, DC 20024

1 Ken Shaw
Unocal Corporation
P.O. Box 4551
Houston, TX 77210-4551

1 Brian Shaw
Pacific Northwest Laboratory
3200 Q Street
Richland, WA 99352

1 John Sinton
Conoco, Inc.
1000 Pine Street
Ponca City, OK 74603

1 Reginal W. Spiller
U.S. DOE
FE-30 FORS
Washington, DC 20585

1 Bill Spurgeon
Kerr-McGee Corporation
P.O. Box 25861/Tech Center
Oklahoma City, OK 73125

1 George Stosur
U.S. DOE
FE-33 GTN
Washington, DC 20545

1 Manik Talwani
Houston Advanced Research Ctr
4800 Research Forest Drive
The Woodlands, TX 77381

1 Henry Tan
Amoco Production Company
P.O. Box 3385
Tulsa, OK 74102

1 Walter R. Turpening
Reservoir Imaging, Inc.
13003 Murphy Road, Ste D-1
Stafford, TX 77477

1 Roger Turpening
Earth Resources Laboratory
Mass. Institute of Technology
42 Carleton Street
Cambridge, MA 02142

1 Harold Vinegar
Shell Development Corporation
P.O. Box 481
Houston, TX 77001-0481

1 Sandra L. Waisley
U.S. DOE
FE-32 FORS
Washington, DC 20585

1 Larry Walter
Bolt Technology Corporation
3024 Rogerdoli Road
Houston, TX 77042

1 Ron Ward
Louisiana Land & Explor. Co.
909 Poydras Street
New Orleans, LA 70160

1 Royal J. Watts
U.S. DOE
3610 Collins Ferry Road
Morgantown, WV 26505

1 Thomas C. Wesson
U.S. DOE
220 N. Virginia Avenue
Bartlesville, OK 74005

1 Bob Whitsett
DOE-Partnership
12434 Perthshire
Houston, TX 77024

1 Graham A. Winbow
Exxon Production Research co.
P.O. Box 2189
Houston, TX

1 Robert Withers
ARCO Expl. & Prod. Tech.
2300 West Plano Pkwy
Plano, TX 75075

1 E. J. Witterholt
BP Exploration
P.O. Box 4587
Houston, TX 77210-4587

Sandia Internal:

MS 0985 John Stichman, 2600
MS 0987 Ron Franco, 2664 (10)
MS 0987 Jeff Morgan, 2664
MS 0987 David Ryerson, 2664
MS 0701 Richard Lynch, 6100
MS 0706 David Northrop, 6112 (10)
MS 0705 Richard S. Harding, 6114
MS 0705 Patrick Drozda, 6114
MS 0705 Bruce Engler, 6114 (50)
MS 0705 Norman Warpinski, 6114
MS 0750 Marianne Walck, 6116
MS 0750 Gregory Elbring, 6116
MS 0843 Gerard Sleefe, 9136
MS 0979 Larry Walker, 9204
MS 0655 Preston Herrington, 9236

MS 9018 Central Tech. Files, 8523-2
MS 0899 Technical Library, 13414 (5)
MS 0619 Technical Publications, 12613
MS 0100 Document Processing for
DOE/OSTI, 7613-2 (2)

•U.S. GOVERNMENT PRINTING OFFICE 1995-0-673-031/00034